Etude de modèles macroscopiques de réseaux de neurones spatialement organisés

Joachim Crevat

▶ **To cite this version:**

HAL Id: tel-02895966

https://hal.science/tel-02895966

Submitted on 10 Jul 2020

THÈSE

En vue de l'obtention du

DOCTORAT DE L'UNIVERSITÉ DE TOULOUSE

Délivré par l'Université Toulouse 3 - Paul Sabatier

Présentée et soutenue par

Joachim CREVAT

Le 3 juillet 2020

Etude de modèles macroscopiques de réseaux de neurones spatialement organisés

Ecole doctorale : **EDMITT - Ecole Doctorale Mathématiques, Informatique et Télécommunications de Toulouse**

Spécialité : **Mathématiques et Applications**

Unité de recherche :
IMT : Institut de Mathématiques de Toulouse

Thèse dirigée par
Francis FILBET et Grégory FAYE

Jury

Mme Delphine SALORT, Rapporteure
M. Daniel HAN-KWAN, Rapporteur
Mme Fanny DELEBECQUE, Examinatrice
M. François DELARUE, Examinateur
M. Francis FILBET, Directeur de thèse
M. Grégory FAYE, Co-directeur de thèse

Remerciements

Je commence ce manuscrit en remerciant tous ceux qui m'ont côtoyé ou que j'ai rencontrés pendant ces trois ans de thèse, à qui je souhaite exprimer ma gratitude.

Je tiens à remercier en tout premier lieu mes directeurs de thèse Francis Filbet et Grégory Faye pour avoir accepté d'encadrer cette thèse. J'avais déjà effectué un stage en M1 avec Grégory, qui avait été un premier pas très motivant dans le monde de la recherche. Puis, alors que le projet initial de stage de M2 avait été construit par Francis, celui-ci m'a proposé de rajouter Grégory en co-directeur pour travailler sur des modèles de réseaux de neurones. J'ai sincèrement apprécié durant ces trois ans la qualité de leur encadrement. Même s'il y a eu des moments difficiles, ils ont réussi à toujours rester disponibles, compréhensifs, et motivants. De plus, ils m'ont toujours donné les meilleurs conseils. Le sujet qu'ils m'ont proposé s'est avéré non seulement très riche et captivant pour moi, mais je me suis rendu compte au fur et à mesure qu'il est aussi intéressant pour la communauté des chercheurs en neurosciences mathématiques.

Nous avons toujours réussi à nous voir régulièrement pour faire le point. Je sortais de nos réunions, qui pouvaient durer plusieurs heures, avec des réponses et des pistes à explorer, et surtout un sentiment d'avoir progressé. Je veux aussi saluer tout le temps que vous avez passé pour me donner des recommandations pour mon projet professionnel (d'abord pour la recherche, puis pour l'enseignement). Vous avez su être particulièrement honnêtes et justes. Même si je n'ai pas suivi tous vos conseils, je vous remercie profondément pour votre bienveillance.

Je me rends compte du travail énorme que vous avez dû fournir pour toujours me pousser en avant, me recommander les bonnes conférences, relire mes travaux et mes présentations. Je souhaite à beaucoup d'autres étudiants de découvrir le travail de chercheur avec vous. Merci pour tout.

Je souhaite aussi remercier Delphine Salort et Daniel Han-Kwan pour avoir accepté de lire et rapporter ce manuscrit. Merci d'avoir pris ce temps, malgré tous les événements imprévus que vous avez sûrement rencontrés pendant cette période de confinement. Je remercie aussi Fanny Delebecque et François Delarue pour avoir accepté de faire partie de mon jury de thèse alors que nous étions encore incertains quant aux modalités de tenue de la soutenance à cause de la situation sanitaire.

En plus de ces trois ans de thèse, j'ai effectué aussi deux stages à l'IMT. J'ai pu rencontrer et partager des moments enrichissants avec quelques chercheurs envers qui je suis reconnaissant. Tout particulièrement, je tiens à remercier ceux qui ont participé à l'organisation du groupe de travail doctorant, c'est-à-dire Violaine Roussier-Michon, Ariane Trescases, Sepideh Mirrahimi et Jean-Michel Roquejoffre. Vos remarques m'ont beaucoup aidé à prendre du recul sur mon travail. Pour les mêmes raisons, j'exprime aussi ma reconnaissance à Jean-François Coulombel pour ses remarques lors d'un groupe de travail en 2017, qui m'ont été très utiles par la suite. Je salue aussi Franck Boyer pour ses nombreux conseils au sujet de l'après-thèse. Ensuite, grâce aux TP que j'ai donnés, j'ai pu échanger entre autres avec Étienne Fieux et Marie-Hélène Vignal, que je tiens à saluer pour avoir toujours été investis, arrangeants et de bon conseil. C'est en partie grâce à eux que mes premières expériences d'enseignement ont été très positives.

Merci aussi à tous les chercheurs que j'ai rencontrés durant les différentes conférences auxquelles j'ai assistées. Je salue en particulier Julien Chevallier et Éric Luçon pour les discussions enrichissantes à l'ICMNS ; Étienne Tanré et Romain Veltz pour l'invitation à un groupe de travail à Paris ; et Daniele Avitabile pour le projet de recherche sur le modèle QIF pendant le confinement. Je veux aussi remercier tout spécialement Jimmy Garnier, qui m'a invité à la première conférence où j'ai dû présenter mes résultats, à Chambéry. J'en ai été très honoré. Je salue aussi Stéphane Brull pour son invitation au congrès franco-coréen à Bordeaux. C'est formidable de voir que même des milliers de kilomètres n'empêchent pas la collaboration scien-

tifique.

Ensuite, l'IMT et l'école doctorale sont dotés d'équipes administratives particulièrement efficaces et sympathiques. Je remercie tout particulièrement Agnès Requis et Martine Labruyère. Toujours disponibles, et assez patientes pour expliquer les différentes démarches à faire. Et bien sûr, j'adresse un remerciement spécial à Monique et Marie-Line, très efficaces dans leur travail, et toujours prêtes à prendre le temps de bavarder un peu quand ça ne va pas.

Durant l'été 2018, j'ai participé au CEMRACS à Marseille. Là-bas, pendant 6 semaines, j'ai pu rencontrer des chercheurs et des doctorants pour travailler tous ensemble sur des sujets de mathématiques appliquées à la biologie. J'ai eu le plaisir de mener un projet de recherche en compagnie de Florian Lavigne, Léonard Dekens et Frédéric Kuczma. Nous étions encadrés par Vincent Calvez et Gaël Raoul, que je ne remercierai jamais assez pour nous avoir donné la motivation et les moyens de même dépasser les objectifs du projet initial.

Ensuite, je dois avouer que je n'aurais eu le courage de tenir 3 ans sans l'appui des amis formidables que je me suis faits au bureau 302, toujours enclins à prendre un petit moment pour s'entraider, ou simplement se remonter le moral. Dans l'ordre d'apparition, un grand merci à Marc, pour tous ses conseils; à Guillaume, toujours calme, sérieux et rassurant; à Baptiste, l'une des personnes les plus gentilles que j'aie jamais rencontrées; à Alexis, pour toutes les pauses où l'on a discuté culture, mathématiques, ou simplement partagé nos problèmes respectifs; à Mathias, pour tous les fous rires dès 8h du matin; et enfin à Louis, toujours incroyablement passionné et investi dans ce qu'il fait, avec qui nous avons passé des moments mémorables.

Si l'ambiance au laboratoire est aussi bonne, c'est notamment grâce à tous les doctorants (et post-doctorants) qui savent se soutenir les uns les autres. Tout d'abord Michelle, la fournisseuse de bonne humeur et kaak bhalib; Anthony, qui gare sa Mercedes n'importe où mais qu'on aime bien quand même; Elena, toujours souriante sous ses cheveux multicolores. Je salue également Susely, Moktar, Sourav, Joe, François, Kuntal, Perla, Paola, Corentin, Phuong pour l'équipe MIP; Valentin, Maylis, William, Joachim, Nathanael, Jens, Laetitia, les deux Clément et Mehdi pour l'équipe ESP ; et Jean-Marc, Florian, Tu, Dimitri et Fabien pour l'équipe Picard. Je suis obligé de faire une liste à la Prévert, vous êtes si nombreux et je vous suis à tous reconnaissant pour tous les bons moments que j'ai passés avec vous.

La thèse est une épreuve de longue haleine qui demande un soutien moral indéfectible. Et pour ça je tiens à remercier tous les gens qui ont partagé mon appartement, qui ont tous su m'apporter un soutien à leur manière. Je salue donc dans l'ordre d'apparition Soso, Mathis, Chloé, Aurélie, Jéromine (deux ans déjà !), Florent, Paola, Cécilianne, et Thomas. Merci aussi à Marius, Nestor et Irène, vous êtes trois amis vraiment extraordinaires. Pendant les trop rares week-ends où je suis rentré à Lyon, j'ai pu y retrouver des amis de longue date, merci à Dimitri, Quentin et Adrien.

Et enfin, merci à ma famille pour m'avoir toujours soutenu et encouragé dans tout ce que j'ai entrepris, y compris ma thèse. Je remercie donc mon frère et ma sœur Florent et Camille, qui à leur manière propre m'ont enseigné d'aller jusqu'au bout des choses. Et bien sûr merci à mes deux parents, toujours aimables et attentionnés, prêts à m'aider lorsqu'ils le peuvent (je pense entre autres à la relecture très précise de l'introduction pour laquelle leur savoir-faire de journaliste a été décisif); c'est très précieux de savoir que des gens bienveillants comme vous me soutiennent quoi qu'il arrive.

Résumé

Dans cette thèse, nous étudions un réseau neuronal spatialement organisé, c'est-à-dire que les interactions entre deux neurones ne dépendent que de leurs positions. Si nous ne considérons qu'un nombre relativement restreint de cellules, l'activité électrique de chaque neurone peut être modélisée grâce au système de FitzHugh-Nagumo. Toutefois, si nous cherchons à étudier le comportement collectif d'un groupe de neurones plus nombreux, il devient essentiel de trouver d'autres modèles, correspondant à une échelle d'observation plus grande. L'objectif de cette thèse est donc d'établir un lien mathématique rigoureux entre le modèle microscopique de FitzHugh-Nagumo, et des modèles macroscopiques qui donnent l'évolution des quantités électriques moyennes à chaque position dans le réseau.

La première étape de notre stratégie consiste à établir un lien rigoureux entre le modèle microscopique et un modèle intermédiaire, en faisant tendre le nombre de neurones vers l'infini. Nous obtenons une équation à dérivées partielles qui donne l'évolution de la densité de probabilité de trouver des neurones à chaque instant en fonction de leur position et de leur potentiel de membrane. Elle décrit alors une échelle mésoscopique d'observation du réseau.

Ensuite, nous étudions les valeurs électriques moyennes calculées à partir du modèle mésoscopique. Afin de trouver un système d'équations satisfait par ces quantités macroscopiques, nous considérons le cas où les interactions locales entre neurones sont fortes. Pour cela, nous proposons deux redimensionnements possibles. En utilisant une méthode d'entropie relative, nous établissons un lien mathématique entre le modèle intermédiaire et un système de réaction-diffusion. Le terme de diffusion sera local ou non local en espace, selon le redimensionnement que nous aurons choisi.

Enfin, nous attaquons l'étude de ce dernier changement d'échelle du point de vue de l'analyse numérique. En particulier, nous présentons une discrétisation du modèle mésoscopique qui préserve l'asymptotique dans le régime des interactions locales fortes. Ainsi, nous sommes capables d'estimer des vitesses de convergence et d'observer des dynamiques du modèle intermédiaire.

Mots-Clés

Abstract

In this thesis, we study a spatially organised neuronal network, that is the interactions between two neurons only depend on their positions. If we only consider a relatively small number of cells, the electric activity of each neuron can be modeled with the FitzHugh-Nagumo system. Yet, if we attempt to study the collective behaviour of a more sizeable assembly of neurons, we must find other models, corresponding to a larger scale of observation. Thus, the purpose of this thesis is to establish a rigourous mathematical link between the microscopic FitzHugh-Nagumo model, and macroscopic models which account for the evolution of average electrical quantities at any position in the network.

The first step of our strategy consists in deriving a rigourous link between the microscopic model and an intermediary model as the number of neurons tends to infinity. We obtain a partial differential equation, which gives the evolution of the probability density of finding neurons at any time depending on their position and membrane potential. Therefore, it describes a mesoscopic scale of observation of the network.

Then, we study the average electrical quantities computed from the mesoscopic model. In order to find a system of equations satisfied by these macroscopic quantities, we consider the regime of strong local interactions. To do so, we provide two different ways of rescaling. Using a relative entropy method, we find a mathematical link between the intermediary model and a reaction-diffusion system. Depending on the rescaling we choose, the diffusion term can be local or non local in space.

Finally, we tackle the study of this last change of scale from a numerical analysis viewpoint. In particular, we introduce a discretization of the mesoscopic model which is asymptotic preserving in the regime of strong local interactions. Hence, we can numerically estimate rates of convergence, and we observe some dynamics of the intermediary model.

Keywords

Contents

Chapter 1

Introduction

Contents

1.1 Préambule

Ce mémoire de thèse porte sur la modélisation de réseaux de neurones du cerveau et leur analyse. Plus précisément, nous nous sommes intéressés à l'étude de modèles macroscopiques déterministes de réseaux de neurones à partir d'un modèle microscopique organisé spatialement. Commençons par passer en revue les différentes problématiques de modélisation de notre sujet, en précisant le contexte dans lequel s'inscrit notre travail.

Les neurones sont des cellules d'organisme vivant constituées d'un corps cellulaire appelé *soma* dans lequel est situé le noyau. Pour communiquer, chaque neurone possède une extension en forme de branche appelée *axone* qui conduit de courtes impulsions électriques appelées *potentiels d'action*. Les axones des autres neurones dans l'environnement sont connectés à un *arbre dendritique* qui conduit les influx nerveux venant de l'extérieur jusqu'au corps cellulaire. La jonction entre les axones et les dendrites se fait par des *synapses* (voir la Figure 1.1).

La Figure 1.2 représente schématiquement une synapse entre deux neurones. Le neurone *présynaptique* est celui auquel est rattaché la terminaison de l'axone (en haut sur le schéma), et le neurone *postsynaptique* est celui à qui appartient la dendrite (en bas). L'impulsion électrique parcourt l'axone du neurone présynaptique jusqu'à sa terminaison. Si son intensité est suffisante, l'arrivée de charges électriques produit des mouvements d'ions qui vont déplacer des vésicules contenant des neurotransmetteurs chimiques jusqu'à la *fente synaptique* (l'espace séparant les deux neurones). Ces neurotransmetteurs vont être relâchés pour parcourir la fente jusqu'à rencontrer des neurorécepteurs au niveau de l'arbre dendritique du neurone postsynaptique. Une réaction chimique intervient, à l'issue de laquelle des mouvements d'ions, et donc de charges électriques, vont se produire pour acheminer le signal jusqu'au corps du neurone.

Un neurone est une cellule excitable, dans le sens où elle produit des influx nerveux en réponse à un stimulus électrique extérieur qui vient perturber son état de repos. Ces impulsions ont notamment été mises en évidence par l'expérience de Hodgkin-Huxley [84], dont le but était de mesurer l'évolution du potentiel électrique d'un point donné de la membrane d'un axone géant de calmar (voir Figure 1.3a). Nous observons que l'influx nerveux se propageant le long de l'axone est une brève perturbation à forte amplitude d'un état de repos du potentiel du neurone. Nous l'appellerons par la suite *potentiel d'action*.

La modélisation de l'activité électrique des neurones est un domaine d'intérêt aussi bien en biologie, pour les neurosciences et l'imagerie médicale, qu'en mathématiques. En effet, ces modèles, bien que simples analytiquement pour modéliser l'activité d'un seul neurone, peuvent présenter des dynamiques complexes pour l'activité couplée d'un réseau de neurones. Tout d'abord, un modèle général et standard pour un simple neurone est le suivant. Notons v le potentiel de membrane d'un neurone. Il évolue en fonction des différents courants parcourant le neurone. Tout d'abord, nous notons u la somme des *courants synaptiques*, c'est-à-dire la somme des courants provenant des dendrites du neurone, générés par les interactions synaptiques avec l'environnement. Nous considérons $-I_{\text{chim}}$ le *courant de membrane*. Il provient de l'ensemble des réactions chimiques internes au neurone qui tendent à ramener le potentiel v vers son état de repos. Enfin, nous ajoutons I_{ext} un autre courant injecté de l'extérieur dans le neurone. Toutes ces quantités électriques sont représentées schématiquement à la Figure 1.3b. En notant C la capacité électrique de la cellule, on obtient d'après [26]:

$$C \frac{\mathrm{d}v}{\mathrm{d}t} = -I_{\text{chim}} + u + I_{\text{ext}}. \tag{1.1.1}$$

On considère que lorsque la tension du neurone atteint un certain seuil à un instant T, il émet un potentiel d'action, puis est réinitialisé à une certaine valeur.
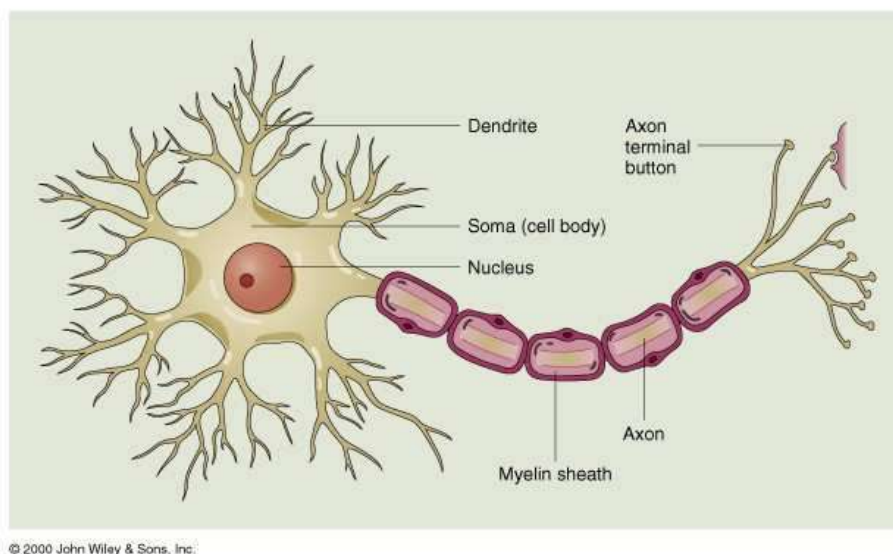
Figure 1.1: Schéma de la structure d'un neurone.

1.1.1 Modèles de Hodgkin-Huxley et de FitzHugh-Nagumo

Dans ce travail de thèse, nous nous intéressons particulièrement à l'évolution de la tension de membrane en elle-même, y compris au cours de l'émission d'un influx nerveux. Afin de décrire précisément la fonction v, dans [85], Alan Hodgkin et Andrew Huxley ont décomposé le courant de membrane I_{chim} en trois différents courants provenant de la circulations d'ions K^+, Na^+ et d'autres ions au rôle réfractaire, c'est-à-dire qui tendent à ramener le potentiel v vers son état de repos. Nous notons ces courants respectivement I_K, I_{Na} et I_l. Un moyen simple de déterminer ces courants est de les modéliser à l'aide de la *conductance* électrique. En utilisant la loi d'Ohm, nous obtenons donc que

$$I_{\text{chim}} = \sum_{s \in \{K, Na, l\}} g_s \, (v - V_s),$$

où V_s et g_s représentent respectivement le potentiel de repos pour la chaîne d'activation de l'ion $s \in \{K, Na, l\}$, et la conductance de la chaîne de l'ion s. D'après [85], si l'on note $\overline{g}_s$ la conductance maximale associée à la chaîne de l'ion s, on obtient:

$$g_K = n^4 \, \overline{g}_K, \quad g_{Na} = m^3 h \, \overline{g}_{Na}, \quad g_l = \overline{g}_l,$$

où m, n et h sont les proportions (variables) de chaînes "ouvertes" respectivements des ions Na^+, K^+ et inhibiteurs. Le modèle (1.1.1) devient le modèle de Hodgkin-Huxley (HH):

$$
\begin{cases}
C \dfrac{\mathrm{d}v}{\mathrm{d}t} + n^4 \, \overline{g}_K \, (v - V_K) + m^3 h \, \overline{g}_{Na} \, (v - V_{Na}) + \overline{g}_l \, (v - V_l) = u + I_{\text{ext}}, \\[2mm]
\dfrac{\mathrm{d}m}{\mathrm{d}t} = \alpha_m(v) \, (1 - m) + \beta_m(v) \, m, \\[2mm]
\dfrac{\mathrm{d}n}{\mathrm{d}t} = \alpha_n(v) \, (1 - n) + \beta_n(v) \, n, \\[2mm]
\dfrac{\mathrm{d}h}{\mathrm{d}t} = \alpha_h(v) \, (1 - h) + \beta_h(v) \, h.
\end{cases}
\tag{1.1.2}
$$

11
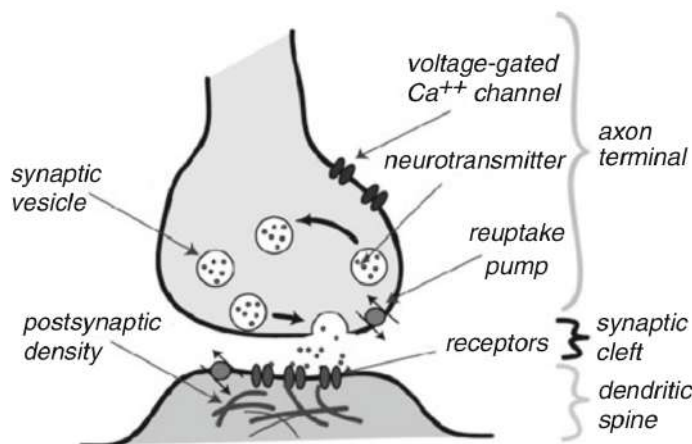
Figure 1.2: Schéma d'une synapse entre deux neurones (source [26]).

De plus, les fonctions (α_s, β_s) pour $s \in \{m, n, h\}$ ont été déterminées dans [85] à partir de données expérimentales.

Dans la suite de notre travail, nous ne nous intéresserons pas au modèle (1.1.2), mais plutôt à une version simplifiée à seulement deux dimensions : le modèle de FitzHugh-Nagumo [71, 108] (abrégé FHN par la suite), développé en 1961. En effet, dans [71], Richard FitzHugh a décomposé le système (1.1.2) en deux sous-systèmes : (v, w) les variables excitatrices du système, qui évoluent rapidement, et (h, n) les variables inhibitrices, qui évoluent lentement. En utilisant deux projections linéaires, il retire une dimension à chacun des sous-systèmes, et se retrouve finalement avec le modèle suivant :

$$\begin{cases} \dfrac{\mathrm{d}v}{\mathrm{d}t} = N(v) - w + u + I_{\text{ext}}, \\[2mm] \dfrac{\mathrm{d}w}{\mathrm{d}t} = \tau\,(v + a - b\,w). \end{cases} \qquad (1.1.3)$$

Ici, nous utilisons la notation v même s'il ne s'agit pas exactement du potentiel de membrane étudié dans le modèle (1.1.2), mais d'une approximation. Nous l'appellerons par la suite aussi *potentiel de membrane* même si ce n'est pas physiquement exact. Ensuite, w ne représente plus vraiment de grandeur physique à proprement parler, mais reste essentielle à la dynamique du système. Nous l'appellerons par la suite *variable d'adaptation*. De plus, $\tau \geq 0$, $a \in \mathbb{R}$ et $b \geq 0$ sont des constantes données. Le paramètre τ est choisi en général assez petit pour que l'évolution de la variable v soit rapide par rapport à celle de w. Enfin, $N(v)$ est la fonction cubique suivante :

$$N : v \mapsto v\,(1 - v)\,(v - \theta), \qquad (1.1.4)$$

où $\theta \in (0, 1)$. Le terme $N(v)$ sert à modéliser l'excitabilité de la cellule[1].

Dans le but de reproduire les dynamiques des neurones que nous avons décrites, nous devons à présent définir la notion de *système excitable*. Il s'agit d'une équation différentielle qui possède comme équilibre un unique point fixe P^* stable. Si la condition initiale est suffisamment proche de P^*, alors la solution est attirée par celui-ci et reste dans son voisinage. Si l'écart entre la

---

[1]Dans la suite, pour les travaux que nous effectuerons, nous pourrons sans perdre de généralité utiliser une fonction N plutôt de la forme

$$N(v) = v\,(\alpha - \beta\,v^2),$$

où $\alpha, \beta \geq 0$.
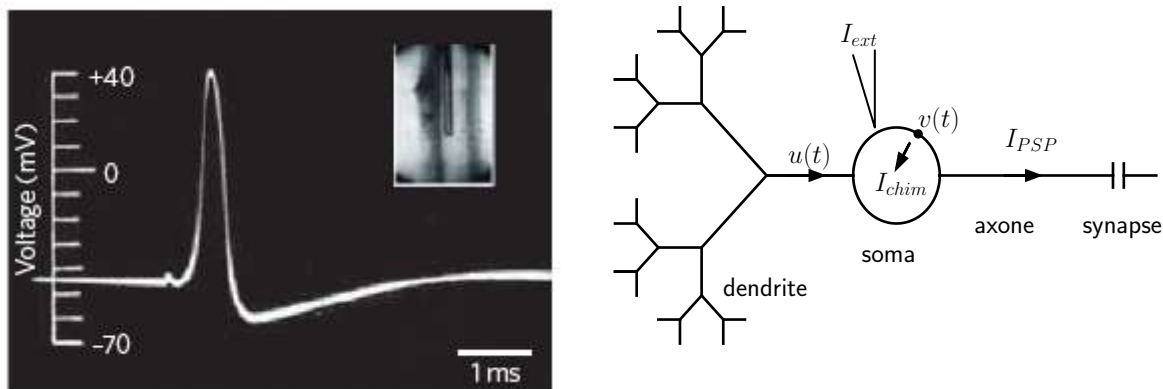
(a) Mesure d'un potentiel d'action mesuré au niveau de la membrane d'un axone d'un neurone géant de calmar (source [84]).

(b) Schéma des différents courants parcourant un neurone. I_{PSP} correspond au courant présynaptique parcourant l'axone.

Figure 1.3: Activité électrique d'un neurone.

condition initiale et P^* dépasse un certain seuil, alors la trajectoire de la solution suit un grand cycle avant de converger vers P^*.

Dans le cas du système de FHN (1.1.3), considérons le cas d'un neurone isolé ($u = I_{\text{ext}} = 0$). Nous avons représenté à la Figure 1.4 deux exemples de solutions de (1.1.3), en ayant fixé des paramètres θ, a et b tels que le système admette un unique point fixe (v^*, w^*), qui est stable. Comme conditions initiales, nous avons choisi deux perturbations différentes du point fixe. Si la perturbation est de trop faible amplitude (en rouge), alors le système retourne à l'état de repos sans détour. Si l'amplitude de la perturbation est suffisante (en bleu), alors comme on peut l'observer sur la Figure 1.4b, la solution suit une longue trajectoire dans l'espace des phases avant de revenir à l'état de repos. En regardant la dynamique de la variable v à la Figure 1.4a, on voit qu'elle est comparable à un potentiel d'action comme représenté à la Figure 1.3a.

Le régime excitable du système de FHN (1.1.3) sert donc à modéliser une unique décharge d'un neurone en réponse à un stimulus. Nous pouvons aussi reproduire une série de décharges régulières en considérant le régime *oscillatoire* de l'équation. Un système oscillatoire est une équation différentielle qui possède un unique point fixe P^*, qui est instable, et une trajectoire cyclique stable. Si le système n'est pas initialisé en P^*, alors la trajectoire des solutions converge vers l'orbite périodique stable.

Dans (1.1.3), en modifiant le paramètre a, nous pouvons rendre le point fixe (v^*, w^*) instable. Comme observé dans [26, 119], il se produit une bifurcation de Hopf, à savoir qu'une orbite cyclique stable apparaît. À la Figure 1.5, nous avons représenté une solution de (1.1.3) dans un régime oscillatoire en modifiant la valeur de a par rapport à ce que nous avions fixé pour le régime excitable. Le système possède toujours un unique point fixe (v^*, w^*), mais il est instable. La solution n'étant pas initialisée en (v^*, w^*), nous observons sur la Figure 1.5b qu'elle converge vers un cycle limite. À la Figure 1.5a, nous remarquons que les deux composantes v et w présentent des oscillations déphasées. Puisque v a la forme d'une série de pics, cette configuration sert à modéliser une série d'impulsions nerveuses.

Dans les modèles (1.1.1), (1.1.2) et (1.1.3), les interactions avec les autres neurones sont exprimées à travers le courant u. Pour simplifier, disons que le réseau ne reçoit aucun autre stimulus extérieur, soit $I_{\text{ext}} = 0$. Dans le cas du système de FHN (1.1.3), associons à chaque neurone un numéro $i \in \{1, ..., n\}$, et notons (v_i, w_i) son binôme potentiel-adaptation, et u_i le courant synaptique qu'il reçoit. On peut coupler l'activité de $n \in \mathbb{N}$ neurones pour étudier un

(a) Graphe de la première composante.

(b) Trajectoire dans l'espace des phases.
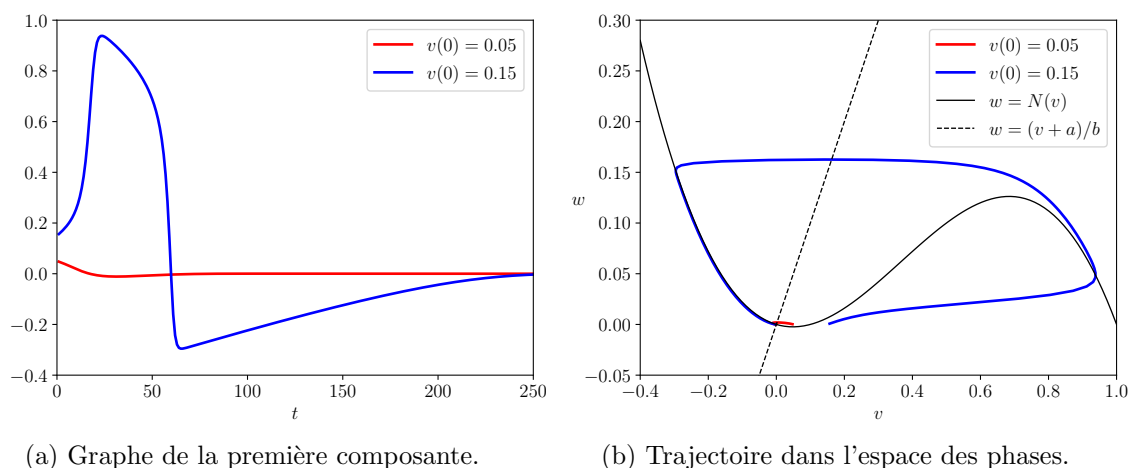
Figure 1.4: **Régime excitable.** Représentations de la solution $t \mapsto (v(t), w(t))$ de l'équation de FHN (1.1.3) pour deux conditions initiales différentes : $v(0) = 0.15$ (rouge), $v(0) = 0.05$ (en bleu), et $w(0) = 0$ dans les deux cas. Les paramètres sont fixés à $\tau = 0.005$, $a = 0$, $b = 1$ et $\theta = 0.1$.

réseau d'un nombre fini de neurones, en écrivant pour tout $i \in \{1, ..., n\}$:

$$u_i = \sum_{j=1}^{n} I_{j \to i}, \tag{1.1.5}$$

où $I_{j \to i}$ est le courant reçu par i venant de j. En utilisant la loi d'Ohm, et en notant $g_{j \to i}$ la conductance de la liaison du neurone j (présynaptique) au i (postsynaptique), nous pouvons déterminer que pour tout $i, j \in \{1, ..., n\}$,

$$I_{j \to i} = g_{j \to i} \, (v_j - v_i). \tag{1.1.6}$$

L'intérêt final d'un modèle de réseau de neurones est de modéliser et reproduire la dynamique collective de portions entières du cortex. Étant donné le très grand nombre de neurones (de l'ordre de 10^{11} neurones dans le cerveau humain, reliés par environ 10^{15} synapses), il est évident que nous ne pouvons pas modéliser précisément l'évolution de chaque neurone. Nous devons changer l'échelle d'observation du réseau, ce qui revient à changer de modèle. Dans la suite de ces travaux, nous distinguerons trois types de modèles.

- Un modèle *microscopique* (échelle 10^{-6}m) étudie l'évolution des quantités électriques associées à chaque neurone en particulier dans un réseau de neurones de taille finie.

- Un modèle *mésoscopique* (échelle 10^{-4}m) est obtenu en faisant tendre le nombre de neurones $n \in \mathbb{N}$ vers l'infini dans un modèle microscopique dont les interactions ont été renormalisées par $1/n$. Ce procédé est appelé *limite champ moyen*. À la limite, la dynamique de chaque neurone a tendance à se décorréler des autres, et l'activité électrique de chaque neurone finit par obéir à la même équation, indépendante du neurone considéré. C'est ce qu'on appelle la *propagation du chaos*.

- Un modèle *macroscopique* (échelle 10^{-2}m) donne l'évolution des quantités électriques moyennes dans un réseau de taille infinie à chaque instant et à chaque position. Dans notre travail, nous ne verrons que des modèles macroscopiques spatialement étendus.

14

(a) Graphes en fonction du temps.

(b) Trajectoire dans l'espace des phases.
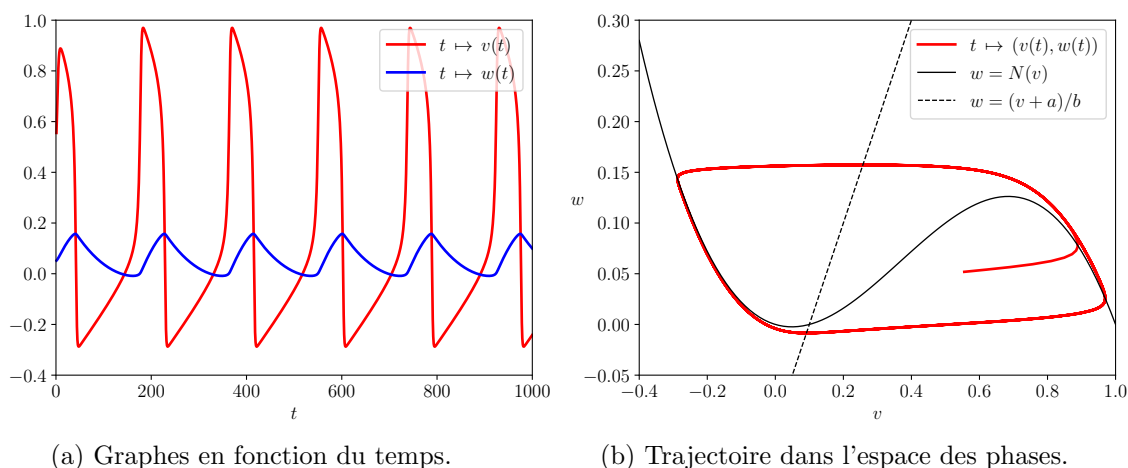
Figure 1.5: **Régime oscillatoire.** Représentations de la solution $t \mapsto (v(t), w(t))$ de l'équation de FHN (1.1.3) en régime oscillatoire. Les paramètres sont fixés à $\tau = 0.01$, $a = -0.1$, $b = 1$ et $\theta = 0.1$. Les conditions initiales sont $(v(0), w(0)) = (0.5, 0)$.

Changer d'échelle d'espace nous permet de décrire des réseaux de neurones plus grands, mais nous perdons des informations sur le système au cours du processus.

Avant tout, nous devons faire notre choix en termes de type de couplage entre les neurones. Ensuite, notre première étape sera de faire tendre le nombre de neurones n vers l'infini, c'est-à-dire d'effectuer une limite champ moyen pour trouver un modèle intermédiaire à l'échelle mésoscopique. À partir de celui-ci, nous pourrons obtenir un modèle macroscopique.

Plusieurs autres travaux ont déjà étudié la limite champ moyen du modèle de FHN. Nous mentionnons tout d'abord l'article de Baladron *et al.* [5], complété plus tard par Bossy *et al.* [15]. Ils étudient un réseau de n neurones de type HH (ou FHN) bruités aléatoirement, interagissant entre eux à travers deux types de synapses: *électriques* et *chimiques*. Dans le cas de synapses chimiques, en reprenant la notation de la conductance comme dans (1.1.6), on obtient que pour tout $i, j \in \{1, .., n\}$, la conductance $g_{j \to i}$ dépend du temps, et pour tout $t > 0$,

$$g_{j \to i}(t) = \overline{g}_{j \to i}(t)\, y_j(t),$$

où $\overline{g}_{j \to i}$ est la conductance maximale, et $y_j(t)$ est la proportion de chaînes de neurotransmetteurs chimiques ouvertes. Ce taux y_j vérifie une équation différentielle similaire aux deuxième, troisième et quatrième équations dans le modèle HH (1.1.2). Quant à la conductance maximale, elle varie aléatoirement en fonction du temps. Ensuite, dans le cas de synapses électriques, le transfert de signal électrique se fait indépendamment des chaînes de neurotransmetteurs chimiques, ce qui donne directement $g_{j \to i}(t) = \overline{g}_{j \to i}(t)$. Les auteurs ont ensuite étudié la limite champ moyen du système d'équations, à savoir la limite en loi de chaque couple (v_i, w_i) pour i allant de 1 à n quand n tend vers l'infini. Ces résultats ont ensuite été repris par Mischler *et al.* dans [106] pour un réseau de neurones de type FHN, reliés par des synapses électriques avec une conductance homogène et constante G. Ils se sont notamment concentrés sur l'équation à dérivées partielles vérifiée par la densité de probabilité $f(t, v, w)$ de trouver des neurones à l'instant $t > 0$ dotés d'un couple potentiel-adaptation égal à $(v, w) \in \mathbb{R}^2$, qui s'écrit

$$\partial_t f + \partial_v \left(f \left[N(v) - w + G \int_{\mathbb{R}^2} (v' - v)\, f(t, v', w')\, \mathrm{d}v'\, \mathrm{d}w' \right] \right) + \partial_w \left(f\, \tau\, (v + \alpha - \gamma\, w) \right) = \partial_{vv}^2 f.$$

$$(1.1.7)$$

Dans cette dernière équation, le terme intégral traduit les interactions entre neurones. En effet, il correspond à la somme des contributions de tous les neurones à l'évolution du potentiel d'un neurone dont le potentiel de membrane est v, avec une conductance uniforme. Les autres termes de réaction locaux représentent l'excitabilité de chaque neurone. Le terme $\partial_{vv}^2 f$ est lui une conséquence du bruit aléatoire dans la première équation du modèle microscopique (1.1.3). Ils ont démontré l'existence et l'unicité de solution, ainsi que la stabilité dans le régime de faible connectivité. Une telle équation et appelée *équation de champ moyen*.

Toutefois, comme il est souligné dans des travaux comme [114, 131], pour que notre modèle soit réaliste biologiquement, il est important que les interconnections entre neurones soient hétérogènes. Nous devons trouver un moyen de les pondérer. D'après des observations biologiques (voir [104] par exemple), l'organisation spatiale de la zone du cerveau a une influence sur les interactions entre neurones. À l'instar d'autres modèles de réseau de neurones spatialement organisés (voir [3, 26]), dans [103] E. Luçon et W. Stannat ont étudié la limite champ moyen d'un réseau de neurones de type FHN, bruités aléatoirement, en pondérant les conductances par la distance séparant chaque neurone. Plus précisément, ils considèrent n neurones uniformément répartis dans l'intervalle $[-1/2, 1/2]$. La conductance du neurone j au neurone i, respectivement localisés aux positions $\mathbf{x}_j$ et $\mathbf{x}_i \in \mathbb{R}^d$ avec $d \in \{1, 2, 3\}$, est donnée par $\Psi(\|\mathbf{x}_i - \mathbf{x}_j\|)$, où Ψ est une fonction à support compact. Ils ont également étudié le cas où chaque neurone ne communique qu'avec ses $p \in \mathbb{N}$ plus proches voisins, en suivant l'idée de [110]. Ensuite, dans [102], E. Luçon a étendu cette analyse aux réseaux dans lesquels les positions des neurones sont aléatoirement distribuées. Il a de même prouvé la convergence du potentiel moyen dans le réseau vers la solution d'une équation de réaction-diffusion, donnant ici une description macroscopique d'un tel réseau.

Dans notre travail, nous étudierons seulement des réseaux de neurones spatialement organisés. Ce choix de modélisation est aussi motivé par le fait que même un couplage spatial relativement simple peut produire des dynamiques complexes dans les réseaux neuronaux. Par exemple, comme nous le verrons plus tard, le potentiel de membrane peut se propager sous forme de pulsations à travers l'espace, ou même former des ondes progressives bidimensionnelles en forme de spirale tournante.

Biologiquement parlant, le cerveau n'est pas homogène : il est divisé en de nombreuses zones dont les répartitions spatiales des neurones ne sont pas identiques. Un exemple est le cas du cortex visuel des primates, dans lequel les neurones sont organisés en colonnes presque homogènes, appelées *colonnes corticales*. Même si ces colonnes communiquent entre elles, deux cellules d'une même colonne, donc proches, vont avoir plus d'interactions que deux cellules sur deux colonnes différentes. À titre d'illustration, la Figure 1.6 montre la reconstitution en 2D d'une section du cortex visuel d'un singe. Les liens entre neurones sont mis en évidence grâce à l'injection d'un traceur. On observe une section des différentes colonnes corticales mises en évidence par cette expérience.

Considérons n neurones de type FHN, sans ajouter de bruit aléatoire. Associons à chaque neurone $i \in \{1, ..., n\}$ une position $\mathbf{x}_i \in \mathbb{R}^d$ où $d \in \{1, 2, 3\}$ est la dimension en espace du modèle. Ces positions sont des paramètres constants. Ici, nous ne prenons en compte que des synapses de type électrique, et la conductance est donnée par un *noyau de connectivité* $\Phi : \mathbb{R}^{2d} \to \mathbb{R}$, qui va modéliser l'effet des positions respectives de deux neurones sur leurs interactions. Ainsi, le
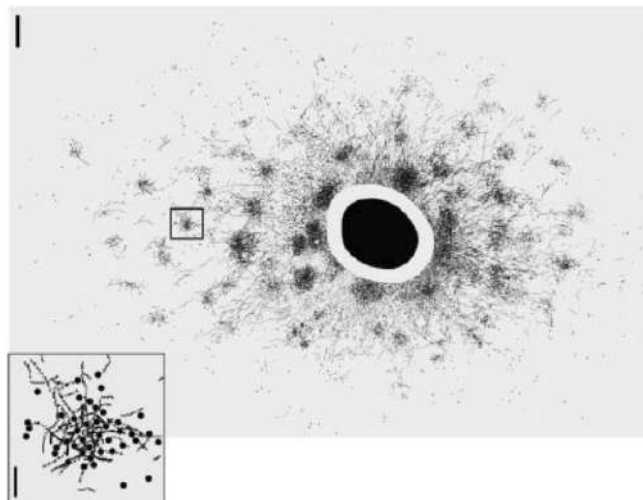
Figure 1.6: Reconstruction d'une vue en 2D d'un réseau de neurones dans une section du cortex visuel d'un singe après l'injection d'un traceur (source [104]) (barres d'échelle: 500 μm et 100 μm).

système (1.1.3) devient :

$$\begin{cases} \dfrac{\mathrm{d}\mathbf{x}_i}{\mathrm{d}t} &=& 0, \\[2mm] \dfrac{\mathrm{d}v_i}{\mathrm{d}t} &=& N(v_i) - w_i - \dfrac{1}{n}\sum_{j=1}^{n}\Phi(\mathbf{x}_i, \mathbf{x}_j)\,(v_i - v_j), \\[2mm] \dfrac{\mathrm{d}w_i}{\mathrm{d}t} &=& \tau\,(v_i + a - b\,w_i). \end{cases} \qquad (1.1.8)$$

D'un point de vue biologique, on considère qu'un neurone ne va interagir qu'avec ses plus proches voisins. Pour tout neurone i, un choix raisonnable pour $\Phi(\mathbf{x}_i, \cdot)$ est la fonction indicatrice d'un voisinage borné de 0, ou bien une fonction gaussienne. De plus, nous avons ajouté un facteur $1/n$ afin de renormaliser la contribution de chaque neurone.

La spécificité du modèle (1.1.8) par rapport à la littérature, est que les interactions ne sont pondérées que par les positions des neurones, et qu'il n'y a pas de bruit aléatoire, ce qui va nous amener à n'utiliser que des méthodes déterministes. Ce modèle microscopique sera notre point de départ pour tous les travaux effectués dans cette thèse. Notre objectif est donc d'obtenir une description macroscopique de (1.1.8) quand le nombre de neurones tend vers l'infini.

1.1.2 Autres modèles de réseau de neurones

La caractéristique commune des modèles que nous avons vus jusqu'ici est le rôle de la conductance dans les interactions synaptiques, qu'elles soient de type chimique ou électrique. Ces modèles donnent accès à un meilleur aperçu des variations des courants synaptiques et des dynamiques spatio-temporelles du réseau. Tous les choix de modélisation que nous avons fait ont été motivés par deux objectifs contradictoires : avoir un modèle réaliste et en même temps simple à analyser mathématiquement. En particulier, le fait de n'avoir considéré que des synapses de type électrique dans (1.1.8) est critiquable du point de vue du réalisme biologique, mais la pondération des conductances par les positions des neurones nous permet de considérer un réseau de neurones à la fois hétérogène et simple à analyser.

Cette difficulté à trouver un juste équilibre entre réalisme et difficulté mathématique a motivé une approche alternative. Dans beaucoup d'autres modèles de réseau de neurones, la forme

précise du potentiel d'action n'a pas d'importance : on ne considère que des neurones *impulsionnels*, c'est-à-dire que le potentiel de chaque cellule évolue en fonction des stimuli extérieurs jusqu'à atteindre un seuil V_T. À ce moment-là, le neurone émet un pic de potentiel instantané, puis son potentiel est réinitialisé à une certaine valeur $V_R < V_T$. Lorsqu'un neurone décharge, il apporte une contribution instantanée au potentiel électrique de tous les neurones auxquels il est lié (parfois avec un certain retard). Ces contributions peuvent être modulées par un poids synaptique.

Ces modèles ne font plus intervenir la conductance. Ils peuvent être vus comme des approximations des modèles que nous avons vus précédemment, même s'il n'existe à notre connaissance aucun passage rigoureux des modèles de type HH ou FHN à des modèles impulsionnels. Étant donné que la modélisation des interactions a été considérablement simplifiée, ces modèles décrivent de manière plus grossière les variations des courants synaptiques et des potentiels de membrane. En revanche, ils sont plus simples à traiter mathématiquement, et il est possible de considérer des synapses de type chimique et électrique à travers les poids synaptiques pour gagner en réalisme.

La littérature autour de la modélisation de réseaux de neurones impulsionnels étant riche, la liste des modèles que nous présentons ici n'est pas exhaustive. Nous ne donnons que les exemples les plus courants.

1.1.2.1   Équations de fréquence de décharge et champs neuronaux

Ce paragraphe suit les arguments du Chapitre 6 du livre [26].

Équation de fréquence de décharge.   Considérons à présent un réseau fini de neurones, répartis en $P \in \mathbb{N}$ populations de même taille $n \in \mathbb{N}$. Chaque neurone est caractérisé par $p \in \{1, ..., P\}$ l'index de la population à laquelle il appartient, et $i \in \{1, ..., n\}$ son numéro au sein de la population p. Pour modéliser la variation du potentiel $v_{i,p}$ de chaque neurone i dans chaque population p, nous reprenons le modèle général (1.1.1), en notant $u_{i,p}$ le courant postsynaptique reçu. Ici encore, comme dans (1.1.5), nous supposons que $u_{i,p}$ est la somme des courants reçus par chaque neurone dans le réseau. Nous considérons qu'il n'y a aucun autre stimulus extérieur, donc $I_{\text{ext}} = 0$.

Pour chaque neurone i dans chaque population p, on note $\{T_{i,p}^m, \ m \in \mathbb{N}\}$ l'ensemble des instants où le neurone émet un potentiel d'action, avec pour tout $m \in \mathbb{N}^*$,

$$T_{i,p}^m := \inf\left\{t, \ t > T_{i,p}^{m-1} \,\Big|\, v_{i,p}(t) = V_T, \ \frac{\mathrm{d}}{\mathrm{d}t}v_{i,p}(t) > 0\right\}, \quad T_{i,p}^0 = 0. \qquad (1.1.9)$$

De plus, nous supposons que les interactions synaptiques entre deux neurones ne dépendent que des populations auxquelles ils appartiennent.

Pour ce modèle, nous ne considérons plus des synapses électriques, mais chimiques. Seuls les potentiels d'action représentent un pic de potentiel assez important pour activer les chaînes de neurotransmetteurs chimiques, et activer un courant postsynaptique. De plus, contrairement à (1.1.6), nous ne modélisons plus les interactions synaptiques à l'aide de conductances, mais seulement par l'ouverture ou non de chaînes de communication chimique. Le courant postsynaptique provenant d'un neurone présynaptique j de la population q jusqu'à un neurone postsynaptique i de la population p est donné par

$$\frac{1}{n} \sum_{m \in \mathbb{N}} \Phi_{pq}(t - T_{j,q}^m),$$

où $\Phi_{pq}(t)/n$ représente les effets du passage du courant à travers la synapse et l'arbre dendritique. Si nous supposons que les courants synaptiques reçus par un neurone i de la population p

s'additionnent, le courant entrant total qu'il reçoit à l'instant $t \in \mathbb{R}$ est donc:

$$\begin{cases} u_{i,p}(t) = \displaystyle\int_{-\infty}^{t} \sum_{q=1}^{P} \frac{1}{n} \sum_{j=1}^{n} \Phi_{pq}(t-t')\, a_{j,q}(t')\, \mathrm{d}t', \\[2ex] a_{j,q}(t) = \displaystyle\sum_{m \in \mathbb{N}} \delta_0(t - T_{j,q}^m). \end{cases} \qquad (1.1.10)$$

Ici, $a_{j,q}(t)$ représente la chaîne d'influx nerveux émis par le neurone j. Dans la suite, nous notons $u_{i,p} = u_p$ pour tout i et p, puisque le courant $u_{i,p}$ ne dépend pas de i mais seulement de p. Ce système (1.1.10) est le point de départ en tant que modèle microscopique pour de nombreux travaux pour obtenir un modèle macroscopique quand le nombre de neurones tend vers l'infini. Nous nous référons à [31, 61] pour l'étude de la limite champ moyen de (1.1.10) quand le nombre de neurones tend vers l'infini dans le cas de poids synaptiques aléatoires, et à [123] pour le cas particulier où les poids synaptiques sont à la fois stochastiques et dépendent de l'organisation spatiale du réseau.

Nous pouvons réécrire le système précédent pour tout $p \in \{1, ..., P\}$ sans la dépendance en fonction de i, ce qui donne :

$$\begin{cases} u_p(t) = \displaystyle\int_{-\infty}^{t} \sum_{q=1}^{P} \Phi_{pq}(t-t')\, a_q(t')\, \mathrm{d}t', \\[2ex] a_q(t) = \displaystyle\frac{1}{n} \sum_{j,\,\kappa(j)=q} a_j(t). \end{cases} \qquad (1.1.11)$$

Faisons à présent une hypothèse importante : nous supposons que chaque population de neurones est proche de l'état *asynchrone*, c'est-à-dire que les chaînes d'influx nerveux entre deux neurones d'une même population n'ont aucun lien entre eux. Nous pouvons approximer $a_p(t)$ par $F[u_p(t)]$, où F est une fonction croissante (généralement une sigmoïde ou une fonction de Heaviside). Ceci nous mène pour tout $p \in \{1, ..., P\}$ au modèle *microscopique* suivant:

$$u_p(t) = \int_{-\infty}^{t} \sum_{q=1}^{P} \Phi_{pq}(t-t')\, F[u_q(t')]\, \mathrm{d}t'. \qquad (1.1.12)$$

Comme nous avons considéré des synapses de type chimique, le modèle (1.1.12) peut modéliser de manière plus réaliste les interactions entre neurones que dans (1.1.8). En revanche, comme nous l'avons vu, il donne accès à moins d'informations sur les variations des quantités électriques du réseau.

Equation de champ neuronal. Le modèle microscopique de fréquence de décharge (1.1.12) est le point de départ de la construction heuristique d'un type particulier de modèle macroscopique : les équations de champ neuronal. Considérons que le réseau de neurones est organisé spatialement dans $\mathbb{R}$. Supposons que chaque population p est constituée de n neurones uniformément répartis dans le segment $[p\,d, (p+1)d]$, où $d > 0$ est fixé. Définissons $\rho = n/d$ la densité de cellules dans le réseau. Ce genre d'hypothèse correspond par exemple à la modélisation de certaines structures de neurones comme les *colonnes corticales* du cortex visuel du primate. Pour tout p et q, on définit pour tout $t > 0$:

$$\Phi_{pq}(t) = \rho\, d\, \Phi(p\,d, q\,d, t), \quad u_p(t) = u(t, p\,d).$$

L'équation (1.1.12) devient :

$$u(t, p\,d) \,=\, \rho\,d \sum_{q \in \mathbb{Z}} \int_{-\infty}^{t} \Phi(p\,d, q\,d, t - t')\, F\left[u(t', q\,d)\right]\, \mathrm{d}t'.$$

En passant à la limite $d \to 0$ (voir [124, 125] pour une justification rigoureuse), nous obtenons pour tout $x \in \mathbb{R}$ et $t > 0$:

$$u(t, x) \,=\, \int_{\mathbb{R}} \int_{-\infty}^{t} \Phi(x, y, t - t')\, F\left[u(t', y)\right]\, \mathrm{d}t'\, \mathrm{d}y. \tag{1.1.13}$$

D'une part, il est courant de faire l'hypothèse que l'on peut décomposer le noyau d'interaction $\Phi(x, y, t) \,=\, w(x, y)\, \varphi(t)$, où $w(x, y)$ représente le poids synaptique moyen des connexions de la position y à la position x. De plus, on définit $\varphi(t) \,=\, e^{-t/\tau}\, H(t)$, $\tau > 0$ est un temps de relaxation, et H est la fonction de Heaviside. La fonction φ vérifie au sens des distributions:

$$\left(\frac{\mathrm{d}}{\mathrm{d}t} \,+\, \frac{1}{\tau} \right) \varphi(t) \,=\, \delta_0(t).$$

Donc si l'on applique l'opérateur $\mathcal{L}_t \,=\, \partial_t + \tau^{-1}$ à la fonction u, on obtient l'*équation de champ neuronal* standard:

$$\partial_t u(t, x) \,=\, -\frac{u(t, x)}{\tau} \,+\, \int_{\mathbb{R}} w(x, y)\, F\left[u(t, y)\right]\, \mathrm{d}y. \tag{1.1.14}$$

Cette équation est un des premiers modèles heuristiquement déterminé dans les années 1970, notamment par S.I. Amari [3]. Nous nous référons à [25, 44] pour une analyse plus poussée des dynamiques des équations de champ neuronal, y compris dans des domaines spatiaux à deux dimensions. Nous mentionnons aussi les articles de Chevallier *et al.* [40, 42], qui parviennent à trouver un modèle microscopique stochastique spatialement organisé associé à (1.1.14) en étudiant plutôt les temps des décharges en séries des différents neurones dans le réseau.

Supposons à présent que les neurones sont divisés en deux classes: les neurones *excitateurs* (E), et les neurones *inhibiteurs* (I). Pour tout $a, b \in \{E, I\}$, on note u_a le courant synaptique moyen des neurones de classe a. τ_a et F_a sont respectivement la constante de relaxation et la fonction de gain associés à la classe a, w_{ab} le noyau d'interaction qui régule les effets des neurones de classe b sur les neurones de classe a. L'équation (1.1.14) devient pour tout $t > 0$ et $x \in \mathbb{R}$:

$$\begin{cases} \partial_t u_E(t, x) \,=\, -\dfrac{u_E(t, x)}{\tau_E} \,+\, \displaystyle\int_{\mathbb{R}} w_{EE}(x, y)\, F_E\left[u_E(t, y)\right]\, \mathrm{d}\mathbf{y} \,+\, \int_{\mathbb{R}} w_{EI}(x, y)\, F_I\left[u_I(t, y)\right]\, \mathrm{d}\mathbf{y}, \\[4mm] \partial_t u_I(t, x) \,=\, -\dfrac{u_I(t, x)}{\tau_I} \,+\, \displaystyle\int_{\mathbb{R}} w_{IE}(x, y)\, F_E\left[u_E(t, y)\right]\, \mathrm{d}\mathbf{y} \,+\, \int_{\mathbb{R}} w_{II}(x, y)\, F_I\left[u_I(t, y)\right]\, \mathrm{d}\mathbf{y}, \end{cases} \tag{1.1.15}$$

où $w_{EE}, w_{IE} \geq 0$ et $w_{EI}, w_{II} \leq 0$. Ce dernier système est une version spatialement organisée des équations de Wilson et Cowan [132, 133], utilisées pour étudier les dynamiques macroscopiques du cortex.

Les modèles (1.1.14) et (1.1.15) sont les descriptions macroscopiques de grands réseaux de neurones les plus connues. Ils ont fait l'objet d'une attention toute particulière dans la littérature. Des phénomènes biologiques observés dans le cerveau ont pu être reproduits grâce à ces modèles, comme les oscillations des électroencéphalogrammes [109], les mécanismes amenant aux hallucinations visuelles [27, 58], à la mémoire à court terme [100, 101] ou à la perception du mouvement [72]. Cependant, à notre connaissance, il n'existe à ce jour toujours pas de lien mathématique rigoureux entre un modèle microscopique de réseau de neurones, et un quelconque modèle macroscopique spatialement organisé comme (1.1.14) ou (1.1.15). C'est le plus grand inconvénient de ces équations par rapport aux modèles que nous étudierons dans cette thèse.

1.1.2.2 Modèle "Intègre et tire"

Reprenons le modèle microscopique standard initial (1.1.1) pour modéliser l'évolution du potentiel v d'un neurone en fonction du courant synaptique reçu u, du courant de membrane $-I_{\text{chim}}$ et d'un courant extérieur I_{ext}. Le modèle de neurone *Intègre et tire* (IT) est, comme précédemment, un modèle de neurone impulsionnel, c'est-à-dire qu'il émet un pic de potentiel lorsque v atteint un seuil V_T, et est alors instantanément réinitialisé à $V_R < V_T$. On considère que le courant $-I_{\text{chim}}$ tend à ramener le potentiel du neurone vers un état de repos V_0. En général, notamment dans le cas du modèle Intègre et tire à fuite (ITF), on choisit:

$$I_{\text{chim}}(t) = -\frac{v(t) - V_0}{R},$$

où R est la résistance électrique de la membrane du neurone. Il s'agit ici d'une approximation des dynamiques internes à chaque neurone plus simple que pour les modèles de HH ou FHN, mais moins précise. Cela permet de concentrer toute la difficulté mathématique dans les interactions entre neurones.

Afin de simplifier les notations, considérons que la capacité C et la résistance R sont fixées à 1, $V_T = 1$, et $V_0 = V_R = 0$. Nous nous intéressons à un réseau de n neurones, chaque neurone étant indexé comme précédemment par $i \in \{1, ..., n\}$. De plus, nous supposons que pour tout i, $I_{\text{ext},i}$ est constant fixé à I_0. Nous définissons $(T_i^m)_{m \in \mathbb{N}}$ les temps d'émissions de potentiels d'action du neurone i comme dans (1.1.9), et $u_i(t)$ le courant postsynaptique reçu au temps $t > 0$. Supposons que les liaisons synaptiques sont de type électrique et chimique à la fois. Alors $u_i(t)$ se décompose en une contribution chimique $u_{\text{chim},i}$ et une contribution électrique $u_{\text{elec},i}$, et s'écrit:

$$\begin{cases} u_i(t) = u_{\text{chim},i}(t) + u_{\text{elec},i}(t), \\[2mm] u_{\text{chim},i}(t) = \dfrac{1}{n}\sum_{j=1}^{n}\sum_{m \in \mathbb{N}} \alpha_{ij}\, \delta_0(t - T_j^m), \\[2mm] u_{\text{elec},i}(t) = \dfrac{1}{n}\sum_{j \neq i} \beta_{ij}\, v_j(t), \end{cases} \qquad (1.1.16)$$

où α_{ij}, β_{ij} sont les poids synaptiques structurant l'influence du neurone j sur le neurone i. En conséquence, pour tout $i \in \{1, ..., n\}$, et pour tout $T_i^m < t < T_i^{m+1}$ avec $m \in \mathbb{N}$:

$$\frac{\mathrm{d}v_i(t)}{\mathrm{d}t} = -v_i(t) + \frac{1}{n}\sum_{j=1}^{n}\sum_{m \in \mathbb{N}} \alpha_{ij}\, \delta_0(t - T_j^m) + \frac{1}{n}\sum_{j \neq i} \beta_{ij}\, v_j(t) + \sigma\, \eta_i(t). \qquad (1.1.17)$$

où $\sigma \geq 0$, et $\eta_i(t)$ est un terme de bruit stochastique.

L'équation (1.1.17) est le modèle microscopique qui sert de point de départ de nombreux travaux pour déterminer des caractérisations mésoscopiques. Par exemple, des travaux ont étudié la limite champ moyen quand n tend vers l'infini d'un modèle ITF (1.1.17) (voir [28] pour des poids synaptiques constants ou [117] pour des poids hétérogènes stochastiques). Ils ont prouvé la propagation du chaos de l'équation (1.1.17), c'est-à-dire que les neurones vont se décorréler quand n tend vers l'infini. En particulier, pour tout i, le potentiel $v_i(t)$ va converger vers une variable aléatoire X_t définie par:

$$X_t = X_0 - \int_0^t X_s\, \mathrm{d}s + \alpha\, e(t) + \sigma\, W_t - M_t, \qquad (1.1.18)$$

où $X_0 < 1$ presque sûrement, α dépend des poids synaptiques (α_{ij}), $(W_t)_{t \geq 0}$ est un mouvement Brownien standard. De plus on définit pour tout $t \geq 0$:

$$\begin{cases} e(t) = \mathbb{E}[M_t], \quad M_t = \sum_{k \geq 1} \chi_{[0,t]}(T_k), \\[2mm] T_k = \inf\{t > T_{k-1} \,|\, X_t = 1\} \text{ pour tout } k \geq 1, \quad T_0 = 0, \end{cases} \tag{1.1.19}$$

où l'on note χ_A la fonction caractéristique de l'ensemble A. La loi de cette variable aléatoire peut être décrite par une équation de Fokker-Planck. En effet, si l'on note $p(t,v)$ la densité de probabilité de trouver des neurones dans le réseau au potentiel $v \in (-\infty, 1)$ à l'instant $t > 0$, d'après [28, 53, 117], celle-ci satisfait l'équation de champ moyen:

$$\begin{cases} \partial_t p(t,v) - \sigma\, \partial_{vv}^2 p(t,v) + \partial_v\left[(-v + \alpha\, e'(t))\, p(t,v)\right] = \delta_0(v)\, e'(t), \\[2mm] p(t,1) = p(t,-\infty) = 0, \\[2mm] e'(t) = \frac{\mathrm{d}}{\mathrm{d}t} \mathbb{E}[M_t] = -\frac{1}{2}\, \partial_v p(t,1). \end{cases} \tag{1.1.20}$$

L'existence d'une solution globale en temps à l'équation (1.1.20) a été établie dans [53] par Delarue *et al.* Toutefois, selon la condition initiale et les paramètres choisis dans ce modèle, il est possible qu'apparaisse un phénomène de *blow-up*, c'est-à-dire un temps $t > 0$ auquel tous les neurones se synchronisent et déchargent en même temps (cela se traduit par $e(t) = +\infty$). Pour une analyse de ces *blow-up*, et de la dynamique des solutions à l'équation (1.1.20), nous nous référons à [32, 37]. Dans [54], Delarue *et al.* ont étudié précisément le cas singulier de décharges simultanées dans le réseau. Ils ont démontré l'existence de solutions faibles à l'équation (1.1.20), ainsi que la convergence et la propagation du chaos du système microscopique (1.1.17) vers (1.1.20) quand le nombre de neurones n tend vers l'infini.

Notons que récemment, dans [116], B. Perthame et D. Salort ont réussi à obtenir rigoureusement une équation semblable à (1.1.20) par la réduction d'un modèle cinétique décrivant un réseau de neurones basé sur des interactions avec conductance. Ceci établit un lien mathématique entre les modèles à conductance et le modèle IT.

D'un côté, le modèle mésoscopique (1.1.20) est suffisamment simplifié pour être traitable mathématiquement. De plus, en choisissant des poids synaptiques hétérogènes et stochastiques, il permet de modéliser des liaisons entre neurones plus réalistes que dans (1.1.8). Toutefois, il reste issu d'approximations importantes sur la dynamique interne de chaque neurone, en plus des limites propres aux neurones impulsionnels.

1.1.2.3 Modèle structuré par l'âge

Une autre approche pour la modélisation de réseaux de neurones impulsionnels est de s'intéresser non plus au potentiel, mais à la probabilité qu'un neurone émette une décharge, en fonction des courants extérieurs qu'il reçoit, et en fonction du temps écoulé depuis la dernière décharge.

Considérons un modèle IT déterministe légèrement différent de (1.1.17), qui s'écrit pour tout i et pour tout $T_i^m < t < T_i^{m+1}$ avec $m \in \mathbb{N}$:

$$\begin{cases} v_i(t) = V_0 + (V_R - V_0)e^{-(t-T_i^m)} + \int_{T_i^m}^t h(t-s)\, a_i(s)\, \mathrm{d}s, \\[2mm] a_i(t) = \frac{1}{n} \sum_{j=1}^n \sum_{m \in \mathbb{N}} \delta_0(t - T_j^m), \end{cases} \tag{1.1.21}$$

où h est une fonction positive représentant le potentiel excitateur postsynaptique. Ici, les interactions ont été traitées différemment : les poids synaptiques sont homogènes sur le réseau, mais dépendent du temps. Cela permet de modéliser le fait que plus le temps écoulé depuis la dernière décharge est long, plus un neurone recevant des stimuli extérieurs est susceptible d'émettre un potentiel d'action. Ce choix de modélisation n'est pas le plus réaliste, le réseau étant considéré comme homogène, mais il permet d'étudier l'influence du temps sur la dynamique du réseau. Le plus réaliste aurait été de concilier les deux approches, en considérant des poids synaptiques hétérogènes dépendant du temps, mais le modèle aurait alors été plus dur à analyser.

Ainsi, la limite champ moyen présentée au dernier paragraphe n'est plus valable. Il faut trouver une autre manière de caractériser l'activité neuronale à l'échelle mésoscopique. Dans [41], Chevallier *et al.* ont démontré que l'on peut considérer l'*âge* d'un neurone, c'est à dire le processus aléatoire qui à un instant t associe le temps écoulé depuis la dernière décharge du neurone, comme un processus de Hawkes. Dans [40], J. Chevallier avait déjà étudié la limite champ moyen de processus stochastiques de Hawkes, ce qui permet d'étudier le comportement du système (1.1.21) quand n tend vers l'infini. Cette limite peut être décrite par une équation qui donne l'évolution de la densité de probabilité $p(t,s)$ de trouver à l'instant t des neurones dans le réseau ayant émis leur dernière décharge à l'instant $t - s$, et s'écrit pour $0 \leq s \leq t$:

$$\begin{cases} \partial_t p(t,s) \,+\, \partial_s p(t,s) \,+\, f(s, X(t))\, p(t,s) \,=\, 0, \\[2mm] N(t) \,:=\, p(t, s=0) \,=\, \int_0^\infty f(s', X(t))\, p(t, s')\, \mathrm{d}s', \\[2mm] X(t) \,=\, J \int_0^t h(u)\, N(t-u)\, \mathrm{d}u, \end{cases} \qquad (1.1.22)$$

où $J \geq 0$. Ce genre de modèle est qualifié de structuré par l'âge, ou *modèle de temps écoulé*. Plus clairement, $N(t)$ représente le nombre de neurones déchargeant à l'instant t, et $f(s, X(t))$ est le taux de neurones dont la dernière décharge date de l'instant $t - s$ qui émettent un pic à t. Pour une étude des différentes dynamiques associées à ce modèle, nous nous référons à [111–113], et à [93] pour l'étude de ce modèle dans le cas d'un réseau inhomogène.

Si ce modèle mésoscopique est capable de montrer l'influence de poids synaptiques dépendants du temps, il ne donne pas accès aux mêmes informations sur le réseau que les modèles vus précédemment. En particulier, il ne donne pas d'information sur le potentiel de membrane moyen dans le réseau, donc il ne permet pas d'obtenir une description macroscopique du système au sens où nous l'entendons.

1.1.3 Plan de la thèse

Les objectifs principaux de cette thèse sont d'une part de déterminer rigoureusement des modèles macroscopiques pour l'équation de FHN spatialement organisée (1.1.8) quand le nombre de neurones n tend vers l'infini, et d'autre part de décrire précisément les hypothèses nécessaires sur les conditions initiales et sur le noyau d'interaction, afin de comprendre dans quel cadre ces modèles macroscopiques sont valables. Pour cela, nous allons procéder en plusieurs étapes successives, qui posent toutes des problèmes intéressants, tant mathématiquement qu'en termes de modélisation biologique. Tout d'abord, nous étudierons la *limite champ moyen* du système (1.1.8) quand le nombre de neurones tend vers l'infini (Chapitre 2). Cette équation de transport nous donnera une description *mésoscopique* du système, dans le sens où même si elle nous donne des informations sur un réseau de neurones de taille infinie, elle ne nous permet pas directement de trouver un système d'équations vérifié par les valeurs moyennes du réseau. Cette équation nous

servira d'étape intermédiaire pour trouver un modèle macroscopique après redimensionnement du couplage entre neurones.

Par la suite, nous étudierons deux *limites macroscopiques* différentes, correspondant à deux manières de redimensionner les interactions dans l'équation de champ moyen (Chapitres 3 et 4). Nous pourrons déterminer deux systèmes de réaction-diffusion étudiant les variations des valeurs moyennes du réseau de neurones, l'un avec un terme de diffusion spatiale non locale, l'autre locale.

Enfin, nous étudierons l'une de ces limites macroscopiques en termes d'analyse numérique (Chapitre 5). En clair, nous allons proposer une discrétisation spatio-temporelle de l'équation de champ moyen intermédiaire qui fournit une approximation consistante du système de réaction-diffusion local en passant à la limite.

1.2 De l'échelle microscopique mésoscopique (Chapitre 2)

1.2.1 Limite champ moyen

Comme les solutions de (1.1.8) sont des vecteurs dans $\mathbb{R}^{2n}$, nous devons trouver un cadre fonctionnel adapté pour étudier la limite quand le nombre de neurones n tend vers l'infini. La méthode classique consiste à étudier l'évolution en temps de la probabilité de trouver des neurones à une certaine position $\mathbf{x} \in \mathbb{R}^d$ et dotés de la paire potentiel-adaptation $(v, w) \in \mathbb{R}^2$ dans le réseau. Pour ce faire, nous travaillerons dans un sous-espace des mesures de probabilité sur $\mathbb{R}^{d+2}$, qui sera indépendant de n. Nous sommes donc amenés à définir la notion de *mesure empirique*.

Definition 1.2.1. *On associe à chaque n-tuplets $\mathbf{X}_n = (\mathbf{x}_i)_{1 \le i \le n} \in (\mathbb{R}^d)^n$, $V_n(t) = (v_i(t))_{1 \le i \le n}$ et $W_n(t) = (w_i(t))_{1 \le i \le n}$ pour $t \ge 0$, sa mesure empirique:*

$$f_n(t, \mathrm{d}\mathbf{x}, \mathrm{d}v, \mathrm{d}w) := \frac{1}{n} \sum_{j=1}^{n} \delta_{(\mathbf{x}_j, v_j(t), w_j(t))}(\mathrm{d}\mathbf{x}, \mathrm{d}v, \mathrm{d}w). \tag{1.2.1}$$

Notons que les mesures empiriques sont des mesures de probabilités sur $\mathbb{R}^{d+2}$. Nous pouvons remarquer que pour tout $n \in \mathbb{N}$, si les n-tuplets $\mathbf{X}_n$, $V_n(t)$ et $W_n(t)$ sont des solutions du système de FHN (1.1.8) pour $t > 0$, alors la mesure empirique associée f_n vérifie formellement l'équation de transport suivante pour $(\mathbf{x}, v, w) \in \mathbb{R}^{d+2}$:

$$\begin{cases} \partial_t f + \partial_v \left(f \left[N(v) - w - \mathcal{K}_\Phi[f] \right] \right) + \partial_w \left(f \, A(v, w) \right) = 0, \\[2mm] \mathcal{K}_\Phi[f](t, \mathbf{x}, v) := \int_{\mathbb{R}^{d+2}} \Phi(\mathbf{x}, \mathbf{x}')(v - v') f(t, \mathrm{d}\mathbf{x}', \mathrm{d}v', \mathrm{d}w'), \\[2mm] A(v, w) := \tau \left(v + a - b \, w \right). \end{cases} \tag{1.2.2}$$

Supposons formellement que f_n converge vers une certaine mesure de probabilité f dans un certain sens quand n tend vers l'infini. D'un point de vue de modélisation, $f(t, \mathrm{d}\mathbf{x}, \mathrm{d}v, \mathrm{d}w)$ est la mesure de probabilité à l'instant $t \ge 0$ de trouver des neurones dans le volume élémentaire $\mathrm{d}\mathbf{x}$, dotés d'un potentiel et d'une variable d'adaptation dans des volumes élémentaires respectivement de taille $\mathrm{d}v$ et $\mathrm{d}w$. Nous doterons par la suite l'équation (1.2.2) de la condition initiale

$$f(0, \cdot) = f_0. \tag{1.2.3}$$

D'un point de vue mathématique, f vérifie aussi formellement l'équation de transport (1.2.2). Détaillons un peu les différents termes de l'équation de champ moyen (1.2.2). Tout d'abord,

le terme $\partial_v \left(f \left[N(v) - w \right] \right) + \partial_w \left(f \, A(v, w) \right)$ représente la réaction due à l'excitabilité de chaque neurone. Ensuite, le terme nonlocal $-\partial_v \left(f \, \mathcal{K}_\Phi[f] \right)$ représente les interactions à travers tout le réseau. En effet, pour tout $n \in \mathbb{N}$, le terme d'interaction dans le système (1.1.8) vérifie:

$$\frac{1}{n} \sum_{j=1}^{n} \Phi(\mathbf{x}, \mathbf{x}_j) \, (v - v_j) = \mathcal{K}_\Phi[f_n] \to \mathcal{K}_\Phi[f],$$

quand n tend vers l'infini.

La limite champ moyen de systèmes à particules vers des équations de Vlasov a déjà été largement étudiée. Les techniques les plus classiques sont par exemple expliquées dans [57], dans lequel R. Dobrushin traite le cas où les interactions entre particules sont pondérées par une fonction globalement Lipschitzienne. Pour cela, il démontre un résultat de stabilité des solutions de l'équation de Vlasov limite pour une topologie de mesure de probabilité adéquate: la métrique de Wasserstein.

Definition 1.2.2 (Distance de Wasserstein d'ordre $k \in \mathbb{N}^*$)**.** *Soient μ et ν deux mesures de probabilité de $\mathbb{R}^{d+2}$ avec des moments d'ordre k finis. La distance de Wasserstein d'ordre k entre μ et ν est définie par*

$$d_k(\mu, \nu) = \left(\inf_{\pi \in \Lambda(\mu, \nu)} \iint_{\mathbb{R}^{d+2} \times \mathbb{R}^{d+2}} \| (\mathbf{x} - \mathbf{x}', v - v', w - w') \|^k \, \pi(\mathrm{d}\mathbf{x}, \mathrm{d}v, \mathrm{d}w, \mathrm{d}\mathbf{x}', \mathrm{d}v', \mathrm{d}w') \right)^{\frac{1}{k}},$$

où $\| (\mathbf{x}, v, w) \|$ dénote la norme euclidienne standard du vecteur $(\mathbf{x}, v, w)$ dans $\mathbb{R}^{d+2}$ pour tout $\mathbf{x} \in \mathbb{R}^d$ et $(v, w) \in \mathbb{R}^2$, et $\Lambda(\mu, \nu)$ est l'ensemble des couplages de μ et ν, c'est-à-dire pour tout $\pi \in \Lambda(\mu, \nu)$, pour toute fonction $\phi \in \mathscr{C}(\mathbb{R}^{d+2})$ telle que $\phi(\mathbf{z}) = \mathcal{O}(\|\mathbf{z}\|^2)$ quand $\|\mathbf{z}\|$ tend vers l'infini,

$$\begin{cases} \iint \phi(\mathbf{x}, v, w) \, \pi(\mathrm{d}\mathbf{x}, \mathrm{d}v, \mathrm{d}w, \mathrm{d}\mathbf{x}', \mathrm{d}v', \mathrm{d}w') = \int \phi(\mathbf{x}, v, w) \, \mu(\mathrm{d}\mathbf{x}, \mathrm{d}v, \mathrm{d}w), \\[2mm] \iint \phi(\mathbf{x}', v', w') \, \pi(\mathrm{d}\mathbf{x}, \mathrm{d}v, \mathrm{d}w, \mathrm{d}\mathbf{x}', \mathrm{d}v', \mathrm{d}w') = \int \phi(\mathbf{x}', v', w') \, \nu(\mathrm{d}\mathbf{x}', \mathrm{d}v', \mathrm{d}w'). \end{cases}$$

On appelle *estimation de Dobrushin* un tel résultat. Cette démonstration a ensuite été étendue à d'autres types de noyau d'interaction, par exemple aux fonctions singulières (voir [81]).

Dans notre cas, comme le noyau d'interaction $(\mathbf{x}, \mathbf{y}, v) \mapsto \Phi(\mathbf{x}, \mathbf{y}) \, v$ est localement lipschitzien, mais pas globalement à cause du facteur v, nous ne pouvons pas utiliser les mêmes stratégies que dans [57, 75]. Nous utiliserons donc les méthodes présentées dans [13], où Bolley *et al.* étendent les résultats de Dobrushin dans le cas d'un noyau d'interaction seulement localement lipschitzien, en utilisant des estimées *a priori* de moments exponentiels des solutions de l'equation (1.2.2)-(1.2.3).

Par souci de concision, nous ne détaillerons pas dans cette introduction ce que nous entendons par solution de l'équation de transport (1.2.2) (voir le Chapitre 2 pour les détails). Avant d'énoncer notre résultat, nous devons préciser les hypothèses sur les conditions initiales. Dans cette sous-section, nous supposons que la donnée initiale f_0 de l'équation (1.2.2) est une mesure de probabilité sur $\mathbb{R}^{d+2}$ vérifiant pour une certaine constante $\alpha_0 > 0$:

$$\int_{\mathbb{R}^{d+2}} \exp \left(\alpha_0 \left(1 + |v|^2 + |w|^2 \right)^{1/2} \right) f_0(\mathrm{d}\mathbf{x}, \mathrm{d}v, \mathrm{d}w) < \infty. \tag{1.2.4}$$

Le résultat démontré est le suivant.

Theorem 1.2.3 (Limite champ moyen). *Soit Φ un noyau de connectivité globalement lipschitzien sur $\mathbb{R}^{2d}$ et uniformément borné. Soit $T > 0$ un temps final.*

1. *Soient $f_{0,1}$ et $f_{0,2}$ deux mesures de probabilité sur $\mathbb{R}^{d+2}$ avec des moments d'ordre 2 finis. On note f_1 et f_2 les solutions de l'équation (1.2.2) respectivement associées. Supposons de plus que $f_{0,2}$ satisfasse l'hypothèse (1.2.4) pour un certain $\alpha_0 > 0$ constant. Alors il existe deux constantes $C_T > 0$ et K_T telles que pour tout $t \in [0, T]$:*

$$d_2\left(f_1(t), f_2(t)\right) \,\le\, K_T \, d_2\left(f_{0,1}, f_{0,2}\right)^{\beta(t)}, \tag{1.2.5}$$

où $\beta(t) = e^{-C_T \, t}$.

2. *Soit f_0 une mesure de probabilité sur $\mathbb{R}^{d+2}$ avec des moments d'ordre 2 finis, et vérifiant l'hypothèse (1.2.4). On note f la solution de l'équation (1.2.2) associée. De plus, pour tout $n \in \mathbb{N}$, on pose les n-tuplets $\mathbf{X} \in \left(\mathbb{R}^d\right)^n$, $V_{i,0}$ et $W_{i,0} \in \mathbb{R}^n$ comme condition initiale au système de FHN (1.1.8). On note $f_{0,n}$ la mesure empirique associée aux conditions initiales, et f_n celle associée à la solution de (1.1.8). Supposons que les données initiales vérifient*

$$\lim_{n \to +\infty} d_2(f_{0,n}, f_0) \,=\, 0. \tag{1.2.6}$$

Alors on a:

$$\lim_{n \to +\infty} \sup_{t \in [0,T]} d_2(f_n(t), f(t)) \,=\, 0. \tag{1.2.7}$$

Dans ce théorème, le résultat (i) est une estimation de stabilité semblable à une estimée de Dobrushin avec la distance de Wasserstein d'ordre 2. La limite champ moyen en elle-même est établie par le résultat (ii) comme une conséquence de (i).

1.2.2 Dynamique du modèle de champ moyen

Dans le Chapitre 2, nous présenterons un schéma numérique pour le modèle à champ moyen (1.2.2)-(1.2.3), basé sur une méthode particulaire. Ce type de méthode a été introduite dans [79, 120] pour des problèmes de dynamique des fluides. Cela consite à approcher la solution de (1.2.2) par un nombre fini de macro-particules, dont les trajectoires sont déterminées par les courbes caractéristiques de (1.2.2). Si l'on note f la solution de l'équation (1.2.2)-(1.2.3), alors le système d'équations caractéristiques s'écrit pour tout $(t, \mathbf{x}) \in \mathbb{R}^+ \times \mathbb{R}^d$ et tout $(v, w) \in \mathbb{R}^2$:

$$\begin{cases} \dfrac{\mathrm{d}\mathcal{V}}{\mathrm{d}t} \,=\, N\left(\mathcal{V}\right) \,-\, \mathcal{W} \,+\, \mathcal{K}_\Phi[f](t, \mathbf{x}, \mathcal{V}), \\[2mm] \dfrac{\mathrm{d}\mathcal{W}}{\mathrm{d}t} \,=\, A\left(\mathcal{V}, \mathcal{W}\right), \\[2mm] \mathcal{V}(0) \,=\, v, \quad \mathcal{W}(0) \,=\, w, \end{cases} \tag{1.2.8}$$

où $\mathcal{K}_\Phi$ est défini dans (1.2.2). Ce type de méthode a ensuite été utilisé dans de nombreux domaines, comme la physique des plasmas par exemple (voir [34, 68, 83]). Quant à la discrétisation en temps, nous utiliserons une méthode de Runge-Kutta explicite d'ordre 2.

En général, il est plus intéressant de simuler le comportement du modèle mésoscopique plutôt que du modèle microscopique pour modéliser la dynamique collective d'un grand nombre de neurones. En effet, même si nous n'aurons pas accès en détail à l'état de chaque neurone dans le réseau, le calcul du terme non local sera beaucoup plus rapide, ce qui nous permettra de considérer des réseaux de neurones plus larges et plus denses.

(a) $t = 0$ (b) $t = 10$ (c) $t = 100$
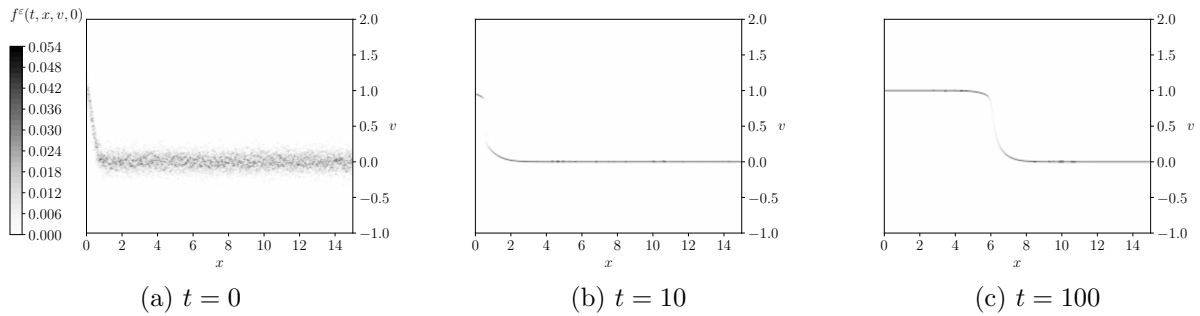
Figure 1.7: Allure de la fonction de densité f solution de (1.2.2) avec comme condition initiale (1.2.9), pour $w = 0$ fixé, et à différents instants t. Les maillages en x et v contiennent 200 points chacun, et nous avons fixé $\Delta t = 0.001$ et $\theta = 0.25$.

À la Figure 1.7, nous étudions l'équation (1.2.2) dans un sous-cas bien particulier : nous choisissons $\tau = 0$ et comme condition initiale pour tout $x \in [0, 15]$, $(v, w) \in \mathbb{R}^2$:

$$f_0(x, v, w) = \frac{1}{\sqrt{0.02\,\pi}} \exp\left(-\frac{|v - V_0(x)|^2}{0.02}\right) \otimes \delta_0(w), \quad V_0(x) = \exp\left(-5\,x^2\right). \qquad (1.2.9)$$

Dans cette configuration, cela revient à retirer l'influence de la variable d'adaptation w. De plus, afin de considérer un réseau de neurones homogènes (ρ_0 constant sur $[0, 15]$ et nul ailleurs), les particules de la méthode numérique sont réparties uniformément dans l'intervalle $[0, 15]$. Ensuite, nous utilisons ici comme noyau d'interaction une fonction gaussienne:

$$\Phi : (x, y) \mapsto G(x - y) := \frac{5}{\sqrt{\pi}} \exp\left(|x - y|^2\right).$$

Sur la Figure 1.7, nous pouvons observer deux phénomènes. Tout d'abord, quand le temps s'écoule, les particules ont tendance à se synchroniser à chaque position. En clair, à chaque position x, le potentiel de chaque particule se rapproche vers la moyenne des potentiels de toutes les particules en x. Ceci implique que la solution f de (1.2.2) semble converger vers une masse de Dirac en v centrée en $V(t, x)$, le potentiel moyen à la position x à l'instant t, quand le temps t tend vers l'infini.

Ensuite, le potentiel moyen V a qualitativement la forme d'un front d'invasion connectant l'état stationnaire $v = 0$ à 1, se propageant à vitesse constante. Or, c'est exactement le comportement que l'on s'attend à obtenir pour la solution de l'équation de réaction-diffusion d'Allen-Cahn non locale, qui s'écrit pour $t > 0$ et $x \in \mathbb{R}$:

$$\partial_t V(t, x) - [G \star V(t, x) - V(t, x)] = N(V(t, x)), \qquad (1.2.10)$$

où $\star$ représente le produit de convolution en espace. L'existence, l'unicité et la stabilité de ces fronts d'invasion solutions de (1.2.10) ont été démontrés dans [8]. Ainsi, comme nous le développerons plus en détail dans le Chapitre 2, il est possible de retrouver qualitativement des comportements attendus pour un modèle macroscopique avec le modèle de champ moyen (1.2.2).

1.3 Limites macroscopiques (Chapitres 3 et 4)

Nous nous intéressons à présent aux quantités macroscopiques du réseau de neurones. Soit f une solution de l'équation de champ moyen (1.2.2)-(1.2.3). Dans la suite, nous considérons que

pour tout $t > 0$, $f(t)$ est une densité, donc une fonction dans $L^1(\mathbb{R}^{d+2})$. Nous définissons pour tout $t > 0$ et pour tout $\mathbf{x} \in \mathbb{R}^d$:

$$\rho(t,\mathbf{x}) \begin{pmatrix} 1 \\ V(t,\mathbf{x}) \\ W(t,\mathbf{x}) \end{pmatrix} := \int_{\mathbb{R}^2} \begin{pmatrix} 1 \\ v \\ w \end{pmatrix} f(t,\mathbf{x},v,w)\, \mathrm{d}v\, \mathrm{d}w. \tag{1.3.1}$$

De plus, la conservation de la masse dans l'équation (1.2.2) nous donne directement que pour tout $t > 0$,

$$\rho(t,\cdot) = \rho(0,\cdot) = \rho_0.$$

Ici, pour tout $t > 0$ et $\mathbf{x} \in \mathbb{R}^d$, $\rho_0(\mathbf{x})$ représente la densité moyenne de neurones dans le réseau à la position $\mathbf{x}$, et $V(t,\mathbf{x})$ et $W(t,\mathbf{x})$ sont les valeurs moyennes du potentiel et de la variable d'adaptation dans le réseau. En utilisant l'équation (1.2.2), nous pouvons déterminer que les quantités macroscopiques vérifient formellement le système d'équations pour $t > 0$ et $\mathbf{x} \in \mathbb{R}^d$:

$$\begin{cases} \partial_t (\rho_0\, V) - \rho_0\, \mathcal{L}_{\rho_0,\Phi}(V) = \rho_0\, [N(V) - W] + \mathcal{E}(f), \\[2mm] \partial_t (\rho_0\, W) = \rho_0\, A(V,W), \end{cases} \tag{1.3.2}$$

où $\mathcal{L}_{\rho_0,\Phi}$ est un opérateur spatial nonlocal défini par

$$\mathcal{L}_{\rho_0,\Phi}(V)(t,\mathbf{x}) := \int_{\mathbb{R}^d} \Phi(\mathbf{x},\mathbf{x}')\, \rho_0(\mathbf{x}')\, \big(V(t,\mathbf{x}') - V(t,\mathbf{x})\big)\, \mathrm{d}\mathbf{x}', \tag{1.3.3}$$

et $\mathcal{E}(f)$ est un terme d'erreur donné ci-dessous:

$$\mathcal{E}(f)(t,\mathbf{x}) = \int_{\mathbb{R}^2} f(t,\mathbf{x},v,w)\, [N(v) - N(V(t,\mathbf{x}))]\, \mathrm{d}v\, \mathrm{d}w. \tag{1.3.4}$$

On observe directement que les grandeurs macroscopiques ne vérifient pas un système d'équations fermé, à cause de la nonlinéarité N qui fait apparaître des moments de f supérieur à 1. Afin de résoudre ce problème, et afin d'être capable de contrôler le terme d'erreur $\mathcal{E}(f)$, nous allons modifier le noyau de connectivité Φ afin de considérer le régime à interactions locales fortes. Pour cela, nous utiliserons deux manières différentes, développées aux Chapitres 3 et 4.

1.3.1 Chapitre 3 : Décomposition des interactions

Soit $\varepsilon > 0$ un paramètre de redimensionnement. Nous commençons par décomposer les interactions entre les interactions locales fortes, et les interactions à longue portée plus faibles. Pour cela, nous remplaçons dans l'équation de transport (1.2.2) le noyau de connectivité Φ par:

$$\Phi(\mathbf{x},\mathbf{y}) = \Psi(\|\mathbf{x} - \mathbf{y}\|) + \frac{1}{\varepsilon}\, \delta_0(\|\mathbf{x} - \mathbf{y}\|), \tag{1.3.5}$$

où δ_0 est la masse de Dirac centrée en 0, et Ψ est une fonction positive vérifiant:

$$\int_{\mathbb{R}^d} \Psi(\|\mathbf{x}\|)\, \mathrm{d}\mathbf{x} < \infty.$$

Ce type d'hypothèse sur les interactions entre neurones est souvent faite pour modéliser les dynamiques du cortex visuel [24]. L'équation de transport (1.2.2) devient pour $t > 0$, $(\mathbf{x},v,w) \in \mathbb{R}^{d+2}$:

$$\begin{cases} \partial_t f^\varepsilon + \partial_v \left(f^\varepsilon\, [N(v) - w - \mathcal{K}_\Psi[f^\varepsilon]]\right) - \dfrac{1}{\varepsilon} \partial_v \left(f^\varepsilon\, \rho_0^\varepsilon\, (v - V^\varepsilon)\right) + \partial_w \left(f^\varepsilon\, A(v,w)\right) = 0, \\[3mm] \mathcal{K}_\Psi[f^\varepsilon](t,\mathbf{x},v) = \displaystyle\int_{\mathbb{R}^{d+2}} \Psi(\|\mathbf{x} - \mathbf{x}'\|)\, (v - v')\, f^\varepsilon(t,\mathbf{x}',v',w')\, \mathrm{d}\mathbf{x}'\, \mathrm{d}v'\, \mathrm{d}w', \end{cases} \tag{1.3.6}$$

et on définit les grandeurs macroscopiques $(\rho_0^\varepsilon, V^\varepsilon, W^\varepsilon)$ à partir de f^ε comme dans (1.3.1). Dans l'équation (1.3.6), nous pouvons faire une analogie avec la théorie cinétique, en remarquant que le terme d'interactions locales a la même forme qu'un terme d'alignement dans une équation de Vlasov. C'est pourquoi nous appelons la limite quand ε tend vers 0 la *limite hydrodynamique*. Formellement, si nous multiplions l'équation (1.3.6) par ε, alors quand ε tend vers 0, le terme d'interactions locales $\partial_v (f^\varepsilon \rho_0^\varepsilon (v - V^\varepsilon))$ tend vers 0. En conséquence, une solution f^ε de l'équation (1.3.6) tend formellement vers une masse de Dirac en v dans un certain sens faible à déterminer. Plus précisément, toujours en faisant une analogie avec la théorie cinétique, f^ε converge vers une *distribution monocinétique*, c'est-à-dire formellement:

$$f^\varepsilon(t, \mathbf{x}, v, w) \underset{\varepsilon \to 0}{\rightharpoonup} F(t, \mathbf{x}, w) \otimes \delta_0(v - V(t, \mathbf{x})), \tag{1.3.7}$$

où l'on définit

$$F(t, \mathbf{x}, w) := \lim_{\varepsilon \to 0} \int_{\mathbb{R}} f^\varepsilon(t, \mathbf{x}, v, w) \, \mathrm{d}v, \quad V(t, \mathbf{x}) := \lim_{\varepsilon \to 0} V^\varepsilon(t, \mathbf{x}).$$

Nous posons

$$\rho(t, \mathbf{x}) = \int_{\mathbb{R}} F(t, \mathbf{x}, w) \, \mathrm{d}w, \quad \rho(t, \mathbf{x}) \, W(t, \mathbf{x}) = \int_{\mathbb{R}} F(t, \mathbf{x}, w) \, w \, \mathrm{d}w.$$

Tout d'abord, la conservation de la masse nous donne directement que pour tout $t > 0$, $\rho(t, \cdot) = \rho(0, \cdot) = \rho_0$. Ensuite, nous pouvons observer que formellement, le terme $\mathcal{E}(f^\varepsilon)$ dans le système (1.3.2) tend vers 0 quand ε tend vers 0, donc la limite formelle V de V^ε vérifie l'équation:

$$\partial_t(\rho_0 \, V) - \rho_0 \, \mathcal{L}_{\rho_0, \Psi}(V) = \rho_0 \, [N(V) - W].$$

Enfin, en intégrant (1.3.6) par rapport à v, et en considérant la limite formelle quand ε tend vers 0, on obtient que F vérifie la fonction de transport suivante:

$$\partial_t F + \partial_w (A(V, w) \, F) = 0.$$

Comme nous le verrons dans le Chapitre 3, les fonctions (ρ_0, V, W) vérifient le système de réaction-diffusion nonlocale de type FitzHugh-Nagumo:

$$\begin{cases} \partial_t V - \mathcal{L}_{\rho_0, \Psi}(V) = N(V) - W, \\ \partial_t W = A(V, W), \end{cases} \tag{1.3.8}$$

où le terme nonlocal $\mathcal{L}_{\rho_0, \Psi}(V)$ est défini dans (1.3.3). Le but de ce chapitre est de démontrer que le système (1.3.8) est une caractérisation macroscopique du réseau de neurones modélisé par l'équation de champ moyen (1.3.6). Le résultat démontré est le suivant.

Theorem 1.3.1. *[Limite hydrodynamique] Soit $T > 0$ un temps final. Pour tout $\varepsilon > 0$, nous considérons une condition initiale f_0^ε à support compact en (v, w), vérifiant*

$$f_0^\varepsilon \geq 0, \quad f_0^\varepsilon, \nabla_{\mathbf{u}} f_0^\varepsilon \in L^\infty(\mathbb{R}^{d+2}),$$

où $\mathbf{u} = (v, w)$, et il existe une constante $C > 0$ indépendante de ε telle que

$$\|\rho_0^\varepsilon\|_{L^\infty} + \int_{\mathbb{R}^{d+2}} \left(1 + \|\mathbf{x}\|^4 + |v|^4 + |w|^4\right) f_0^\varepsilon(\mathbf{x}, v, w) \, \mathrm{d}\mathbf{x} \, \mathrm{d}v \, \mathrm{d}w \leq C.$$

Soit (ρ_0, V_0, W_0) un triplet de données initiales vérifiant

$$\rho_0 \geq 0, \quad \rho_0 \in L^1 \cap L^\infty(\mathbb{R}^d), \quad V_0, W_0 \in L^\infty(\mathbb{R}^d),$$

et supposons de plus qu'il existe une constante $C > 0$ telle que

$$\|\rho_0 - \rho_0^\varepsilon\|_{L^2}^2 + \int_{\mathbb{R}^d} \rho_0^\varepsilon \left[|V_0 - V_0^\varepsilon|^2 + |W_0 - W_0^\varepsilon|^2\right] \mathrm{d}\mathbf{x} \leq C \, \varepsilon^{1/(d+6)}.$$

Alors les quantités macroscopiques $(\rho_0^\varepsilon, V^\varepsilon, W^\varepsilon)$ calculées à partir de f^ε la solution de (1.3.6) avec pour condition initiale f_0^ε vérifient pour tout $t \in [0, T]$

$$\int_{\mathbb{R}^d} \rho_0^\varepsilon(\mathbf{x}) \left[|V - V^\varepsilon|^2(t, \mathbf{x}) + |W - W^\varepsilon|^2(t, \mathbf{x})\right] \mathrm{d}\mathbf{x} \leq C_T \, \varepsilon^{1/(d+6)}, \tag{1.3.9}$$

où le triplet (ρ_0, V, W) vérifient le système d'équation (1.3.8).

1.3.2 Chapitre 4 : Redimensionnement des interactions

Dans le travail précédent, nous avons considéré que les neurones conservent des interactions à longue portée, même à l'échelle macroscopique. En fonction de la zone du cerveau considérée, ce n'est pas forcément le choix de modélisation le plus pertinent. Puisque les neurones communiquent surtout avec leurs plus proches voisins, considérons $\varepsilon > 0$ un paramètre de redimensionnement, et remplaçons dans l'équation (1.2.2) le noyau d'interaction Φ par:

$$\Phi(\mathbf{x}, \mathbf{y}) = \frac{1}{\varepsilon^2} \Psi_\varepsilon(\|\mathbf{x} - \mathbf{y}\|), \quad \Psi_\varepsilon : r \mapsto \frac{1}{\varepsilon^d} \Psi\left(\frac{r}{\varepsilon}\right),$$

où Ψ est un noyau d'interaction vérifiant

$$\Psi > 0, \quad \int_{\mathbb{R}^d} \Psi(\|\mathbf{x}\|) \, \mathrm{d}\mathbf{x} = 1, \quad \sigma := \int_{\mathbb{R}^d} \Psi(\|\mathbf{x}\|) \frac{\|\mathbf{x}\|^2}{2} \, \mathrm{d}\mathbf{x} < \infty. \tag{1.3.10}$$

L'équation de transport (1.2.2) devient pour $t > 0$, et $(\mathbf{x}, v, w) \in \mathbb{R}^{d+2}$:

$$\begin{cases} \partial_t f^\varepsilon + \partial_v \left(f^\varepsilon \left[N(v) - w - \mathcal{K}_\varepsilon[f^\varepsilon]\right]\right) + \partial_w \left(f^\varepsilon A(v, w)\right) = 0, \\[2mm] \mathcal{K}_\varepsilon[f^\varepsilon](t, \mathbf{x}, v) := \frac{1}{\varepsilon^{d+2}} \int_{\mathbb{R}^{d+2}} \Psi\left(\frac{\|\mathbf{x} - \mathbf{x}'\|}{\varepsilon}\right) (v - v') f^\varepsilon(t, \mathrm{d}\mathbf{x}', \mathrm{d}v', \mathrm{d}w'). \end{cases} \tag{1.3.11}$$

Ce genre de redimensionnement a déjà été utilisé dans [6, 7] pour prouver la convergence des solutions de type onde progressive d'une équation bistable nonlocale vers celles d'une équation bistable standard. En conséquence, nous pouvons nous attendre à obtenir un laplacien en espace à la limite $\varepsilon \to 0$. Nous devrons donc être prudent quant à la régularité en espace des solutions.

Étudions formellement la limite de f^ε une solution de (1.3.11) quand ε tend vers 0. Soit $t > 0$, $\mathbf{x} \in \mathbb{R}^d$ et $\mathbf{u} = (v, w) \in \mathbb{R}^2$. En utilisant le changement de variables $\mathbf{y} = (\mathbf{x} - \mathbf{x}')/\varepsilon$, nous obtenons

$$f^\varepsilon(t, \mathbf{x}, \mathbf{u}) \, \mathcal{K}_\varepsilon[f^\varepsilon](t, \mathbf{x}, v) = \varepsilon^{-2} \iint_{R^{d+2}} \Psi(\|\mathbf{y}\|) (v - v') f^\varepsilon(t, \mathbf{x} - \varepsilon\mathbf{y}, \mathbf{u}') f^\varepsilon(t, \mathbf{x}, \mathbf{u}) \, \mathrm{d}\mathbf{y} \, \mathrm{d}\mathbf{u}'.$$

Ensuite, en utilisant un développement de Taylor sur le terme $f^\varepsilon(t, \mathbf{x} - \varepsilon\mathbf{y}, \mathbf{u}')$ quand ε tend vers 0, et en utilisant les hypothèses vérifiées par Ψ, notamment le fait que Ψ est radialement symétrique pour simplifier les termes d'ordre impair en $\mathbf{y}$, on a:

$$f^\varepsilon(t, \mathbf{x}, \mathbf{u}) \, \mathcal{K}_\varepsilon[f^\varepsilon](t, \mathbf{x}, v) = \varepsilon^{-2} \int_{\mathbb{R}^2} (v - v') f^\varepsilon(t, \mathbf{x}, \mathbf{u}') f^\varepsilon(t, \mathbf{x}, \mathbf{u}) \, \mathrm{d}\mathbf{u}'$$

$$+ \sigma \int_{\mathbb{R}^2} (v - v') \Delta_\mathbf{x} f^\varepsilon(t, \mathbf{x}, \mathbf{u}') f^\varepsilon(t, \mathbf{x}, \mathbf{u}) \, \mathrm{d}\mathbf{u}' + R_\varepsilon(t, \mathbf{x}, \mathbf{u}), \quad (1.3.12)$$

où $R_\varepsilon(t, \mathbf{x}, \mathbf{u})$ rassemble tous les termes d'ordre plus élevé en ε, ce qui nous amène à supposer que R_ε tend vers 0 quand $\varepsilon \to 0$. Supposons que f^ε converge formellement vers une distribution f quand ε tend vers 0. Dans la suite, on note $(\rho_0^\varepsilon, V^\varepsilon, W^\varepsilon)$ et (ρ_0, V, W) les quantités macroscopiques respectivement calculées à partir de f^ε et f, comme dans (1.3.1). Alors, en injectant le développement (1.3.12) dans l'équation (1.3.11), et en faisant tendre ε vers 0, nous pouvons identifier les ordres -2 et 0. Nous obtenons les deux équations suivantes vérifiées par f au sens des distributions pour $t > 0$, $\mathbf{x} \in \mathbb{R}^d$ et $(v, w) \in \mathbb{R}^2$:

$$\mathcal{O}(\varepsilon^{-2}): \qquad \iint (v - v')\, f(t, \mathbf{x}, v', w')\, f(t, \mathbf{x}, v, w)\, \mathrm{d}v'\, \mathrm{d}w' = 0, \qquad (1.3.13)$$

$$\mathcal{O}(1): \qquad \begin{aligned} \partial_t f &+ \partial_v \left[f\, (N(v) - w) \right] + \partial_w \left[f\, A(v, w) \right] \\ &- \sigma\, \partial_v \left[f\, (\Delta_\mathbf{x} \rho_0\, v - \Delta_\mathbf{x}(\rho_0\, V)) \right] = 0. \end{aligned} \qquad (1.3.14)$$

La première équation (1.3.13) nous donne que f est proportionnelle à une masse de Dirac en v centrée en $V(t, \mathbf{x})$. En effet, (1.3.13) implique que $(v - V(t, \mathbf{x}))\, \rho_0(\mathbf{x})\, f(t, \mathbf{x}, v, w) = 0$ au sens des distributions, puisque pour tout $\phi \in \mathscr{C}_c^\infty(\mathbb{R}^{d+2})$ et $t > 0$, on a :

$$\left| \iint f(t, \mathbf{x}, v, w)\, \rho_0(\mathbf{x})\, \phi(\mathbf{x}, v, w)\, \mathrm{d}\mathbf{x}\, \mathrm{d}v\, \mathrm{d}w - \int F(t, \mathbf{x}, w)\, \rho_0(\mathbf{x})\, \phi(\mathbf{x}, V(t, \mathbf{x}), w)\, \mathrm{d}\mathbf{x}\, \mathrm{d}w \right|$$
$$\leq \|\nabla_v \phi\|_{L^\infty} \iint_{\mathrm{Supp}(\phi)} f(t, \mathbf{x}, v, w)\, \rho_0(\mathbf{x})\, |v - V(t, \mathbf{x})|\, \mathrm{d}\mathbf{x}\, \mathrm{d}v\, \mathrm{d}w,$$

qui est égal à 0. En d'autres termes, comme au paragraphe précédent, (1.3.7) est vérifiée. On définit par la suite pour tout $t > 0$, $(\mathbf{x}, w) \in \mathbb{R}^{d+1}$:

$$F(t, \mathbf{x}, w) := \int_\mathbb{R} f(t, \mathbf{x}, v, w)\, \mathrm{d}v, \quad \rho_0(\mathbf{x})\, W(t, \mathbf{x}) := \int_{\mathbb{R}^2} f(t, \mathbf{x}, v, w)\, w\, \mathrm{d}v\, \mathrm{d}w.$$

Comme précédemment, nous pouvons établir que (V, F) vérifie le système d'équations pour $t > 0$, $(\mathbf{x}, w) \in \mathbb{R}^{d+1}$:

$$\begin{cases} \partial_t F + \partial_w \left(A(V, w)\, F \right) = 0, \\[2mm] \partial_t(\rho_0\, V) - \sigma \left[\rho_0\, \Delta_\mathbf{x}(\rho_0\, V) - (\Delta_\mathbf{x} \rho_0)\, \rho_0\, V \right] = \rho_0\, N(V) - \rho_0\, W. \end{cases} \qquad (1.3.15)$$

Là encore, dans un souci de concision, nous verrons dans le Chapitre 4 en quoi le système (1.3.15) revient à étudier le système de réaction-diffusion local de type FitzHugh-Nagumo, qui s'écrit pour $t > 0$ en $\mathbf{x} \in \mathbb{R}^d$:

$$\begin{cases} \partial_t V(t, \mathbf{x}) - \sigma \left[\Delta_\mathbf{x}(\rho_0\, V)(t, \mathbf{x}) - \Delta_\mathbf{x} \rho_0(\mathbf{x})\, V(t, \mathbf{x}) \right] = N(V(t, \mathbf{x})) - W(t, \mathbf{x}), \\[2mm] \partial_t W(t, \mathbf{x}) = A(V(t, \mathbf{x}), W(t, \mathbf{x})), \end{cases} \qquad (1.3.16)$$

qui est un autre modèle macroscopique pour le système de FHN défini par (1.3.11). Le principal résultat démontré dans le Chapitre 4 est le suivant.

Theorem 1.3.2. *[Limite asymptotique] Soit Ψ un noyau d'interaction vérifiant (1.3.10). Soit $T > 0$ un temps final. Pour tout $\varepsilon > 0$, nous considérons une condition initiale f_0^ε à support compact en (v, w), vérifiant*

$$f_0^\varepsilon \geq 0, \quad f_0^\varepsilon, \nabla_\mathbf{u} f_0^\varepsilon \in L^\infty(\mathbb{R}^{d+2}),$$

où $\mathbf{u} = (v, w)$, *et il existe une constante* $C > 0$ *indépendante de* ε *telle que*

$$\|\rho_0^\varepsilon\|_{L^\infty} + \int_{\mathbb{R}^{d+2}} \left(1 + \|\mathbf{x}\|^4 + |v|^4 + |w|^4\right) f_0^\varepsilon(\mathbf{x}, v, w) \, \mathrm{d}\mathbf{x} \, \mathrm{d}v \, \mathrm{d}w \leq C.$$

Soit (ρ_0, V_0, W_0) *un triplet de données initiales vérifiant*

$$\rho_0 \geq 0, \quad \rho_0 \in \mathcal{C}_b^3(\mathbb{R}^d), \quad \rho_0 \in L^1(\mathbb{R}^d), \quad V_0, W_0 \in H^2(\mathbb{R}^d),$$

et supposons de plus que quand $\varepsilon \to 0$,

$$\frac{1}{\varepsilon^2} \|\rho_0 - \rho_0^\varepsilon\|_{L^2}^2 + \int_{\mathbb{R}^d} \rho_0^\varepsilon \left[|V_0 - V_0^\varepsilon|^2 + |W_0 - W_0^\varepsilon|^2\right] \mathrm{d}\mathbf{x} \longrightarrow 0.$$

Alors les quantités macroscopiques $(\rho_0^\varepsilon, V^\varepsilon, W^\varepsilon)$ *calculées à partir de* f^ε *la solution de* (1.3.11) *avec pour condition initiale* f_0^ε *vérifient pour tout* $t \in [0, T]$

$$\int_{\mathbb{R}^d} \rho_0^\varepsilon(\mathbf{x}) \left[|V - V^\varepsilon|^2(t, \mathbf{x}) + |W - W^\varepsilon|^2(t, \mathbf{x})\right] \mathrm{d}\mathbf{x} \longrightarrow 0, \tag{1.3.17}$$

où (ρ_0, V, W) *vérifient le système d'équation* (1.3.16).

1.3.3 Entropie relative

Dans les Chapitres 3 et 4, pour démontrer respectivement les Théorèmes 1.3.1 et 1.3.2, nous utiliserons une méthode d'entropie relative. Ce genre de technique a été développée par M. Dafermos [51] et R. DiPerna [56] pour des lois de conservation. Cela consiste à perturber l'entropie du système considéré, ce qui nous permet de mesurer la distance entre les solutions du système et le système limite.

Ici, des travaux comme [63, 94, 95], où les auteurs étudient la limite hydrodynamique d'équations cinétiques nonlocales spatialement organisées, montrent qu'une technique d'entropie relative est tout à fait adaptée. En revanche, puisqu'il n'y a pas de bruit dans le modèle microscopique, il n'y a pas de Laplacien en v dans l'équation de transport (1.2.2), contrairement au cas traité dans [95]. Comme dans [63, 94], sans l'effet régularisant du laplacien, la solution de l'équation cinétique converge vers solution monocinétique, comme explicité dans (1.3.7). Pour des raisons de régularité, nous ne pouvons pas utiliser une entropie classique de la forme $f \log(f)$.

De manière similaire à [63, 94], nous considérons comme entropie pour tout triplet $\mathcal{Z} = (\rho, \rho V, \rho W)$ où ρ, V et W sont des fonctions de $\mathbb{R}^d$ dans $\mathbb{R}$:

$$\eta(\mathcal{Z}) := \rho \frac{|V|^2 + |W|^2}{2}. \tag{1.3.18}$$

Si on note $P = \rho V$ et $Q = \rho W$, nous obtenons pour tout $\mathbf{x} \in \mathbb{R}^d$:

$$\eta(\mathcal{Z})(\mathbf{x}) = \begin{cases} \dfrac{P^2(\mathbf{x}) + Q^2(\mathbf{x})}{2\rho(\mathbf{x})} & \text{if } \rho(\mathbf{x}) \neq 0, \\ \\ 0 & \text{else.} \end{cases}$$

La différentielle de η par rapport à ses variables est :

$$D\eta(\mathcal{Z}) = \begin{pmatrix} D_\rho \eta \\ D_P \eta \\ D_Q \eta \end{pmatrix} = \begin{pmatrix} -\dfrac{|V|^2 + |W|^2}{2} \\ V \\ W \end{pmatrix}.$$

On définit l'entropie relative entre les deux triplets $\mathcal{Z}_1 = (\rho_1, \rho_1 V_1, \rho_1 W_1)$ et $\mathcal{Z}_2 = (\rho_2, \rho_2 V_2, \rho_2 W_2)$ comme suit:

$$
\begin{aligned}
\eta(\mathcal{Z}_1 \,|\, \mathcal{Z}_2) \;\; &:= \;\; \eta(\mathcal{Z}_1) \, - \, \eta(\mathcal{Z}_2) \, - \, D\eta(\mathcal{Z}_2) \cdot (\mathcal{Z}_1 - \mathcal{Z}_2) \\
&= \;\; \rho_1 \, \frac{|V_1 - V_2|^2 \, + \, |W_1 - W_2|^2}{2}.
\end{aligned}
\tag{1.3.19}
$$

Dans le cas que nous étudions ici, nous avons choisi comme entropie l'énergie du système. La méthode d'entropie relative peut ici être rapprochée de la stratégie d'estimation de l'énergie modulée. Ce genre de technique a notamment été utilisée dans [20, 21] par Brenier *et al.* pour démontrer la convergence d'un système de Vlasov-Poisson dans le régime quasi-neutre, vers les équations d'Euler incompressible. Elle consiste là encore à perturber l'énergie du système avec la solution de l'équation limite.

Considérons le triplet $\mathcal{Z} = (\rho_0, V, W)$, où (V, W) est une solution du système de réaction-diffusion (1.3.8) (resp. (1.3.16)), et $\mathcal{Z}^\varepsilon = (\rho_0^\varepsilon, V^\varepsilon, \rho_0^\varepsilon W^\varepsilon)$ les quantités macroscopiques calculées à partir d'une solution f^ε de l'équation de transport (1.3.6) (resp. (1.3.11)). La preuve du Théorème 1.3.1 (resp. Théorème 1.3.2) repose sur le contrôle de l'entropie relative $\eta(\mathcal{Z}^\varepsilon \,|\, \mathcal{Z})$. La difficulté et l'originalité de ces problèmes vient du fait que nous devons aussi estimer une dissipation pour montrer que le terme d'erreur $\mathcal{E}(f^\varepsilon)$ tend vers 0 quand ε tend vers 0.

Dans le cas étudié dans le Chapitre 4, une difficulté s'ajoute : nous devons être particulièrement vigilant quant à la régularité en espace des solutions.

1.4 Schéma numérique asymptotiquement stable (Chapitre 5)

Dans le Chapitre 5, nous chercherons à construire un schéma numérique de l'équation de champ moyen (1.3.11), qui reste stable quand le paramètre de redimensionnement ε tend vers 0, et qui à la limite $\varepsilon \to 0$ fournit une approximation numérique de l'équation de réaction-diffusion (1.3.16). Ce type de discrétisation est appelé schéma *Asymptotic Preserving* (abrégé AP par la suite). Commençons par énoncer quelques généralités sur les schémas AP, puis nous détaillerons plus précisément le cas qui nous intéresse.

1.4.1 Définition et propriétés d'un schéma AP

Soit $\varepsilon > 0$ un paramètre. Considérons P_ε un système de Cauchy, dépendant du paramètre ε, n'admettant qu'une seule solution u_ε. Supposons que u_ε converge dans un certain sens quand ε tend vers 0 vers u_0 la solution d'un problème limite P_0. La limite du problème P_ε vers P_0 peut poser quelques problèmes analytiques. Par exemple, ils peuvent ne pas être de la même nature mathématique. Plus précisément dans le cas que nous étudierons, P_ε sera une équation de transport, tandis que P_0 sera une équation de réaction-diffusion. Les méthodes analytiques ou numériques valables pour le problème P_ε ne le seront peut-être pas pour P_0. Nous ne pouvons pas non plus nous restreindre à n'étudier que le système limite P_0 pour deux raisons principales. Tout d'abord, il y a généralement une perte d'informations dans le passage à la limite $\varepsilon \to 0$. Ensuite, si nous considérons des problèmes de modélisation concrets, les données expérimentales ne donnent parfois des informations que sur P_ε.

Il est donc nécessaire de déterminer un schéma numérique pour le problème P_ε. Or, les méthodes numériques classiques peuvent faire apparaître des conditions de stabilité qui dépendent de ε. Si bien que pour des valeurs de ε petites, nous devrons prendre des pas de temps et d'espace de l'ordre de ε, ce qui n'est pas souhaitable en termes de temps de calcul.

Soit $\mathbf{h} = (\Delta t, \Delta x)$ les paramètres numériques que nous considérons. Un schéma AP est une discrétisation consistante du problème P_ε, notée $P_{\varepsilon,\mathbf{h}}$, qui converge quand ε tend vers 0 vers une
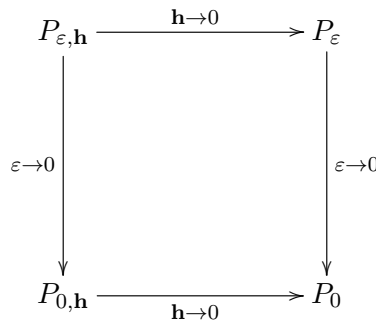
Figure 1.8: Diagramme commutatif expliquant les propriétés d'un schéma AP.

discrétisation consistante du problème limite P_0, notée $P_{0,\mathbf{h}}$. La Figure 1.8 montre un diagramme commutatif explicitant les différentes convergences. Les schémas AP sont des outils nécessaires pour le traitement numérique de problèmes singuliers en ε, utilisés pour toute une variété de problèmes. Par exemple, dans [52], P. Degond passe en revue différentes discrétisations AP pour différents modèles de plasma. Plus particulièrement, nous mentionnons [68], dans lequel F. Filbet et L.M. Rodrigues proposent un schéma AP pour l'équation de Vlasov-Poisson avec un champ magnétique externe fort, avec une méthode particulaire. Nous citons aussi [65, 115] pour des discrétisations AP de l'équation de Boltzmann dans différents régimes. D'une manière plus générale, S. Jin [90] et A. Klar [98] ont exposé plusieurs techniques de discrétisations AP pour des équations de transport avec un terme singulier. Dans [91], S. Jin passe en revue non seulement des techniques de schémas AP pour des équations cinétiques ou de transport linéaire, mais aussi pour des systèmes hyperboliques avec termes de relaxation raide. Dans le cas de l'équation de transport (1.3.11), il y a bien entendu un terme singulier comme dans les cas traités par la littérature, mais la difficulté provient surtout de la discrétisation du terme non local.

1.4.2 Schéma AP pour l'équation (1.3.11)

Afin de trouver une approximation adéquate pour l'équation (AP), nous devons commencer par la discrétisation spatiale, puis celle en temps. Dans l'esprit de [68], cité plus haut, nous choisissons d'utiliser de nouveau une méthode particulaire. Si l'on note f^ε la solution de l'équation (1.3.11) avec une condition initiale f_0^ε, alors le système d'équations caractéristiques s'écrit pour tout $(t,\mathbf{x}) \in \mathbb{R}^+ \times \mathbb{R}^d$ et tout $(v,w) \in \mathbb{R}^2$:

$$\begin{cases} \dfrac{\mathrm{d}\mathcal{V}^\varepsilon}{\mathrm{d}t} = N\left(\mathcal{V}^\varepsilon\right) - \mathcal{W}^\varepsilon + \mathcal{K}_\varepsilon[f^\varepsilon](t,\mathbf{x},\mathcal{V}^\varepsilon), \\[2mm] \dfrac{\mathrm{d}\mathcal{W}^\varepsilon}{\mathrm{d}t} = A\left(\mathcal{V}^\varepsilon, \mathcal{W}^\varepsilon\right), \\[2mm] \mathcal{V}^\varepsilon(0) = v, \quad \mathcal{W}^\varepsilon(0) = w, \end{cases} \tag{1.4.1}$$

où $\mathcal{K}_\varepsilon$ est défini dans (1.3.11). Toutefois, on peut réécrire le terme non local comme suit:

$$\mathcal{K}_\varepsilon[f^\varepsilon](\cdot,v) = \frac{1}{\varepsilon^2}\left[\Psi_\varepsilon \star (\rho_0^\varepsilon V^\varepsilon) - \Psi_\varepsilon \star \rho_0^\varepsilon v\right]. \tag{1.4.2}$$

Une manière efficace de discrétiser des produits de convolution est d'utiliser une méthode spectrale. Ce genre de méthode a été utilisé par exemple dans [29], pour l'étude numérique
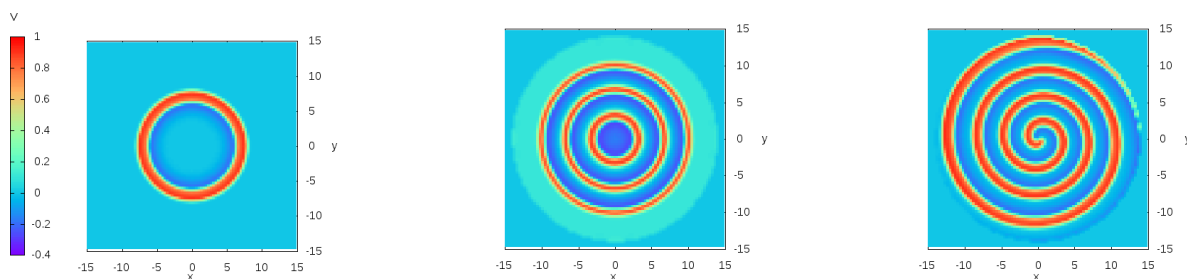
(a) Pic de potentiel se propageant radialement.

(b) Oscillations du potentiel se propageant radialement.

(c) Onde rotative en spirale.

Figure 1.9: Différentes dynamiques du potentiel moyen V^ε calculé à partir de la solution f^ε de (1.3.11). (a): $t = 280$, $\tau = 0.005$, $a = 0$ et $b = 5$. (b): $t = 280$, $\tau = 0.01$, $a = -0.1$ et $b = 1$. (c): $t = 2000$, $\tau = 0.005$, $a = 0$ et $b = 5$.

d'équations de réaction-diffusion à diffusion non locale. D'une part, leur méthode peut s'appliquer à des diffusions locales comme dans (1.3.15), et d'autre part, elle est adaptée à la discrétisation de termes intégraux comme $\mathcal{K}_\varepsilon[f^\varepsilon]$. Les méthodes spectrales sont particulièrement utilisées pour la discrétisation de l'opérateur non local de Boltzmann [64, 66, 67, 69, 114]. Dans le cas du système caractéristique (1.4.1), nous ne pouvons pas procéder de la même manière à cause de la nonlinéarité N. La méthode de collocation spectrale que nous utiliserons consiste à étudier seulement le terme raide $\mathcal{K}_\varepsilon[f^\varepsilon]$ dans l'espace de Fourier.

Comme il sera établi dans le Chapitre 4, à la limite $\varepsilon \to 0$, la solution f^ε de l'équation de transport (1.3.11) converge dans un certain sens vers une masse de Dirac en v. Numériquement, ici, nous utiliserons le terme raide pour prouver que toutes les particules situées à la même position dans le réseau se synchronisent.

Quant à la discrétisation temporelle, nous construirons dans le Chapitre deux schémas numériques différents, respectivement d'ordre 1 et 2 en temps. Nous prouverons qu'il s'agit bien là de schémas AP. Nous déterminerons numériquement l'ordre de ces deux schémas par rapport à **h** le paramètre numérique, et l'ordre en ε de convergence vers la solution du problème limite (1.3.15).

1.4.3 Exemples de dynamique dans un réseau de neurones spatialement organisé

Dans le Chapitre 5, nous étudierons numériquement des comportements plus complexes de l'équation (1.3.11), dans le cas d'un milieu hétérogène, et la génération d'ondes bidimensionnelles rotatives en forme de spirale. Ici, nous montrons quelques simulations numériques de l'équation (1.2.2), afin de montrer des exemples de dynamiques possibles pour le modèle de FHN spatialement organisé. Considérons comme noyau d'interaction une fonction Gaussienne:

$$\Psi : r \mapsto \frac{1}{2\,\pi\,\sigma^2}\,\exp\left(-\frac{r^2}{2\,\sigma}\right),$$

où $\sigma > 0$ est une constante (que l'on fixera à 0.005 dans cette sous-section). Soit f_0^ε de l'équation (1.3.11), telle que la densité de neurone ρ_0^ε (calculée comme dans (1.3.1)) est une approximation régulière de la fonction $\chi_{B(0,15)}$. Les simulations sont faites dans le compact $(-15, 15)^2$. Nous avons fixé les paramètres $\varepsilon = 0.001$, $\theta = 0.1$, le pas de temps $\Delta t = 0.1$, dans un maillage de l'espace avec $n = 256$ points par côté, $M = 100$ neurones dans chaque cellule.

Comme nous l'avons expliqué précédemment, un réseau de neurones spatialement couplé peut générer des dynamiques assez complexes. En effet, pour l'équation de réaction-diffusion limite (1.3.16), l'existence de pulsations se propageant dans l'espace a été prouvée dans [36, 80], l'existence d'oscillations se propageant a été démontrée dans [38], et l'apparition d'ondes bidimensionnelles en spirale a été observée numériquement dans [29]. Nous présentons à la Figure 1.9 quelques exemples de simulations numériques dans un espace à deux dimensions pour le potentiel moyen dans le réseau calculé à partir d'une solution de l'équation (1.2.2), pour différents jeux de paramètres. Comme conditions initiales, nous choisissons pour tout $(\mathbf{x}, v, w) \in \mathbb{R}^{d+2}$

$$f_0^{\varepsilon}(\mathbf{x}, v, w) = \rho_0(\mathbf{x})\,\delta_0(v - V_0(\mathbf{x})) \otimes \delta_0(w - W_0(\mathbf{x})),$$

avec

$$V_0(\mathbf{x}) = \begin{cases} \chi_{B(0,1)} & \text{dans les cas (a) et (b),} \\ \chi_{[-15,0]^2} & \text{dans le cas (c),} \end{cases} \qquad W_0(\mathbf{x}) = \begin{cases} 0 & \text{dans les cas (a) et (b),} \\ 0.1\,\chi_{[-15,0]\times[0,15]} & \text{dans le cas (c).} \end{cases}$$

Il s'agit ici d'un pic de potentiel unique se propageant radialement (panneau (a)), d'une série de pics de potentiels se propageant radialement (panneau (b)), et d'une onde en spirale rotative (panneau (c)). Ainsi, nous parvenons à reproduire numériquement avec l'équation de transport (1.3.11) des comportements macroscopiques proches de ceux attendus pour l'équation de réaction-diffusion limite. De plus, ces dynamiques sont observées biologiquement sur des portions du cerveau [11]. Nous mentionnons particulièrement que des ondes en spirales ont été observées *in vivo* dans un cortex de primate [86].

1.5 Appendice A : Projet CEMRACS

Durant l'été 2018, j'ai suivi une école de recherche au Centre d'Eté Mathématique de Recherche Avancée en Calcul Scientifique (CEMRACS), sur le thème "Modélisation numérique et mathématique pour des applications biologiques et médicales : descriptions déterministes, probabilistiques et statistiques". J'y ai participé à un projet de recherche en groupe encadré par Vincent Calvez et Gaël Raoul, en collaboration avec Léonard Dekens, Florian Lavigne et Frédéric Kuczma. Ce travail a été suivi d'une publication dans la revue *ESAIM: Proceedings and Surveys*. Même si son sujet ne s'accorde pas avec le reste de la thèse présentée ici, dans un souci de montrer l'entièreté du travail effectué, un appendice a été ajouté pour présenter nos résultats.

Nous nous intéressons à un modèle de réaction-diffusion-reproduction d'une population, répartie de manière hétérogène en espace. Le phénotype de chaque individu caractérise sa dispersion spatiale. Dans le cas d'un mode de reproduction asexué, il a été prouvé dans la littérature que le front d'invasion de la population accélère lorsque le temps s'écoule (voir [10, 19]). Plus précisément, la position du front est proportionnelle à $t^{3/2}$, où t est le temps. Nous pouvons remplacer le terme de reproduction asexuée par un terme nonlocal, qui modélise une reproduction-mutation sexuée. Notre objectif était d'estimer formellement et numériquement l'accélération quand on change le mode de reproduction. Pour cela, nous avons fait l'hypothèse que la solution de l'équation de réaction-diffusion-reproduction est une gaussienne à chaque instant. Ainsi, en changeant de variables et d'inconnue, nous avons pu nous ramener à l'étude d'une équation de Hamilton-Jacobi. De plus, nous avons effectué des simulations numériques pour étudier la dynamique de la solution en temps long. La difficulté, tant dans l'analyse formelle que dans l'analyse mathématique, provient du terme de reproduction nonlocal.

Chapter 2

Mean-field limit of a spatially-extended FitzHugh-Nagumo neural network

Contents

Abstract

We consider a spatially-extended model for a network of interacting FitzHugh-Nagumo neurons without noise, and rigorously establish its mean-field limit towards a nonlocal transport equation as the number of neurons goes to infinity. Our approach is based on deterministic methods, and namely on the stability of the solutions of the mean-field equation with respect to their initial data. The main difficulty lies in the adaptation in a deterministic framework of arguments previously introduced for the mean-field limit of stochastic systems of interacting particles with a certain class of locally Lipschitz continuous interaction kernels. This result establishes a rigorous link between the microscopic and mesoscopic scales of observation of the network, which can be further used as an intermediary step to derive macroscopic models. We also propose a numerical scheme for the discretization of the solutions of the mean-field model, based on a particle method, in order to study the dynamics of its solutions, and to compare it with the microscopic model.

2.1 Introduction

The interest of the analysis of neural networks is to study the collective behaviour of large assemblies of neurons. Consequently, even if microscopic models can accurately provide information on a finite-size neural network, they are too costly to consider a realistic amount of neurons. Therefore, the first step for the derivation of mesoscopic and macroscopic descriptions of neural networks is to consider that there are an infinite number of neurons, which leads to consider the mean-field limit (see [5, 15, 40, 41, 54, 103, 106, 123–126] for instance).

In this chapter, we adress the mean-field limit of the spatially-extended FHN system for a finite size neuronal network, as the number of neurons $n \in \mathbb{N}$ goes to infinity. Each neuron in the network is indexed by $i \in \{1, ..., n\}$, and characterized by a pair voltage-adaptation $(v_i, w_i) \in \mathbb{R}^2$ and a spatial position $\mathbf{x}_i \in \mathbb{R}^d$ with $d \in \{1, 2, 3\}$. The FHN system reads

$$\begin{cases} \dfrac{\mathrm{d}\mathbf{x}_i}{\mathrm{d}t} &= 0, \\ \dfrac{\mathrm{d}v_i}{\mathrm{d}t} &= N(v_i) - w_i - \dfrac{1}{n}\sum_{j=1}^n \Phi(\mathbf{x}_i, \mathbf{x}_j)(v_i - v_j), \\ \dfrac{\mathrm{d}w_i}{\mathrm{d}t} &= \tau\,(v_i + a - b\,w_i), \end{cases} \tag{2.1.1}$$

where $\Phi : \mathbb{R}^{2d} \to \mathbb{R}$ is a connectivity weight which models the influence of the positions of two neurons on their interactions, and N is a nonlinear function which models the cell excitability. A typical choice for the nonlinearity N (see for instance [5, 15, 106, 108]) is the cubic function

$$N : v \mapsto v\,(\alpha - \beta\,v^2), \tag{2.1.2}$$

for any $\alpha, \beta \geq 0$. The classical method to derive a mean-field description from an individually based model is to study the time evolution at each location of the probability of finding neurons characterized by a certain couple potential-adaptation variable. The framework of this approach is to work in a probability measure set independent on the number of neurons. Thus, we consider empirical measures associated with solutions of (2.1.1). Let us highlight that an empirical measure is a probability measure on $\mathbb{R}^{d+2}$. Our purpose is thus to prove the convergence of the empirical measures associated to the solutions of the FHN system (2.1.1) towards $f(t, \mathrm{d}\mathbf{x}, \mathrm{d}v, \mathrm{d}w)$ is the probability measure of finding neurons in an elementary volume of size $\mathrm{d}\mathbf{x}$ with a potential membrane and an adaptation variable in an elementary interval respectively of length $\mathrm{d}v$ and $\mathrm{d}w$ at time $t \geq 0$ within the cortex. Such a probability measure f satisfying the nonlocal transport

equation :

$$\partial_t f + \partial_v \left(f \left[N(v) - w - \mathcal{K}[f] \right] \right) + \partial_w \left(f \, A(v, w) \right) = 0, \quad t > 0, \quad (\mathbf{x}, v, w) \in \mathbb{R}^{d+2}, \qquad (2.1.3)$$

where

$$\begin{cases} \mathcal{K}[f](t, \mathbf{x}, v) & := \displaystyle\int_{\mathbb{R}^{d+2}} \Phi(\mathbf{x}, \mathbf{x}')(v - v') f(t, d\mathbf{x}', dv', dw'), \\[2mm] A(v, w) & := \tau \, (v + a - b \, w). \end{cases}$$

Let us comment the mean-field equation (2.1.3). The term $-\partial_v \left(f \mathcal{K}[f] \right)$ describes nonlocal interactions through the whole network, and $\partial_v \left(f(N(v) - w) \right) + \partial_w \left(f \, A(v, w) \right)$ accounts for the local reaction due to the excitability of nerve cells. Since this PDE can be written in a divergence form, we directly have the conservation of mass, which leads us to complement (2.1.3) with an initial condition:

$$f(0, \cdot) = f_0. \qquad (2.1.4)$$

It is worth noticing that for all $n \in \mathbb{N}$, for all n-tuples $\mathbf{X}_n = (\mathbf{x}_i)_{1 \le i \le n} \in (\mathbb{R}^d)^n$, $V_n = (v_i)_{1 \le i \le n} \in \mathbb{R}^n$ and $W_n = (w_i)_{1 \le i \le n} \in \mathbb{R}^n$, $(\mathbf{X}_n, V_n, W_n)$ is a solution to the spatially-extended FHN system (2.1.1) if and only if the associated empirical measure f_n is a solution to the transport equation (2.1.3).

The derivation of the transport equation (2.1.3) joins a large literature in mathematical neuroscience and kinetic theory. Indeed, the problem of the mean-field limit of systems of interacting particles towards kinetic models has been widely investigated, varying the types of interactions. We mention the work of Dobrushin [57], who introduced some classical methods to prove the mean-field limit of an individual-based model of interacting particles with a bounded globally Lipschitz continuous interaction kernel towards a Vlasov equation, using a stability result of the solutions to the kinetic model with respect to their initial data, in a suitable topology of probability measures. Such a stability result is called Dobrushin's estimate. See for instance [75] for a more recent review of this approach. Then, similar results have been proved for a larger variety of interaction kernels. For example, in [81], the authors proved the mean-field limit towards a Vlasov equation, in the case where the interaction kernel has a singularity. Besides, in [13], the authors introduced an extension of the classical mean-field theory from [57] which also works for a certain class of locally Lipschitz continuous interaction kernels.

The main contribution of this chapter is the rigorous justification of the model (2.1.3) we considered in [49] as the mean-field limit of the FHN system (2.1.1). It provides a mesoscopic description of the neural network, which can be used as an intermediary step for the derivation of macroscopic models from the FHN system (2.1.1), as in [49]. Here, we work with an initial data for (2.1.3) which is not compactly supported in general, but with finite exponential moments. Even though the main mathematical methods that we use were introduced in [13], to our knowledge, they have not been applied for the FHN system in a deterministic and spatially structured framework. Furthermore, in order to display some numerical simulations of the mean-field model (2.1.3), we consider a numerical scheme for this model using a particle method, that is we consider a set of particles approximating the solution of the characteristic system associated to (2.1.3) instead of the finite-size model (2.1.1). It appears that for certain sets of parameters, we observe some dynamics usually expected for macroscopic models. We also compare this scheme with the FHN system (2.1.1), to get some numerical evidence of the relevance of the transport equation (2.1.3).

Here, in our framework the interaction kernel $(\mathbf{x}, \mathbf{y}, v) \mapsto \Phi(\mathbf{x}, \mathbf{y}) \, v$ is locally Lipschitz continuous but not globally because of the factor v. Indeed, it is Lipschitz continuous on every bounded sets of $\mathbb{R}^{d+1}$ but its Lipschitz constant goes to infinity with the diameter of the set considered. Therefore some terms of higher order arise in the computation of a Dobrushin's

estimate. Thus, we need additional assumptions to control these terms, and hence to compute a similar stability estimate. In the spirit of [13], we circumvent this issue with the estimate of exponential moments of the solution of the transport equation (2.1.3), and with an appropriate division of the set of integration in the nonlocal terms, to get a suitable estimate. We mention that in [30, 77], the authors tackled a similar difficulty for some kinetic models of collective motion, and they chose to work with compactly supported solutions specifically to overcome this problem, controling the growth of velocity support to construct measure solutions.

2.2 Main result

This section is devoted to the statement of our main result on the mean-field limit from the solution of the microscopic model (2.1.1) towards the solution of the equation (2.1.3) as the number of neurons n goes to infinity.

Before stating our main result, let us precisely define the notion of solution of the equation (2.1.3) we use in this chapter. In the following, we denote by $\mathcal{P}_2(\mathbb{R}^{d+2})$ the set of probability measures on $\mathbb{R}^{d+2}$ with finite moments of order 2.

Definition 2.2.1 (Measure solution of (2.1.3)). *Consider an initial data $f_0 \in \mathcal{P}_2(\mathbb{R}^{d+2})$. Let $T > 0$. Then, f is said to be a measure solution of (2.1.3) with initial data f_0 if $f \in \mathscr{C}([0,T], \mathcal{P}_2(\mathbb{R}^{d+2}))$ and for all $t \in [0,T]$,*

$$f(t) = \mathcal{Z}_{f_0}(t, \cdot) \# f_0,$$

where $\#$ is our notation for the push-forward[1], and $\mathcal{Z}_{f_0}$ is defined for all $t \in [0,T]$ and all $\mathbf{z} = (\mathbf{x}, v, w) \in \mathbb{R}^{d+2}$ through

$$\mathcal{Z}_{f_0}(t, \mathbf{z}) := (\mathbf{x}, \mathcal{V}_{f_0}(t, \mathbf{z}), \mathcal{W}_{f_0}(t, \mathbf{z})), \tag{2.2.1}$$

where $(\mathcal{V}_{f_0}, \mathcal{W}_{f_0})$ is a solution of the characteristic system associated to (2.1.3) for $t > 0$ and $\mathbf{z} = (\mathbf{x}, v, w) \in \mathbb{R}^{d+2}$:

$$\begin{cases} \partial_t \mathcal{V}(t, \mathbf{z}) = N(\mathcal{V}(t, \mathbf{z})) - \mathcal{W}(t, \mathbf{z}) \\ \qquad\qquad - \int \Phi(\mathbf{x}, \mathbf{x}') \left(\mathcal{V}(t, \mathbf{z}) - \mathcal{V}(t, \mathbf{z}') \right) f_0(\mathrm{d}\mathbf{x}', \mathrm{d}v', \mathrm{d}w'), \\ \partial_t \mathcal{W}(t, \mathbf{z}) = A(\mathcal{V}(t, \mathbf{z}), \mathcal{W}(t, \mathbf{z})), \\ \mathcal{V}(0, \mathbf{z}) = v, \quad \mathcal{W}(0, \mathbf{z}) = w. \end{cases} \tag{2.2.2}$$

Remark 2.2.2. *In the rest of this paper, for the sake of clarity, we will use the notation $\mathbf{z} = (\mathbf{x}, v, w) \in \mathbb{R}^{d+2}$ and $\mathbf{z}' = (\mathbf{x}', v', w') \in \mathbb{R}^{d+2}$.*

As we can expect from this notion of measure solution to (2.1.3), the regularity of the solution to the characteristic system (2.2.2) is crucial. Therefore, we need to clearly define our framework for the connectivity kernel Φ and the nonlinear function N to prove, on the one hand, the existence and uniqueness of solutions to the FHN system (2.1.1) and the transport equation

---

[1]For all h, map from $\mathbb{R}^{d+2}$ to itself, for all probability measure μ, the notation $\nu = h\#\mu$ is equivalent to

$$\int \mathbb{1}_B(z)\nu(\mathrm{d}z) = \int \mathbb{1}_B(h(y))\mu(\mathrm{d}y)$$

for all B measurable subset of $\mathbb{R}^{d+2}$.

(2.1.3), and on the other hand, to prove our result of mean-field limit. In the following, in the spirit of [13, 30], we choose a connectivity kernel $\Phi : \mathbb{R}^{2d} \to \mathbb{R}$ satisfying

$$\Phi \in \mathrm{Lip}_b(\mathbb{R}^{2d}), \tag{2.2.3}$$

where $\mathrm{Lip}_b(\mathbb{R}^{2d})$ is the set of bounded and globally Lipschitz continuous functions from $\mathbb{R}^{2d}$ to $\mathbb{R}$. In the following, we note $L > 0$ the Lipschitz constant of the connectivity kernel Φ, and

$$\|\Phi\|_\infty := \sup_{(\mathbf{x},\mathbf{y})} |\Phi(\mathbf{x},\mathbf{y})|.$$

Here, the Lipschitz continuity of the connectivity kernel is only a technical assumption. On the other hand, the choice of a bounded Φ seems to be reasonable from a biological viewpoint, since currents transmitted through synapses are bounded. We also choose a locally Lipschitz continuous nonlinearity $N : \mathbb{R} \to \mathbb{R}$ such that there exist two constants $\kappa, \tilde{\kappa} > 0$ satisfying:

$$\begin{cases} v\, N(v) \leq \kappa\, |v|^2 & \forall v \in \mathbb{R}, \\ (v - u)\, (N(v) - N(u)) \leq \tilde{\kappa}\, |v - u|^2 & \forall (v, u) \in \mathbb{R}^2. \end{cases} \tag{2.2.4}$$

Then, it remains to choose a suitable topology on $\mathcal{P}_2(\mathbb{R}^{d+2})$ to state our result of mean-field limit. The most convenient distance to describe the convergence of an empirical measure in such problems is the Wasserstein distance [13, 30, 75, 77], recalled in the next definition.

Definition 2.2.3 (Wasserstein distance of order 2). *Let μ and ν be two probability measures of $\mathbb{R}^{d+2}$ with finite moments of second order. The Wasserstein distance of order 2 between μ and ν is defined by*

$$d_2(\mu, \nu) = \left(\inf_{\pi \in \Lambda(\mu,\nu)} \iint_{\mathbb{R}^{d+2} \times \mathbb{R}^{d+2}} \|(\mathbf{x} - \mathbf{x}', v - v', w - w')\|^2\, \pi(\mathrm{d}\mathbf{x}, \mathrm{d}v, \mathrm{d}w, \mathrm{d}\mathbf{x}', \mathrm{d}v', \mathrm{d}w') \right)^{\frac{1}{2}},$$

where $\|(\mathbf{x}, v, w)\|$ stands for the euclidean norm of the vector $(\mathbf{x}, v, w)$ in $\mathbb{R}^{d+2}$ for all $\mathbf{x} \in \mathbb{R}^d$ and $(v, w) \in \mathbb{R}^2$, and $\Lambda(\mu, \nu)$ is the set of couplings of μ and ν, that is to say for all $\pi \in \Lambda(\mu, \nu)$, for all function $\varphi \in \mathscr{C}(\mathbb{R}^{d+2})$ such that $\varphi(\mathbf{z}) = \mathcal{O}(\|\mathbf{z}\|^2)$ as $\|\mathbf{z}\|$ goes to infinity,

$$\iint \varphi(\mathbf{x}, v, w)\, \pi(\mathrm{d}\mathbf{x}, \mathrm{d}v, \mathrm{d}w, \mathrm{d}\mathbf{x}', \mathrm{d}v', \mathrm{d}w') = \int \varphi(\mathbf{x}, v, w)\, \mu(\mathrm{d}\mathbf{x}, \mathrm{d}v, \mathrm{d}w),$$

and

$$\iint \varphi(\mathbf{x}', v', w')\, \pi(\mathrm{d}\mathbf{x}, \mathrm{d}v, \mathrm{d}w, \mathrm{d}\mathbf{x}', \mathrm{d}v', \mathrm{d}w') = \int \varphi(\mathbf{x}', v', w')\, \nu(\mathrm{d}\mathbf{x}', \mathrm{d}v', \mathrm{d}w').$$

In this paper, we choose to work with the Wasserstein distance of order 2 instead of 1 as in [30, 57, 75] to deal with the nonlinearity N, which naturally makes appear some moments of second order in v and w in the computation of the stability estimate.

Then, as explained in the introduction, to circumvent the issues caused by the class of interaction kernel we consider, even if it is not needed for the existence and uniqueness of a measure solution to (2.1.3), we make some assumptions on the initial data of the equation (2.1.3). Thus, we consider an initial data $f_0 \in \mathcal{P}_2(\mathbb{R}^{d+2})$ satisfying:

$$\int e^{\alpha_0 \langle v, w \rangle}\, f_0(\mathrm{d}\mathbf{x}, \mathrm{d}v, \mathrm{d}w) < +\infty, \tag{2.2.5}$$

for some constant $\alpha_0 > 0$, using the notation for all $(v, w) \in \mathbb{R}^2$:

$$\langle v, w \rangle := (1 + |v|^2 + |w|^2)^{1/2}. \tag{2.2.6}$$

Now, we have all the tools we need to state our main theorem.

Theorem 2.2.4 (Mean-field limit)**.** *We consider a connectivity kernel Φ satisfying* (2.2.3)*, and a locally Lipschitz continuous nonlinearity N satisfying* (2.2.4)*. Let $T > 0$.*

1. *Consider two initial data $f_{0,1}$ and $f_{0,2} \in \mathcal{P}_2(\mathbb{R}^{d+2})$ such that $d_2(f_{0,1}, f_{0,2}) < 1$. Assume that $f_{0,2}$ satisfies* (2.2.5) *for some constant $\alpha_0 > 0$. Further assume that there exist f_1 and $f_2 \in \mathscr{C}([0,T], \mathcal{P}_2(\mathbb{R}^{d+2}))$ two measure solutions of the equation* (2.1.3) *respectively with initial conditions $f_{0,1}$ and $f_{0,2}$. Then there exist two positive constants $C_T > 0$ and $K_T > 0$ such that for all $t \in [0,T]$,*

$$d_2(f_1(t), f_2(t)) \leq K_T \, d_2(f_{0,1}, f_{0,2})^{\beta(t)}, \tag{2.2.7}$$

   where $\beta(t) := e^{-C_T \, t}$.

2. *For all $n \in \mathbb{N}$, consider the initial data $(\mathbf{x}_i, v_{0,i}, w_{0,i})_{1 \leq i \leq n} \in \left(\mathbb{R}^{d+2}\right)^n$ and its associated empirical measure $f_{0,n}$. Consider an initial data $f_0 \in \mathcal{P}_2(\mathbb{R}^{d+2})$. Then, for all $n \in \mathbb{N}$, there exists a unique solution $(\mathbf{x}_i, v_i, w_i)_{1 \leq i \leq n} \in \left(\mathbb{R}^{d+2}\right)^n$ of the FHN system* (2.1.1) *with initial data $(\mathbf{x}_i, v_{0,i}, w_{0,i})_{1 \leq i \leq n}$, and for all $t \in [0,T]$, we note its associated empirical measures $f_n(t)$. There also exists a unique measure solution $f \in \mathscr{C}([0,T], \mathcal{P}_2(\mathbb{R}^{d+2}))$ to* (2.1.3) *with initial data f_0. Further assume that f_0 satisfies* (2.2.5) *for some positive constant $\alpha_0 > 0$ and that*

$$\lim_{n \to +\infty} d_2(f_{0,n}, f_0) = 0. \tag{2.2.8}$$

   Then, we get:

$$\lim_{n \to +\infty} \sup_{t \in [0,T]} d_2(f_n(t), f(t)) = 0. \tag{2.2.9}$$

Remark 2.2.5. *Let us discuss the dependance of the two constants C_T and K_T mentioned in Theorem* 2.2.4 *(i) with respect to the initial data. First of all, C_T and K_T depend on T, N, τ, a, b, and on the exponential moment of only one of the two initial data, say $f_{0,2}$. Actually, we need the assumption $d_2(f_{0,1}, f_{0,2}) < 1$ so that K_T does not depend on the Wasserstein distance between the two initial data.*

The proof of Theorem 2.2.4 is postponed to Section 2.5. The first part (i) is the stability result of the measure solutions to (2.1.3) with respect to their initial data. Our approach follows the idea from [13, 30, 57, 75]. Indeed, the main difficulty comes from the interaction kernel of the form $(\mathbf{x}, \mathbf{x}', v) \mapsto \Phi(\mathbf{x}, \mathbf{x}') \, v$, which is only locally Lipschitz continuous.

As for the second part (ii), the existence and uniqueness of the FHN system (2.1.1) follows from the Cauchy-Lipschitz Theorem, and the proof of the well-posedness of the transport equation (2.1.3) relies on the well-posedness of the characteristic system (2.2.2) using classical arguments as in [75]. Then, the mean-field limit from (2.1.1) towards (2.1.3) is just a consequence of the first part (i).

Remark 2.2.6. *We can extend the result of existence and uniqueness of the solution to* (2.1.1) *and the Definition* 2.2.1 *of measure solutions of* (2.1.3) *to the case where Φ is only bounded and continuous with respect to its first variable uniformly relative to its second variable.*

The rest of this paper is organized as follows. In Section 2.3, we prove an *a priori* estimate for the solution of the transport equation (2.1.3) which will be crucial for the proof of Theorem 2.2.4. Then, in Section 2.4, we present the proof of the existence and uniqueness of the measure solution of the equation (2.1.3). Furthermore, we prove our main result of mean-field limit in Section 2.5 and present as an application a stability result regarding monokinetic solutions in the following Section 2.6. Finally, in Section 2.7, we provide a numerical scheme for the transport equation (2.1.3) based on a particle method, and we display some numerical simulations, to illustrate the results established in Sections 2.5 and 2.6, and to show that this numerical scheme accurately reproduces the behavior of a large neural network.

2.3 *A priori* estimate

The purpose of this section is to prove an *a priori* estimate of the exponential moments of a solution of the equation (2.1.3). But first, we start by proving a technical lemma which will be useful all along the rest of the chapter. We will need to work with the characteristic system (2.2.2). In Section 2.4, we will prove that for all $T > 0$, the characteristics are well-defined in $\mathscr{C}([0, T], \mathcal{E})$, where

$$\mathcal{E} := \left\{ \mathcal{U} \in \mathscr{C}(\mathbb{R}^{d+2}, \mathbb{R}) \mid \|\mathcal{U}\|_{\mathcal{E}} < \infty \right\}, \tag{2.3.1}$$

with

$$\|\mathcal{U}\|_{\mathcal{E}} := \sup_{(\mathbf{x}, v, w) \in \mathbb{R}^{d+2}} \frac{|\mathcal{U}(\mathbf{x}, v, w)|}{\langle v, w \rangle}. \tag{2.3.2}$$

This choice of Banach space is justified since in general, the characteristics are not bounded, so we need to control some moments in v and w.

Lemma 2.3.1 (Technical lemma). *Let $T > 0$. We consider a connectivity kernel Φ satisfying (2.2.3) and a locally Lipschitz continuous nonlinearity N satisfying (2.2.4). Let $f_{0,1}$ and $f_{0,2} \in \mathcal{P}(\mathbb{R}^{d+2})$, and $\mathcal{U}_1$ and $\mathcal{U}_2 \in \mathscr{C}([0, T], \mathcal{E})$. Assume that for all $i \in \{1, 2\}$, there exists $(\mathcal{V}_i, \mathcal{W}_i)$ in $\mathscr{C}([0, T], \mathcal{E})^2$ of class $\mathscr{C}^1$ in time, such that for all $t \in (0, T]$ and $\mathbf{z} = (\mathbf{x}, v, w) \in \mathbb{R}^{d+2}$, the couple $(\mathcal{V}_i, \mathcal{W}_i)$ satisfies*

$$\begin{cases} \partial_t \mathcal{V}_i(t, \mathbf{z}) = N(\mathcal{V}_i(t, \mathbf{z})) - \mathcal{W}_i(t, \mathbf{z}) - \int \Phi(\mathbf{x}, \mathbf{x}') \left(\mathcal{U}_i(t, \mathbf{z}) - \mathcal{U}_i(t, \mathbf{z}') \right) f_{0,i}(\mathrm{d}\mathbf{z}'), \\[2mm] \partial_t \mathcal{W}_i(t, \mathbf{z}) = A(\mathcal{V}_i(t, \mathbf{z}), \mathcal{W}_i(t, \mathbf{z})), \\[2mm] \mathcal{V}_i(0, \mathbf{z}) = v, \quad \mathcal{W}_i(0, \mathbf{z}) = w. \end{cases}$$

Then, we have for all $t \in [0, T]$ and all $\mathbf{z} = (\mathbf{x}, v, w) \in \mathbb{R}^{d+2}$:

$$\frac{1}{2} \partial_t \left(|\mathcal{V}_i(t, \mathbf{z})|^2 + |\mathcal{W}_i(t, \mathbf{z})|^2 \right)$$
$$\leq \left(\kappa + \frac{1}{2} + \tau \right) \left(|\mathcal{V}_i(t, \mathbf{z})|^2 + |\mathcal{W}_i(t, \mathbf{z})|^2 \right) + \frac{\tau a^2}{2} + \mathcal{T}_{nl,i}(t), \tag{2.3.3}$$

$$\frac{1}{2} \partial_t \left(|\mathcal{V}_1(t, \mathbf{z}) - \mathcal{V}_2(t, \mathbf{z})|^2 + |\mathcal{W}_1(t, \mathbf{z}) - \mathcal{W}_2(t, \mathbf{z})|^2 \right)$$
$$\leq \left(\tilde{\kappa} + \frac{\tau + 1}{2} \right) \left(|\mathcal{V}_1(t, \mathbf{z}) - \mathcal{V}_2(t, \mathbf{z})|^2 + |\mathcal{W}_1(t, \mathbf{z}) - \mathcal{W}_2(t, \mathbf{z})|^2 \right) + \mathcal{T}_{nl,12}(t), \tag{2.3.4}$$

where κ and $\tilde{\kappa}$ are the two constants defined in (2.2.4), and for all $t \in [0, T]$, for all $i \in \{1, 2\}$, using the shorthand $\mathcal{U}_i = \mathcal{U}_i(t, \mathbf{z})$ and $\mathcal{U}_i' = \mathcal{U}_i(t, \mathbf{z}')$,

$$\begin{cases} \mathcal{T}_{nl,i}(t) := -\mathcal{V}_i(t, \mathbf{z}) \int \Phi(\mathbf{x}, \mathbf{x}') \left[\mathcal{U}_i - \mathcal{U}_i' \right] f_{0,i}(\mathrm{d}\mathbf{z}'), \\[2mm] \mathcal{T}_{nl,12}(t) := -(\mathcal{V}_1(t, \mathbf{z}) - \mathcal{V}_2(t, \mathbf{z})) \\[1mm] \qquad \times \left(\int \Phi(\mathbf{x}, \mathbf{x}') \left[\mathcal{U}_1 - \mathcal{U}_1' \right] f_{0,1}(\mathrm{d}\mathbf{z}') - \int \Phi(\mathbf{x}, \mathbf{x}') \left[\mathcal{U}_2 - \mathcal{U}_2' \right] f_{0,2}(\mathrm{d}\mathbf{z}') \right). \end{cases}$$

Proof. The proof is straightforward, and mainly lies on Young's inequality and the properties (2.2.4) satisfied by the nonlinearity N. $\square$

Now, let us prove the *a priori* estimate of the exponential moments.

Lemma 2.3.2. *Let $T > 0$. We consider a connectivity kernel Φ satisfying (2.2.3) and a locally Lipschitz continuous nonlinearity N satisfying (2.2.4). Let $p \geq 1$. Consider an initial data $f_0 \in \mathcal{P}_2(\mathbb{R}^{d+2})$ satisfying (2.2.5) for some $\alpha_0 > 0$. Assume that there exists $f \in \mathscr{C}([0,T], \mathcal{P}_2(\mathbb{R}^{d+2}))$ a measure solution of (2.1.3) and a couple $(\mathcal{V}_{f_0}, \mathcal{W}_{f_0}) \in \mathscr{C}([0,T], \mathcal{E})^2$ solution of the characteristic system (2.2.2), such that if we define $\mathcal{Z}_{f_0} := (id_{\mathbb{R}^d}, \mathcal{V}_{f_0}, \mathcal{W}_{f_0})$, then for all $t \in [0,T]$,*

$$f(t) = \mathcal{Z}_{f_0}(t) \# f_0.$$

Then, there exists a constant $C_{f_0}^T > 0$ which depends only on the parameters of the equation (2.1.3), on T and on the moments of f_0, such that for all $t \in [0,T]$, if we define $\alpha(t) := \alpha_0 \, e^{-p \, C_{f_0}^T \, T}$, we have:

$$\int e^{\alpha(t) \, \langle v, w \rangle^p} f(t, \mathrm{d}\mathbf{x}, \mathrm{d}v, \mathrm{d}w) \leq \int e^{\alpha_0 \, \langle v, w \rangle^p} f_0(\mathrm{d}\mathbf{x}, \mathrm{d}v, \mathrm{d}w). \tag{2.3.5}$$

Proof. Consider $\alpha \in \mathscr{C}^1([0,T], \mathbb{R})$ a positive function to be determined later. Let $t \in [0,T]$. According to the inequality (2.3.3) from Lemma 2.3.1, we have the following estimate:

$$\frac{1}{2} \frac{\mathrm{d}}{\mathrm{d}t} \int e^{\alpha(t) \, \langle \mathcal{V}_{f_0}(t,\mathbf{z}), \mathcal{W}_{f_0}(t,\mathbf{z}) \rangle^p} f_0(\mathrm{d}\mathbf{z}) \leq \int \left[\frac{1}{2} \alpha'(t) \, \langle \mathcal{V}_{f_0}(t,\mathbf{z}), \mathcal{W}_{f_0}(t,\mathbf{z}) \rangle^p \right.$$
$$\left. + \frac{p}{2} \alpha(t) \, \langle \mathcal{V}_{f_0}(t,\mathbf{z}), \mathcal{W}_{f_0}(t,\mathbf{z}) \rangle^{p-2} \left(\mathcal{T}_l(t) + \mathcal{T}_{nl}(t) \right) \right] e^{\alpha(t) \, \langle \mathcal{V}_{f_0}(t,\mathbf{z}), \mathcal{W}_{f_0}(t,\mathbf{z}) \rangle^p} f_0(\mathrm{d}\mathbf{z}),$$

where

$$\begin{cases} \mathcal{T}_l(t) := \left(\kappa + \dfrac{1}{2} + \tau \right) \left(|\mathcal{V}_{f_0}(t,\mathbf{z})|^2 + |\mathcal{W}_{f_0}(t,\mathbf{z})|^2 \right) + \dfrac{\tau \, a^2}{2}, \\[2mm] \mathcal{T}_{nl}(t) := - \mathcal{V}_{f_0}(t,\mathbf{z}) \displaystyle\int \Phi(\mathbf{x}, \mathbf{x}') \left[\mathcal{V}_{f_0}(t,\mathbf{z}) - \mathcal{V}_{f_0}(t,\mathbf{z}') \right] f_0(\mathrm{d}\mathbf{z}'). \end{cases}$$

First of all, we can easily estimate the first term $\mathcal{T}_l(t)$ factorizing by $|\langle \mathcal{V}_{f_0}(t,\mathbf{z}), \mathcal{W}_{f_0}(t,\mathbf{z}) \rangle|^2$ as follows:

$$\mathcal{T}_l(t) \leq \left(\frac{(2 + a^2) \, \tau + 1}{2} + \kappa \right) |\langle \mathcal{V}_{f_0}(t,\mathbf{z}), \mathcal{W}_{f_0}(t,\mathbf{z}) \rangle|^2.$$

Then, we treat the second term $\mathcal{T}_{nl}(t)$ using the moment estimate (2.2.5) satisfied by f_0, with Young's inequality and then factorizing by $|\langle \mathcal{V}_{f_0}(t,\mathbf{z}), \mathcal{W}_{f_0}(t,\mathbf{z}) \rangle|^2$ as follows:

$$\mathcal{T}_{nl}(t) \leq \frac{3}{2} |\mathcal{V}_{f_0}(t,\mathbf{z})|^2 \int |\Phi(\mathbf{x}, \mathbf{x}')| f_0(\mathrm{d}\mathbf{z}') + \frac{1}{2} \int |\Phi(\mathbf{x}, \mathbf{x}')| |\mathcal{V}_{f_0}(t,\mathbf{z}')|^2 f_0(\mathrm{d}\mathbf{z}')$$
$$\leq \frac{1}{2} \|\Phi\|_\infty \left(3 \, |\mathcal{V}_{f_0}(t,\mathbf{z})|^2 + \int |\mathcal{V}_{f_0}(t,\mathbf{z}')|^2 f_0(\mathrm{d}\mathbf{z}') \right)$$
$$\leq \frac{1}{2} \|\Phi\|_\infty \left(3 + \sup_{s \in [0,T]} \|\mathcal{V}_{f_0}(s)\|_{\mathcal{E}}^2 \int |\langle v', w' \rangle|^2 f_0(\mathrm{d}\mathbf{z}') \right)$$
$$\times |\langle \mathcal{V}_{f_0}(t,\mathbf{z}), \mathcal{W}_{f_0}(t,\mathbf{z}) \rangle|^2.$$

Finally, we get that there exists a positive constant $C_{f_0}^T > 0$ such that:

$$\frac{1}{2} \frac{\mathrm{d}}{\mathrm{d}t} \int e^{\alpha(t) \, \langle \mathcal{V}_{f_0}(t,\mathbf{z}), \mathcal{W}_{f_0}(t,\mathbf{z}) \rangle^p} f_0(\mathrm{d}\mathbf{z})$$
$$\leq \int \left[\frac{1}{2} \alpha'(t) + \frac{p}{2} C_{f_0}^T \, \alpha(t) \right] \langle \mathcal{V}_{f_0}(t,\mathbf{z}), \mathcal{W}_{f_0}(t,\mathbf{z}) \rangle^p \, e^{\alpha(t) \, \langle \mathcal{V}_{f_0}(t,\mathbf{z}), \mathcal{W}_{f_0}(t,\mathbf{z}) \rangle^p} f_0(\mathrm{d}\mathbf{z}).$$

We choose for all $s \in [0, T]$, $\alpha(s) := \alpha_0 \, e^{-p \, C_{f_0}^T \, s}$, so that for all $s \in [0, T]$,

$$\alpha'(s) + p \, C_{f_0}^T \, \alpha(s) = 0, \quad \alpha(0) = \alpha_0.$$

Hence,

$$\frac{\mathrm{d}}{\mathrm{d}t} \int e^{\alpha(t) \, \langle \mathcal{V}_{f_0}(t, \mathbf{z}), \mathcal{W}_{f_0}(t, \mathbf{z}) \rangle^p} f_0(\mathrm{d}\mathbf{z}) \leq 0.$$

Consequently, to conclude the proof, we integrate this last inequality between 0 and $t \in [0, T]$ to get the estimate (2.3.5). $\qquad \square$

2.4 Proof of the well-posedness of the mean-field equation (2.1.3)

This section is devoted to the proof of existence and uniqueness of a measure solution to the transport equation (2.1.3), in the sense of Definition 2.2.1. Let $T > 0$ be a fixed final time and $f_0 \in \mathcal{P}_2(\mathbb{R}^{d+2})$. First, we focus on the well-posedness of the characteristic system (2.2.2), and then we will conclude by defining the measure solution to (2.1.3) as the push-forward of the initial data by the solution of the characteristic system.

2.4.1 Proof of the well-posedness of the characteristic system (2.2.2)

As a preliminary step, we establish the existence and uniqueness of the solution of the characteristic system (2.2.2) in $\mathscr{C}([0, T], \mathcal{E})$, where $\mathcal{E}$ is defined with (2.3.1)-(2.3.2).

Proposition 2.4.1. *Let $T > 0$. Consider an initial data $f_0 \in \mathcal{P}_2(\mathbb{R}^{d+2})$. Then, there exists a unique couple $(\mathcal{V}_{f_0}, \mathcal{W}_{f_0})$ solution of (2.2.2) on $[0, T]$ such that*

$$\mathcal{V}_{f_0}, \mathcal{W}_{f_0} \in \mathscr{C}([0, T], \mathcal{E}).$$

Proof. Since we cannot directly conclude with the Cauchy-Lipschitz theorem because of the term resulting from the nonlocal interactions in (2.2.2), our approach is based on the construction of a Cauchy sequence $(\mathcal{V}_p, \mathcal{W}_p)_{p \in \mathbb{N}}$ in $\mathscr{C}([0, T], \mathcal{E})$, in order to circumvent this difficulty. Then, we will define the couple $(\mathcal{V}_{f_0}, \mathcal{W}_{f_0})$ as its limit as p tends to infinity.

Step 1: construction of the sequences

First, we prove the following lemma, which yields the existence and uniqueness of the solution of a system of equations approximating (2.2.2), in which we consider the contribution of the interactions as a source term.

Lemma 2.4.2. *Let $T > 0$. Consider $f_0 \in \mathcal{P}(\mathbb{R}^{d+2})$, and let $\mathcal{U} \in \mathscr{C}([0, T], \mathcal{E})$. Then, there exists a unique couple $(\mathcal{V}, \mathcal{W}) \in \mathscr{C}([0, T], \mathcal{E})^2$ solution of class $\mathscr{C}^1$ in time of the following system for $t > 0$ and $\mathbf{z} = (\mathbf{x}, v, w) \in \mathbb{R}^{d+2}$:*

$$\begin{cases} \partial_t \mathcal{V}(t, \mathbf{z}) = N(\mathcal{V}(t, \mathbf{z})) - \mathcal{W}(t, \mathbf{z}) - \displaystyle\int \Phi(\mathbf{x}, \mathbf{x}')(\mathcal{U}(t, \mathbf{z}) - \mathcal{U}(t, \mathbf{z}')) \, f_0(\mathrm{d}\mathbf{z}'), \\[2mm] \partial_t \mathcal{W}(t, \mathbf{z}) = A(\mathcal{V}(t, \mathbf{z}), \mathcal{W}(t, \mathbf{z})), \\[2mm] \mathcal{V}(0, \mathbf{z}) = v, \quad \mathcal{W}(0, \mathbf{z}) = w. \end{cases} \qquad (2.4.1)$$

The proof of Lemma 2.4.2 only relies on classical arguments, but for the sake of completeness, it is postponed to the Appendix 2.9. Then, by induction, Lemma 2.4.2 implies the existence and uniqueness of a sequence $(\mathcal{V}_p, \mathcal{W}_p)_{p \in \mathbb{N}}$, such that $(\mathcal{V}_0, \mathcal{W}_0) := (0, 0)$, and for all $p \in \mathbb{N}$, for all $t \in [0, T]$ and $\mathbf{z} = (\mathbf{x}, v, w) \in \mathbb{R}^{d+2}$,

$$
\begin{cases}
\mathcal{V}_{p+1}(t, \mathbf{z}) = v + \int_0^t \Big[N(\mathcal{V}_{p+1}(s, \mathbf{z})) - \mathcal{W}_{p+1}(s, \mathbf{z}) \\
\qquad\qquad\qquad\qquad - \int \Phi(\mathbf{x}, \mathbf{x}')(\mathcal{V}_p(s, \mathbf{z}) - \mathcal{V}_p(s, \mathbf{z}'))\, f_0(\mathrm{d}\mathbf{z}') \Big]\, \mathrm{d}s, \\
\mathcal{W}_{p+1}(t, \mathbf{z}) = w + \int_0^t A(\mathcal{V}_{p+1}(s, \mathbf{z}), \mathcal{W}_{p+1}(s, \mathbf{z}))\, \mathrm{d}s.
\end{cases} \tag{2.4.2}
$$

Step 2: Cauchy sequences

Now, we want to prove that for all $t \in [0, T]$, $\{\mathcal{V}_p(t)\}_{p \in \mathbb{N}}$ and $\{\mathcal{W}_p(t)\}_{p \in \mathbb{N}}$ are two Cauchy sequences in $\mathcal{E}$. For all $p \in \mathbb{N}$, we define:

$$
G_{p+1}(t) := \left(\|\mathcal{V}_{p+1}(t) - \mathcal{V}_p(t)\|_{\mathcal{E}}^2 + \|\mathcal{W}_{p+1}(t) - \mathcal{W}_p(t)\|_{\mathcal{E}}^2 \right)^{\frac{1}{2}},
$$

and we want to prove by induction that this quantity is summable. Let $p \in \mathbb{N}$, $t \in [0, T]$ and $\mathbf{z} = (\mathbf{x}, v, w)$. Thus, according to the inequality (2.3.4) from Lemma 2.3.1, we have:

$$
\frac{1}{2} \left(|\mathcal{V}_{p+2}(t, \mathbf{z}) - \mathcal{V}_{p+1}(t, \mathbf{z})|^2 + |\mathcal{W}_{p+2}(t, \mathbf{z}) - \mathcal{W}_{p+1}(t, \mathbf{z})|^2 \right) \leq \int_0^t [\mathcal{T}_l(s) + \mathcal{T}_{nl}(s)]\, \mathrm{d}s,
$$

where for all $s \in [0, t]$,

$$
\begin{cases}
\mathcal{T}_l(s) := \left(\tilde{\kappa} + \dfrac{\tau + 1}{2} \right) \\
\qquad\qquad \times \left(|\mathcal{V}_{p+2}(t, \mathbf{z}) - \mathcal{V}_{p+1}(t, \mathbf{z})|^2 + |\mathcal{W}_{p+2}(t, \mathbf{z}) - \mathcal{W}_{p+1}(t, \mathbf{z})|^2 \right), \\
\mathcal{T}_{nl}(s) := -\left(\mathcal{V}_{p+2}(s, \mathbf{z}) - \mathcal{V}_{p+1}(s, \mathbf{z}) \right) \\
\qquad\qquad \times \int \Phi(\mathbf{x}, \mathbf{x}') \left[(\mathcal{V}_{p+1}(s, \mathbf{z}) - \mathcal{V}_{p+1}(s, \mathbf{z}')) - (\mathcal{V}_p(s, \mathbf{z}) - \mathcal{V}_p(s, \mathbf{z}')) \right]\, f_0(\mathrm{d}\mathbf{z}').
\end{cases}
$$

Let $s \in [0, t]$. The first term $\mathcal{T}_l(s)$ is easily controled factorizing by $|\langle v, w \rangle|^2 \geq 1$, and then taking the supremum on $\mathbb{R}^2$, as follows:

$$
\mathcal{T}_l(s) \leq \left(\tilde{\kappa} + \frac{\tau + 1}{2} \right) |\langle v, w \rangle|^2\, |G_{p+2}(s)|^2 \tag{2.4.3}
$$

Then, to deal with the nonlocal term $\mathcal{T}_{nl}(s)$, using the boundedness of Φ and Young's inequality, we can compute:

$$
\begin{aligned}
\mathcal{T}_{nl}(s) &= \left(\mathcal{V}_{p+2}(s, \mathbf{z}) - \mathcal{V}_{p+1}(s, \mathbf{z}) \right) \\
&\quad \times \int \Phi(\mathbf{x}, \mathbf{x}') \left[(\mathcal{V}_{p+1}(s, \mathbf{z}') - \mathcal{V}_p(s, \mathbf{z}')) - (\mathcal{V}_{p+1}(s, \mathbf{z}) - \mathcal{V}_p(s, \mathbf{z})) \right]\, f_0(\mathrm{d}\mathbf{z}') \\
&\leq \frac{1}{2} |\mathcal{V}_{p+2}(s, \mathbf{z}) - \mathcal{V}_{p+1}(s, \mathbf{z})|^2 \\
&\quad + \frac{1}{2} \|\Phi\|_\infty^2 \int \left(|\mathcal{V}_{p+1}(s, \mathbf{z}') - \mathcal{V}_p(s, \mathbf{z}')|^2 + |\mathcal{V}_{p+1}(s, \mathbf{z}) - \mathcal{V}_p(s, \mathbf{z})|^2 \right)\, f_0(\mathrm{d}\mathbf{z}').
\end{aligned}
$$

Moreover, factorizing each term with $|\langle v, w \rangle|^2$, we get:

$$
\begin{aligned}
\mathcal{T}_{nl}(s) &\leq \frac{1}{2} |\langle v, w \rangle|^2\, \|\mathcal{V}_{p+2}(s) - \mathcal{V}_{p+1}(s)\|_{\mathcal{E}}^2 \\
&\quad + \frac{1}{2} \|\Phi\|_\infty^2 \left(\int |\langle v', w' \rangle|^2\, f_0(\mathrm{d}\mathbf{z}') + |\langle v, w \rangle|^2 \right) \|\mathcal{V}_{p+1}(s) - \mathcal{V}_p(s)\|_{\mathcal{E}}^2 \\
&\leq \frac{1}{2} |\langle v, w \rangle|^2 \left[|G_{p+2}(s)|^2 + \|\Phi\|_\infty^2 \left(\int |\langle v', w' \rangle|^2\, f_0(\mathrm{d}\mathbf{z}') + 1 \right) |G_{p+1}(s)|^2 \right] \tag{2.4.4}
\end{aligned}
$$

Finally, the estimates (2.4.3) and (2.4.4) together yield that there exist two positive constants $C_1 > 0$ and $C_2 > 0$ independent of p such that:

$$|\mathcal{V}_{p+2}(t, \mathbf{z}) - \mathcal{V}_{p+1}(t, \mathbf{z})|^2 \, + \, |\mathcal{W}_{p+2}(t, \mathbf{z}) - \mathcal{W}_{p+1}(t, \mathbf{z})|^2$$
$$\leq |\langle v, w \rangle|^2 \left[C_1 \int_0^t |G_{p+1}(s)|^2 \, \mathrm{d}s \, + \, C_2 \int_0^t |G_{p+2}(s)|^2 \, \mathrm{d}s \right],$$

which implies, by dividing this inequality by $|\langle v, w \rangle|^2$ and then taking the supremum on $\mathbb{R}^{d+2}$:

$$|G_{p+2}(t)|^2 \, \leq \, C_1 \int_0^t |G_{p+1}(s)|^2 \, \mathrm{d}s \, + \, C_2 \int_0^t |G_{p+2}(s)|^2 \, \mathrm{d}s. \tag{2.4.5}$$

On the one hand, one can check with a straightforward induction argument that G_{p+2} is continuous with respect to time. Hence, using Grönwall's lemma, we have for all $t \in [0, T]$:

$$|G_{p+2}(t)|^2 \, \leq \, C_1 \, e^{C_2 T} \int_0^t |G_{p+1}(s)|^2 \, \mathrm{d}s. \tag{2.4.6}$$

On the other hand, for all $t \in [0, T]$,

$$|G_1(t)|^2 \, = \, \|\mathcal{V}_1(t)\|_{\mathcal{E}}^2 \, + \, \|\mathcal{W}_1(t)\|_{\mathcal{E}}^2 \, \leq \, C_T, \tag{2.4.7}$$

for some constant $C_T > 0$, since $\mathcal{V}_1$ and $\mathcal{W}_1 \in \mathscr{C}([0, T], \mathcal{E})$ according to Lemma 2.4.2. Hence, by induction, we can deduce from (2.4.6) and (2.4.7) that for all $p \in \mathbb{N}$ and all $t \in [0, T]$:

$$|G_{p+1}(t)|^2 \, \leq \, C_T \frac{\left(C_1 \, e^{C_2 T} t \right)^p}{p!}, \tag{2.4.8}$$

which is summable. Consequently, for all $t \in [0, T]$, $\{\mathcal{V}_p(t)\}_{p \in \mathbb{N}}$ and $\{\mathcal{W}_p(t)\}_{p \in \mathbb{N}}$ are Cauchy sequences in $\mathcal{E}$. Since $\mathcal{E}$ is a Banach space, and since for all $p \in \mathbb{N}$, $\mathcal{V}_p$ and $\mathcal{W}_p \in \mathscr{C}([0, T], \mathcal{E})$, there exist $\mathcal{V}_{f_0}$ and $\mathcal{W}_{f_0} \in \mathscr{C}([0, T], \mathcal{E})$ such that for all $t \in [0, T]$, $\mathcal{V}_p(t, \cdot)$ (respectively $\mathcal{W}_p$) converges towards $\mathcal{V}_{f_0}(t, \cdot)$ (respectively $\mathcal{W}_{f_0}$) uniformly in $\mathcal{E}$. Thus, passing to the limit $p \to +\infty$ in (2.4.2), we get that for all $\mathbf{z} \in \mathbb{R}^{d+2}$, $(\mathcal{V}_{f_0}(\cdot, \mathbf{z}), \mathcal{W}_{f_0}(\cdot, \mathbf{z}))$ is a solution in $\mathscr{C}([0, T], \mathcal{E})^2$ of the characteristic system (2.2.2) in the integral form. Furthermore, since the nonlinearity N is locally Lipschitz continuous and $\mathcal{V}_{f_0}$ and $\mathcal{W}_{f_0}$ are continuous with respect to time, we directly have from the integral form of (2.2.2) that $(\mathcal{V}_{f_0}(\cdot, \mathbf{z}), \mathcal{W}_{f_0}(\cdot, \mathbf{z}))$ is of class $\mathscr{C}^1$ in time.

Step 3: Uniqueness

Now, we want to check that the solution of (2.2.2) is unique. Suppose that there exist $(\mathcal{V}_1, \mathcal{W}_1)$ and $(\mathcal{V}_2, \mathcal{W}_2)$ two solutions of (2.2.2) in $\mathscr{C}([0, T], \mathcal{E})^2$. We define for all $t \in [0, T]$:

$$G(t) \, := \, \left(\|\mathcal{V}_1(t) - \mathcal{V}_2(t)\|_{\mathcal{E}}^2 \, + \, \|\mathcal{W}_1(t) - \mathcal{W}_2(t)\|_{\mathcal{E}}^2 \right)^{\frac{1}{2}}. \tag{2.4.9}$$

Thus, using similar computations as previously, we get that there exists a positive constant C such that for all $t \in [0, T]$:

$$|G(t)|^2 \, \leq \, C \int_0^t |G(s)|^2 \, \mathrm{d}s.$$

Since $\mathcal{V}_i, \mathcal{W}_i$ are continuous with respect to time for $i \in \{1, 2\}$, using Grönwall's inequality, we get that $(V_1, W_1) = (V_2, W_2)$. $\qquad \square$

2.4.2 Construction of the measure solution to (2.1.3)

We have proved so far that there exists a unique map $\mathcal{Z}_{f_0} := (\text{id}_{\mathbb{R}^d}, \mathcal{V}_{f_0}, \mathcal{W}_{f_0})$ such that $(\mathcal{V}_{f_0}, \mathcal{W}_{f_0})$ is a solution of the characteristic system (2.2.2) in $\mathscr{C}([0, T], \mathcal{E})$. We define:

$$f : t \mapsto \mathcal{Z}_{f_0}(t) \# f_0. \tag{2.4.10}$$

Thus, for all $t \in [0, T]$:

$$\int \left(\|\mathbf{x}\|^2 + |v|^2 + |w|^2 \right) f(t, \mathrm{d}\mathbf{z}) = \int \left(\|\mathbf{x}\|^2 + |\mathcal{V}_{f_0}(t, \mathbf{z})|^2 + |\mathcal{W}_{f_0}(t, \mathbf{z})|^2 \right) f_0(\mathrm{d}\mathbf{z})$$

$$\leq \int \|\mathbf{x}\|^2 f_0(\mathrm{d}\mathbf{z}) + \left(\|\mathcal{V}_{f_0}(t)\|_{\mathcal{E}}^2 + \|\mathcal{W}_{f_0}(t)\|_{\mathcal{E}}^2 \right) \int |\langle v, w \rangle|^2 f_0(\mathrm{d}\mathbf{z}),$$

which is uniformly bounded. Hence, for all $t \in [0, T]$:

$$f(t) \in \mathcal{P}_2(\mathbb{R}^{d+2}).$$

Then, we want to prove that $f \in \mathscr{C}([0, T], \mathcal{P}_2(\mathbb{R}^{d+2}))$, where $\mathcal{P}_2(\mathbb{R}^{d+2})$ is equiped with the Wasserstein distance d_2. Let t and $t' \in [0, T]$. Notice that the measure $(\mathcal{Z}_{f_0}(t) \times \mathcal{Z}_{f_0}(t')) \# f_0 \in \Lambda(f(t), f(t'))$. Therefore, we have:

$$d_2^2(f(t), f(t')) = \inf_{\pi \in \Lambda(f(t), f(t'))} \iint |\mathbf{z}_1 - \mathbf{z}_2|^2 \, \pi(\mathrm{d}\mathbf{z}_1 \mathrm{d}\mathbf{z}_2)$$

$$\leq \int |\mathcal{Z}_{f_0}(t, \mathbf{z}) - \mathcal{Z}_{f_0}(t', \mathbf{z})|^2 f_0(\mathrm{d}\mathbf{z})$$

$$\leq \left(\|\mathcal{V}_{f_0}(t) - \mathcal{V}_{f_0}(t')\|_{\mathcal{E}}^2 + \|\mathcal{W}_{f_0}(t) - \mathcal{W}_{f_0}(t')\|_{\mathcal{E}}^2 \right) \int |\langle v, w \rangle|^2 f_0(\mathrm{d}\mathbf{z}).$$

Since $\mathcal{V}_{f_0}$ and $\mathcal{W}_{f_0} \in \mathscr{C}([0, T], \mathcal{E})$, and $f_0 \in \mathcal{P}_2(\mathbb{R}^{d+2})$, we have that:

$$f \in \mathscr{C}([0, T], \mathcal{P}_2(\mathbb{R}^{d+2})).$$

Hence, f is a measure solution of (2.1.3) in the sense of definition 2.2.1.

2.5 Proof of Theorem 2.2.4

This section is devoted to the proof of our main result Theorem 2.2.4. We start with the stability result (i). Our approach consists in using an estimate of the Wasserstein distance between two measure solutions of (2.1.3). Then, we will show how this stability result implies the mean-field limit result (ii).

2.5.1 Proof of the stability result

For $j \in \{1, 2\}$, we define the map $\mathcal{Z}_j$ such that for all $t \in [0, T]$ and all $\mathbf{z} = (\mathbf{x}, v, w) \in \mathbb{R}^{d+2}$:

$$\mathcal{Z}_j(t, \mathbf{z}) := (\mathbf{x}, \mathcal{V}_j(t, \mathbf{z}), \mathcal{W}_j(t, \mathbf{z})),$$

where $(\mathcal{V}_j, \mathcal{W}_j)$ is the solution of the characteritic system (2.2.2) with initial data $f_{0,j}$. $\mathcal{V}_j$ and $\mathcal{W}_j$ are in $\mathscr{C}([0, T], \mathcal{E})$ according to Proposition 2.4.1. Let $\pi \in \Lambda(f_{0,1}, f_{0,2})$ be the optimal measure to compute $d_2(f_{0,1}, f_{0,2})$, that is

$$d_2(f_{0,1}, f_{0,2}) = \left(\iint \|\mathbf{z}_1 - \mathbf{z}_2\|^2 \, \pi(\mathrm{d}\mathbf{z}_1, \mathrm{d}\mathbf{z}_2) \right)^{\frac{1}{2}}.$$

The existence of such a minimizing measure is proved in [130]. First, we want to estimate the function $D[\pi]$ defined for all $t \in [0, T]$ with

$$D[\pi](t) := \left(\iint \|\mathcal{Z}_1(t, \mathbf{z}_1) - \mathcal{Z}_2(t, \mathbf{z}_2)\|^2 \, \pi(\mathrm{d}\mathbf{z}_1, \mathrm{d}\mathbf{z}_2) \right)^{\frac{1}{2}}.$$

Then, we will be able to conclude using the fact that for all $t \in [0, T]$,

$$d_2(f_1(t), f_2(t)) \leq D[\pi](t).$$

Step 1: Estimate of $D[\pi]$

Let $t \in [0, T]$, $\mathbf{z}_1 = (\mathbf{x}_1, v_1, w_1)$ and $\mathbf{z}_2 = (\mathbf{x}_2, v_2, w_2) \in \mathbb{R}^{d+2}$. We start by estimating the integrand $\|\mathcal{Z}_1(t, \mathbf{z}_1) - \mathcal{Z}_2(t, \mathbf{z}_2)\|^2$. Then, we will integrate with respect to the measure $\pi(\mathrm{d}\mathbf{z}_1, \mathrm{d}\mathbf{z}_2)$ in order to estimate $D[\pi]^2(t)$. In the following, for $j \in \{1, 2\}$, we use the shorthand notations $\mathcal{V}_j := \mathcal{V}_j(t, \mathbf{z}_j)$ and $\mathcal{V}_j' := \mathcal{V}_j(t, \mathbf{z}_j')$, and the same for $\mathcal{W}_j$. First, since $\mathcal{V}_j$ and $\mathcal{W}_j$ are of class $\mathscr{C}^1$ with respect to time for $j \in \{1, 2\}$, according to the inequality (2.3.4) from Lemma 2.3.1, we have:

$$\frac{1}{2} \frac{\mathrm{d}}{\mathrm{d}t} \|\mathcal{Z}_1(t, \mathbf{z}_1) - \mathcal{Z}_2(t, \mathbf{z}_2)\|^2 \leq \mathcal{T}_l + \mathcal{T}_{nl}, \tag{2.5.1}$$

where

$$\begin{cases} \mathcal{T}_l := \left(\tilde{\kappa} + \frac{\tau + 1}{2} \right) \left(|\mathcal{V}_1 - \mathcal{V}_2|^2 + |\mathcal{W}_1 - \mathcal{W}_2|^2 \right), \\[2mm] \mathcal{T}_{nl} := -(\mathcal{V}_1 - \mathcal{V}_2) \\[1mm] \qquad \times \left[\int \Phi(\mathbf{x}_1, \mathbf{x}_1') \, (\mathcal{V}_1 - \mathcal{V}_1') \, f_{0,1}(\mathrm{d}\mathbf{z}_1') - \int \Phi(\mathbf{x}_2, \mathbf{x}_2') \, (\mathcal{V}_2 - \mathcal{V}_2') \, f_{0,2}(\mathrm{d}\mathbf{z}_2') \right]. \end{cases}$$

By integrating (2.5.1) with respect to the measure $\pi(\mathrm{d}\mathbf{z}_1, \mathrm{d}\mathbf{z}_2)$, we get:

$$\frac{1}{2} \frac{\mathrm{d}}{\mathrm{d}t} D[\pi](t)^2 \leq \iint [\mathcal{T}_l + \mathcal{T}_{nl}] \, \pi(\mathrm{d}\mathbf{z}_1, \mathrm{d}\mathbf{z}_2). \tag{2.5.2}$$

We easily treat the first term $\mathcal{T}_l$ using the definition of $D[\pi]$:

$$\iint \mathcal{T}_l \, \pi(\mathrm{d}\mathbf{z}_1, \mathrm{d}\mathbf{z}_2) \leq \left(\tilde{\kappa} + \frac{\tau + 1}{2} \right) D[\pi](t)^2. \tag{2.5.3}$$

Now, we deal with the nonlocal terms $\mathcal{T}_{nl}$. Since we have:

$$\Phi(\mathbf{x}_1, \mathbf{x}_1') \, (\mathcal{V}_1 - \mathcal{V}_1') + \Phi(\mathbf{x}_2, \mathbf{x}_2') \, (\mathcal{V}_2 - \mathcal{V}_2') \\ = \Phi(\mathbf{x}_1, \mathbf{x}_1') \left[(\mathcal{V}_1 - \mathcal{V}_2) - (\mathcal{V}_1' - \mathcal{V}_2') \right] + \left(\Phi(\mathbf{x}_1, \mathbf{x}_1') - \Phi(\mathbf{x}_2, \mathbf{x}_2') \right) (\mathcal{V}_2 - \mathcal{V}_2'),$$

we get:

$$\iint \mathcal{T}_{nl} \, \pi(\mathrm{d}\mathbf{z}_1, \mathrm{d}\mathbf{z}_2) \leq J_1 + J_2 + J_3,$$

where

$$\begin{cases} J_1 := \iint \iint |\Phi(\mathbf{x}_1, \mathbf{x}_1')| \, |\mathcal{V}_1 - \mathcal{V}_2|^2 \, \pi(\mathrm{d}\mathbf{z}_1', \mathrm{d}\mathbf{z}_2') \, \pi(\mathrm{d}\mathbf{z}_1, \mathrm{d}\mathbf{z}_2), \\[2mm] J_2 := \iint \iint |\Phi(\mathbf{x}_1, \mathbf{x}_1')| \, |\mathcal{V}_1 - \mathcal{V}_2| \, |\mathcal{V}_1' - \mathcal{V}_2'| \, \pi(\mathrm{d}\mathbf{z}_1', \mathrm{d}\mathbf{z}_2') \, \pi(\mathrm{d}\mathbf{z}_1, \mathrm{d}\mathbf{z}_2), \\[2mm] J_3 := \iint \iint |\Phi(\mathbf{x}_1, \mathbf{x}_1') - \Phi(\mathbf{x}_2, \mathbf{x}_2')| \, |\mathcal{V}_1 - \mathcal{V}_2| \, |\mathcal{V}_2 - \mathcal{V}_2'| \, \pi(\mathrm{d}\mathbf{z}_1', \mathrm{d}\mathbf{z}_2') \, \pi(\mathrm{d}\mathbf{z}_1, \mathrm{d}\mathbf{z}_2). \end{cases}$$

The two first terms J_1 and J_2 are easy to estimate, using the fact that Φ is bounded and Young's inequality. We find:

$$\begin{cases} J_1 \leq \|\Phi\|_\infty D[\pi](t)^2, \\[2mm] J_2 \leq \|\Phi\|_\infty D[\pi](t)^2. \end{cases}$$

Furthermore, since Φ satisfies the assumption (2.2.3), we have for all $(\mathbf{x}_1, \mathbf{x}_1')$ and $(\mathbf{x}_2, \mathbf{x}_2') \in \mathbb{R}^{2d}$:

$$\left| \Phi(\mathbf{x}_1, \mathbf{x}_1') - \Phi(\mathbf{x}_2, \mathbf{x}_2') \right| \leq \min \left\{ L \left(|\mathbf{x}_1 - \mathbf{x}_2| + |\mathbf{x}_1' - \mathbf{x}_2'| \right), 2 \|\Phi\|_\infty \right\}. \tag{2.5.4}$$

Let $R(t) > 0$ to be determined later. We define the sets

$$\begin{cases} \varepsilon_{R(t)} := \left\{ \mathbf{z} \in \mathbb{R}^{d+2}, |\mathcal{V}_2(t, \mathbf{z})| \leq R(t) \right\}, \\[2mm] \Theta_{R(t)} := \left(\mathbb{R}^{d+2} \times \varepsilon_{R(t)} \right)^2. \end{cases} \tag{2.5.5}$$

Then, we can deal with the third term J_3 using (2.5.4) and then splitting the set of integration into $\Theta_{R(t)}$ and its complementary $\Theta_{R(t)}^C$:

$$\begin{aligned} J_3 \leq \iint \iint \min \Big\{ L \left(|\mathbf{x}_1 - \mathbf{x}_2| + |\mathbf{x}_1' - \mathbf{x}_2'| \right), 2 \|\Phi\|_\infty \Big\} & \\ \times |\mathcal{V}_1 - \mathcal{V}_2| \, |\mathcal{V}_2 - \mathcal{V}_2'| \, \pi(\mathrm{d}\mathbf{z}_1', \mathrm{d}\mathbf{z}_2') \, \pi(\mathrm{d}\mathbf{z}_1, \mathrm{d}\mathbf{z}_2) & \\ \leq J_{31} + J_{32}, & \end{aligned}$$

where

$$\begin{cases} J_{31} := \\ \quad L \iint \underset{\Theta_{R(t)}}{\iint} |\mathcal{V}_1 - \mathcal{V}_2| \left(|\mathbf{x}_1 - \mathbf{x}_2| + |\mathbf{x}_1' - \mathbf{x}_2'| \right) |\mathcal{V}_2 - \mathcal{V}_2'| \, \pi(\mathrm{d}\mathbf{z}_1', \mathrm{d}\mathbf{z}_2') \pi(\mathrm{d}\mathbf{z}_1, \mathrm{d}\mathbf{z}_2), \\[3mm] J_{32} := 2 \|\Phi\|_\infty \iint \underset{\Theta_{R(t)}^C}{\iint} |\mathcal{V}_1 - \mathcal{V}_2| \, |\mathcal{V}_2 - \mathcal{V}_2'| \, \pi(\mathrm{d}\mathbf{z}_1', \mathrm{d}\mathbf{z}_2') \, \pi(\mathrm{d}\mathbf{z}_1, \mathrm{d}\mathbf{z}_2). \end{cases}$$

We can treat the term J_{31} with the Cauchy-Schwarz inequality:

$$\begin{aligned} J_{31} &\leq 2 L R(t) \iint \underset{\Theta_{R(t)}}{\iint} |\mathcal{V}_1 - \mathcal{V}_2| \left(|\mathbf{x}_1 - \mathbf{x}_2| + |\mathbf{x}_1' - \mathbf{x}_2'| \right) \pi(\mathrm{d}\mathbf{z}_1', \mathrm{d}\mathbf{z}_2') \, \pi(\mathrm{d}\mathbf{z}_1, \mathrm{d}\mathbf{z}_2) \\ &\leq 2 L R(t) \, D[\pi](t)^2 \\ &\quad + 2 L R(t) \left(\iint |\mathcal{V}_1 - \mathcal{V}_2|^2 \, \pi(\mathrm{d}\mathbf{z}_1, \mathrm{d}\mathbf{z}_2) \right)^{\frac{1}{2}} \left(\iint |\mathbf{x}_1' - \mathbf{x}_2'|^2 \, \pi(\mathrm{d}\mathbf{z}_1', \mathrm{d}\mathbf{z}_2') \right)^{\frac{1}{2}} \\ &\leq 4 L R(t) \, D[\pi](t)^2. \end{aligned}$$

Then, using the Young and Cauchy-Schwarz inequalities, we can estimate the second term J_{32} as follows:

$$\begin{aligned} J_{32} &\leq \|\Phi\|_\infty D[\pi](t)^2 + \|\Phi\|_\infty \iint \underset{\Theta_{R(t)}^C}{\iint} |\mathcal{V}_2 - \mathcal{V}_2'|^2 \, \pi(\mathrm{d}\mathbf{z}_1', \mathrm{d}\mathbf{z}_2') \, \pi(\mathrm{d}\mathbf{z}_1, \mathrm{d}\mathbf{z}_2) \\ &\leq \|\Phi\|_\infty D[\pi](t)^2 + \|\Phi\|_\infty \left(\iint \iint |\mathcal{V}_2 - \mathcal{V}_2'|^4 \, \pi(\mathrm{d}\mathbf{z}_1', \mathrm{d}\mathbf{z}_2') \, \pi(\mathrm{d}\mathbf{z}_1, \mathrm{d}\mathbf{z}_2) \right)^{\frac{1}{2}} \end{aligned}$$

$$\times \left(\iint_{\Theta_{R(t)}^C} \iint \pi(\mathrm{d}\mathbf{z}_1', \mathrm{d}\mathbf{z}_2') \, \pi(\mathrm{d}\mathbf{z}_1, \mathrm{d}\mathbf{z}_2) \right)^{\frac{1}{2}}$$

$$\leq \|\Phi\|_\infty \, D[\pi](t)^2 \,+\, C \left(\int |\mathcal{V}_2|^4 \, f_{0,2}(\mathrm{d}\mathbf{z}_2) \right)^{\frac{1}{2}} \left(\int_{\varepsilon_{R(t)}^C} f_{0,2}(\mathrm{d}\mathbf{z}_2) \right)^{\frac{1}{2}}.$$

On the one hand, according to Lemma 2.3.2, there exists a positive function $\alpha : [0, T] \mapsto \mathbb{R}$ such that if we define $\alpha_T := \alpha(T) > 0$, we have:

$$\int_{\varepsilon_{R(t)}^C} f_{0,2}(\mathrm{d}\mathbf{z}_2) \leq \int_{\varepsilon_{R(t)}^C} \frac{e^{\alpha_T |\mathcal{V}_2|}}{e^{\alpha_T R(t)}} f_{0,2}(\mathrm{d}\mathbf{z}_2) \leq e^{-\alpha_T R(t)} \int e^{\alpha_0 \langle v_2, w_2 \rangle} f_{0,2}(\mathrm{d}\mathbf{z}_2).$$

On the other hand, there exists a constant $C > 0$ such that

$$\int |\mathcal{V}_2|^4 \, f_{0,2}(\mathrm{d}\mathbf{z}_2) \leq C \int \left(1 + e^{\alpha_T |\mathcal{V}_2|} \right) f_{0,2}(\mathrm{d}\mathbf{z}_2) < \infty,$$

according to Lemma 2.3.2. Finally, there exists a constant $C > 0$ such that

$$J_{32} \leq C \left(1 + R(t) \right) D[\pi](t)^2 + C \, e^{-\frac{\alpha_T}{2} R(t)}.$$

and consequently, there exists a constant $\widetilde{C} > 0$ such that

$$\iint \mathcal{T}_{nl} \, \pi(\mathrm{d}\mathbf{z}_1 \mathrm{d}\mathbf{z}_2) \leq \widetilde{C} \left(1 + R(t) \right) D[\pi](t)^2 + \widetilde{C} \, e^{-\frac{\alpha_T}{2} R(t)}. \tag{2.5.6}$$

Now, we use (2.5.3) and (2.5.6) to estimate respectively the local terms $\mathcal{T}_l$ and the nonlocal terms $\mathcal{T}_{nl}$ in (2.5.2). Finally, we get that there exists a constant $C_T > 0$ such that for all $t \in [0, T]$ and all $R(t) > 0$:

$$\frac{\mathrm{d}}{\mathrm{d}t} D[\pi](t)^2 \leq C_T \left(1 + R(t) \right) D[\pi](t)^2 + C_T \, e^{-\frac{\alpha_T}{2} R(t)}. \tag{2.5.7}$$

First, if we choose $R(t) = 1$ for all $t \in [0, T]$ in the inequality (2.5.7), since $D[\pi]$ is continous with respect to time because $\mathcal{Z}_1$ and $\mathcal{Z}_2$ are continuous, Grönwall's lemma yields that there exists a constant $K_T > 0$ such that for all $t \in [0, T]$, $D[\pi](t)^2 < K_T$. Then, we define the function

$$u : t \mapsto \frac{D[\pi](t)^2}{e \, K_T},$$

so that for all $t \in [0, T]$ such that $u(t) > 0$, we have $1 \leq -\ln(u(t))$. Let $t \in [0, T]$ such that $u(t) > 0$. Then, we choose the quantity $R(t)$ in (2.5.7) as follows:

$$R(t) := -\frac{2}{\alpha_T} \ln\left(u(t) \right).$$

Hence, (2.5.7) becomes

$$u'(t) \leq C_T \left(1 - \frac{2}{\alpha_T} \ln\left(u(t) \right) \right) u(t) + \frac{C_T}{e \, K_T} u(t)$$

$$\leq -C_T \left(1 + \frac{2}{\alpha_T} \right) u(t) \ln\left(u(t) \right) - \frac{C_T}{e \, K_T} u(t) \ln\left(u(t) \right)$$

$$\leq -\widetilde{C}_T \, u(t) \ln\left(u(t) \right),$$

for some constant $\widetilde{C}_T > 0$. Since $u(t) > 0$, we can divide the last inequality by $u(t)$, which yields:

$$(\ln(u(t)))' \leq -\widetilde{C}_T \ln(u(t))$$

Consequently, since u is continuous with respect to time, using Grönwall's inequality to $\ln(u)$, if we define the function

$$\beta : t \mapsto e^{-\widetilde{C}_T \, t}, \tag{2.5.8}$$

we get that for all $t \in [0, T]$:

$$u(t) \leq u(0)^{\beta(t)},$$

and this remains true if $u(t) = 0$. Finally, we can conclude that for all $t \in [0, T]$

$$
\begin{aligned}
D[\pi](t) &\leq (e \, K_T)^{\frac{1-\beta(t)}{2}} \, D[\pi](0)^{\beta(t)} \\
&\leq \widetilde{K}_T \, D[\pi](0)^{\beta(t)},
\end{aligned}
\tag{2.5.9}
$$

where $\widetilde{K}_T > 0$ is a positive constant.

Step 2: Conclusion of the estimate of the Wasserstein distance

We note for all $j \in \{1 \, , \, 2\}$ and all $t \in [0, T]$

$$f_j(t) := \mathcal{Z}_j(t) \# f_{0,j}.$$

Thus, for all $t \in [0, T]$ and for all $\pi \in \Lambda(f_{0,1}, f_{0,2})$,

$$(\mathcal{Z}_1(t) \times \mathcal{Z}_2(t)) \, \# \pi \in \Lambda(f_1(t) \, , \, f_2(t)),$$

and therefore,

$$d_2(f_1(t), f_2(t)) \leq \left(\iint \|\mathcal{Z}_1(t, \mathbf{z}_1) - \mathcal{Z}_2(t, \mathbf{z}_2)\|^2 \, \pi(\mathrm{d}\mathbf{z}_1 \, \mathrm{d}\mathbf{z}_2) \right)^{\frac{1}{2}} = D[\pi](t).$$

Finally, we can conclude using the estimate (2.5.1):

$$
\begin{aligned}
d_2(f_1(t), f_2(t)) &\leq \widetilde{K}_T \, D[\pi](0)^{\beta(t)} \\
&= \widetilde{K}_T \, d_2(f_{0,1}, f_{0,2})^{\beta(t)}.
\end{aligned}
$$

Remark 2.5.1. *If we make the additional assumption that there exists $p > 1$ such that*

$$\int e^{\langle v, w \rangle^p} f_{0,2}(\mathrm{d}\mathbf{z}) < \infty,$$

then instead of the estimate (2.5.6), we can conclude using a similar argument that there exists a constant $C_T > 0$ such that for all $t \in [0, T]$,

$$\frac{\mathrm{d}}{\mathrm{d}t} D[\pi](t)^2 \leq C_T \, (1 + R) D[\pi](t)^2 + C_T \, e^{-\frac{\alpha_T}{2} \, R^p}.$$

Hence, since $D[\pi]$ is continuous with respect to time, Grönwall's lemma yields that for all $R > 0$ and all $t \in [0, T]$,

$$D[\pi](t)^2 \leq \left(D[\pi](0)^2 + \frac{e^{-\frac{\alpha_T}{2} \, R^p}}{1 + R} \right) e^{C_T \, (1+R) \, t}.$$

Therefore, this implies that for all $t \in [0, T]$ and all $R > 0$,

$$d_2^2(f_1(t), f_2(t)) \leq D[\pi](t)^2 \leq \left(d_2^2(f_{0,1}, f_{0,2}) + \frac{e^{-\frac{\alpha_T}{2} \, R^p}}{1 + R} \right) e^{C_T \, (1+R) \, t}. \tag{2.5.10}$$

Choosing for instance

$$R = -\frac{1}{2\,C_T\,T}\ln\left(d_2^2(f_{0,1}, f_{0,2})\right),$$

the estimate (2.5.10) *is enough to prove the part (ii) of Theorem* 2.2.4*. Indeed, since* $(f_{0,n})_{n\in\mathbb{N}}$ *and* f_0 *satisfy assumption* (2.2.8)*, we get*

$$\lim_{n\to+\infty}\sup_{t\in[0,T]} d_2(f_n(t), f(t)) = 0.$$

2.5.2   Proof of the mean-field limit from (2.1.1) towards (2.1.3)

First, the existence and uniqueness of the solution to the FHN system is a direct consequence of the Cauchy-Lipschitz theorem. Then, we have already proved the well-posedness of the transport equation (2.1.3) in Section 2.4.

Now, let us conclude the proof using the stability result from the first part of Theorem 2.2.4. We notice that for all $n \in \mathbb{N}$, the empirical measure f_n is the measure solution of the equation (2.1.3) with initial condition $f_{0,n}$. Then, the part (i) of Theorem 2.2.4 yields that there exist two positive constants C_T and K_T independent of n such that for all $t \in [0,T]$ and for all $n \in \mathbb{N}$,

$$d_2(f_n(t), f(t)) \,\leq\, K_T\, d_2(f_{0,n}, f_0)^{\beta(t)},$$

where

$$\beta(t) \,:=\, e^{-C_T\,t}.$$

Finally, using the assumption (2.2.8), we get that

$$\lim_{n\to+\infty}\sup_{t\in[0,T]} d_2(f_n(t), f(t)) = 0,$$

which concludes the proof of Theorem 2.2.4.

2.6   Application: Stability of monokinetic solutions

One of the motivations to study the mean-field model is the analysis of the macroscopic quantities computed from a measure solution to (2.1.3), though the equation formally satisfied by the average membrane potential in the network is not closed. A way to overcome this difficulty is to look for monokinetic solutions of (2.1.3), that is solutions f of the form

$$f(t, \mathrm{d}\mathbf{x}, \mathrm{d}v, \mathrm{d}w) \,=\, \rho_0(\cdot)\,\mathrm{d}\mathbf{x} \otimes \delta_{V(t,\cdot)}(\mathrm{d}v) \otimes \delta_{W(t,\cdot)}(\mathrm{d}w), \tag{2.6.1}$$

where ρ_0 is the average density of neurons, and (V, W) is the average couple membrane potential-adaptation variable in the network. Therefore, if f is a monokinetic solution of (2.1.3), then the couple (V, W) formally satisfies the nonlocal reaction-diffusion FHN system:

$$\begin{cases} \partial_t V(t, \mathbf{x}) - \displaystyle\int \Phi(\mathbf{x}, \mathbf{x}')\,(V(t, \mathbf{x}') - V(t, \mathbf{x}))\,\rho_0(\mathbf{x}')\,\mathrm{d}\mathbf{x}' \,=\, N(V(t, \mathbf{x})) - W(t, \mathbf{x}), \\[2mm] \partial_t W(t, \mathbf{x}) \,=\, \tau\,(V(t, \mathbf{x}) + a - b\,W(t, \mathbf{x})). \end{cases} \tag{2.6.2}$$

In this subsection, we consider a connectivity kernel Φ of the form:

$$\Phi(\mathbf{x}, \mathbf{y}) \,=\, \Psi(\mathbf{x} - \mathbf{y}),$$

where $\Psi : \mathbb{R}^d \to \mathbb{R}$ is symmetric, which means that the conductance between two neurons only depends on the distance between them. We want to use the stability result from Theorem 2.2.4 to prove that monokinetic solutions of the equation (2.1.3) are stable with respect to the Wasserstein distance d_2. Under some additional assumptions, we can state the following well-posedness result.

Lemma 2.6.1. *Assume that Ψ is a non-negative symmetric connectivity kernel in $L^1(\mathbb{R}^d)$, and N is the nonlinearity defined through:*

$$N : v \mapsto v - v^3. \tag{2.6.3}$$

Consider an initial data (ρ_0, V_0, W_0) satisfying

$$\rho_0 \in L^1 \cap L^\infty(\mathbb{R}^d), \quad \rho_0 \geq 0, \quad V_0, W_0 \in L^\infty(\mathbb{R}^d). \tag{2.6.4}$$

Then for any $T > 0$, there exists a unique couple (V, W) which is a classical solution to the nonlocal reaction-diffusion system (2.6.2) with initial data (V_0, W_0), where

$$V, W \in \mathscr{C}^1([0, T], L^\infty(\mathbb{R}^d)).$$

The proof of Lemma 2.6.1 is based on a classical fixed point argument, and we refer to [49] for the details. Now, as a direct consequence of Theorem 2.2.4, we get the following result of stability of monokinetic solution of the equation (2.1.3).

Proposition 2.6.2 (Stability of monokinetic solutions). *Let $T > 0$. Assume that Φ is a non-negative symmetric connectivity kernel in $L^1(\mathbb{R}^d)$, and N is the nonlinearity defined through (2.6.3). Consider the initial data $f_0 \in \mathcal{P}_2(\mathbb{R}^{d+2})$, and (ρ_0, V_0, W_0) satisfying (2.6.4) and*

$$\int_{\mathbb{R}^d} \rho_0(\mathbf{x}) \, d\mathbf{x} = 1, \quad \int_{\mathbb{R}^d} \left(\|\mathbf{x}\|^2 + e^{\alpha_0 \langle V_0(\mathbf{x}), W_0(\mathbf{x}) \rangle} \right) \rho_0(\mathbf{x}) \, d\mathbf{x} < \infty, \tag{2.6.5}$$

for some positive constant $\alpha_0 > 0$. Let (V, W) be the solution of (2.6.2) with initial data (V_0, W_0) provided by Lemma 2.6.1, and let $f \in \mathscr{C}([0, T], \mathcal{P}_2(\mathbb{R}^{d+2}))$ be the measure solution of (2.1.3) with initial data f_0. Then there exist two positive constants $C_T > 0$ and $K_T > 0$ such that for all $t \in [0, T]$,

$$d_2 \left(f(t), \rho_0(\cdot) \, d\mathbf{x} \otimes \delta_{V(t, \cdot)}(dv) \otimes \delta_{W(t, \cdot)}(dw) \right)$$
$$\leq K_T \, d_2 \left(f_0, \rho_0 \, d\mathbf{x} \otimes \delta_{V_0}(dv) \otimes \delta_{W_0}(dw) \right)^{\beta(t)}, \tag{2.6.6}$$

where $\beta(t) := e^{-C_T t}$.

Proof. According to the assumption (2.6.5), we have:

$$\int \left(\|\mathbf{x}\|^2 + e^{\alpha_0 \langle v, w \rangle} \right) \rho_0(\mathbf{x}) \, d\mathbf{x} \otimes \delta_{V_0(\mathbf{x})}(dv) \otimes \delta_{W_0(\mathbf{x})}(dw) < \infty,$$

so $\rho_0 \, d\mathbf{x} \otimes \delta_{V_0}(dv) \otimes \delta_{W_0}(dw) \in \mathcal{P}_2(\mathbb{R}^{d+2})$ and satisfies (2.2.5). Moreover, $\rho_0 \, d\mathbf{x} \otimes \delta_V(dv) \otimes \delta_W(dw) \in \mathscr{C}([0, T], \mathcal{P}_2(\mathbb{R}^{d+2}))$ is a measure solution of (2.1.3) since (V, W) is a classical solution of (2.6.2). Thus, we can apply Theorem 2.2.4, which yields (2.6.6). $\qquad\square$

2.7 Numerical simulations

In this section, we approximate the solution f of the mean-field equation (2.1.3) for a one-dimensional network (*i.e.* $d = 1$), normalized to $[0, 1]$. There are few numerical methods specifically adapted to kinetic theory. In [4], the authors numerically approximate a mean-field model of neural network of FHN type using finite differences without considering any space dependence. On the contrary, we are particularly interested in the influence of space in the mean-field model (2.1.3). In order to approximate (2.1.3), we use a particle method. This kind of numerical scheme was first introduced by Harlow [79] for the numerical computation of specific problems in fluid dynamics, and precisely mathematically studied later [120]. Then, a large diversity of particle methods were introduced for simulations in fluid mechanics and plasma physics (see for instance [34, 68, 83] and references therein). Throughout this section, we fix $N(v)$ to be the following cubic nonlinearity:

$$N : v \mapsto v\,(1 - v)\,(v - 0.25). \tag{2.7.1}$$

2.7.1 Principle of the particle method

For $T > 0$, the standard particle method consists in approximating the solution f of the mean-field equation (2.1.3) on $[0, T]$ by a finite sum of Dirac masses

$$f_M(t, \mathrm{d}\mathbf{x}, \mathrm{d}v, \mathrm{d}w) := \frac{1}{M} \sum_{i=1}^{M} \delta_{\mathbf{x}_i}(\mathrm{d}\mathbf{x}) \otimes \delta_{\mathcal{V}_i(t)}(\mathrm{d}v) \otimes \delta_{\mathcal{W}_i(t)}(\mathrm{d}w),$$

where M is the number of distinct particles considered in the network, and for all $1 \leq i \leq M$, $(\mathcal{V}_i, \mathcal{W}_i)$ is the solution of the characteristic system (2.2.2) provided by Proposition 2.4.1 with initial condition $(\mathbf{x}_i, v_{0,i}, w_{0,i}) \in \mathbb{R}^3$ and initial measure $f_M(0, \cdot)$. In order to provide an approximation of the macroscopic quantities necessary to solve (2.2.2), we approach the Dirac masses by $\varphi_h := h^{-d}\,\varphi(\cdot/h)$, where $h > 0$ is a small fixed parameter, and

$$\varphi : z \mapsto \begin{cases} 0 & \text{if } |z| \geq 1, \\ 1 + z & \text{if } |z| \in [-1, 0], \\ 1 - z & \text{if } |z| \in [0, 1]. \end{cases}$$

Therefore, we can define the discrete densities on a mesh $(\mathbf{y}_i)_{1 \leq i \leq n_{\mathbf{y}}}$ of step size $h > 0$ of the considered interval $[0, 1]$, where $n_{\mathbf{y}} \in \mathbb{N}$ and $h > 0$ satisfy $h = 1/(n_{\mathbf{y}} - 1)$, with for all $1 \leq i \leq M$:

$$\begin{cases} \rho_{M,h}(\mathbf{y}_i) & := \dfrac{1}{M} \sum_{j=1}^{M} \varphi_h(\mathbf{y}_i - \mathbf{x}_j), \\ j_{M,h}(t, \mathbf{y}_i) & := \dfrac{1}{M} \sum_{j=1}^{M} \varphi_h(\mathbf{y}_i - \mathbf{x}_j)\,\mathcal{V}_j(t). \end{cases} \tag{2.7.2}$$

The whole point of the particle method is that $n_{\mathbf{y}} \ll M$. Now, for all $1 \leq i \leq M$, the couple $(\mathcal{V}_i, \mathcal{W}_i)$ is approached by a solution of an approximated characteristic system, noted (V_i, W_i), in which we replace the nonlocal term in (2.2.2) with

$$\int \Phi(\mathbf{x}_i, \mathbf{x}')\,\big(\rho_{M,h}(\mathbf{x}')\,V_i(t) \,-\, j_{M,h}(t, \mathbf{x}')\big)\,\mathrm{d}\mathbf{x}', \tag{2.7.3}$$

with the same initial data, and we approximate the integral terms in (2.7.3) with the rectangle method using the mesh $(\mathbf{y}_i)_{1 \leq i \leq n_{\mathbf{y}}}$. Finally, for the time discretization, we use a Runge-Kutta

scheme of second order, with a time grid of step 0.01. In the following, we work in the case where the neurons in the network are homogeneously distributed in the interval $[0, 1]$. Consequently, we choose the parameters $(\mathbf{x}_i)_{1 \leq i \leq M}$ forming a regular mesh of the interval $[0, 1]$, and we fix for the rest of this section $M = 5001$ and $n_{\mathbf{y}} = 501$.

2.7.2 Numerical investigation of three different regimes

In this subsection, we display some numerical simulations of the mean-field model (2.1.3) to observe its dynamics for different sets of parameters. The dynamics of the microscopic system (2.1.1) when the number of neurons is large and of the transport equation (2.1.3) are both rich, but not well known. Nevertheless, the model FHN for one isolated neuron

$$\begin{cases} \dfrac{\mathrm{d}}{\mathrm{d}t} v = N(v) - w, \\[2mm] \dfrac{\mathrm{d}}{\mathrm{d}t} w = A(v, w), \end{cases} \tag{2.7.4}$$

has been extensively studied, and its asymptotic behaviors are perfectly predictable. Thus, we consider three different sets of parameters corresponding to three different regimes of the FHN model (2.7.4).

(i) Bistable regime: we remove the influence of the adaptation variable w, that is we consider $\tau = 0$. In this case, the equation (2.7.4) admits exactly two stable fixed points at $v = 0$ and $v = 1$ and one unstable at $v = 0.25$. Thus, the solution $v(t)$ of the equation (2.7.4) converges towards 0 as $t \to +\infty$ if $v(0) < 0.25$, or towards 1 if $v(0) > 0.25$.

(ii) Oscillatory regime: we choose $a = -0.25$ and $b = 3$, so that the system (2.7.4) admits a unique fixed point $(0.25, 0)$, which is unstable. We also consider $\tau = 0.02$. Consequently, in this setting, the solution of the system (2.7.4) converges towards a stable limit cycle if it is not initialized at the fixed point.

(iii) Excitable regime: we choose $a = 0$ and $b = 7$, so that the system (2.7.4) admits a unique fixed point $(0, 0)$, which is stable. All the solutions of (2.7.4) converge towards $(0, 0)$ as $t \to +\infty$. Moreover, we fix $\tau = 0.002$, so that (2.7.4) exhibits a slow/fast dynamics.

From now on, we define the connectivity kernel to be

$$\Phi(\mathbf{x}, \mathbf{y}) = G_\varepsilon(\mathbf{x} - \mathbf{y}) \quad \forall (\mathbf{x}, \mathbf{y}) \in \mathbb{R}^2 \quad \text{with} \quad G_\varepsilon(\mathbf{x}) := \frac{1}{\sqrt{2\pi\,\varepsilon}} \exp\left(-\frac{|\mathbf{x}|^2}{2\,\varepsilon}\right), \tag{2.7.5}$$

where $\varepsilon > 0$ is a rescaling parameter.

Let us discuss this choice of connectivity kernel in (2.7.5). First of all, since Φ is non-negative, we consider a purely excitatory regime. Then, the parameter $\varepsilon > 0$ varies between 1 and very small values, in order to consider the regime of strong local interactions, which seems reasonable from a biological point of view since two neurons interact only through their contact point provided by their shared synapse.

We are interested in the dynamics of the average macroscopic couple (V_f, W_f) computed from the solution f of the mean-field model (2.1.3). In the previous section, we have proved the stability of monokinetic solutions (2.6.1) from well-prepared initial data (see Proposition 2.6.2). In the following, we present in the three regimes discussed above some numerical evidences that monokinetic solutions have a larger basin of attraction in the sense that the dynamics of (V_f, W_f) is found to be close to the dynamics of the solutions of the nonlocal reaction-diffusion system (2.6.2). To conclude this section, we will compare the dynamics between the FHN system (2.1.1), and the mean-field model (2.1.3) in the oscillatory regime for different values of n the number of neurons.

Figure 2.1: **Bistable regime.** (a)-(b) Spatio-temporal evolution of the macroscopic function V_f computed from the solution f of the equation (2.1.3) with $\tau = 0$, and different values of the parameter ε, fixed at (a) 10^{-1}, (b) 10^{-3}. (c) Profile of the macroscopic function $V_f(t, \cdot)$ at different fixed times, computed with $\varepsilon = 10^{-3}$ and with $\tau = 0$.

Case (i) − Bistable regime.

We study the mean-field model (2.1.3) in the bistable regime with $\tau = 0$. As initial condition for our numerical scheme, we choose for all $1 \leq i \leq M$,

$$v_{0,i} = \frac{1}{2} \operatorname{erfc}\left(\sqrt{5000}(\mathbf{x}_i - 0.05)\right), \quad w_{0,i} = 0,$$

where erfc is the complementary error function.

In Figure 2.1, we show the spatio-temporal evolution of the macroscopic quantity V_f for different values of the parameter ε. First, in the case (a), $\varepsilon = 10^{-1}$ is large compared to the width of the considered interval $[0, 1]$. Thus, the space influence is almost homogenized, and the interactions between the particles of the neural network are expected to vanish after a few time. Consequently, for t large enough and for all fixed position $\mathbf{x} \in [0, 1]$, the macroscopic quantity $V_f(\cdot, \mathbf{x})$ is expected to behave as a solution of the one-neuron equation (2.7.4) in the same framework, that is to converge towards one of the two stable fixed points. Indeed, we can observe that it converges towards 0. Then, in the case (b), $\varepsilon = 10^{-3}$ is sufficiently small to observe another dynamic. Here, the behavior of the function V_f qualitatively looks like an invasion front, connecting the steady state 0 to 1, propagating at constant speed. Moreover, as shown in (c), after an initial transition phase, the shape of the front seems to be invariant and smooth.

We note that the qualitative behavior of the macroscopic function V_f when ε is small enough corresponds well to the dynamics of the nonlocal reaction-diffusion system (2.6.2) for which traveling front solutions are known to exist [6] when considered on the real line. Regarding the density function f, we show in Figure 2.2 its temporal evolution for $\varepsilon = 10^{-3}$. We observe that the density f remains concentrated around the states $v = 1$ in an interval $[0, \mathbf{x}_0(t)]$ and then around $v = 0$ in the complementary interval $[\mathbf{x}_0(t), 1]$ for some $\mathbf{x}_0(t) \in (0, 1)$ propagating at a constant speed. This shows that f remains close to a monokinetic solution of the form $\rho_0 \, d\mathbf{x} \otimes \delta_{V_f(t,\cdot)}(dv)$, where the qualitative behavior of V_f is that of a traveling front, as previously detailed. This validates the fact monokinetic solutions seem to have a large basin of attraction.

As explained in [6], the macroscopic speed of propagation is proportional to the integral $\int_0^1 N(u) \, du$. Thus, if we rather work with the nonlinearity

$$N : v \mapsto v \, (1 - v) \, (v - 0.75),$$

we observe a similar behaviour, where the state $V_f = 0$ invades the state $V_f = 1$. Furthermore,

57
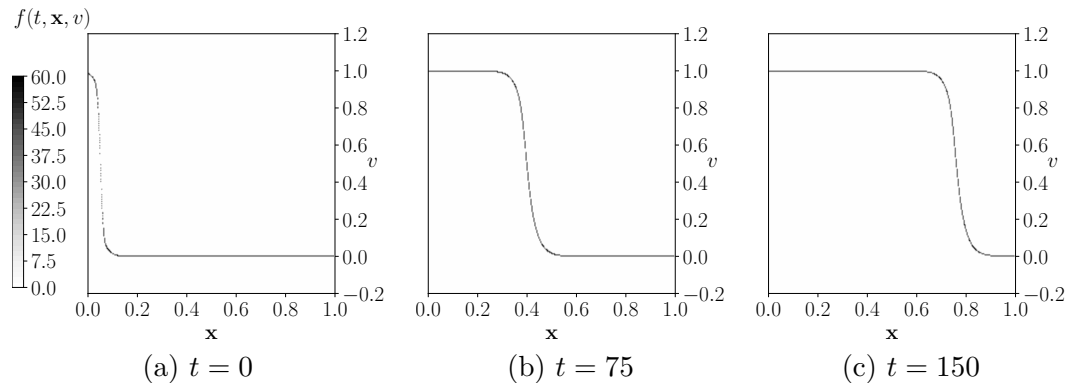
Figure 2.2: **Bistable regime.** Numerical approximation of the density function f solution of the transport equation (2.1.3) at fixed time (a) $t = 0$, (b) $t = 75$ and (c) $t = 150$, computed with the parameters $\varepsilon = 10^{-3}$ and $\tau = 0$.

in the specific case of a nonlinearity satisfying $\int_0^1 N(u)\,\mathrm{d}u = 0$, for instance

$$N : v \mapsto v\,(1 - v)\,(v - 0.5),$$

there is no invasion.

Case (ii) – Oscillatory regime

In the oscillatory regime, we choose as initial data a perturbation of the steady state $(0.25, 0)$ concentrated around the position $\mathbf{x} = 0$:

$$v_{0,i} = 0.25 + 0.5\,\exp\left(-5000\,\mathbf{x}_i^2\right), \quad w_{0,i} = 0.$$

In Figure 2.3, we display the spatio-temporal evolution of the macroscopic function V_f computed from the solution f of the transport equation (2.1.3) with three different values of the variance ε. In the first case (a), we fix the parameter $\varepsilon = 10^{-1}$. In that case, we expect that the space dependence of V_f to be suppressed and we indeed observe synchronized homogeneous oscillations. Then, we reduce the value of ε to localize the interactions and enforce the spatial dependence. For both $\varepsilon = 10^{-3}$ and $\varepsilon = 10^{-5}$, we observe temporal oscillations whose phase is modulated spatially, similar to what is usually found for the local FHN reaction-diffusion system in the oscillatory regime [38]. More precisely, the dynamics is that of a modulated traveling wave propagating at constant speed from 0 towards the right, and leaving in the wake an oscillatory pattern with a constant frequency and amplitude. This is illustrated in Figure 2.3 panel (f) where the trajectory followed by the average couple (V_f, W_f) in the phase space at a given time converges towards a limit cycle.

Case (iii) – Excitable regime

We consider an initial condition that is a perturbation of the steady state $(0, 0)$ concentrated at the middle of the interval $[0, 1]$, that is for all $1 \leq i \leq M$:

$$v_{0,i} = \exp\left(-5000\,|\mathbf{x}_i - 0.5|^2\right), \quad w_{0,i} = 0.$$

We report in Figure 2.4, panel (a), the space-time representation of the macroscopic function V_f for $\varepsilon = 10^{-5}$. In that case, we see that the dynamics generates two counter-propagating traveling pulses. Once again, the behavior of the function V_f is qualitatively the same as the
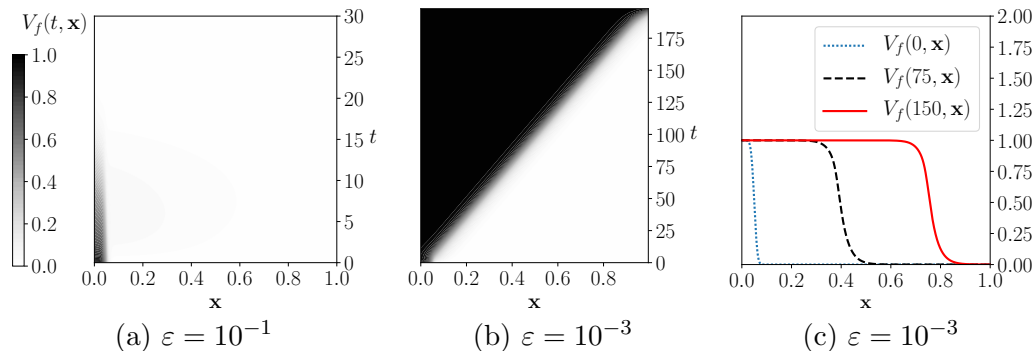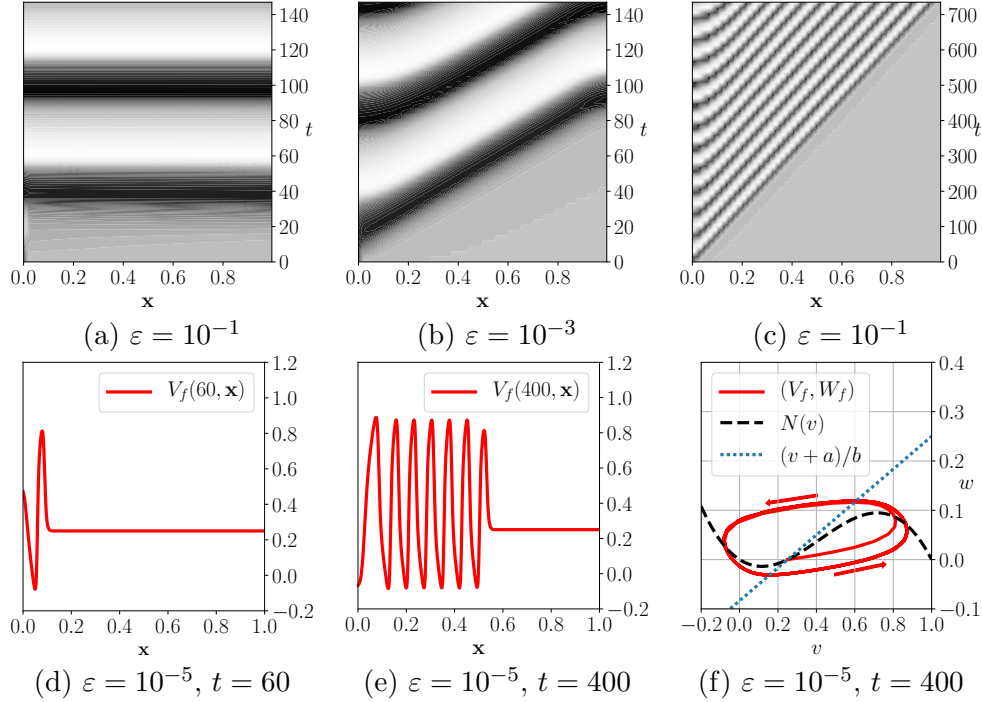
Figure 2.3: **Oscillatory regime.** (a)-(b)-(c) Spatio-temporal evolution of the macroscopic function V_f computed from the solution f of the transport equation (2.1.3) with three different values of the parameter ε, fixed at (a) $\varepsilon = 10^{-1}$, (b) $\varepsilon = 10^{-3}$ and (c) $\varepsilon = 10^{-5}$. (d)-(e) Profile of the macroscopic function $V_f(t, \cdot)$ computed with $\varepsilon = 10^{-5}$ at time $t = 60$ and $t = 400$ respectively. (f) Trajectory in the phase space (v, w) of the couple (V_f, W_f) at fixed position $\mathbf{x} = 0.2$ between times 0 and $t = 400$ computed with $\varepsilon = 10^{-5}$. The other parameters are fixed at $a = -0.25$, $b = 3$, and $\tau = 0.02$.

expected dynamics of the corresponding macroscopic model (2.6.2), where it is well known that the nonlocal reaction-diffusion FHN system supports traveling pulse solution [62]. We have drawn in Figure 2.4 panel (b) the profile of the v-component of the traveling pulse at different times and the corresponding trajectory in the phase plane in Figure 2.4 panel (c) where we recover that the profile of the traveling pulse is a homoclinic orbit to the stable fixed point $(0, 0)$. The study of traveling pulses in excitable media has received lots of interests in the past decades, especially for the local reaction-diffusion FHN system, and to our best knowledge, it is the first time that traveling pulses are reported for the FHN mean-field model.

2.7.3 Numerical comparison between the FHN system and the mean-field model

We consider a set of parameters corresponding to the oscillatory regime of the FHN model (2.7.4), that is the same parameters and initial condition as in paragraph above. We also fix $\varepsilon = 10^{-4}$, so that the average couple (V_f, W_f) computed from the solution to the transport equation (2.1.3) presents an oscillatory pattern modulated by a traveling wave propagating through space as previously.

In Figure 2.5, we display the profile of the macroscopic function V_f at fixed time $t = 225$ with respect to $\mathbf{x}$, together with the points $(\mathbf{x}_i, v_i)_{1 \leq i \leq n}$ standing for the solution of the FHN system (2.1.1) approximated with a Runge-Kutta scheme of second order, for different values of n. We choose $n = 50$ in the case (a), $n = 100$ in the case (b) and $n = 500$ in the case (c). In
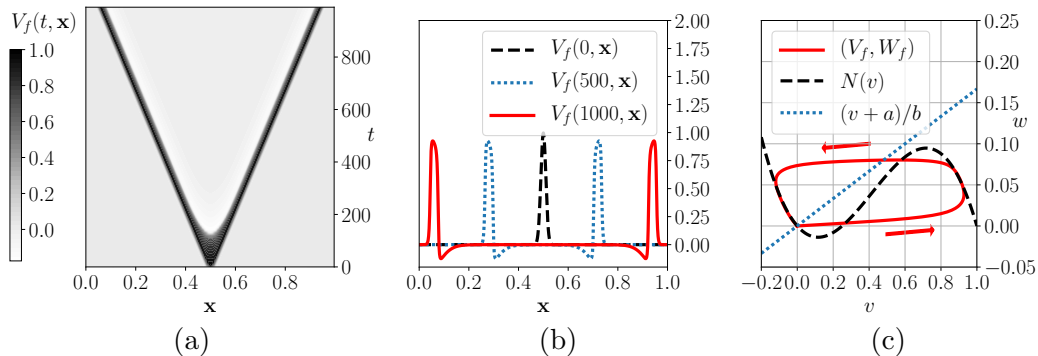
Figure 2.4: **Excitable regime.** (a) Spatio-temporal evolution of the macroscopic function V_f computed from the solution f of the transport equation (2.1.3) with $\varepsilon = 10^{-5}$. (b) Corresponding profile of the macroscopic function $V_f(t, \cdot)$ computed at different times. (c) Trajectory in the phase space (v, w) of the couple (V_f, W_f) at fixed position $\mathbf{x} = 0.2$ between times 0 and $t = 1000$ computed with $\varepsilon = 10^{-5}$. The other parameters are fixed at $a = 0$, $b = 7$, and $\tau = 0.002$.

the case (a), n is large enough so that the oscillatory pattern emerges. Though, the frequency of these oscillations seems to be slightly higher than for the mean-field model (2.1.3). Then, we observe that for a relatively small number of neurons n in the network, the points $(\mathbf{x}_i, v_i)_{1 \le i \le n}$ match with the trajectory of $V(t, \cdot)$. Indeed, in the case (b), the oscillations of both models (2.1.1) and (2.1.3) are almost synchronized, and in the case (c), the points $(\mathbf{x}_i, v_i)_{1 \le i \le n}$ overlay the trajectory of V_f. It seems that the microscopic system (2.1.1) does not vary much any more for higher values of n, and quickly converges towards the solution of (2.1.3) as n tends to infinity.

On the one hand, the computations are obviously quicker than for the microscopic model (2.1.1) with a too large value of n. This is natural since in the numerical scheme of (2.1.3), we replace the sum over all the neurons in the network with a mean-field operator. On the other hand, the transport equation (2.1.3) manages to accurately represent the behavior of a large neural network, and we still have access to more information than with a macroscopic model. Indeed, the mean-field model focuses on an approximation of the density of neurons rather than the average membrane potential. This shows the whole interest of the mean-field model (2.1.3) compared to the microscopic model (2.1.1) and to macroscopic models.

We mention that in the presence of noise as in [119], the authors showed some numerical simulations of the FHN system (2.1.1) with homogeneous interactions, where the finite number of neurons can cause the emergence of relaxation cycles near the transition from the excitable regime to the oscillatory regime, whereas the deterministic model still presents a unique stable fixed point.

2.8   Discussion

In this paper, we have proved the mean-field limit of the deterministic spatially-extended FHN model for neural networks towards a nonlocal transport equation as the number of neurons goes to infinity. Our approach is based on a stability estimate of solutions of the transport equation (2.1.3) with respect to their initial data. We have also proved the well-posedness of the transport equation in the space of probability measures with finite second moments, equiped with the Wasserstein distance of order 2. This mean-field limit provides a rigorous link between the microscopic scale of the neural network and a mesoscopic scale, which can then be used as an intermediary step for the derivation of macroscopic description of the neural network. Our microscopic model was obtained coupling the FHN model for a finite number of neurons, whose

(a) $n = 50$ (b) $n = 100$ (c) $n = 500$
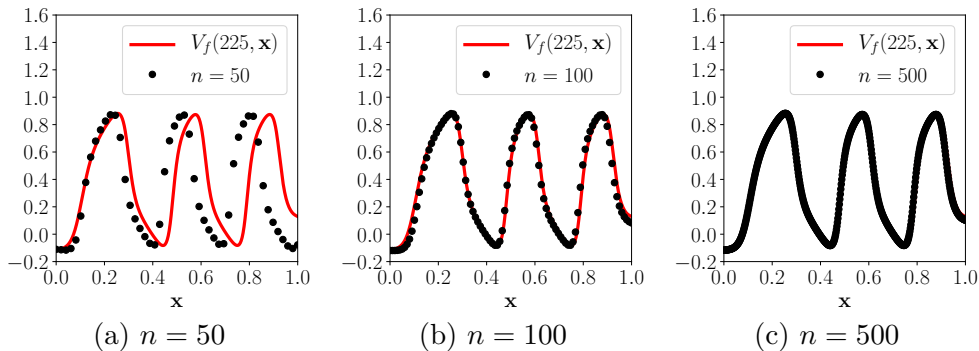
Figure 2.5: Profile of the macroscopic function V_f computed from the solution f of the transport equation (2.1.3) with $\varepsilon = 10^{-4}$, and with the points $(\mathbf{x}_i, v_i)_{1 \le i \le n}$ from the solution of the FHN system (2.1.1), at fixed time $t = 225$. The other parameters are the same as in Figure 2.3.

interactions with their neighbours are modulated only with their spatial position in the network with a connectivity kernel Φ. Moreover, we have ignored the noise in the interactions, so that we only used deterministic tools. Finally, our numerical simulations showed that the mean-field model (2.1.3), with a sufficiently localized connectivity kernel, is robust enough to display some qualitative behaviors expected for macroscopic quantities in some specific frameworks, while retaining more information than macroscopic models.

Several extensions to this work seem natural. For example, taking inspiration from [31], a possibility could be to randomly choose the connectivity weights $\Phi_{i,j}$ in (2.1.1) with a probability law which depends only on the distance between the neurons i and j. A direct consequence of a mean-field limit result could be the propagation of chaos in the network as the number of neurons goes to infinity, that is the neurons become less and less correlated as their number gets large. Furthermore, another interesting extension comes from the recent work of Chiba and Medvedev [43] for the Kuramoto model, and to study the mean-field limit of the FHN model on various types of random graphs.

2.9 Appendix: proof of lemma 2.4.2

We start by proving that for all fixed $\mathbf{z} \in \mathbb{R}^{d+2}$, there exists a unique solution $(\mathcal{V}(\cdot, \mathbf{z}), \mathcal{W}(\cdot, \mathbf{z})) \in \mathscr{C}^1([0,T])^2$ of (2.4.1) such that for all $t \in [0,T]$, $(\mathcal{V}(t, \cdot), \mathcal{W}(t, \cdot)) \in \mathscr{C}(\mathbb{R}^{d+2}, \mathbb{R})^2$. Then, we prove that $\mathcal{V}$ and $\mathcal{W} \in \mathscr{C}([0,T], \mathcal{E})$, where $\mathcal{E}$ is defined with (2.3.1)-(2.3.2).

Step 1: Existence and uniqueness of the solution of (2.4.1)

First of all, the function
$$\begin{pmatrix} v \\ w \end{pmatrix} \mapsto \begin{pmatrix} N(v) - w \\ A(v, w) \end{pmatrix}$$

is locally Lipschitz continuous in $\mathbb{R}^2$. Moreover, since $\mathcal{U} \in \mathscr{C}([0,T], \mathcal{E})$, then for all $\mathbf{z} = (\mathbf{x}, v, w) \in \mathbb{R}^{d+2}$, the function
$$t \mapsto \int \Phi(\mathbf{x}, \mathbf{x}') \left(\mathcal{U}(t, \mathbf{z}) - \mathcal{U}(t, \mathbf{z}') \right) f_0(\mathrm{d}\mathbf{z}')$$

is continuous on $[0,T]$. Therefore, for all $\mathbf{z} \in \mathbb{R}^{d+2}$, the Cauchy-Lipschitz Theorem gives us the local existence and uniqueness of the solution $(\mathcal{V}(\cdot, \mathbf{z}), \mathcal{W}(\cdot, \mathbf{z}))$ of class $\mathscr{C}^1$. Then, using an energy estimate, we want to prove that for all $\mathbf{z} \in \mathbb{R}^{d+2}$, the couple $(\mathcal{V}(\cdot, \mathbf{z}), \mathcal{W}(\cdot, \mathbf{z}))$ is well-defined on $[0,T]$. According to the definition of $\mathcal{E}$, we know that for all $(t, \mathbf{z}) \in [0,T] \times \mathbb{R}^{d+2}$:

$$|\mathcal{U}(t,\mathbf{z})| \leq \langle v, w \rangle \sup_{s \in [0,T]} \|\mathcal{U}(s)\|_{\mathcal{E}}. \tag{2.9.1}$$

Let $\mathbf{z} \in \mathbb{R}^{d+2}$ and $t \in [0,T]$ small enough so that $(\mathcal{V}, \mathcal{W})$ exists in $(t, \mathbf{z})$. According to the inequality (2.3.3) from Lemma 2.3.1, we have the following energy estimate:

$$\frac{1}{2} \partial_t \left(|\mathcal{V}(t,\mathbf{z})|^2 + |\mathcal{W}(t,\mathbf{z})|^2 \right) \leq \mathcal{T}_l + \mathcal{T}_{nl},$$

where

$$\begin{cases} \mathcal{T}_l := \left(\tau + \dfrac{1}{2} + \kappa \right) \left(|\mathcal{V}(t,\mathbf{z})|^2 + |\mathcal{W}(t,\mathbf{z})|^2 \right) + \dfrac{\tau\, a^2}{2}, \\[2mm] \mathcal{T}_{nl} := -\mathcal{V}(t,\mathbf{z}) \displaystyle\int \Phi(\mathbf{x}, \mathbf{x}') \left(\mathcal{U}(t,\mathbf{z}) - \mathcal{U}(t,\mathbf{z}') \right) f_0(\mathrm{d}\mathbf{z}'). \end{cases}$$

We estimate the second term $\mathcal{T}_{nl}$ using Young's inequality, the assumption that Φ is bounded and the estimate (2.9.1):

$$\begin{aligned} \mathcal{T}_{nl} &\leq \frac{1}{2} |\mathcal{V}(t,\mathbf{z})|^2 + \frac{1}{2} \int |\Phi(\mathbf{x}, \mathbf{x}')|^2 \left(|\mathcal{U}(t,\mathbf{z})|^2 + |\mathcal{U}(t,\mathbf{z}')|^2 \right) f_0(\mathrm{d}\mathbf{z}') \\ &\leq \frac{1}{2} |\mathcal{V}(t,\mathbf{z})|^2 + \frac{1}{2} \|\Phi\|_{\infty}^2 \left(|\mathcal{U}(t,\mathbf{z})|^2 + \int |\mathcal{U}(t,\mathbf{z}')|^2 f_0(\mathrm{d}\mathbf{z}') \right) \\ &\leq \frac{1}{2} |\mathcal{V}(t,\mathbf{z})|^2 + \frac{1}{2} \|\Phi\|_{\infty}^2 \left(|\langle v, w \rangle|^2 + \int |\langle v', w' \rangle|^2 f_0(\mathrm{d}\mathbf{z}') \right) \sup_{s \in [0,T]} \|\mathcal{U}(s)\|_{\mathcal{E}}^2 \\ &\leq \frac{1}{2} |\mathcal{V}(t,\mathbf{z})|^2 + \frac{1}{2} \|\Phi\|_{\infty}^2 \left(1 + \int |\langle v', w' \rangle|^2 f_0(\mathrm{d}\mathbf{z}') \right) \sup_{s \in [0,T]} \|\mathcal{U}(s)\|_{\mathcal{E}}^2 \, |\langle v, w \rangle|^2. \end{aligned}$$

Hence, there exist two constants $C_1 > 0$ and $C_2 > 0$ such that for all $t \in [0,T]$ and $\mathbf{z} \in \mathbb{R}^{d+2}$,

$$\partial_t \left(|\mathcal{V}(t,\mathbf{z})|^2 + |\mathcal{W}(t,\mathbf{z})|^2 \right) \leq C_1 \left(|\mathcal{V}(t,\mathbf{z})|^2 + |\mathcal{W}(t,\mathbf{z})|^2 \right) + C_2 \, |\langle v, w \rangle|^2.$$

Therefore, since $\mathcal{V}$ and $\mathcal{W}$ are continuous with respect to time, Grönwall's inequality yields that for all $t \in [0,T]$,

$$\left(|\mathcal{V}(t,\mathbf{z})|^2 + |\mathcal{W}(t,\mathbf{z})|^2 \right) \leq \left(|v|^2 + C_2\, t\, |\langle v, w \rangle|^2 \right) e^{C_1\, t}. \tag{2.9.2}$$

This implies that $\mathcal{V}(\cdot, \mathbf{z})$ and $\mathcal{W}(\cdot, \mathbf{z})$ are defined on $[0,T]$, and thus we get:

$$(\mathcal{V}(\cdot, \mathbf{z}), \mathcal{W}(\cdot, \mathbf{z})) \in \mathscr{C}^1([0,T]).$$

Moreover, if we divide (2.9.2) by $|\langle v, w \rangle|^2$ and if we take the supremum on $\mathbb{R}^{d+2}$, we conclude that for all $t \in [0,T]$,

$$\|\mathcal{V}(t)\|_{\mathcal{E}}^2 \leq (1 + C_2\, t)\, e^{C_1\, t}. \tag{2.9.3}$$

Moreover, since Φ is continuous with respect to its first variable uniformly relative to its second variable, and since $\mathcal{U} \in \mathscr{C}([0,T], \mathcal{E})$, we get that the function

$$(t, \mathbf{z}) = (t, \mathbf{x}, v, w) \mapsto \int \Phi(\mathbf{x}, \mathbf{x}') \left(\mathcal{U}(t,\mathbf{z}) - \mathcal{U}(t,\mathbf{z}') \right) f_0(\mathrm{d}\mathbf{z}')$$

is continous on $[0,T] \times \mathbb{R}^{d+2}$. Therefore, one can check that for all $t \in [0,T]$,

$$(\mathcal{V}(t, \cdot), \mathcal{W}(t, \cdot)) \in \mathscr{C}(\mathbb{R}^{d+2}, \mathbb{R})^2. \tag{2.9.4}$$

Furthermore, (2.9.3) together with (2.9.4) yield that for all $t \in [0, T]$,

$$(\mathcal{V}(t, \cdot), \mathcal{W}(t, \cdot)) \in \mathcal{E}^2. \tag{2.9.5}$$

Step 2: $\mathcal{V}$ and $\mathcal{W}$ are in $\mathscr{C}([0, T], \mathcal{E})$

It remains to prove that $(\mathcal{V}, \mathcal{W}) \in \mathscr{C}([0, T], \mathcal{E})^2$. Let us fix $t \in [0, T]$. Consider $\tilde{t} \in [0, T]$ and $\mathbf{z} = (\mathbf{x}, v, w) \in \mathbb{R}^{d+2}$. Thus, according to the inequality (2.3.4) from Lemma 2.3.1, we have:

$$\frac{1}{2} \partial_t \left(\left| \mathcal{V}(t, \mathbf{z}) - \mathcal{V}(\tilde{t}, \mathbf{z}) \right|^2 + \left| \mathcal{W}(t, \mathbf{z}) - \mathcal{W}(\tilde{t}, \mathbf{z}) \right|^2 \right) \leq \mathcal{T}_l + \mathcal{T}_{nl},$$

where

$$
\begin{cases}
\mathcal{T}_l := \left(\tilde{\kappa} + \dfrac{\tau + 1}{2} \right) \left(\left| \mathcal{V}(t, \mathbf{z}) - \mathcal{V}(\tilde{t}, \mathbf{z}) \right|^2 + \left| \mathcal{W}(t, \mathbf{z}) - \mathcal{W}(\tilde{t}, \mathbf{z}) \right|^2 \right), \\
\mathcal{T}_{nl} := - \left(\mathcal{V}(t, \mathbf{z}) - \mathcal{V}_{p+1}(\tilde{t}, \mathbf{z}) \right) \\
\qquad \times \displaystyle\int \left[\Phi(\mathbf{x}, \mathbf{x}') \left(\mathcal{U}(t, \mathbf{z}) - \mathcal{U}(t, \mathbf{z}') \right) + \Phi(\mathbf{x}, \mathbf{x}') \left(\mathcal{U}(\tilde{t}, \mathbf{z}) - \mathcal{U}(\tilde{t}, \mathbf{z}') \right) \right] f_0(\mathrm{d}\mathbf{z}').
\end{cases}
$$

To deal with the nonlocal term $\mathcal{T}_{nl}$, we use Young's inequality and the assumption that Φ is bounded:

$$
\begin{aligned}
\mathcal{T}_{nl} &= - \left(\mathcal{V}(t, \mathbf{z}) - \mathcal{V}(\tilde{t}, \mathbf{z}) \right) \left(\left(\mathcal{V}(t, \mathbf{z}) - \mathcal{V}(\tilde{t}, \mathbf{z}) \right) \int \Phi(\mathbf{x}, \mathbf{x}') \, f_0(\mathrm{d}\mathbf{z}') \right. \\
&\qquad \left. + \int \Phi(\mathbf{x}, \mathbf{x}') \left(\mathcal{U}(t, \mathbf{z}') - \mathcal{U}(\tilde{t}, \mathbf{z}') \right) \, f_0(\mathrm{d}\mathbf{z}') \right) \\
&\leq \frac{1}{2} \left| \mathcal{V}(t, \mathbf{z}) - \mathcal{V}(\tilde{t}, \mathbf{z}) \right|^2 \\
&\quad + \frac{1}{2} \| \Phi \|_\infty^2 \left| \mathcal{U}(t, \mathbf{z}) - \mathcal{U}(\tilde{t}, \mathbf{z}) \right|^2 + \frac{1}{2} \| \Phi \|_\infty^2 \| \mathcal{U}(t) - \mathcal{U}(\tilde{t}) \|_\mathcal{E}^2 \int |\langle v', w' \rangle|^2 \, f_0(\mathrm{d}\mathbf{z}').
\end{aligned}
$$

Then, dividing $\mathcal{T}_l$ and $\mathcal{T}_{nl}$ by $|\langle v, w \rangle|^2$ and taking the supremum on $\mathbb{R}^{d+2}$, we get that there exist two constants C_1 and C_2 such that:

$$
\begin{aligned}
\frac{\mathrm{d}}{\mathrm{d}t} &\left(\| \mathcal{V}(t) - \mathcal{V}(\tilde{t}) \|_\mathcal{E}^2 + \| \mathcal{W}(t) - \mathcal{W}(\tilde{t}) \|_\mathcal{E}^2 \right) \\
&\qquad \leq C_1 \left(\| \mathcal{V}(t) - \mathcal{V}(\tilde{t}) \|_\mathcal{E}^2 + \| \mathcal{W}(t) - \mathcal{W}(\tilde{t}) \|_\mathcal{E}^2 \right) + C_2 \| \mathcal{U}(t) - \mathcal{U}(\tilde{t}) \|_\mathcal{E}^2.
\end{aligned}
$$

Since $\mathcal{V}$ and $\mathcal{W}$ are continuous with respect to time, using Grönwall's lemma and the assumption $\mathcal{U} \in \mathscr{C}([0, T], \mathcal{E})$, we conclude that

$$\lim_{\tilde{t} \to t} \left(\| \mathcal{V}(t) - \mathcal{V}(\tilde{t}) \|_\mathcal{E}^2 + \| \mathcal{W}(t) - \mathcal{W}(\tilde{t}) \|_\mathcal{E}^2 \right) = 0,$$

and consequently,

$$(\mathcal{V}, \mathcal{W}) \in \mathscr{C}([0, T], \mathcal{E})^2.$$

Chapter 3

Rigorous derivation of the nonlocal reaction-diffusion FitzHugh-Nagumo system

Contents

Abstract

We introduce a spatially extended transport kinetic FitzHugh-Nagumo model with forced local interactions and prove that its hydrodynamic limit converges towards the classical nonlocal reaction-diffusion FitzHugh-Nagumo system. Our approach is based on a relative entropy method, where the macroscopic quantities of the kinetic model are compared with the solution to the nonlocal reaction-diffusion system. This approach allows to make the rigorous link between kinetic and reaction-diffusion models.

3.1 Introduction

In the last chapter, we established the mean-field limit of a spatially-extended FHN model towards the following transport equation, which reads for all position $\mathbf{x} \in \mathbb{R}^d$ with $d \in \{1, 2, 3\}$, for all time $t > 0$ and for all pair voltage-adaptation $(v, w) \in \mathbb{R}^2$:

$$\partial_t f^\varepsilon + \partial_v \left(f^\varepsilon N(v) - f^\varepsilon w - f^\varepsilon \mathcal{K}_{\Phi_\varepsilon}[f^\varepsilon] \right) + \partial_w \left(A(v, w) f^\varepsilon \right) = 0, \tag{3.1.1}$$

where the operator $\mathcal{K}_{\Phi_\varepsilon}[f^\varepsilon]$ and the convective term A are given by

$$\begin{cases} \mathcal{K}_{\Phi_\varepsilon}[f^\varepsilon](t, \mathbf{x}, v) := \displaystyle\int_{\mathbb{R}^{d+2}} \Phi_\varepsilon(\mathbf{x} - \mathbf{x}')(v - v') \, f^\varepsilon(t, \mathbf{x}', v', w') \, \mathrm{d}w' \mathrm{d}v' \mathrm{d}\mathbf{x}', \\[2mm] A(v, w) := \tau(v + a - b\,w), \end{cases}$$

where $\tau \geq 0$, $a \in \mathbb{R}$ and $b \geq 0$ are fixed constant. Even if we have to consider the variable $v + a$ instead of v, we consider $a = 0$. In our framework, Φ_ε is a connectivity weight which models the influence of the relative positions of two neurons on their interactions, which depends on a small rescaling paramter $\varepsilon > 0$, and N is a nonlinear function which models the cell excitability. In this part, without loss of generality (see [5, 71, 106, 108]), we consider the cubic function[1]

$$N : v \mapsto v - v^3. \tag{3.1.2}$$

Such an equation models the evolution of the density function $f^\varepsilon(t, \mathbf{x}, v, w)$ of finding neurons with a potential membrane $v \in \mathbb{R}$ and an adaptation variable $w \in \mathbb{R}$ at time $t \geq 0$ and position $\mathbf{x} \in \mathbb{R}^d$ within the cortex. The term $\mathcal{K}_\varepsilon[f^\varepsilon]$ describes nonlocal interactions through the whole field, whereas the other terms account for the local reactions due to the excitability of nerve cells.

We introduce the following macroscopic quantities for f^ε a solution of (3.1.1):

$$\begin{cases} \rho^\varepsilon(t, \mathbf{x}) := \displaystyle\int_{\mathbb{R}^2} f^\varepsilon(t, \mathbf{x}, v, w) \, \mathrm{d}v \mathrm{d}w, \\[3mm] \rho^\varepsilon(t, \mathbf{x}) V^\varepsilon(t, \mathbf{x}) = j^\varepsilon(t, \mathbf{x}) := \displaystyle\int_{\mathbb{R}^2} v f^\varepsilon(t, \mathbf{x}, v, w) \, \mathrm{d}v \mathrm{d}w, \\[3mm] \rho^\varepsilon(t, \mathbf{x}) W^\varepsilon(t, \mathbf{x}) = q^\varepsilon(t, \mathbf{x}) := \displaystyle\int_{\mathbb{R}^2} w f^\varepsilon(t, \mathbf{x}, v, w) \, \mathrm{d}v \mathrm{d}w, \end{cases} \tag{3.1.3}$$

where ρ^ε stands for the averaged neuron density, V^ε is the average membrane potential, and W^ε is the average adaptation variable. As explained in the general introduction, the equation

---

[1] All our results remain true for $N(v) = v\,(\alpha - \beta\,v)$ with any $\alpha, \beta > 0$ or $N(v) = v\,(1 - v)\,(v - \theta)$ with $\theta \in (0, 1)$.

formally satisfied by j^ε is not closed because of the presence of the reaction term $\partial_v \left(f^\varepsilon(N(v)) \right)$ in (3.1.1), which introduces higher moments of f^ε in v. To circumvent this difficulty and obtain a closed macroscopic system, we consider a specific form for the connectivity function Φ_ε. We will assume that it can be decomposed by the superposition of strong local interactions modeled by $\frac{1}{\varepsilon}\delta_0$, where δ_0 is the Dirac distribution centered at 0 and weak lateral interactions described by a non-negative connectivity kernel Ψ. As a consequence, for all $\varepsilon > 0$, we work with

$$\Phi_\varepsilon(\mathbf{x}) = \Psi(\mathbf{x}) + \frac{1}{\varepsilon}\delta_0(\mathbf{x}), \quad \forall \mathbf{x} \in \mathbb{R}^d. \tag{3.1.4}$$

Note that such an assumption of strong local interactions and weak lateral interactions is often used when modeling visual cortex [24]. We can then rewrite the kinetic equation (3.1.1) as

$$\partial_t f^\varepsilon + \partial_v \left(f^\varepsilon N(v) - f^\varepsilon w - f^\varepsilon \mathcal{K}_\Psi[f^\varepsilon] \right) - \frac{1}{\varepsilon}\partial_v \left(f^\varepsilon(\rho^\varepsilon v - j^\varepsilon) \right) + \partial_w \left(A(v,w)f^\varepsilon \right) = 0 \tag{3.1.5}$$

for $(t, \mathbf{x}, v, w) \in (0, \infty) \times \mathbb{R}^{d+2}$, and the macroscopic quantities $(\rho^\varepsilon, \rho^\varepsilon V^\varepsilon, \rho^\varepsilon W^\varepsilon)$ formally verify the system of equations:

$$\begin{cases} \partial_t \rho^\varepsilon = 0, \\[2mm] \partial_t \left(\rho^\varepsilon V^\varepsilon \right) - \rho^\varepsilon \mathcal{L}_{\rho^\varepsilon}(V^\varepsilon) = \rho^\varepsilon \left[N(V^\varepsilon) - W^\varepsilon \right] + \mathcal{E}(f^\varepsilon), \\[2mm] \partial_t \left(\rho^\varepsilon W^\varepsilon \right) = \rho^\varepsilon A(V^\varepsilon, W^\varepsilon), \end{cases} \tag{3.1.6}$$

for $(t, \mathbf{x}) \in (0, \infty) \times \mathbb{R}^d$, where the spatial nonlocal operator $\mathcal{L}_\rho$ is defined through

$$\mathcal{L}_\rho(V) := -(\Psi \star \rho)V + \Psi \star [\rho V], \tag{3.1.7}$$

whereas $\star$ stands for the convolution product in $\mathbb{R}^d$ only with respect to space. Furthermore, we have set

$$\mathcal{E}(f^\varepsilon)(t, \mathbf{x}) := \int_{\mathbb{R}^2} f^\varepsilon(t, \mathbf{x}, v, w) \left[N(v) - N(V^\varepsilon(t, \mathbf{x})) \right] \mathrm{d}v \mathrm{d}w. \tag{3.1.8}$$

It is worth noticing that v is a collisional invariant for the operator $\partial_v \left(f^\varepsilon(\rho^\varepsilon v - j^\varepsilon) \right)$ such that the macroscopic system (3.1.6) does not naturally present terms of order $\mathcal{O}(1/\varepsilon)$.

In the formal limit $\varepsilon \to 0$, the solution f^ε to (3.1.5) should converge in some weak sense towards the mono-kinetic distribution in v:

$$f^\varepsilon(t, \mathbf{x}, v, w) \underset{\varepsilon \to 0}{\rightharpoonup} F(t, \mathbf{x}, w) \otimes \delta_0(v - V(t, \mathbf{x})), \tag{3.1.9}$$

where the limit (F, V) has to be determined. First we set

$$\rho(t, \mathbf{x}) := \int_{\mathbb{R}} F(t, \mathbf{x}, w)\mathrm{d}w, \quad \rho(t, \mathbf{x})\, W(t, \mathbf{x}) := \int_{\mathbb{R}} F(t, \mathbf{x}, w)\, w\, \mathrm{d}w.$$

Then, assuming that $\mathcal{E}(f^\varepsilon) \to 0$ as $\varepsilon \to 0$ in the second equation of (3.1.6), we get that the pair (F, V) formally satisfies

$$\begin{cases} \partial_t \left(\rho V \right) - \rho \mathcal{L}_\rho(V) = \rho \left[N(V) - W \right], \\[2mm] \partial_t F + \partial_w \left(A(V, w) F \right) = 0. \end{cases}$$

Therefore, the limit function $\mathcal{Z} := (\rho, \rho V, \rho W)$ is expected to verify the following nonlocal reaction diffusion system:

$$\partial_t \mathcal{Z} = \mathcal{F}(\mathcal{Z}), \quad t > 0, \mathbf{x} \in \mathbb{R}^d, \tag{3.1.10}$$

with $\mathcal{F}$ given by

$$\mathcal{F}(\mathcal{Z}) := \rho \begin{pmatrix} 0 \\ \mathcal{L}_\rho(V) + N(V) - W \\ A(V, W) \end{pmatrix}. \tag{3.1.11}$$

It is interesting to note that although we obtain a mono-kinetic distribution in the v variable only, it is enough to obtain a closed macroscopic model. Indeed, the kinetic equation (3.1.5) is linear in the w variable which allows to close the system when integrating in w.

Let us first make some comments on the structure of the macroscopic model (3.1.10)-(3.1.11). For all $\mathbf{x} \in \mathbb{R}^d$ such that $\rho(t, \mathbf{x}) = \rho_0(\mathbf{x}) > 0$, the system (3.1.10) reduces to the usual nonlocal reaction-diffusion system of FitzHugh-Nagumo type

$$\begin{cases} \partial_t V - \mathcal{L}_{\rho_0}(V) = N(V) - W, \\ \\ \partial_t W = \tau(V + a - bW), \end{cases} \tag{3.1.12}$$

for $\mathbf{x} \in \mathbb{R}^d$ and $t > 0$, where $\mathcal{L}_{\rho_0}(V)$ can be interpreted as a nonlocal diffusion operator in $\mathbf{x}$. In the limiting case $\rho_0 \equiv 1$[2], such a system has already been well studied especially regarding the formation of propagating waves (traveling fronts and pulses) in both cases $\tau = 0$ and $0 < \tau \ll 1$ [8, 62]. We also mention the classical works regarding the local FitzHugh-Nagumo system, that is when $\mathcal{L}_{\rho_0}(V)$ is replaced by the standard diffusion operator [36, 80, 92], and the more recent advances for the discrete case [88, 89]. The present work is then a rigorous justification of the nonlocal reaction-diffusion system of FitzHugh-Nagumo type (3.1.10) that is obtained as the hydrodynamic limit of the kinetic equation (3.1.5) as $\varepsilon \to 0$.

The main challenge towards a rigorous proof of this hydrodynamic limit stems from the Dirac singularity of the mono-kinetic distribution which prevents us from using a classical entropy of the form $f \log(f)$ since it would not be well-defined. Following ideas from [63], who proved a similar hydrodynamic limit of the kinetic Cucker-Smale model for collective motion with forced local alignment towards the pressureless Euler equation with a nonlocal force, we shall overcome this problem by the mean of a relative entropy argument. Let us also mention the work of [94] in which the hydrodynamic limit of a collisionless and non-diffusive kinetic equation under strong local alignment regime is rigorously established *via* a relative entropy argument. The specific difficulty here is that, instead of having a transport term as in [63], the presence of the reaction term $\partial_v(f^\varepsilon N(v))$ in (3.1.5) introduces higher order moments of f^ε in v which we will need to control. In fact, it will be enough to have a priori estimates of second and fourth order moments of f^ε in (v, w) to circumvent this difficulty.

The rest of this chapter is organized as follows. In Section 3.2, we state our main result about the hydrodynamic limit of (3.1.5) towards (3.1.10). Then, in Section 3.3, we derive some a priori estimates that will be crucial for our relative entropy argument. The proof of our main result is contained in Section 3.4.

3.2 Preliminaries and main result

In this section, we present our main result on the hydrodynamic limit from a weak solution $(f^\varepsilon)_{\varepsilon>0}$ of the kinetic equation (3.1.5) to a classical solution $(\rho_0, \rho_0 V, \rho_0 W)$ of the asymptotic system (3.1.10). For that, we first need to present the existence result for the weak solution of (3.1.5) and the classical solution of (3.1.10).

---

[2]In our setting, ρ_0 is probability density function such that the case $\rho_0 \equiv 1$ is excluded from our hypotheses. Nevertheless, system (3.1.12) is still well defined for $\rho_0 \equiv 1$, see Proposition 3.2.3.

First we set the hypotheses we make for the study of the kinetic FHN equation (3.1.5) and the limit system (3.1.10). We consider a connectivity kernel Ψ in (3.1.4) which is non-negative, symmetric and satisfies

$$\Psi \in L^1(\mathbb{R}^d). \tag{3.2.1}$$

This last assumption models the fact that if two neurons are far away from each other, they have weak mutual interactions. The other condition is a natural biological assumption and expresses the symmetric and excitatory nature of the considered underlying neural network.

3.2.1 Existence of weak solution to (3.1.5)

We here say that f^ε is a weak solution of (3.1.5) if for any $T > 0$, $f^\varepsilon(0,.) = f_0^\varepsilon \geq 0$ in $\mathbb{R}^{d+2}$,

$$f^\varepsilon \in \mathscr{C}^0([0,T], L^1(\mathbb{R}^{d+2})) \cap L^\infty((0,T) \times \mathbb{R}^{d+2}),$$

and (3.1.5) holds in the sense of distribution, that is, for any $\varphi \in \mathscr{C}_c^\infty([0,T] \times \mathbb{R}^{d+2})$, the weak formulation holds

$$\int_0^T \int f^\varepsilon \left[\partial_t \varphi + \left(N(v) - w - \mathcal{K}_\Psi[f^\varepsilon] - \frac{1}{\varepsilon}(\rho^\varepsilon v - j^\varepsilon) \right) \partial_v \varphi + A(v,w)\partial_w \varphi \right] \mathrm{d}\mathbf{z}\,\mathrm{d}t$$

$$+ \int f_0^\varepsilon \varphi(0)\,\mathrm{d}\mathbf{z} = 0 \tag{3.2.2}$$

where $\mathbf{z} = (\mathbf{x}, v, w) \in \mathbb{R}^{d+2}$.

Remark 3.2.1. *Using the mass conservation property of equation (3.1.5), we can easily check that the time varying macroscopic quantities $(\rho^\varepsilon, V^\varepsilon, W^\varepsilon)$ defined in (3.1.3) simplify to*

$$\rho^\varepsilon(t,\mathbf{x}) := \int_{\mathbb{R}^2} f^\varepsilon(t,\mathbf{x},v,w)\,\mathrm{d}v\,\mathrm{d}w = \int_{\mathbb{R}^2} f_0^\varepsilon(\mathbf{x},v,w)\,\mathrm{d}v\,\mathrm{d}w = \rho_0^\varepsilon(\mathbf{x}), \tag{3.2.3}$$

hence we have

$$\begin{cases} \rho_0^\varepsilon(\mathbf{x})V^\varepsilon(t,\mathbf{x}) := \displaystyle\int_{\mathbb{R}^2} v\, f^\varepsilon(t,\mathbf{x},v,w)\,\mathrm{d}v\,\mathrm{d}w, \\[3mm] \rho_0^\varepsilon(\mathbf{x})W^\varepsilon(t,\mathbf{x}) := \displaystyle\int_{\mathbb{R}^2} w\, f^\varepsilon(t,\mathbf{x},v,w)\,\mathrm{d}v\,\mathrm{d}w, \end{cases}$$

for all $\mathbf{x} \in \mathbb{R}^d$ and all $t > 0$ where f^ε is well-defined.

First, let us prove the well-posedness of the kinetic equation (3.1.5).

Proposition 3.2.2. *For any $\varepsilon > 0$ we choose Ψ to be non-negative, symmetric and satisfies (3.2.1), we also assume that f_0^ε satisfies*

$$f_0^\varepsilon \geq 0, \quad f_0^\varepsilon \in L^1(\mathbb{R}^{d+2}), \quad f_0^\varepsilon, \nabla_\mathbf{u} f_0^\varepsilon \in L^\infty(\mathbb{R}^{d+2}), \tag{3.2.4}$$

where $\mathbf{u} = (v,w)$ and for all $\mathbf{x} \in \mathbb{R}^d$,

$$\mathrm{Supp}(f_0^\varepsilon(\mathbf{x},\cdot,\cdot)) \subseteq B(0, R_0^\varepsilon) \subset \mathbb{R}^2. \tag{3.2.5}$$

Then for any $T > 0$, there exists a unique f^ε weak solution to (3.1.5) in the sense of (3.2.2), which is compactly supported in $\mathbf{u} = (v,w) \in \mathbb{R}^2$.

The proof relies on a classical fixed point argument, but for the sake of completeness, it is postponed to the Appendix 3.5.

3.2.2 Existence of classical solution to the nonlocal FitzHugh-Nagumo system

Let us now state the result of existence and uniqueness for the nonlocal reaction-diffusion FitzHugh-Nagumo system defined as

$$
\begin{cases}
\partial_t V - \mathcal{L}_{\rho_0}(V) = N(V) - W, & \\
& t > 0 \text{ and } \mathbf{x} \in \mathbb{R}^d, \\
\partial_t W = \tau(V + a - bW), & \\
V(0, \mathbf{x}) = V_0(\mathbf{x}), \quad W(0, \mathbf{x}) = W_0(\mathbf{x}), \quad \mathbf{x} \in \mathbb{R}^d.
\end{cases}
\tag{3.2.6}
$$

Before describing precisely the existence and uniqueness of solution (V, W) to the hydrodynamical system (3.2.6), let us emphasize that this system is more convenient to analyse than (3.1.10)-(3.1.11) verified by $\mathcal{Z} = (\rho_0, \rho_0 V, \rho_0 W)$. Indeed, as we will see, both solutions coincide in the region of interest where $\rho_0 > 0$, but the study of (3.2.6) allows to construct a solution such that for all $t \in [0, T]$

$$
V(t), W(t) \in L^\infty(\mathbb{R}^d).
$$

This property is crucial to apply the relative entropy method in the asymptotic analysis of (3.1.5) when $\varepsilon \to 0$.

Proposition 3.2.3. *We choose Ψ to be non-negative, symmetric and satisfies (3.2.1), we also suppose that ρ_0 and the initial data (V_0, W_0) satisfies,*

$$
\rho_0 \geq 0, \quad \rho_0 \in L^1 \cap L^\infty(\mathbb{R}^d), \quad V_0, W_0 \in L^\infty(\mathbb{R}^d).
\tag{3.2.7}
$$

Then for any $T > 0$, there exists a unique classical solution $(V, W) \in \mathscr{C}^1([0, T], L^\infty(\mathbb{R}^d))$ to the equation (3.2.6). Furthermore, $\mathcal{Z} = (\rho_0, \rho_0 V, \rho_0 W)$ is a solution to (3.1.10)-(3.1.11).

The proof of this proposition also relies on a classical fixed point argument. For the sake of completeness, it is postponed to the Appendix 3.6. Then as a direct consequence, for a given initial data (F_0, V_0), it leads to the existence and uniqueness of solution (F, V) to the following system of equations

$$
\begin{cases}
\partial_t F + \partial_w \left(A(V, w) F\right) = 0, & \\
\rho_0 \partial_t V - \rho_0 \mathcal{L}_{\rho_0}(V) = \rho_0 \left[N(V) - W\right], & \\
\rho_0(\mathbf{x}) = \displaystyle\int_{\mathbb{R}} F(t, \mathbf{x}, w) \, \mathrm{d}w, & \\
V(t, \mathbf{x}) = 0, \quad t > 0 \text{ and } \mathbf{x} \in \mathbb{R}^d \setminus \mathrm{Supp}_{\mathrm{ess}}(\rho_0), & \\
W(t, \mathbf{x}) = \begin{cases} \dfrac{1}{\rho_0(\mathbf{x})} \displaystyle\int_{\mathbb{R}} F(t, \mathbf{x}, w) \, w \, \mathrm{d}w, & \text{if } \rho_0(\mathbf{x}) > 0, \\ 0, & \text{else.} \end{cases}
\end{cases}
\tag{3.2.8}
$$

More precisely we have the following result.

Corollary 3.2.4. *Consider $V_0 \in L^\infty(\mathbb{R}^d)$ and $F_0 \in \mathcal{M}(\mathbb{R}^{d+1})$ such that*

$$
\int_{\mathbb{R}^{d+1}} w^2 F_0(\mathrm{d}\mathbf{x}, \mathrm{d}w) < \infty
$$

and for almost every $\mathbf{x} \in \mathbb{R}^d$,

$$\rho_0(\mathbf{x}) = \int_{\mathbb{R}} F_0(\mathbf{x}, w) \, \mathrm{d}w, \quad W_0(\mathbf{x}) := \begin{cases} \dfrac{1}{\rho_0(\mathbf{x})} \displaystyle\int_{\mathbb{R}} F_0(\mathbf{x}, w) \, w \, \mathrm{d}w, & \textit{if } \rho_0(\mathbf{x}) > 0, \\ \\ 0, & \textit{else}, \end{cases}$$

where $\rho_0 \in L^1 \cap L^\infty(\mathbb{R}^d)$ *and* $W_0 \in L^\infty(\mathbb{R}^d)$. *We further assume that* $V_0 = 0$ *on* $\mathbb{R}^d \setminus \mathrm{Supp}_{ess}(\rho_0)$. *Then for any* $T > 0$, *there exists a unique couple* (F, V) *solution to* (3.2.8), *where*

$$(F, V) \in L^\infty((0, T), \mathcal{M}(\mathbb{R}^{d+1})) \times \mathscr{C}^1([0, T], L^\infty(\mathbb{R}^d)),$$

and F *is a measure solution to the first equation* (3.2.8), *that is, for any* $\varphi \in \mathscr{C}_c^1(\mathbb{R}^{d+1})$

$$\frac{\mathrm{d}}{\mathrm{d}t} \int_{\mathbb{R}^{d+1}} \varphi(\mathbf{x}, w) \, F(t, \mathrm{d}\mathbf{x}, \mathrm{d}w) - \int_{\mathbb{R}^{d+1}} A(V(t, \mathbf{x}), w) \, \partial_w \varphi(\mathbf{x}, w) \, F(t, \mathrm{d}\mathbf{x}, \mathrm{d}w) = 0 \qquad (3.2.9)$$

such that there exists a constant $C_T > 0$,

$$\int_{\mathbb{R}^{d+1}} w^2 F(t, \mathrm{d}\mathbf{x}, \mathrm{d}w) < C_T, \quad t \in [0, T].$$

Proof. We first apply Proposition 3.2.3 with (ρ_0, V_0, W_0), where (ρ_0, W_0) is computed from the moments with respect to $(1, w)$ of the initial distribution F_0, that is, for almost every $\mathbf{x} \in \mathbb{R}^d$,

$$\rho_0(\mathbf{x}) = \int_{\mathbb{R}} F_0(\mathbf{x}, w) \, \mathrm{d}w, \quad W_0(\mathbf{x}) := \begin{cases} \dfrac{1}{\rho_0(\mathbf{x})} \displaystyle\int_{\mathbb{R}} F_0(\mathbf{x}, w) \, w \, \mathrm{d}w, & \text{if } \rho_0(\mathbf{x}) > 0, \\ \\ 0, & \text{else.} \end{cases}$$

We then denote by $(\widetilde{V}, \widetilde{W})$ the corresponding unique classical solution to (3.2.6) starting from such an initial condition. Finally, we define

$$V(t, \mathbf{x}) := \begin{cases} \widetilde{V}(t, \mathbf{x}), & \text{if } \rho_0(\mathbf{x}) > 0, \\ \\ 0, & \text{else.} \end{cases} \qquad (3.2.10)$$

As ρ_0 is independent of time, we note that $V \in \mathscr{C}^1([0, T], L^\infty(\mathbb{R}^d))$.

We now prove that for any couple solution $(\overline{F}, \overline{V})$ of (3.2.8) then $\overline{V}$ is precisely given by (3.2.10). Thus, let us suppose that $(\overline{F}, \overline{V})$ is a well-defined solution of (3.2.8) on $[0, T]$ with finite second moment. We necessarily get that $\rho_0 \overline{W}$ has to satisfy

$$\partial_t(\rho_0 \overline{W}) - \rho_0 A(\overline{V}, \overline{W}) = 0,$$

together with

$$\rho_0 \partial_t \overline{V} - \rho_0 \mathcal{L}_{\rho_0}(\overline{V}) = \rho_0 \left[N(\overline{V}) - \overline{W} \right].$$

Thus, for any $\mathbf{x} \in \mathbb{R}^d$ such that $\rho_0(\mathbf{x}) > 0$, the couple $(\overline{V}, \overline{W})$ coincides with the unique solution to (3.2.6) with initial condition (ρ_0, V_0, W_0). This is ensured from the fact that the convolution in the nonlocal part $\Psi * (\rho_0 \overline{V})$ of the linear operator $\mathcal{L}_{\rho_0}(\overline{V})$ is only evaluated on the regions where $\rho_0 > 0$. Then, this uniquely defines $\overline{V}(t, \mathbf{x}) = \widetilde{V}(t, \mathbf{x})$ on $\rho_0 > 0$. By definition of a solution to (3.2.8), whenever $\rho_0 = 0$, we have that $\overline{V}(, \mathbf{x}) = 0$. As a conclusion, we have just shown that if $(\overline{F}, \overline{V})$ is a well-defined solution of (3.2.8) on $[0, T]$ with finite second moment then necessarily $\overline{V} = V$ where V is uniquely defined in (3.2.10).

For V defined as above in (3.2.10), we consider the transport equation

$$\begin{cases} \partial_t F + \partial_w \left(A(V, w) \, F \right) \, = \, 0, \\[2mm] F(0) \, = \, F_0. \end{cases} \qquad (3.2.11)$$

Then, for almost every $\mathbf{x} \in \mathbb{R}^d$ and all $(t, w) \in [0; T] \times \mathbb{R}$, we introduce the system of characteristic curves associated to (3.2.11), that is,

$$\begin{cases} \dfrac{\mathrm{d}}{\mathrm{d}s} \mathcal{W}(s) \, = \, A \left(V(s, \mathbf{x}), \, \mathcal{W}(s) \right), \\[3mm] \mathcal{W}(t) \, = \, w, \end{cases} \qquad (3.2.12)$$

where V is defined in (3.2.10). From the regularity with respect to $(t, w) \in [0, T] \times \mathbb{R}$ of the functions $A(.,.)$ and $V(.,.)$ and since $A(.,.)$ grows at most linearly with respect to w, we get global existence and uniqueness of a solution to (3.2.12). This solution is denoted by $\mathcal{W}(s, t, \mathbf{x}, w)$, then we verify using the theory of characteristics that the unique solution to the transport equation (3.2.11) is given by

$$F(t, \mathbf{x}, w) = F_0(\mathbf{x}, \mathcal{W}(0, t, \mathbf{x}, w)) \, e^{\tau \, b \, t}.$$

From the above expression, it easy to compute the second order moment of F with respect to w and get that there exists $C_T > 0$ such that

$$\int_{\mathbb{R}^{d+1}} w^2 F(t, \mathrm{d}\mathbf{x}, \mathrm{d}w) < C_T, \quad t \in [0, T].$$

As a final consequence of the above computations, we have that

$$\frac{1}{\rho_0(\mathbf{x})} \int_{\mathbb{R}} F(t, \mathbf{x}, w) \, w \, \mathrm{d}w = \widetilde{W}(t, \mathbf{x}), \text{ for all } \mathbf{x} \in \mathbb{R}^d \text{ such that } \rho_0(\mathbf{x}) > 0,$$

by uniqueness of the solutions of (3.2.6). This shows that the couple (F, V) is the unique solution to (3.2.8) where V is given in (3.2.10) and F is the unique measure solution of (3.2.11). $\qquad \square$

3.2.3 Main result

Now, we are ready to state our main result about the hydrodynamic limit. To this aim we consider a non-negative initial data $(f_0^\varepsilon)_{\varepsilon > 0}$ and suppose that there exists a constant $C > 0$, such that for all $\varepsilon > 0$,

$$\|\rho_0^\varepsilon\|_{L^\infty} \leq C \qquad (3.2.13)$$

and

$$\int \left(1 + |\mathbf{x}|^4 + |v|^4 + |w|^4 \right) f_0^\varepsilon(\mathbf{x}, v, w) \mathrm{d}w \mathrm{d}v \mathrm{d}\mathbf{x} \leq C. \qquad (3.2.14)$$

Theorem 3.2.5. *Let $T > 0$, Ψ be a non-negative, symmetric kernel verifying (3.2.1) and $(f_0^\varepsilon)_\varepsilon$, a sequence of initial data such that for all $\varepsilon > 0$, (3.2.4), (3.2.5), (3.2.13) and (3.2.14) are satisfied. Assume that (ρ_0, V_0, W_0) verifies (3.2.7), and*

$$\|\rho_0^\varepsilon - \rho_0\|_{L^2}^2 + \int \rho_0^\varepsilon(\mathbf{x}) \left[|V_0^\varepsilon(\mathbf{x}) - V_0(\mathbf{x})|^2 + |W_0^\varepsilon(\mathbf{x}) - W_0(\mathbf{x})|^2 \right] \mathrm{d}\mathbf{x} \leq C \, \varepsilon^{1/(d+6)}. \qquad (3.2.15)$$

Then, the macroscopic quantities $(\rho_0^\varepsilon, V^\varepsilon, W^\varepsilon)$, computed from the solution f^ε to (3.1.5), verify that for all $t \in [0, T]$,

$$\int_{\mathbb{R}^d} \left[|V^\varepsilon(t, \mathbf{x}) - V(t, \mathbf{x})|^2 + |W^\varepsilon(t, \mathbf{x}) - W(t, \mathbf{x})|^2 \right] \rho_0^\varepsilon(\mathbf{x}) \, \mathrm{d}\mathbf{x} \le C_T \, \varepsilon^{1/(d+6)},$$

where (V, W) is the unique solution to (3.1.12).

Let further assume that (ρ_0, V_0, W_0) are such that,

$$\rho_0(\mathbf{x}) = \int_{\mathbb{R}} F_0(\mathbf{x}, w) \, \mathrm{d}w, \quad W_0(\mathbf{x}) = \begin{cases} \dfrac{1}{\rho_0(\mathbf{x})} \displaystyle\int_{\mathbb{R}} F_0(\mathbf{x}, w) \, w \, \mathrm{d}w, & \text{if } \rho_0(\mathbf{x}) > 0, \\[4mm] 0, & \text{else,} \end{cases}$$

for $F_0 \in \mathcal{M}(\mathbb{R}^{d+1})$, and $V_0 = 0$ on $\mathbb{R}^d \backslash \mathrm{Supp}_{ess}(\rho_0)$. Moreover, consider the function F_0^ε such that for all $\mathbf{x} \in \mathbb{R}^d$ and all $w \in \mathbb{R}$,

$$F_0^\varepsilon(\mathbf{x}, w) = \int f_0^\varepsilon(\mathbf{x}, v, w) \, \mathrm{d}v.$$

If $F_0^\varepsilon \rightharpoonup F_0$ weakly-$\star$ in $\mathcal{M}\left(\mathbb{R}^{d+1}\right)$ then we have for all $\varphi \in \mathscr{C}_b^0(\mathbb{R}^{d+2})$:

$$\int \varphi(\mathbf{x}, v, w) \, f^\varepsilon(t, \mathbf{x}, v, w) \, \mathrm{d}v \, \mathrm{d}w \, \mathrm{d}\mathbf{x} \to \int \varphi(\mathbf{x}, V(t, \mathbf{x}), w) \, F(t, \mathrm{d}\mathbf{x}, \mathrm{d}w),$$

strongly in $L_{loc}^1(0, T)$ as $\varepsilon \to 0$, where (F, V) is the unique solution to (3.2.8).

Sketch of the Proof of Theorem 3.2.5. Our approach is based on the application of relative entropy method [51, 56] and more recently [94] , and will be explained in section 3.4. The first step of the proof is to introduce a relative entropy which allows us to compare solutions of (3.1.10) with those of (3.1.6), and then derive an estimate which will enable us to prove that this relative entropy tends to 0 as ε vanishes. Deriving such an estimate is the most difficult part of the analysis. More precisely, the difficulties come from: (i) the reaction term $\partial_v(f^\varepsilon N(v))$ which introduces moments of order 4 that we will need to control, and (ii) the fact that V^ε and W^ε are not a priori bounded in $L^\infty(\mathbb{R}^d)$. We will overcome this problem using two entropy inequalities that will be proved in Section 3.3.

The rest of the paper is devoted to the proof of Theorem 3.2.5, where we get *a priori* estimates uniformly with respect to $\varepsilon > 0$ on the solution $(f^\varepsilon)_{\varepsilon > 0}$ constructed in Proposition 3.2.2 and study the behavior of a relative entropy [51, 56].

3.3 A priori estimates

In this section, we prove some a priori estimates of the moments of a solution to (3.1.5) which will be crucial for the proof of Theorem 3.2.5. For all $i \in \mathbb{N}$ and $z \in \{\mathbf{x}, v, w\}$, we denote by μ_i^z the moment of order i in z of f^ε, defined as

$$\mu_i^z(t) := \int_{\mathbb{R}^{d+2}} |z|^i f^\varepsilon(t, \mathbf{x}, v, w) \, \mathrm{d}\mathbf{x} \mathrm{d}v \mathrm{d}w.$$

whereas μ_i is given by

$$\mu_i(t) := \mu_i^{\mathbf{x}}(t) + \mu_i^v(t) + \mu_i^w(t).$$

Throughout this sequel, let $T > 0$ and $\varepsilon > 0$, and suppose that f^ε is a well-defined solution to (3.1.5) for all $t \in (0, T]$ obtained in Proposition 3.2.2. For any $p \in \mathbb{N}^*$, we first establish some a priori estimates on μ_{2p}^v and μ_{2p}^w.

Lemma 3.3.1 (Moment estimates). *Consider the solution f^ε to* (3.1.5) *given by Proposition* 3.2.2 *and* $p^* \in \mathbb{N}^*$

$$\mu^v_{2p^*}(0) + \mu^w_{2p^*}(0) < \infty.$$

Then there exists $C > 0$, only depending on p^* and τ, such that for all $p \in [1, p^*]$,

$$\frac{1}{2p} \frac{\mathrm{d}}{\mathrm{d}t} \left[\mu^v_{2p} + \mu^w_{2p} \right](t) + \mu^v_{2p+2}(t) + \frac{1}{\varepsilon} \mathcal{D}_p(t) \leq C \left(\left[\mu^v_{2p} + \mu^w_{2p} \right](t) + 1 \right), \qquad (3.3.1)$$

where $\mathcal{D}_p(t)$ is non-negative and defined as

$$\mathcal{D}_p(t) := \int_{\mathbb{R}^{d+2}} f^\varepsilon \, v^{2p-1} \, (v - V^\varepsilon) \, \rho^\varepsilon_0 \, \mathrm{d}\mathbf{x}\mathrm{d}v\mathrm{d}w.$$

Proof. Consider f^ε a well-defined solution to (3.1.5) and $p \in \mathbb{N}^*$, we compute the time evolution of moments in $|v|^{2p}$ and $|w|^{2p}$, hence we have

$$\frac{1}{2p} \frac{\mathrm{d}}{\mathrm{d}t} \left[\mu^v_{2p} + \mu^w_{2p} \right](t) = I_1 + I_2 + I_3 + I_4 + I_5,$$

where

$$\begin{cases} I_1 &:= + \int_{\mathbb{R}^{d+2}} v^{2p-1} \, N(v) \, f^\varepsilon \, \mathrm{d}\mathbf{x}\mathrm{d}v\mathrm{d}w, \\[2mm] I_2 &:= -\frac{1}{\varepsilon} \int_{\mathbb{R}^{d+2}} f^\varepsilon \, \rho^\varepsilon \, v^{2p-1} \, (v - V^\varepsilon) \, \mathrm{d}\mathbf{x}\mathrm{d}v\mathrm{d}w, \\[2mm] I_3 &:= - \int_{\mathbb{R}^{d+2}} v^{2p-1} \, \mathcal{K}_\Psi[f^\varepsilon] \, f^\varepsilon \, \mathrm{d}\mathbf{x}\mathrm{d}v\mathrm{d}w, \\[2mm] I_4 &:= - \int_{\mathbb{R}^{d+2}} v^{2p-1} \, w \, f^\varepsilon \, \mathrm{d}\mathbf{x}\mathrm{d}v\mathrm{d}w, \\[2mm] I_5 &:= + \int_{\mathbb{R}^{d+2}} w^{2p-1} \, A(v, w) \, f^\varepsilon \, \mathrm{d}\mathbf{x}\mathrm{d}v\mathrm{d}w. \end{cases}$$

First of all we treat the term I_1, since $v^{2p-1} \, N(v) = |v|^{2p} - |v|^{2p+2}$, we get

$$I_1 = \int_{\mathbb{R}^{d+2}} \left(|v|^{2p} - |v|^{2p+2} \right) f^\varepsilon \, \mathrm{d}\mathbf{x}\mathrm{d}v\mathrm{d}w = \mu^v_{2p}(t) - \mu^v_{2p+2}(t).$$

Furthermore, we estimate the second term I_2 and show that it is non-positive. Indeed, from the definition of V^ε, we observe that

$$\int \rho^\varepsilon \, (V^\varepsilon)^{2p-1} \left(\int f^\varepsilon \, (v - V^\varepsilon) \, \mathrm{d}v \, \mathrm{d}w \right) \mathrm{d}\mathbf{x} = 0.$$

Therefore, since $p \geq 1$, the function $v \mapsto v^{2p-1}$ is non-decreasing, which yields

$$\varepsilon I_2 = - \int f^\varepsilon \left[\left(v^{2p-1} - (V^\varepsilon)^{2p-1} \right) + (V^\varepsilon)^{2p-1} \right] (v - V^\varepsilon) \, \rho^\varepsilon \, \mathrm{d}v\mathrm{d}w\mathrm{d}\mathbf{x}$$

$$= - \int f^\varepsilon \left(v^{2p-1} - (V^\varepsilon)^{2p-1} \right) (v - V^\varepsilon) \, \rho^\varepsilon \, \mathrm{d}v\mathrm{d}w\mathrm{d}\mathbf{x} \leq 0.$$

As a consequence, we obtain that $\varepsilon I_2 = -\mathcal{D}_p \leq 0$.

Then, we deal with I_3 and prove that it contributes to the dissipation of moments. Indeed, by symmetry of Ψ we may reformulate I_3, using the shorthand notation $f^{\varepsilon\prime} = f^\varepsilon(\mathbf{x}', v', w')$ and $f^\varepsilon = f^\varepsilon(\mathbf{x}, v, w)$, as

$$
\begin{aligned}
I_3 &= -\frac{1}{2} \iint \Psi(\mathbf{x} - \mathbf{x}')\, v^{2p-1} \left(v - v'\right)\, f^{\varepsilon\prime}(t)\, f^\varepsilon(t)\, \mathrm{d}\mathbf{x}\mathrm{d}v\mathrm{d}w\mathrm{d}\mathbf{x}'\mathrm{d}v'\mathrm{d}w' \\
&\quad - \frac{1}{2} \iint \Psi(\mathbf{x} - \mathbf{x}')\, v'^{2p-1} \left(v' - v\right)\, f^{\varepsilon\prime}(t)\, f^\varepsilon(t)\, \mathrm{d}\mathbf{x}\mathrm{d}v\mathrm{d}w\mathrm{d}\mathbf{x}'\mathrm{d}v'\mathrm{d}w' \\
&\leq 0.
\end{aligned}
$$

Finally, we can easily compute I_4, which yields

$$
\begin{aligned}
I_4 &\leq \int f^\varepsilon \left(\frac{2p-1}{2p} |v|^{2p} + \frac{1}{2p} |w|^{2p} \right) \mathrm{d}\mathbf{x}\mathrm{d}v\mathrm{d}w \\
&\leq \frac{2p-1}{2p}\, \mu_{2p}(t),
\end{aligned}
$$

whereas the last term I_5 gives

$$
\begin{aligned}
I_5 &= \tau \int \left[w^{2p-1} v + a\, w^{2p-1} - b\,|w|^{2p} \right] f^\varepsilon\, \mathrm{d}\mathbf{x}\mathrm{d}v\mathrm{d}w \\
&\leq \tau \int \left[\frac{1}{2p} |v|^{2p} + \frac{2p-1}{2p} |w|^{2p} + \frac{2p-1}{2p} |w|^{2p} + \frac{|a|^{2p}}{2p} \right] f^\varepsilon\, \mathrm{d}\mathbf{x}\mathrm{d}v\mathrm{d}w \\
&\leq \tau \frac{2p-1}{p}\, \mu_{2p}(t) + \frac{\tau |a|^{2p}}{2p}.
\end{aligned}
$$

Therefore, gathering the previous results, we get the entropy inequality (3.3.1) with $C > 0$, only depending on p, τ and a. $\qquad\square$

This Lemma will be helpful to pass to the limit $\varepsilon \to 0$ in (3.1.5). The first consequence is some moment estimates in $\mathbf{u} = (v, w)$ and also $\mathbf{x}$.

Corollary 3.3.2. *Under the assumptions of Lemma 3.3.1 with $p^* = 2$, we choose an initial datum f_0^ε such that (3.2.14) is satisfied. Then, there exists a constant $C_T > 0$, which does not depend on $\varepsilon > 0$, such that for any $k \in [0, 4]$,*

$$
\begin{cases}
\mu_k(t) \leq C_T, \quad t \in [0, T], \\[2mm]
\displaystyle\int_0^T \mu_{k+2}^v(t)\, \mathrm{d}t \leq C_T.
\end{cases}
\tag{3.3.2}
$$

Proof. First we observe that

$$
\mu_0(t) = 3 \int_{\mathbb{R}^{d+2}} f^\varepsilon(t)\, \mathrm{d}v\mathrm{d}w\mathrm{d}\mathbf{x} = 3 \|\rho_0^\varepsilon\|_{L^1},
\tag{3.3.3}
$$

which gives the result with $k = 0$.

Then for $k = 4$, we apply Lemma 3.3.1 with $p = 2$ and integrate with respect to $t \in [0, T]$ and by the Grönwall's lemma, it yields the estimates on the second order moment in $\mathbf{u} = (v, w)$, there exists a constant $C_T > 0$ such that for any $t \in [0, T]$

$$
\mu_4^v(t) + \mu_4^w(t) \leq C_T.
$$

Furthermore, since ρ^ε does not depend on time, we also have for all $t \in [0, T]$,

$$\mu_4^{\mathbf{x}}(t) = \int_{\mathbb{R}^d} |\mathbf{x}|^4 \, \rho_0^\varepsilon \, \mathrm{d}\mathbf{x} < \infty,$$

hence from hypothesis (3.2.14) which gives us the uniform control of the moment of order 4 in $\mathbf{x}$ of f_0^ε, there exists a constant $C_T > 0$, independent of $\varepsilon > 0$, such that for all $t \in [0, T]$,

$$\mu_4(t) \leq C_T. \tag{3.3.4}$$

On the other hand, from the latter result and the dissipative terms obtained in Lemma 3.3.1, there exists a constant $C_T > 0$ such that

$$\int_0^T \mu_6^v(t) \, \mathrm{d}t \leq C_T. \tag{3.3.5}$$

Interpolating (3.3.3) and (3.3.4)-(3.3.5), it yields the result with $0 \leq k \leq 4$. $\qquad\square$

Another consequence of Lemma 3.3.1 is the control of the dissipation $\mathcal{D}_1(.)$, which is a crucial step to characterize the limit of the sequence $(f^\varepsilon)_{\varepsilon > 0}$ when $\varepsilon \to 0$.

Corollary 3.3.3. *Under the assumptions of Lemma 3.3.1 with $p^* = 1$, we choose an initial datum f_0^ε such that (3.2.14) is satisfied. Then, there exists a constant $C_T > 0$, such that*

$$\int_0^T \int_{\mathbb{R}^{d+2}} f^\varepsilon(t) \, |v - V^\varepsilon(t, \mathbf{x})|^2 \, \rho_0^\varepsilon(\mathbf{x}) \, \mathrm{d}\mathbf{x} \, \mathrm{d}v \, \mathrm{d}w \, \mathrm{d}t \leq C_T \, \varepsilon. \tag{3.3.6}$$

Proof. We first apply Corollary 3.3.2 to obtain a uniform estimate on the moments $\mu_2(.)$,

$$\mu_2(t) \leq C_T, \quad t \in [0, T].$$

Then, integrating the entropy inequality (3.3.1) between 0 and T and using the positivity of $\mathcal{D}_1(.)$, we find

$$\frac{1}{\varepsilon} \int_0^T \int_{\mathbb{R}^{d+2}} f^\varepsilon(t, \mathbf{x}, v, w) \, |v - V^\varepsilon(t, \mathbf{x})|^2 \, \rho_0^\varepsilon(\mathbf{x}) \mathrm{d}\mathbf{x} \, \mathrm{d}v \, \mathrm{d}w \, \mathrm{d}t$$

$$\leq \mu_2(0) + 2C \int_0^T (1 + \mu_2(t)) \, \mathrm{d}t \leq C_T,$$

from which we easily deduce (3.3.6). $\qquad\square$

This last result is not enough to justify the asymptotic limit. Hopefully, it can be improved by removing the weight ρ_0^ε in the previous estimate.

Lemma 3.3.4. *Consider the solution f^ε to (3.1.5) given by Proposition 3.2.2, where the initial datum f_0^ε satisfies (3.2.14). Then, there exists a constant $C_T > 0$, independent of $\varepsilon > 0$, such that*

$$\int_0^T \int_{\mathbb{R}^{d+2}} f^\varepsilon(t, \mathbf{x}, v, w) |v - V^\varepsilon(t, \mathbf{x})|^2 \, \mathrm{d}\mathbf{x} \, \mathrm{d}v \, \mathrm{d}w \, \mathrm{d}t \leq C_T \, \varepsilon^{2/(d+6)}. \tag{3.3.7}$$

Proof. Let us fix $\varepsilon > 0$ and $T > 0$. First, we set

$$I^\varepsilon = \int_0^T \int f^\varepsilon |v - V^\varepsilon|^2 \, \mathrm{d}w \, \mathrm{d}v \, \mathrm{d}\mathbf{x} \, \mathrm{d}t$$

and notice that according to the definition of V^ε,

$$
\begin{aligned}
I^\varepsilon &= \int_0^T \int f^\varepsilon \left(|v|^2 + |V^\varepsilon|^2 - 2vV^\varepsilon \right) \mathrm{d}w \, \mathrm{d}v \, \mathrm{d}\mathbf{x} \, \mathrm{d}t \\
&\leq \int_0^T \int f^\varepsilon |v|^2 \mathrm{d}w \, \mathrm{d}v \, \mathrm{d}\mathbf{x} \, \mathrm{d}t \, < \, +\infty.
\end{aligned}
$$

So it gives that $f^\varepsilon |v - V^\varepsilon|^2 \in L^1([0,T] \times \mathbb{R}^{d+2})$. Our strategy to prove (3.3.7) is to divide $\mathbb{R}^d$ into several subsets where $f^\varepsilon |v - V^\varepsilon|^2$ is easier to control.

We consider any $\eta > 0$ and define the set $\mathcal{A}_\varepsilon$

$$
\mathcal{A}_\varepsilon := \left\{ \mathbf{x} \in \mathbb{R}^d \;\; | \;\; \rho_0^\varepsilon(\mathbf{x}) = 0 \right\},
$$

and $\mathcal{B}_\varepsilon^\eta$ given by

$$
\mathcal{B}_\varepsilon^\eta := \left\{ \mathbf{x} \in \mathbb{R}^d \;\; | \;\; \rho_0^\varepsilon(\mathbf{x}) > \eta \right\},
$$

whereas $\mathcal{C}_\varepsilon^\eta = \mathbb{R}^d \backslash (\mathcal{A}_\varepsilon \cup \mathcal{B}_\varepsilon^\eta)$, that is,

$$
\mathcal{C}_\varepsilon^\eta := \left\{ \mathbf{x} \in \mathbb{R}^d \;\; | \;\; 0 < \rho_0^\varepsilon(\mathbf{x}) \leq \eta \right\}.
$$

Thus, we have $I^\varepsilon = I_1^\varepsilon + I_2^\varepsilon + I_3^\varepsilon$, where

$$
\begin{cases}
I_1^\varepsilon := \displaystyle\int_0^T \int_{\mathcal{A}_\varepsilon} \int f^\varepsilon |v - V^\varepsilon|^2 \mathrm{d}w \, \mathrm{d}v \, \mathrm{d}\mathbf{x} \, \mathrm{d}t, \\[2ex]
I_2^\varepsilon := \displaystyle\int_0^T \int_{\mathcal{B}_\varepsilon^\eta} \int f^\varepsilon |v - V^\varepsilon|^2 \mathrm{d}w \, \mathrm{d}v \, \mathrm{d}\mathbf{x} \, \mathrm{d}t, \\[2ex]
I_3^\varepsilon := \displaystyle\int_0^T \int_{\mathcal{C}_\varepsilon^\eta} \int f^\varepsilon |v - V^\varepsilon|^2 \mathrm{d}w \, \mathrm{d}v \, \mathrm{d}\mathbf{x} \, \mathrm{d}t.
\end{cases}
$$

On the one hand, since $f^\varepsilon \geq 0$, we directly have that $f^\varepsilon = 0$ when $\rho_0^\varepsilon = 0$, that is when $\mathbf{x} \in \mathcal{A}_\varepsilon$, thus we have

$$
I_1^\varepsilon = \int_0^T \int_{\mathcal{A}_\varepsilon} \int f^\varepsilon |v - V^\varepsilon|^2 \mathrm{d}\mathbf{x} \mathrm{d}v \mathrm{d}w \mathrm{d}t = 0. \tag{3.3.8}
$$

On the other hand, for $\mathbf{x} \in \mathcal{B}_\varepsilon^\eta$, we know that $\rho_0^\varepsilon(\mathbf{x}) > \eta$, therefore it yields that

$$
\begin{aligned}
I_2^\varepsilon &\leq \int_0^T \int_{\mathcal{B}_\varepsilon^\eta} \int f^\varepsilon \, |v - V^\varepsilon|^2 \, \frac{\rho_0^\varepsilon}{\eta} \, \mathrm{d}\mathbf{x} \, \mathrm{d}v \, \mathrm{d}w \, \mathrm{d}t \\
&\leq \frac{1}{\eta} \int_0^T \int f^\varepsilon \, |v - V^\varepsilon|^2 \, \rho_0^\varepsilon \, \mathrm{d}\mathbf{x} \, \mathrm{d}v \, \mathrm{d}w \, \mathrm{d}t.
\end{aligned}
$$

Hence, by application of Corollary 3.3.3, we get the following estimate:

$$
I_2^\varepsilon = \mathcal{O}\left(\frac{\varepsilon}{\eta} \right). \tag{3.3.9}
$$

It remains to control the last term I_3^ε. To this aim we bound it by the sum of three terms : for any $R > 0$, we have

$$
I_3^\varepsilon \leq \int_0^T \int_{\mathcal{C}_\varepsilon^\eta} \int f^\varepsilon |v|^2 \mathrm{d}v \, \mathrm{d}\mathbf{x} \, \mathrm{d}w \, \mathrm{d}t =: I_{3,1}^\varepsilon \, + \, I_{3,2}^\varepsilon \, + \, I_{3,3}^\varepsilon,
$$

where

$$
\begin{cases}
I_{3,1}^{\varepsilon} := \displaystyle\int_0^T \int_{\mathcal{C}_\varepsilon^\eta} \int_{\{|v|>R\}} f^\varepsilon |v|^2 \mathrm{d}v \,\mathrm{d}\mathbf{x}\,\mathrm{d}w\,\mathrm{d}t, \\[2em]
I_{3,2}^{\varepsilon} := \displaystyle\int_0^T \int_{\mathcal{C}_\varepsilon^\eta \cap B^c(0,R)} \int_{\{|v|\leq R\}} f^\varepsilon |v|^2 \mathrm{d}v \,\mathrm{d}\mathbf{x}\,\mathrm{d}w\,\mathrm{d}t, \\[2em]
I_{3,3}^{\varepsilon} := \displaystyle\int_0^T \int_{\mathcal{C}_\varepsilon^\eta \cap B(0,R)} \int_{\{|v|\leq R\}} f^\varepsilon |v|^2 \mathrm{d}v \,\mathrm{d}\mathbf{x}\,\mathrm{d}w\,\mathrm{d}t.
\end{cases}
$$

For $k > 2$, the estimates on moments in velocity gives that

$$
I_{3,1}^{\varepsilon} \leq \frac{1}{R^{k-2}} \int_0^T \int f^\varepsilon |v|^k \,\mathrm{d}v\,\mathrm{d}\mathbf{x}\,\mathrm{d}w\,\mathrm{d}t = \frac{1}{R^{k-2}} \int_0^T \mu_k^v(t)\,\mathrm{d}t, \tag{3.3.10}
$$

where the last term is uniformly bounded according to Corollary 3.3.2 for $k \in [0,6]$.

Furthermore, we estimate $I_{3,2}^{\varepsilon}$ using a similar argument as for $I_{3,1}^{\varepsilon}$ but now using moments in space, that is, for $p \in [2,4]$,

$$
I_{3,2}^{\varepsilon} \leq \int_0^T \int \frac{|\mathbf{x}|^p}{R^p} f^\varepsilon(t)\, R^2 \,\mathrm{d}w\,\mathrm{d}v\,\mathrm{d}\mathbf{x}\,\mathrm{d}t \leq \frac{1}{R^{p-2}} \int_0^T \mu_p^{\mathbf{x}}(t)\,\mathrm{d}t, \tag{3.3.11}
$$

where $\mu_p^{\mathbf{x}}(.)$ is uniformly bounded according to Corollary 3.3.2 for $p \in [0,4]$. Finally, the last term $I_{3,3}^{\varepsilon}$ can be computed as

$$
I_{3,3}^{\varepsilon} \leq R^2 \int_0^T \int_{\mathcal{C}_\varepsilon^\eta \cap B(0,R)} \rho_0^\varepsilon \,\mathrm{d}\mathbf{x}\,\mathrm{d}t \leq \tilde{C}\,T\,R^{d+2}\,\eta, \tag{3.3.12}
$$

where $\tilde{C}$ is the positive constant such that $|B(0,R)| = \tilde{C}R^d$. By summing (3.3.10), (3.3.11) and (3.3.12), we can conclude that there exists a constant $C = C(T)$ independent on R, η and ε such that

$$
I_3^{\varepsilon} \leq C \left(R^{d+2}\,\eta + \frac{1}{R^{p-2}} + \frac{1}{R^{k-2}} \right).
$$

For simplicity we choose $p = k = 4$ and optimize the value of R, which leads to

$$
I_3^{\varepsilon} \leq C_T\,\eta^{2/(d+4)}. \tag{3.3.13}
$$

Finally by summing (3.3.8), (3.3.9) and (3.3.13), we get that there exists a positive constant $C_T > 0$ independent on η and ε, such that,

$$
I^{\varepsilon} \leq C_T \left(\eta^{2/(d+4)} + \frac{\varepsilon}{\eta} \right).
$$

Hence, we can choose $\eta = \varepsilon^{(d+4)/(d+6)}$ and

$$
\int_0^T \int f^\varepsilon |v - V^\varepsilon|^2 \,\mathrm{d}\mathbf{x}\,\mathrm{d}v\,\mathrm{d}w\,\mathrm{d}t \leq C_T\,\varepsilon^{2/(d+6)}.
$$

$\square$

3.4   Relative entropy estimate and proof of Theorem 3.2.5

Following ideas from [63, 94], our proof of Theorem 3.2.5 relies on a relative entropy argument to estimate the distance between a solution of (3.1.6) and a solution of (3.1.10) on $[0, T]$ for some finite $T > 0$ as $\varepsilon \to 0$, with well-prepared initial conditions. Throughout this section, by a solution $(\rho_0, \rho_0 V, \rho_0 W)$ of (3.1.10), we refer to the solution constructed in Proposition 3.2.3. We start this section with the definition of the relative entropy that we will be using. Then, we present an equality satisfied by the relative entropy, which will be useful to estimate it. This estimate will finally be the key argument to conclude the proof.

3.4.1   Definition of relative entropy

We want to use a relative entropy argument which enables us to compare solutions of (3.1.10) with the solutions of (3.1.5) seen on its hydrodynamic form (3.1.6). We first introduce the notion of entropy.

Definition 3.4.1 (Entropy). *For all functions V and $W : \mathbb{R}^d \longrightarrow \mathbb{R}$, and for any non-negative function $\rho : \mathbb{R}^d \to \mathbb{R}$, we define for $\mathcal{Z} = (\rho, \rho V, \rho W)$, the entropy $\eta(\mathcal{Z})$ by*

$$\eta(\mathcal{Z}) := \rho \, \frac{|V|^2 + |W|^2}{2}. \tag{3.4.1}$$

Note that if we define $P = \rho V$ and $Q = \rho W$, then we have

$$\eta(\mathcal{Z}) = \frac{P^2 + Q^2}{2\,\rho}.$$

As a consequence, the differential of η with respect to its variables $\mathcal{Z}$ is given by

$$D\eta(\mathcal{Z}) = \begin{pmatrix} D_\rho \eta \\ D_P \eta \\ D_Q \eta \end{pmatrix} = \begin{pmatrix} -\dfrac{|V|^2 + |W|^2}{2} \\ V \\ W \end{pmatrix}. \tag{3.4.2}$$

Using the definition of entropy (3.4.1), we can now introduce the notion of relative entropy or Bregman divergence.

Definition 3.4.2 (Relative Entropy). *For all functions V_1, W_1, V_2 and $W_2 : \mathbb{R}^d \to \mathbb{R}$ and for all non-negative functions ρ_1 and $\rho_2 : \mathbb{R}^d \to \mathbb{R}$, we define for $\mathcal{Z}_i = (\rho_i, \rho_i V_i, \rho_i W_i)$, with $i = 1, 2$, the relative entropy*

$$\eta(\mathcal{Z}_1 | \mathcal{Z}_2) := \eta(\mathcal{Z}_1) - \eta(\mathcal{Z}_2) - D\eta(\mathcal{Z}_2) \cdot (\mathcal{Z}_1 - \mathcal{Z}_2)$$

which gives us after computation

$$\eta(\mathcal{Z}_1 | \mathcal{Z}_2) = \rho_1 \, \frac{|V_2 - V_1|^2 + |W_2 - W_1|^2}{2}. \tag{3.4.3}$$

This relative entropy will be useful to "compare" the weak solution $(\rho_0^\varepsilon, \rho_0^\varepsilon V^\varepsilon, \rho_0^\varepsilon W^\varepsilon)$ to (3.1.6) with the classical solution $(\rho_0, \rho_0 V, \rho_0 W)$ to (3.1.10). Let us finally remark that in the simplified case where we assume $\rho_0 = \rho_0^\varepsilon$, then η reduces to the Euclidean norm $\|\cdot\|_2$.

3.4.2 Relative entropy equality

In this subsection, we prove an equality satisfied by the relative entropy defined by (3.4.3) between an arbitrary smooth function and a solution of the hydrodynamic equations (3.1.10). The purpose of this result is to split the relative entropy dissipation into one part due to the macroscopic solution (3.1.10) and another part which estimates the difference between the two solutions.

Lemma 3.4.3. *Under the assumption that Ψ is non-negative, symmetric and satisfies (3.2.1), we consider (V, W) the solution to the hydrodynamic equation (3.2.6) given by Proposition 3.2.3. Then, for any $\widetilde{\mathcal{Z}} = (\widetilde{\rho}, \widetilde{\rho}\widetilde{V}, \widetilde{\rho}\widetilde{W})$ such that $\widetilde{\rho}$ is non-negative, $\widetilde{\rho} \in L^1 \cap L^\infty(\mathbb{R}^d)$, whereas $\widetilde{V}$ and $\widetilde{W}$ are both differentiable in time and such that for any $t \in [0, T]$,*

$$\widetilde{\rho}\left(|\widetilde{V}(t)|^4 + |\widetilde{W}(t)|^4\right) \in L^1(\mathbb{R}^d),$$

the following equality holds:

$$\frac{\mathrm{d}}{\mathrm{d}t} \int \eta(\widetilde{\mathcal{Z}}|\mathcal{Z}) \,\mathrm{d}\mathbf{x} = \frac{\mathrm{d}}{\mathrm{d}t} \int \eta(\widetilde{\mathcal{Z}})\mathrm{d}\mathbf{x} \tag{3.4.4}$$
$$- \int D\eta(\mathcal{Z}) \left[\partial_t \widetilde{\mathcal{Z}} - \mathcal{F}(\widetilde{\mathcal{Z}})\right] \mathrm{d}\mathbf{x} + \mathcal{R}(\widetilde{\mathcal{Z}}|\mathcal{Z}) + \mathcal{S}(\widetilde{\mathcal{Z}}),$$

with $\mathcal{R} = \mathcal{R}_l + \mathcal{R}_{nl}$ and $\mathcal{S} = \mathcal{S}_l + \mathcal{S}_{nl}$, where $\mathcal{R}_l$ and $\mathcal{S}_l$ contain local terms

$$\begin{cases} \mathcal{R}_l(\widetilde{\mathcal{Z}}|\mathcal{Z}) := \int \widetilde{\rho}\left(V - \widetilde{V}\right)\left(N(V) - W - N(\widetilde{V}) + \widetilde{W}\right) \mathrm{d}\mathbf{x} \\ \qquad\qquad\qquad + \int \widetilde{\rho}\left(W - \widetilde{W}\right)\left(A(V, W) - A(\widetilde{V}, \widetilde{W})\right) \mathrm{d}\mathbf{x}, \\ \mathcal{S}_l(\widetilde{\mathcal{Z}}) := -\int \widetilde{\rho}\left[\widetilde{V} N(\widetilde{V}) - \widetilde{V}\widetilde{W} + \widetilde{W} A(\widetilde{V}, \widetilde{W})\right] \mathrm{d}\mathbf{x}. \end{cases} \tag{3.4.5}$$

whereas $\mathcal{R}_{nl}(\widetilde{\mathcal{Z}}|\mathcal{Z})$ and $\mathcal{S}_{nl}(\widetilde{\mathcal{Z}})$ gather nonlocal terms

$$\begin{cases} \mathcal{R}_{nl}(\widetilde{\mathcal{Z}}|\mathcal{Z}) := \int \widetilde{\rho}\left[(V - \widetilde{V})\left(\mathcal{L}_{\rho_0}(V) - \mathcal{L}_{\widetilde{\rho}}(\widetilde{V})\right)\right] \mathrm{d}\mathbf{x}, \\ \mathcal{S}_{nl}(\widetilde{\mathcal{Z}}) := -\frac{1}{2}\iint \Psi(\mathbf{x} - \mathbf{y})\,\widetilde{\rho}(\mathbf{x})\,\widetilde{\rho}(\mathbf{y})\left|\widetilde{V}(t, \mathbf{x}) - \widetilde{V}(t, \mathbf{y})\right|^2 \mathrm{d}\mathbf{x}\,\mathrm{d}\mathbf{y} \end{cases} \tag{3.4.6}$$

Proof. First of all, it is worth noticing that for all $t \in [0; T]$, since $V(t)$ and $W(t) \in L^\infty(\mathbb{R}^d)$ and since $\rho_0 \in L^1(\mathbb{R}^d)$, then for all $i \in \mathbb{N}$, $\rho_0\left(|V(t)|^i + |W(t)|^i\right) \in L^1(\mathbb{R}^d)$. From the definition (3.4.2) of $\eta(\widetilde{\mathcal{Z}}|\mathcal{Z})$, we have

$$\frac{\mathrm{d}}{\mathrm{d}t} \int \eta(\widetilde{\mathcal{Z}}|\mathcal{Z}) \,\mathrm{d}\mathbf{x} = \int \left[\partial_t \eta(\widetilde{\mathcal{Z}}) - \partial_t \eta(\mathcal{Z}) - \partial_t D\eta(\mathcal{Z}) \cdot \left(\widetilde{\mathcal{Z}} - \mathcal{Z}\right) - D\eta(\mathcal{Z}) \cdot \partial_t\left(\widetilde{\mathcal{Z}} - \mathcal{Z}\right)\right] \mathrm{d}\mathbf{x}$$
$$= I_1 + I_2,$$

with

$$\begin{cases} I_1 := \int \partial_t \eta(\widetilde{\mathcal{Z}}) - D\eta(\mathcal{Z}) \cdot \left[\partial_t \widetilde{\mathcal{Z}} - \mathcal{F}(\widetilde{\mathcal{Z}})\right] \mathrm{d}\mathbf{x}, \\ I_2 := -\int \left[\partial_t D\eta(\mathcal{Z}) \cdot \left(\widetilde{\mathcal{Z}} - \mathcal{Z}\right) + D\eta(\mathcal{Z}) \cdot \mathcal{F}(\widetilde{\mathcal{Z}})\right] \mathrm{d}\mathbf{x}, \end{cases}$$

where $\mathcal{F}$ is defined in (3.1.10)-(3.1.11).

On the one hand, the term I_1 corresponds to the variation of entropy which simply gives

$$I_1 = \frac{\mathrm{d}}{\mathrm{d}t} \int \eta(\widetilde{\mathcal{Z}}) \, \mathrm{d}\mathbf{x} - \int D\eta(\mathcal{Z}) \cdot \left[\partial_t \widetilde{\mathcal{Z}} - \mathcal{F}(\widetilde{\mathcal{Z}}) \right] \mathrm{d}\mathbf{x}. \tag{3.4.7}$$

On the other hand, we decompose I_2 as $I_2 = I_{21} + I_{22}$ with

$$\begin{cases} I_{21} := \int \partial_t D\eta(\mathcal{Z}) \cdot \left(\widetilde{\mathcal{Z}} - \mathcal{Z} \right) \mathrm{d}\mathbf{x}, \\[3mm] I_{22} := -\int D\eta(\mathcal{Z}) \cdot \mathcal{F}(\widetilde{\mathcal{Z}}) \mathrm{d}\mathbf{x}. \end{cases}$$

Using the definition of $D\eta(\mathcal{Z})$ in (3.4.2) and since $\mathcal{Z}$ is solution to (3.1.10), we have

$$\begin{aligned} I_{21} &:= -\int \partial_t \begin{pmatrix} -\dfrac{|V|^2 + |W|^2}{2} \\ V \\ W \end{pmatrix} \cdot \begin{pmatrix} \widetilde{\rho} - \rho_0 \\ \widetilde{\rho}\widetilde{V} - \rho_0 V \\ \widetilde{\rho}\widetilde{W} - \rho_0 W \end{pmatrix} \mathrm{d}\mathbf{x} \\[2mm] &= \int (\widetilde{\rho} - \rho_0) \left[V \left(\mathcal{L}_{\rho_0}(V) + N(V) - W \right) + W \, A(V,W) \right] \mathrm{d}\mathbf{x} \\[2mm] &\quad - \int \left(\widetilde{\rho}\widetilde{V} - \rho_0 V \right) \left(\mathcal{L}_{\rho_0}(V) + N(V) - W \right) \mathrm{d}\mathbf{x} \\[2mm] &\quad - \int \left(\widetilde{\rho}\widetilde{W} - \rho_0 W \right) A(V,W) \, \mathrm{d}\mathbf{x}, \end{aligned}$$

hence it yields

$$I_{21} = \int \widetilde{\rho} \left[\left(V - \widetilde{V} \right) \left[\mathcal{L}_{\rho_0}(V) + N(V) - W \right] + A(V,W) \left(W - \widetilde{W} \right) \right] \mathrm{d}\mathbf{x}.$$

Furthermore, from the definition of $\mathcal{F}(\widetilde{\mathcal{Z}})$ in (3.1.10)-(3.1.11) and $D\eta(\mathcal{Z})$ in (3.4.2), we obtain

$$I_{22} = -\int \widetilde{\rho} \left(V \left[\mathcal{L}_{\widetilde{\rho}}(\widetilde{V}) + N(\widetilde{V}) - \widetilde{W} \right] + W \, A(\widetilde{V}, \widetilde{W}) \right) \mathrm{d}\mathbf{x}.$$

Then, gathering the latter two equalities and after reordering, we have

$$\begin{aligned} I_2 &= \int \widetilde{\rho} \left[(V - \widetilde{V}) \left(\mathcal{L}_{\rho_0}(V) - \mathcal{L}_{\widetilde{\rho}}(\widetilde{V}) \right) - \widetilde{V} \, \mathcal{L}_{\widetilde{\rho}}(\widetilde{V}) \right] \mathrm{d}\mathbf{x} \\[2mm] &\quad + \int \widetilde{\rho} \left[\left(V - \widetilde{V} \right) \left(N(V) - N(\widetilde{V}) - W + \widetilde{W} \right) - \widetilde{V} \, N(\widetilde{V}) + \widetilde{V} \, \widetilde{W} \right] \mathrm{d}\mathbf{x} \\[2mm] &\quad + \int \widetilde{\rho} \left[\left(W - \widetilde{W} \right) \left(A(V,W) - A(\widetilde{V}, \widetilde{W}) \right) - \widetilde{W} \, A(\widetilde{V}, \widetilde{W}) \right] \mathrm{d}\mathbf{x}, \end{aligned}$$

which can be also written as

$$I_2 = \mathcal{I}_\psi + \mathcal{R}_l(\widetilde{\mathcal{Z}}|\mathcal{Z}) + \mathcal{S}_l(\widetilde{\mathcal{Z}}), \tag{3.4.8}$$

where $\mathcal{R}_l$ and $\mathcal{S}_l$ are given in (3.4.5) whereas the first term $\mathcal{I}_\psi$ is given by

$$\mathcal{I}_\psi := \int \widetilde{\rho} \left[(V - \widetilde{V}) \left(\mathcal{L}_{\rho_0}(V) - \mathcal{L}_{\widetilde{\rho}}(\widetilde{V}) \right) - \widetilde{V} \, \mathcal{L}_{\widetilde{\rho}}(\widetilde{V}) \right] \mathrm{d}\mathbf{x}.$$

Thus, we set

$$
\begin{cases}
\mathcal{R}_{nl} = \displaystyle\int \tilde{\rho}\left[(V - \widetilde{V})\left(\mathcal{L}_{\rho_0}(V) - \mathcal{L}_{\tilde{\rho}}(\widetilde{V})\right)\right]\mathrm{d}\mathbf{x}, \\[3mm]
\mathcal{S}_{nl} = -\displaystyle\int \tilde{\rho}\,\widetilde{V}\,\mathcal{L}_{\tilde{\rho}}(\widetilde{V})\mathrm{d}\mathbf{x}
\end{cases}
$$

and a direct computation gives

$$
\mathcal{S}_{nl} = -\frac{1}{2}\iint \Psi(\mathbf{x} - \mathbf{y})\,\widetilde{\rho}(\mathbf{x})\,\widetilde{\rho}(\mathbf{y})\left|\widetilde{V}(t, \mathbf{x}) - \widetilde{V}(t, \mathbf{y})\right|^2\,\mathrm{d}\mathbf{x}\,\mathrm{d}\mathbf{y}.
$$

We conclude the proof by gathering the last equality together with (3.4.7) and (3.4.8). $\qquad\square$

3.4.3 Relative entropy estimate

Now that we have established the relative entropy equality (3.4.4), we apply it with $\tilde{\rho} = \rho_0^\varepsilon$, $\widetilde{V} = V^\varepsilon$ and $\widetilde{W} = W^\varepsilon$ to estimate the relative entropy between the weak solution $(V^\varepsilon, W^\varepsilon)$ and the classical solution (V, W). More precisely, we prove the following result.

Proposition 3.4.4. *Under the assumptions of Theorem 3.2.5, there exists $C_T > 0$ such that we have for all $t \in (0, T]$:*

$$
\int_{\mathbb{R}^d} \rho_0^\varepsilon(\mathbf{x})\left(|V^\varepsilon(t, \mathbf{x}) - V(t, \mathbf{x})|^2 + |W^\varepsilon(t, \mathbf{x}) - W(t, \mathbf{x})|^2\right)\mathrm{d}\mathbf{x} \leq C_T\,\varepsilon^{1/(d+6)}, \tag{3.4.9}
$$

where (V, W) is the solution to (3.2.6) and $(\rho_0^\varepsilon, \rho_0^\varepsilon V^\varepsilon, \rho_0^\varepsilon W^\varepsilon)$ are the macroscopic quantities computed from f^ε the solution to (3.1.5) on $[0, T]$.

Proof. Consider f^ε a solution to (3.1.5) on $[0, T]$ given in Proposition 3.2.2. From Corollary 3.3.2, we get that for any $t \in [0, T]$, the moment $\mu_4(t)$ is uniformly bounded with respect to $\varepsilon > 0$. Therefore applying the Hölder inequality, we obtain that for all $\mathbf{x} \in \mathbb{R}^d$ such that $\rho_0^\varepsilon(\mathbf{x}) > 0$ and for all $t \in [0; T]$,

$$
\begin{aligned}
\rho_0^\varepsilon(\mathbf{x})|V^\varepsilon(t, \mathbf{x})|^4 &= \frac{1}{|\rho_0^\varepsilon(\mathbf{x})|^3}\left(\int v f^\varepsilon(t, \mathbf{x}, v, w)\mathrm{d}v\,\mathrm{d}w\right)^4, \\
&\leq \int |v|^4 f^\varepsilon(t, \mathbf{x}, v, w)\,\mathrm{d}v\,\mathrm{d}w. \tag{3.4.10}
\end{aligned}
$$

Note that the last inequality remains true when $\rho_0^\varepsilon(\mathbf{x}) = 0$ and the same argument applies when we replace V^ε by W^ε.

Consequently, since $\rho^\varepsilon \in L^1(\mathbb{R}^d)$, we get for any $0 \leq p \leq 4$ and $t \in [0, T]$,

$$
\rho_0^\varepsilon\left(|V^\varepsilon(t)|^p + |W^\varepsilon(t)|^p\right) \in L^1(\mathbb{R}^d).
$$

Thus, we can compute the time evolution of the entropy $\eta(\mathcal{Z}^\varepsilon)$ where $\mathcal{Z}^\varepsilon = (\rho_0^\varepsilon, \rho_0^\varepsilon V^\varepsilon, \rho_0^\varepsilon W^\varepsilon)$ corresponds to the moments of f^ε with respect to $(1, v, w)$, that is $\mathcal{Z}^\varepsilon$ is solution to (3.1.6). It yields that

$$
\frac{\mathrm{d}}{\mathrm{d}t}\int \eta(\mathcal{Z}^\varepsilon(t))\,\mathrm{d}\mathbf{x} + \mathcal{S}(\mathcal{Z}^\varepsilon(t)) = \int V^\varepsilon(t)\,\mathcal{E}(f^\varepsilon(t))\,\mathrm{d}\mathbf{x}, \tag{3.4.11}
$$

where $\mathcal{S}(\mathcal{Z}^\varepsilon)$ is given by (3.4.5)-(3.4.6) when $\widetilde{\mathcal{Z}} = \mathcal{Z}^\varepsilon$ and the error term $\mathcal{E}(f^\varepsilon)$ is defined in (3.1.8).

Then we consider (V, W) the solution to (3.2.6) given in Proposition 3.2.3, hence we have for $\mathcal{Z} = (\rho_0, \rho_0\, V, \rho_0\, W)$,

$$\int D\eta(\mathcal{Z}(t))\, [\partial_t \mathcal{Z}^\varepsilon(t) - \mathcal{F}(\mathcal{Z}^\varepsilon(t))]\, \mathrm{d}\mathbf{x} \;=\; \int V(t)\, \mathcal{E}(f^\varepsilon(t))\mathrm{d}\mathbf{x}. \tag{3.4.12}$$

Therefore, applying Lemma 3.4.3 with $\widetilde{\mathcal{Z}} = (\rho_0^\varepsilon, \rho_0^\varepsilon\, V^\varepsilon, \rho_0^\varepsilon\, W^\varepsilon)$ and using (3.4.11) and (3.4.12), we simply get the following equality

$$\frac{d}{dt} \int \eta(\mathcal{Z}^\varepsilon(t)|\mathcal{Z}(t))\, \mathrm{d}\mathbf{x} \;=\; \int (V^\varepsilon - V)\, \mathcal{E}(f^\varepsilon)(t, \mathbf{x})\mathrm{d}\mathbf{x} \;+\; \mathcal{R}(\mathcal{Z}^\varepsilon|\mathcal{Z}), \tag{3.4.13}$$

where $\mathcal{R} = \mathcal{R}_l + \mathcal{R}_{nl}$ is given in (3.4.5)-(3.4.6). On the one hand, we estimate the term $\mathcal{R}_l$ by

$$
\begin{aligned}
\mathcal{R}_l(\mathcal{Z}^\varepsilon|\mathcal{Z}) \;&\leq\; \int \rho_0^\varepsilon\, (V - V^\varepsilon)\, (N(V) - N(V^\varepsilon) - (W - W^\varepsilon))\, \mathrm{d}\mathbf{x} \\
&\quad + \int \rho_0^\varepsilon\, (W - W^\varepsilon)\, (A(V, W) - A(V^\varepsilon, W^\varepsilon))\, \mathrm{d}\mathbf{x} \\
&\leq\; \int \left(|V - V^\varepsilon|^2 + \frac{1}{2}\, (|V - V^\varepsilon|^2 + |W - W^\varepsilon|^2) \right) \rho_0^\varepsilon\, \mathrm{d}\mathbf{x} \\
&\quad + \frac{\tau}{2} \int (|V - V^\varepsilon|^2 + |W - W^\varepsilon|^2)\, \rho_0^\varepsilon\, \mathrm{d}\mathbf{x} \\
&\leq\; \frac{3 + \tau}{2} \int \eta(\mathcal{Z}^\varepsilon|\mathcal{Z})\mathrm{d}\mathbf{x}.
\end{aligned}
$$

On the other hand, we estimate the second term $\mathcal{R}_{nl}(\mathcal{Z}^\varepsilon|\mathcal{Z})$ as

$$
\begin{aligned}
|\mathcal{R}_{nl}&(\mathcal{Z}^\varepsilon|\mathcal{Z})| \\
&\leq\; \iint \Psi(\mathbf{x} - \mathbf{y})\, \rho_0^\varepsilon(\mathbf{x})\, |\rho_0(\mathbf{y}) - \rho_0^\varepsilon(\mathbf{y})|\, |V(t, \mathbf{y}) - V(t, \mathbf{x})|\, |V(t, \mathbf{x}) - V^\varepsilon(t, \mathbf{x})|\, \mathrm{d}\mathbf{x}\, \mathrm{d}\mathbf{y} \\
&\leq\; \|V\|_{L^\infty} \|\Psi\|_{L^1} \left(\|\rho_0^\varepsilon\|_{L^\infty} \|\rho_0 - \rho_0^\varepsilon\|_{L^2}^2 + \int \eta(\mathcal{Z}^\varepsilon|\mathcal{Z})\mathrm{d}\mathbf{x} \right).
\end{aligned}
$$

Gathering these last inequalities, using the uniform control of $\|\rho_0^\varepsilon\|_{L^\infty}$ given by hypothesis (3.2.13), we have shown that there exists a constant $C_T > 0$, which does not depend on $\varepsilon > 0$ such that for all $t \in [0, T]$,

$$\int_0^t |\mathcal{R}(\mathcal{Z}^\varepsilon(s)|\mathcal{Z}(s))|\mathrm{d}s \;\leq\; C_T \left[\|\rho_0 - \rho_0^\varepsilon\|_{L^2}^2 + \int_0^t \int \eta(\mathcal{Z}^\varepsilon(s)|\mathcal{Z}(s))\, \mathrm{d}\mathbf{x}\, \mathrm{d}s \right]. \tag{3.4.14}$$

It remains to estimate the error term

$$
\begin{aligned}
\left| \int (V^\varepsilon(t) - V(t))\, \mathcal{E}(f^\varepsilon)(t)\mathrm{d}\mathbf{x} \right| \;&\leq\; \frac{3}{2} \int |V^\varepsilon(t) - V(t)|\, |V^\varepsilon(t) - v|\, \left[(V^\varepsilon(t))^2 + v^2 \right] f^\varepsilon(t)\mathrm{d}v\mathrm{d}w\mathrm{d}\mathbf{x} \\
&\leq\; \alpha(t) \left(\int |V^\varepsilon(t) - v|^2\, f^\varepsilon(t)\, \mathrm{d}v\, \mathrm{d}w\, \mathrm{d}\mathbf{x} \right)^{1/2},
\end{aligned}
$$

where $\alpha(t)$ is given by

$$\alpha(t) := \frac{3}{2} \left(\int \left[(V^\varepsilon(t))^2 + v^2 \right]^2 [V^\varepsilon(t) - V(t)]^2\, f^\varepsilon(t)\, \mathrm{d}v\, \mathrm{d}w\, \mathrm{d}\mathbf{x} \right)^{1/2}.$$

Using that V is uniformly bounded in L^∞ according to Proposition 3.2.3 and since

$$\rho_0^\varepsilon \, |V^\varepsilon(t,\mathbf{x})|^6 \le \int |v|^6 f^\varepsilon(t,\mathbf{x},v,w) \mathrm{d}v \mathrm{d}w$$

we deduce from Corollary 3.3.2 that there exists a constant $C_T > 0$, which does not depend on ε, such that

$$\int_0^T \alpha^2(s)\, \mathrm{d}s \le C_T.$$

It yields from Lemma 3.3.7 and the Cauchy-Schwarz inequality that

$$\int_0^T \left| \int \left(V^\varepsilon(t) - V(t) \right) \mathcal{E}(f^\varepsilon)(t) \mathrm{d}\mathbf{x} \right| \mathrm{d}t \le C_T\, \varepsilon^{1/(d+6)}. \tag{3.4.15}$$

Finally integrating (3.4.13) on the time interval $[0,t]$ we get from the previous estimates (3.4.14) and (3.4.15) and using the Grönwall's lemma that

$$\int \eta(\mathcal{Z}^\varepsilon(t)|\mathcal{Z}(t))\, \mathrm{d}\mathbf{x} \;\; \le \;\; C_T \left[\int \eta(\mathcal{Z}^\varepsilon(0)|\mathcal{Z}(0))\, \mathrm{d}\mathbf{x} + \|\rho_0 - \rho_0^\varepsilon\|_{L^2}^2 + \varepsilon^{1/(d+6)} \right]$$

From the assumption (3.2.15), we get that for all $t \in [0,T]$,

$$\int \eta(\mathcal{Z}^\varepsilon(t)|\mathcal{Z}(t))\, \mathrm{d}\mathbf{x} \;\; \le \;\; C_T\, \varepsilon^{1/(d+6)},$$

which concludes the proof. $\qquad\qquad\square$

3.4.4   Conclusion – Proof of Theorem 3.2.5

In this section, we complete the proof of Theorem 3.2.5 using the entropy estimates previously established to show the convergence of f^ε in the limit $\varepsilon \to 0$.

First, we set

$$F^\varepsilon(t,\mathbf{x},w) := \int f^\varepsilon(t,\mathbf{x},v,w)\, \mathrm{d}v,$$

with an initial datum F_0^ε given by

$$F_0^\varepsilon = \int_\mathbb{R} f_0^\varepsilon\, \mathrm{d}v.$$

Noticing that since f^ε is compactly supported in v for any $\varepsilon > 0$, we can choose a test function in (3.2.2) independent of $v \in \mathbb{R}$, hence the distribution F^ε satisfies the following equation, (3.1.5)

$$\int_0^T \int_{\mathbb{R}^{d+1}} F^\varepsilon\, \partial_t \varphi + \tau \left[\int_\mathbb{R} v f^\varepsilon \mathrm{d}v + (a - b\,w)\, F^\varepsilon \right] \partial_w \varphi\, \mathrm{d}\mathbf{x}\mathrm{d}w\mathrm{d}t$$

$$+ \int_{\mathbb{R}^{d+1}} F_0^\varepsilon\, \varphi(0)\, \mathrm{d}\mathbf{x}\mathrm{d}w = 0, \quad \forall \varphi \in \mathscr{C}_c^\infty([0,T) \times \mathbb{R}^{d+1}),$$

or after reordering

$$\int_0^T \int_{\mathbb{R}^{d+1}} F^\varepsilon \left[\partial_t \varphi + A(V(t,\mathbf{x}),w)\, \partial_w \varphi \right] \mathrm{d}\mathbf{x}\mathrm{d}w\mathrm{d}t + \int_{\mathbb{R}^{d+1}} F_0^\varepsilon\, \varphi(0)\, \mathrm{d}\mathbf{x}\mathrm{d}w$$

$$= \tau \int_0^T \int_{\mathbb{R}^{d+2}} (V(t,\mathbf{x}) - v)\, f^\varepsilon\, \partial_w \varphi\, \mathrm{d}v\mathrm{d}\mathbf{x}\mathrm{d}w\mathrm{d}t, \quad \forall \varphi \in \mathscr{C}_c^1([0,T) \times \mathbb{R}^{d+1}),$$

where V is solution to (3.1.10).

On the one hand, using that up to a subsequence F^ε converges weakly-$\star$ in $\mathcal{M}((0,T) \times \mathbb{R}^{d+1})$ to a limit $F \in \mathcal{M}((0,T) \times \mathbb{R}^{d+1})$, we can pass to the limit on the left hand side by linearity. On the other hand, from Lemma 3.3.4 and Proposition 3.4.4, we get when $\varepsilon \to 0$,

$$
\begin{aligned}
\int_0^T \int f^\varepsilon |v - V(t,\mathbf{x})|^2 \mathrm{d}\mathbf{x}\mathrm{d}v\mathrm{d}w\mathrm{d}s \; &\leq \; \int_0^T \int f^\varepsilon \left(|v - V^\varepsilon(t,\mathbf{x})|^2 + |V^\varepsilon(t,\mathbf{x}) - V(t,\mathbf{x})|^2 \right) \mathrm{d}\mathbf{z}\mathrm{d}s \\
&\leq \; C_T\, \varepsilon^{1/(d+6)},
\end{aligned}
$$

hence it yields that since ρ^ε does not depend on time,

$$
\left| \int (V(t,\mathbf{x}) - v)\, f^\varepsilon\, \partial_w \varphi \, \mathrm{d}v\mathrm{d}\mathbf{x}\mathrm{d}w\mathrm{d}t \right| \leq C_T\, \|\partial_w \varphi\|_{L^\infty}\, \|\rho_0^\varepsilon\|_{L^1}^{1/2}\, \varepsilon^{1/(2d+12)}.
$$

Thus, passing to the limit $\varepsilon \to 0$, it proves that F is a measure solution of (3.2.8). Furthermore, by uniqueness of the solution to (3.1.5), we get the convergence for the sequence $(F^\varepsilon)_{\varepsilon>0}$.

Finally let us show that for any $\varphi \in \mathscr{C}_b^0(\mathbb{R}^{d+2})$,

$$
\int \varphi(\mathbf{x}, v, w)\, f^\varepsilon(t, \mathbf{x}, v, w) \, \mathrm{d}v\, \mathrm{d}w\, \mathrm{d}\mathbf{x} \to \int \varphi(\mathbf{x}, V(t,\mathbf{x}), w)\, F(t, \mathrm{d}\mathbf{x}, \mathrm{d}w),
$$

strongly in $L^1_{\mathrm{loc}}(0,T)$ as $\varepsilon \to 0$. Consider $0 < t < t' \leq T$. We start with showing the convergence for any $\varphi \in \mathscr{C}_c^1(\mathbb{R}^{d+2})$, and then we will conclude using a density argument. Consider $\varphi \in \mathscr{C}_c^1(\mathbb{R}^{d+2})$, we have:

$$
\begin{aligned}
\mathcal{I} := \int_t^{t'} \left| \int \varphi(\mathbf{x}, v, w)\, f^\varepsilon(s, \mathbf{x}, v, w)\, \mathrm{d}v\, \mathrm{d}w\, \mathrm{d}\mathbf{x} - \int \varphi(\mathbf{x}, V(s,\mathbf{x}), w)\, F(s, \mathrm{d}\mathbf{x}, \mathrm{d}w) \right| \mathrm{d}s \\
\leq \mathcal{I}_1 + \mathcal{I}_2,
\end{aligned}
$$

where

$$
\begin{cases}
\mathcal{I}_1 &:= \displaystyle\int_t^{t'} \left| \int (\varphi(\mathbf{x}, v, w) - \varphi(\mathbf{x}, V(s,\mathbf{x}), w))\, f^\varepsilon(s, \mathbf{x}, v, w)\, \mathrm{d}v\, \mathrm{d}w\, \mathrm{d}\mathbf{x} \right| \mathrm{d}s, \\[2mm]
\mathcal{I}_2 &:= \displaystyle\int_t^{t'} \left| \int \varphi(\mathbf{x}, V(s,\mathbf{x}), w)\, (F^\varepsilon(s, \mathrm{d}\mathbf{x}, \mathrm{d}w) - F(s, \mathrm{d}\mathbf{x}, \mathrm{d}w)) \right| \mathrm{d}s.
\end{cases}
$$

We estimate the first term $\mathcal{I}_1$ using the regularity of φ and the Cauchy-Schwarz inequality:

$$
\begin{aligned}
\mathcal{I}_1 &\leq \|\partial_v \varphi\|_{L^\infty} \int_0^T \int |v - V(s,\mathbf{x})|\, f^\varepsilon(s, \mathbf{x}, v, w)\, \mathrm{d}v\, \mathrm{d}w\, \mathrm{d}\mathbf{x}\, \mathrm{d}s \\
&\leq \|\partial_v \varphi\|_{L^\infty} \left(\int_0^T \int f^\varepsilon(s, \mathbf{x}, v, w)\, \mathrm{d}v\, \mathrm{d}w\, \mathrm{d}\mathbf{x}\, \mathrm{d}s \right)^{1/2} \\
&\quad \times \left(\int_0^T \int f^\varepsilon(s, \mathbf{x}, v, w)\, |v - V(s,\mathbf{x})|^2\, \mathrm{d}v\, \mathrm{d}w\, \mathrm{d}\mathbf{x}\, \mathrm{d}s \right)^{1/2} \\
&\leq \|\partial_v \varphi\|_{L^\infty}\, (T\, \|f_0^\varepsilon\|_{L^1}\, C_T)^{1/2}\, \varepsilon^{1/(2d+12)},
\end{aligned}
$$

whereas the second term $\mathcal{I}_2$ also converges to zero when ε goes to zero since F^ε converges weakly-$\star$ in $\mathcal{M}((0,T) \times \mathbb{R}^{d+1})$ to F. Using a density argument, this shows the convergence of f^ε in $L^1_{\mathrm{loc}}((0,T), \mathcal{M}(\mathbb{R}^{d+2}))$, so this concludes the proof of Theorem 3.2.5.

3.5 Appendix: proof of Proposition 3.2.2

This appendix is devoted to the proof of the existence and uniqueness of a solution f^ε to (3.1.5). Let $T > 0$ and $\varepsilon > 0$ be fixed. The main difficulty is that we cannot use a compactness argument based on an average lemma as in [96] for example, since there is no transport term of the form $v \nabla_x f^\varepsilon$ in (3.1.5). Thus, our strategy is to linearize the equation (3.1.5) in order to construct a Cauchy sequence which converges towards a solution to (3.1.5). First of all, we need to prove some extra a priori estimates on f^ε. In the rest of this section, since ε is fixed, for the sake of clarity, we will note f instead of f^ε, but all the following estimates are not uniform in ε.

3.5.1 A priori estimates

We recall that for any solution f of (3.1.5) and for all $t \in [0, T]$, $\|f(t)\|_{L^1} = \|f(0)\|_{L^1}$. This subsection is devoted to the proof of some a priori estimates.

First of all, we set the system of characteristic equations associated to (3.1.5) for all $(\mathbf{x}, v, w) \in \mathbb{R}^{d+2}$ and all $s \in [0, T]$:

$$\begin{cases} \dfrac{\mathrm{d}\mathcal{V}(s)}{\mathrm{d}s} = N(\mathcal{V}(s)) - \mathcal{W}(s) - [\Phi_\varepsilon \star \rho_0](\mathbf{x})\mathcal{V}(s) + [\Phi_\varepsilon \star j_f(s)](\mathbf{x}), \\[3mm] \dfrac{\mathrm{d}\mathcal{W}(s)}{\mathrm{d}s} = A(\mathcal{V}(t), \mathcal{W}(t)), \end{cases} \tag{3.5.1}$$

where f is a solution of (3.1.5) and j_f is defined with:

$$j_f := \int f \, v \, \mathrm{d}v \, \mathrm{d}w.$$

We define the flow of (3.5.1) for all $\mathbf{z} = (\mathbf{x}, v, w) \in \mathbb{R}^{d+2}$ for all s, t in $[0, T]$:

$$\Sigma(s, t, \mathbf{z}) = (\mathcal{V}(s, t, \mathbf{z}), \mathcal{W}(s, t, \mathbf{z})) \quad , \quad \Sigma(t, t, \mathbf{z}) = (v, w).$$

We start with proving the well-posedness of the flow of the characteristic equation (3.5.1) and an estimate of the support of a solution to (3.1.5).

Lemma 3.5.1 (Well-posedness of the characteristic system and estimate of the support). *Consider an initial data f_0 satisfying (3.2.4) and (3.2.5), and suppose that there exists f a smooth non-negative solution to (3.1.5) such that for all $t \in [0; T]$, $\|f(t)\|_{L^1} = \|f(0)\|_{L^1}$. Then, the characteristic system (3.5.1) is well-posed. Furthermore, there exists a positive constant $R_{T,\varepsilon}$ such that:*

$$\sup_{\substack{t \in [0,T] \\ \mathbf{x} \in \mathbb{R}^d}} \mathrm{Supp}(f(t, \mathbf{x}, \cdot, \cdot)) \subset B(0, R_{T,\varepsilon}), \tag{3.5.2}$$

and there exist two positive constants C_1 and C_2 such that:

$$R_{T,\varepsilon} \leq C_2 e^{C_1(1+\frac{1}{\varepsilon})T}. \tag{3.5.3}$$

Proof. The Cauchy-Lipschitz Theorem yields the local existence and uniqueness of the flow of the characteristic equation (3.5.1). Define for all $s \in [0, T]$:

$$R_\varepsilon(s) := \sup \left\{ \|\Sigma(s', 0, \mathbf{z})\| \quad | \quad s' \in [0; s], \mathbf{z} \in \mathbb{R}^d \times B(0, R_0^\varepsilon) \right\}.$$

Our purpose is to estimate R_ε using the following energy estimate. Let $s \in [0; T]$, $\mathbf{z} = (\mathbf{x}, v, w) \in \mathbb{R}^d \times B(0, R_0^\varepsilon)$. We have:

$$\|\Sigma(s,0,\mathbf{z})\|^2 = \|(v,w)\|^2 + 2 \int_0^s \Sigma(s',0,\mathbf{z}) \cdot \partial_s \Sigma(s',0,\mathbf{z}) \, \mathrm{d}s'$$

$$= \|(v,w)\|^2 + 2 \int_0^s \left[\mathcal{V} \, N(\mathcal{V}) - \mathcal{V} \, \mathcal{W} \right.$$

$$\left. - [\Phi_\varepsilon \star \rho_0](\mathbf{x}) \, |\mathcal{V}|^2 + [\Phi_\varepsilon \star j_f(s')](\mathbf{x}) \, \mathcal{V} + \mathcal{W} \, A(\mathcal{V},\mathcal{W}) \right] \mathrm{d}s'$$

$$\leq |R_0^\varepsilon|^2 + 2 \int_0^s \left[|\mathcal{V}|^2 + \frac{1}{2} \left(|\mathcal{V}|^2 + |\mathcal{W}|^2 \right) \right.$$

$$\left. + R_\varepsilon(s) \left[\phi_\varepsilon \star \rho_0 \right](\mathbf{x}) \, \mathcal{V} + \frac{\tau}{2} \left(|\mathcal{V}|^2 + |\mathcal{W}|^2 \right) + \frac{\tau}{2} \left(a^2 + |\mathcal{W}|^2 \right) \right] \mathrm{d}s'$$

$$\leq |R_0^\varepsilon|^2 + T \, \tau \, a^2 + \int_0^s \left(3 + 2\,\tau + 2 \, \|\rho_0\|_{L^\infty} \, \|\Psi\|_{L^1} + \frac{2}{\varepsilon} \, \|\rho_0\|_{L^\infty} \right) |R_\varepsilon(s')|^2 \, \mathrm{d}s'.$$

Thus, passing to the supremum in $\mathbf{x} \in \mathbb{R}^d$ and in $(v,w) \in B(0,R_0^\varepsilon)$, we get that for all $s \in [0,T]$:

$$|R_\varepsilon(s)|^2 \leq |R_0^\varepsilon|^2 + T \, \tau \, a^2 + \int_0^s \left(3 + 2\,\tau + 2 \, \|\rho_0\|_{L^\infty} \, \|\Psi\|_{L^1} + \frac{2}{\varepsilon} \, \|\rho_0\|_{L^\infty} \right) |R_\varepsilon(s')|^2 \, \mathrm{d}s'.$$

Using the Grönwall's inequality, we get that there exist two positive constants C_1 and C_2 which depend only on T, R_0^ε, $\|\Psi\|_{L^1}$, ρ_0, τ and a such that for all $s \in [0,T]$:

$$|R_\varepsilon(s)|^2 \leq C_2 \, e^{C_1 \left(1 + \frac{1}{\varepsilon}\right) T}.$$

Therefore, the function $\Sigma(\cdot,0,\cdot)$ is well-posed in $\mathscr{C}^1\left([0,T]^2 \times B(0,R_0^\varepsilon), \, L^\infty(\mathbb{R}^d_{\mathbf{x}})\right)$. Similarly, for all $t \in [0,T]$, we show that $\Sigma(\cdot,t,\cdot)$ is well-posed in $\mathscr{C}^1\left([0,T]^2 \times B(0,R_\varepsilon(t)), \, L^\infty(\mathbb{R}^d_{\mathbf{x}})\right)$. Furthermore, we can conclude that

$$\sup_{\substack{t \in [0,T] \\ \mathbf{x} \in \mathbb{R}^d}} \mathrm{Supp}(f(t,\mathbf{x},\cdot,\cdot)) \subset B(0,R_\varepsilon(T)).$$

$\square$

Now, using this estimate on the propagation of the support in $\mathbf{u} = (v,w)$ of any solution f to (3.1.5), we can estimate f and $\nabla_{\mathbf{u}} f$ in L^∞.

Lemma 3.5.2 (Estimates in L^∞). *Consider an initial data f_0 satisfying (3.2.4) and (3.2.5), and suppose that there exists f a smooth non-negative solution to (3.1.5) such that for all $t \in [0,T]$, $\|f(t)\|_{L^1} = \|f_0\|_{L^1}$. Then, there exists a positive constant $C_{T,\varepsilon}$ such that for all $t \in [0,T]$,*

$$\|f(t)\|_{L^\infty} \leq C_{T,\varepsilon} \quad, \text{ and } \quad \|\nabla_{\mathbf{u}} f(t)\|_{L^\infty} \leq C_{T,\varepsilon}. \tag{3.5.4}$$

Proof. We write (3.1.5) in a non-conservative form:

$$\partial_t f + \mathbf{A} \cdot \nabla_{\mathbf{u}} f = - \operatorname{div}_{\mathbf{u}}(\mathbf{A}) \, f, \tag{3.5.5}$$

where $\mathbf{A}$ is the advection field of (3.1.5) given for all $t \in [0,T]$ and all $\mathbf{z} = (\mathbf{x},v,w) \in \mathbb{R}^{d+2}$ by:

$$\mathbf{A}(t,\mathbf{z}) := \begin{pmatrix} N(v) - w - [\Phi_\varepsilon \star \rho_0](\mathbf{x}) \, v + [\Phi_\varepsilon \star j_f(t)](\mathbf{x}) \\ \\ A(v,w) \end{pmatrix}.$$

Thus, for all $t \in [0, T]$ and all $\mathbf{z} = (\mathbf{x}, v, w) \in \mathbb{R}^{d+2}$, we note $\mathbf{u} = (v, w)$ and we have:

$$
\begin{aligned}
- \operatorname{div}_{\mathbf{u}} (\mathbf{A}(t, \mathbf{z})) &= -N'(v) + [\Phi_\varepsilon \star \rho_0](\mathbf{x}) + \tau \, b \\
&= 3 \, v^2 - 1 + [\Phi_\varepsilon \star \rho_0](\mathbf{x}) + \tau \, b.
\end{aligned}
$$

Then, we get that for all $t \in [0, T]$ and $\mathbf{z} = (\mathbf{x}, v, w) \in \mathbb{R}^{d+2}$:

$$
f(t, \mathbf{z}) = f_0(\mathbf{x}, \Sigma(0, t, \mathbf{z})) - \int_0^t \left(\operatorname{div}_{\mathbf{u}} (\mathbf{A}) \, f \right) (s, \mathbf{x}, \Sigma(s, t, \mathbf{z})) \, \mathrm{d}s.
$$

Consequently, we have for all $t \in [0, T]$:

$$
\| f(t) \|_{L^\infty} \leq \| f_0 \|_{L^\infty} + \int_0^t \| \operatorname{div}_{\mathbf{u}} (\mathbf{A}(s, \cdot)) \, f(s) \|_{L^\infty} \, \mathrm{d}s.
$$

Moreover, according to Lemma 3.5.1, there exists a positive constant $R_{T,\varepsilon}$ satisfying (3.5.2), and therefore, for all s, $t \in [0, T]$ and $\mathbf{z} = (\mathbf{x}, \mathbf{u}) \in \mathbb{R}^d \times B(0, R_{T,\varepsilon})$,

$$
| \operatorname{div}_{\mathbf{u}} (\mathbf{A}(s, \mathbf{z})) | \leq 3 \, |R_{T,\varepsilon}|^2 + 1 + \| \Phi_\varepsilon \|_{L^1} \| \rho_0 \|_{L^\infty} + \tau \, b.
$$

Therefore, the Grönwall's inequality gives us that there exists a positive constant C_1 such that for all $t \in [0, T]$:

$$
\| f(t) \|_{L^\infty} \leq \| f_0 \|_{L^\infty} e^{C_1 \, t}.
$$

Then, by differentiating (3.5.5) with respect to v and w, we have:

$$
\begin{cases}
\partial_t (\partial_v f) + \mathbf{A} \cdot \nabla_{\mathbf{u}} (\partial_v f) &= S^v(t, \mathbf{z}) \, \partial_v f - \tau \, \partial_w f - N''(v) \, f, \\[2mm]
\partial_t (\partial_w f) + \mathbf{A} \cdot \nabla_{\mathbf{u}} (\partial_w f) &= S^w(t, \mathbf{z}) \, \partial_w f + \partial_v f,
\end{cases}
$$

where S^v and S^w are given for all $t \in [0, T]$ and all $\mathbf{z} = (\mathbf{x}, v, w) \in \mathbb{R}^{d+2}$ by:

$$
\begin{cases}
S^v(t, \mathbf{z}) := -2 \, N'(v) + 2 \, [\Phi_\varepsilon \star \rho_0] (\mathbf{x}) + \tau \, b, \\[2mm]
S^w(t, \mathbf{z}) := -N'(v) + [\Phi_\varepsilon \star \rho_0] (\mathbf{x}) + 2 \, \tau \, b.
\end{cases}
$$

Therefore, using the estimate of the support of f (3.5.2), the Grönwall's inequality gives us that there exist two positive constants C_2 and C_3 such that for all $t \in [0, T]$:

$$
\| \nabla_{\mathbf{u}} f(t) \|_{L^\infty} \leq C_3 \, e^{C_2 \, t}.
$$

<div style="text-align: right;">□</div>

3.5.2 Proof of existence and uniqueness

Let $\varepsilon > 0$. We proceed with a linearization of the equation (3.1.5) in order to construct a Cauchy sequence $\{ f_n \}_{n \in \mathbb{N}}$ of non-negative functions. In the following, we use the shorthand notation $\mathbf{u} = (v, w) \in \mathbb{R}^2$. Let us define $f_0 := f_0^\varepsilon$, and for all $n \in \mathbb{N}$, $f^{n+1} \in \mathscr{C}^0([0, T] \times \mathbb{R}^2_{\mathbf{u}}, L^\infty(\mathbb{R}^d_{\mathbf{x}}))$ is a weak solution of the transport equation which reads for $t > 0$ and $(\mathbf{x}, v, w) \in \mathbb{R}^{d+2}$:

$$
\begin{cases}
\partial_t f_{n+1} + \partial_v [f_{n+1} \, P_n] + \partial_w [f_{n+1} \, A(v, w)] = 0, \\[2mm]
P_n(t, \mathbf{x}, v, w) = N(v) - w - [\Psi \star \rho_0] \, v + [\Psi \star j_n] - \dfrac{1}{\varepsilon} \, (\rho_0 \, v - j_{n+1}), \\[2mm]
f_{n+1}|_{t=0} = f_0^\varepsilon,
\end{cases}
\tag{3.5.6}
$$

where $j_n := \int f_n \, v \, m dv \, dw$ and $\rho_0 = \int f_n \, dv \, dw$. We admit the well-posedness of the sequence $\{f_n\}_{n\in\mathbb{N}}$. Using similar arguments as in Lemmas 3.5.1 and 3.5.2, we get that there exist two positive constants $R_{T,\varepsilon}$ and $C_{T,\varepsilon}$ independent on n such that for all $n \in \mathbb{N}$:

$$\sup_{\substack{t\in[0,T]\\ \mathbf{x}\in\mathbb{R}^d}} \mathrm{Supp}(f_n(t,\mathbf{x},\cdot,\cdot)) \subset B(0, R_{T,\varepsilon}), \tag{3.5.7}$$

$$\|f_n(t)\|_{L^\infty} \leq C_{T,\varepsilon} \quad \text{and} \quad \|\nabla_{\mathbf{u}} f_n(t)\|_{L^\infty} \leq C_{T,\varepsilon}. \tag{3.5.8}$$

3.5.2.1 Cauchy sequence

For all $n \in \mathbb{N}$, we define $g_n := f_{n+1} - f_n$, so g_{n+1} is a weak solution to

$$\begin{cases} \partial_t g_{n+1} + \partial_v \left[g_{n+1} \, P_{n+1} \right] + \partial_w \left[g_{n+1} \, A(v,w) \right] \\ \qquad + \partial_v \left[f_n \left(\Psi \star (j_{n+1} - j_n) + \dfrac{1}{\varepsilon} (j_{n+2} - j_{n+1}) \right) \right] = 0, \\ \\ g_{n+1}|_{t=0} = 0, \end{cases} \tag{3.5.9}$$

where P_{n+1} is defined in (3.5.6). Let us fix $t \in [0,T]$ and $n \in \mathbb{N}$. We want to estimate $\|g_{n+1}(t,\mathbf{x})\|_{L^\infty(\mathbb{R}^{d+2})}$. To do so, we use the property that

$$\|g_{n+1}(t,\mathbf{x})\|_{L^p(\mathbb{R}^2_{\mathbf{u}})} \longrightarrow \|g_{n+1}(t,\mathbf{x})\|_{L^\infty(\mathbb{R}^2_{\mathbf{u}})}$$

as p goes to infinity, since $g_{n+1}(t) \in L^1(\mathbb{R}^{d+2})$. Let $p > 1$. We compute:

$$\frac{1}{p} \frac{\mathrm{d}}{\mathrm{d}t} \|g_{n+1}(t)\|_{L^p}^p = I_1 + I_2 + I_3 + I_4,$$

where

$$\begin{cases} I_1 := -\displaystyle\int_{\mathbb{R}^{d+2}} |g_{n+1}|^{p-1} \, \partial_v \, (g_{n+1} \, P_{n+1}) \, \mathrm{sign}(g_{n+1}) \, \mathrm{d}\mathbf{z}, \\ \\ I_2 := -\displaystyle\int_{\mathbb{R}^{d+2}} |g_{n+1}|^{p-1} \, \partial_w \, (g_{n+1} \, A(\mathbf{u})) \, \mathrm{sign}(g_{n+1}) \, \mathrm{d}\mathbf{z}, \\ \\ I_3 := -\displaystyle\int_{\mathbb{R}^{d+2}} |g_{n+1}|^{p-1} \, \partial_v f_{n+1} \, \Psi \star [j_{n+1} - j_n] \, \mathrm{sign}(g_{n+1}) \, \mathrm{d}\mathbf{z}, \\ \\ I_4 := -\displaystyle\int_{\mathbb{R}^{d+2}} |g_{n+1}|^{p-1} \, \partial_v f_{n+1} \, [j_{n+1} - j_n] \, \mathrm{sign}(g_{n+1}) \, \mathrm{d}\mathbf{z}. \end{cases}$$

To treat the first term I_1, we compute:

$$I_1 = -\int |g_{n+1}|^p \, \partial_v \, (P_{n+1}) \, \mathrm{d}\mathbf{z} - \int |g_{n+1}|^{p-1} \, \partial_v \, |g_{n+1}| \, P_{n+1} \, \mathrm{d}\mathbf{z}$$

$$= -\int |g_{n+1}|^p \, \partial_v \, (P_{n+1}) \, \mathrm{d}\mathbf{z} - \frac{1}{p} \int \partial_v \, |g_{n+1}|^p \, P_{n+1} \, \mathrm{d}\mathbf{z}.$$

By integrating the second term by parts in v, we get that

$$\begin{aligned} I_1 &\leq \frac{p-1}{p} \int |g_{n+1}|^p \, |\partial_v P_{n+1}| \, \mathrm{d}\mathbf{z} \\ &= \frac{p-1}{p} \int |g_{n+1}|^p \left| 3 \, v^2 - 1 - \Psi \star \rho_0 - \frac{1}{\varepsilon}\rho_0 \right| \mathrm{d}v \, \mathrm{d}w \, \mathrm{d}\mathbf{x} \\ &\leq C_1 \frac{p-1}{p} \int |g_{n+1}|^p \, \mathrm{d}\mathbf{z}, \end{aligned} \tag{3.5.10}$$

where $C_1 > 0$ is a positive constant which only depends on $R_{T,\varepsilon}$, ε, $\|\Psi\|_{L^1}$ and $\|\rho_0\|_{L^\infty}$. Similarly for the second term I_2, we also have that:

$$I_2 \leq C_2 \frac{p-1}{p} \int |g_{n+1}|^p \, d\mathbf{z}, \tag{3.5.11}$$

where $C_2 > 0$ is a positive constant. As for the third term I_3, Hölder's inequality and the estimate (3.5.8) yield that

$$\begin{aligned} I_3 &\leq C_{T,\varepsilon} \, \|g_{n+1}(t)\|_{L^p}^{p/(p-1)} \, \|\Psi \star [j_{n+1} - j_n] \, (t)\|_{L^p(\mathbb{R}_{\mathbf{x}}^d)} \\ &\leq C_{T,\varepsilon} \, \|\Psi\|_{L^1} \, \|g_{n+1}(t)\|_{L^p}^{p/(p-1)} \, \|(j_{n+1} - j_n)(t)\|_{L^p(\mathbb{R}_{\mathbf{x}}^d)}. \end{aligned}$$

Moreover, according to the definition of j_n and the estimate (3.5.7), we also have

$$\|(j_{n+1} - j_n)(t)\|_{L^p(\mathbb{R}_{\mathbf{x}}^d)} \leq R_{T,\varepsilon} \, \|g_{n+1}(t)\|_{L^p}.$$

Consequently, we get:

$$I_3 \leq C_{T,\varepsilon} \, R_{T,\varepsilon} \, \|\Psi\|_{L^1} \, \|g_{n+1}(t,\mathbf{x})\|_{L^p}^p. \tag{3.5.12}$$

Similarly, using Young's inequality, we get that:

$$\begin{aligned} I_4 &\leq C_{T,\varepsilon} \, R_{T,\varepsilon} \, \frac{1}{\varepsilon} \, \|g_{n+1}(t,\mathbf{x})\|_{L^p}^{p-1} \, \|g_n(t,\mathbf{x})\|_{L^p} \\ &\leq C_{T,\varepsilon} \, R_{T,\varepsilon} \, \frac{1}{\varepsilon} \left(\frac{p-1}{p} \|g_{n+1}(t,\mathbf{x})\|_{L^p}^p + \frac{1}{p} \|g_{n+1}(t,\mathbf{x})\|_{L^p}^p \right). \end{aligned} \tag{3.5.13}$$

Consequently, (3.5.10)-(3.5.13) together give us that there exists a positive constant $C > 0$ independent of n and p such that for all $t \in [0,T]$:

$$\frac{d}{dt} \|g_{n+1}(t)\|_{L^p} \leq C^{-p} \left(\|g_n(t)\|_{L^p} + (p-1)^{-p} \|g_{n+1}(t)\|_{L^p} \right).$$

Thus, Grönwall's inequality yields that

$$\|g_{n+1}(t)\|_{L^p} \leq C^{-p} \exp\left(C^{-p} (p-1)^{-p} t \right) \int_0^t \|g_n(s)\|_{L^p} \, ds.$$

Therefore, in the limit $p \to +\infty$, we finally get for all $t \in [0,T]$:

$$\|g_{n+1}(t)\|_{L^\infty} \leq \int_0^t \|g_n(s)\|_{L^\infty} \, ds. \tag{3.5.14}$$

Furthermore, the estimate (3.5.8) yields that for $n = 0$,

$$\|g_1(t)\|_{L^\infty} \leq 2 \, C_{T,\varepsilon}. \tag{3.5.15}$$

We deduce from (3.5.14)-(3.5.15) that for all $n \in \mathbb{N}$,

$$\|g_{n+1}(t)\|_{L^\infty} \leq 2 \, C_{T,\varepsilon} \, \frac{t^n}{n!}. \tag{3.5.16}$$

which is summable. Hence, we can deduce that $\{f_n\}_{n \in \mathbb{N}}$ is a Cauchy sequence in $\mathscr{C}([0,T] \times \mathbb{R}_{\mathbf{u}}^2, \mathbb{R}_{\mathbf{x}}^d)$, which is a Banach space. Consequently, there exists f^ε a non-negative function in $\mathscr{C}([0,T] \times \mathbb{R}_{\mathbf{u}}^2, \mathbb{R}_{\mathbf{x}}^d)$ such that $\{f_n\}_{n \in \mathbb{N}}$ strongly converges towards f^ε in $\mathscr{C}([0,T] \times \mathbb{R}_{\mathbf{u}}^2, \mathbb{R}_{\mathbf{x}}^d)$.

3.5.2.2 Passing to the limit $n \to +\infty$

Let us pass to the limit $n \to +\infty$ in the weak formulation of (3.5.6). Here, we only give details for the nonlinear term. Let $n \in \mathbb{N}$ and $t \in [0, T]$. Since $\|j_n(t) - j(t)\|_{L^\infty(\mathbb{R}^d)} \leq R_{T,\varepsilon} \|f_n(t) - f(t)\|_{L^\infty}$, the sequence $\{j_n(t)\}_{n \in \mathbb{N}}$ strongly converges towards j in $L^\infty([0, T], L^\infty(\mathbb{R}^d))$. Thus, for all φ in $\mathscr{C}_c^\infty([0, T] \times \mathbb{R}^{d+2})$, as n goes to infinity,

$$\int_0^t \int_{R^{d+2}} j_n \, f_n \, \partial_v \varphi \, \mathrm{d}\mathbf{z} \, \mathrm{d}s \; \longrightarrow \; \int_0^t \int_{R^{d+2}} j \, f \, \partial_v \varphi \, \mathrm{d}\mathbf{z} \, \mathrm{d}s. \tag{3.5.17}$$

Therefore, f^ε is a weak solution of (3.1.5) in the sense of (3.2.2) which satisfies the support estimate (3.5.2). Consequently, we deduce

$$f^\varepsilon \in \mathscr{C}^0\left([0, T], L^1(\mathbb{R}^{d+2})\right),$$

hence we can apply Lemma 3.5.1 with f^ε, which yields that the characteristics $\Sigma \in \mathscr{C}^1([0, T]^2 \times \mathbb{R}_{\mathbf{u}}^2, L^\infty(\mathbb{R}_{\mathbf{x}}^d)^2)$ are well-defined. As previously, we note $\mathbf{A}$ the advection field of (3.1.5). Therefore, for all $t \in [0, T]$, $\mathbf{u} = (v, w) \in \mathbb{R}^2$ and $\mathbf{x} \in \mathbb{R}^d$,

$$f^\varepsilon(t, \mathbf{x}, \mathbf{u}) \,=\, f_0^\varepsilon(\mathbf{x}, \Sigma(0, t, \mathbf{x}, \mathbf{u})) \, \exp\left(-\int_0^t \operatorname{div}_{\mathbf{u}} \mathbf{A}(s, \mathbf{x}, \Sigma(s, t, \mathbf{x}, \mathbf{u})) \mathrm{d}s\right).$$

Finally, using the regularity of $\operatorname{div}_{\mathbf{u}} \mathbf{A}$, Σ and f_0^ε which satisfies (3.2.4), we get that

$$f^\varepsilon, \nabla_{\mathbf{u}} f^\varepsilon \in L^\infty((0, T) \times \mathbb{R}^{d+2}).$$

3.5.2.3 Proof of uniqueness

Suppose that there exists two functions f_1 and $f_2 \in \mathscr{C}([0, T] \times \mathbb{R}_{\mathbf{u}}^2, \mathbb{R}_{\mathbf{x}}^d)$ weak solutions to (3.1.5) with f_0 as initial data. Define $g := f_2 - f_1$. Thus, g satisfies the following equation:

$$\begin{cases} \partial_t g \,+\, \partial_v \left[g \left(N(v) - w - [\Phi_\varepsilon \star \rho_0] \, v + [\Phi_\varepsilon \star j_2] \right) \right] \,+\, \partial_w \left[g \, A(v, w) \right] \\ \qquad +\, \partial_v \left(f_1 \, \Phi_\varepsilon \star [j_2 - j_1] \right) \,=\, 0, \\[2mm] g|_{t=0} \,=\, 0. \end{cases} \tag{3.5.18}$$

Using the same computations as before, we get that there exists a positive constant $C > 0$ such that for all $t \in [0, T]$:

$$\frac{\mathrm{d}}{\mathrm{d}t} \|g(t)\|_{L^\infty} \,\leq\, C \, \|g(t)\|_{L^\infty}.$$

Hence, Grönwall's inequality yields that for all $t \in [0, T]$, $\|g(t)\|_{L^\infty} \,=\, 0$. Therefore, $f_1 = f_2$ almost everywhere.

3.6 Appendix: proof of Proposition 3.2.3

This appendix is devoted to the proof of Proposition 3.2.3. We apply a fixed point argument to get the existence and uniqueness of a classical solution (V, W) of (3.2.6). We first set

$$\mathscr{E} \,:=\, \mathscr{C}^0([0, T], L^\infty(\mathbb{R}^d))$$

and for a fixed $M > 0$ we define

$$\mathscr{K}_T \,:=\, \left\{ (V, W) \in \mathscr{E}^2 \,;\, \|V(t) - V_0\|_{L^\infty(\mathbb{R}^d)} + \|W(t) - W_0\|_{L^\infty(\mathbb{R}^d)} \leq M, \,\forall t \in [0, T] \right\},$$

equipped with the norm for $U = (V, W) \in \mathscr{K}_T$,

$$\|\|U\|\| := \sup_{t \in [0,T]} \left(\|V(t)\|_{L^\infty(\mathbb{R}^d)} + \|W(t)\|_{L^\infty(\mathbb{R}^d)} \right).$$

Consider the application Γ such that for all $U = (V, W) \in \mathscr{K}_T$, for all $t \in [0, T]$ and almost every $\mathbf{x} \in \mathbb{R}^d$,

$$\Gamma[U](t, \mathbf{x}) := U_0(\mathbf{x}) + \int_0^t \left[\begin{array}{c} \mathcal{L}_{\rho_0}(V)(s, \mathbf{x})\mathrm{d}s + N(V(s, \mathbf{x})) - W(s, \mathbf{x}) \\ A(V, W)(s, \mathbf{x}) \end{array} \right] \mathrm{d}s.$$

On the one hand, since $\Psi \in L^1(\mathbb{R}^d)$ and $N \in \mathscr{C}^1(\mathbb{R})$, we prove that Γ is well-defined

$$\|\|\Gamma[U] - U_0\|\| \leq C\,T$$

for some constant $C > 0$ independent of time. As a consequence, we can choose T small enough so that $\Gamma[U] \in \mathscr{K}_T$. On the other hand, Γ is contractive : for U_1 $U_2 \in \mathscr{K}_T$ and $(t, \mathbf{x})$ be in $[0, T] \times \mathbb{R}^d$, we have

$$|\Gamma[U_1] - \Gamma[U_2]|\,(t, \mathbf{x}) \leq C\,t\,\|\|U_1 - U_2\|\|,$$

where $C > 0$ does not depend of time $t > 0$, hence for T small enough, Γ is a contraction from $\mathscr{K}_T$ to $\mathscr{K}_T$, which is a complete for the distance associated to the norm $\|\|.\|\|$ previously defined. Therefore, using the Banach fixed point theorem, there exists a unique $U \in \mathscr{K}_T$ such that $\Gamma[U] = U$, that is, $U = (V, W)$ is solution to (3.2.6) for the initial condition $U_0 = (V_0, W_0)$. Moreover since V and $W \in \mathscr{C}^0([0, T], L^\infty(\mathbb{R}^d))$ and using the Duhamel's formula, it yields that

$$V,\, W \in \mathscr{C}^1([0, T], L^\infty(\mathbb{R}^d)).$$

Finally, an energy estimate gives that

$$\begin{aligned} \frac{1}{2} \frac{\mathrm{d}}{\mathrm{d}t} \left(|V(t, \mathbf{x})|^2 + |W(t, \mathbf{x})|^2 \right) &\leq \left(\frac{3 + \tau}{2} + \|\Psi\|_{L^1} \|\rho_0\|_{L^\infty} \right) \|V(t)\|_{L^\infty(\mathbb{R}^d)}^2 \\ &+ \frac{1 + 2\,\tau}{2} \|W(t)\|_{L^\infty(\mathbb{R}^d)}^2 + \frac{\tau\,a^2}{2}. \end{aligned}$$

Using Grönwall's lemma, we can conclude that there exists a constant $C > 0$, only depending on a, τ and Ψ, such that

$$\|\|(V, W)\|\| \leq (\|\|(V_0, W_0)\|\| + C)\,e^{C\,T}.$$

It allows to prove that this unique solution is global in time.

Chapter 4

Asymptotic limit of a spatially-extended mean-field FitzHugh-Nagumo model

Article à paraître en 2020 dans *M³AS: Mathematical Models and Methods in Applied Sciences*, en tant que seul auteur.

Contents

Abstract

We consider a spatially extended mean-field model of a FitzHugh-Nagumo neural network, with a rescaled interaction kernel. Our main purpose is to prove that its asymptotic limit in the regime of strong local interactions converges toward a system of reaction-diffusion equations taking account for the average quantities of the network. Our approach is based on a modulated energy argument, to compare the macroscopic quantities computed from the solution of the transport equation, and the solution of the limit system. The main difficulty, compared to the literature, lies in the need of regularity in space of the solutions of the limit system and a careful control of an internal nonlocal dissipation.

4.1   Introduction

In this chapter, we consider the following nonlocal FHN transport equation for all $\varepsilon > 0$, $t > 0$, $\mathbf{x} \in \mathbb{R}^d$ with $d \in \{1, 2, 3\}$, and $\mathbf{u} = (v, w) \in \mathbb{R}^2$:

$$\begin{cases} \partial_t f^\varepsilon(t, \mathbf{x}, \mathbf{u}) + \partial_v \left[f^\varepsilon(t, \mathbf{x}, \mathbf{u}) \left(N(v) - w - \mathcal{K}_\varepsilon[f^\varepsilon](t, \mathbf{x}, v) \right) \right] + \partial_w \left[f^\varepsilon(t, \mathbf{x}, \mathbf{u}) A(v, w) \right] = 0, \\[2mm] \mathcal{K}_\varepsilon[f^\varepsilon](t, \mathbf{x}, v) := \dfrac{1}{\varepsilon^{d+2}} \iint_{\mathbb{R}^{d+2}} \Psi \left(\dfrac{\|\mathbf{x} - \mathbf{x}'\|}{\varepsilon} \right) (v - v') f^\varepsilon(t, \mathbf{x}', \mathbf{u}') \, \mathrm{d}\mathbf{x}' \, \mathrm{d}\mathbf{u}', \\[2mm] A(v, w) := \tau(v + a - b\,w), \\[2mm] f^\varepsilon|_{t=0} = f_0^\varepsilon, \end{cases}$$
$$(4.1.1)$$

using the shorthand notation $\mathbf{u}' = (v', w')$. As precedently in this framework, each neuron is characterized by three quantities: a pair voltage-adaptation $(v, w) \in \mathbb{R}^2$, and $\mathbf{x} \in \mathbb{R}^d$ its spatial position in the network. Furthermore, $f^\varepsilon(t, \mathbf{x}, \mathbf{u})$ is the density function of finding neurons at time t at position $\mathbf{x}$ and at the electrical state $\mathbf{u} = (v, w)$ within the cortex.

Let us clarify the notations. First of all τ and b are non-negative constant. Then, even if we have to consider the variable $v + a$ instead of v, we consider $a = 0$. Here, we consider small values of $\tau > 0$ to account for the slow evolution of the adaptation variable. Then, the purpose of the function N is to model the excitability of each neuron. In the rest of this chapter, as in [36, 38, 88, 89, 92, 119], we consider the following cubic nonlinearity

$$N(v) := v(1 - v)(v - \theta), \quad v \in \mathbb{R}, \tag{4.1.2}$$

where $\theta \in (0, 1)$ is fixed. Such a nonlinearity satisfies the following properties for four fixed positive constants κ_1, κ_1', κ_2 and κ_3:

$$\begin{cases} v\,N(v) \leq \kappa_1 |v|^2 - \kappa_1' |v|^4, & v \in \mathbb{R}, \\[2mm] (v - u)(N(v) - N(u)) \leq \kappa_2 |v - u|^2, & v, u \in \mathbb{R}, \\[2mm] |N(v) - N(u)| \leq \kappa_3 |v - u| \left(1 + |v|^2 + |u|^2 \right), & v, u \in \mathbb{R}. \end{cases} \tag{4.1.3}$$

In the rest of this chapter, we consider a small scaling parameter $\varepsilon > 0$ and

$$\Psi_\varepsilon(\|\mathbf{x}\|) := \frac{1}{\varepsilon^d} \Psi \left(\frac{\|\mathbf{x}\|}{\varepsilon} \right), \quad \mathbf{x} \in \mathbb{R}^d, \quad \varepsilon > 0, \tag{4.1.4}$$

where $\Psi : \mathbb{R} \to \mathbb{R}^+$ is a connectivity kernel modeling the influence of the distance between two neurons on their interactions. Notice that in this model, interactions are only modulated by

distance and the electrical voltage between neurons. In the following, we assume that Ψ satisfies the following assumptions:

$$\Psi > 0 \text{ a.e.,} \quad \int \Psi(\|\mathbf{y}\|) \, \mathrm{d}\mathbf{y} = 1, \quad 0 < \sigma = \int \Psi(\|\mathbf{y}\|) \frac{\|\mathbf{y}\|^2}{2} \, \mathrm{d}\mathbf{y} < \infty. \tag{4.1.5}$$

Let us discuss the hypotheses on Ψ. First, the choice of a positive and integrable connectivity kernel implies that we only consider activatory interactions, and that neurons which are far away from each other have few interactions. Moreover, we restrict our framework to positive functions only for technical reasons. Then, the assumptions of finite moments and symmetry are crucial hypotheses to derive the asymptotic limit as ε goes to 0. Indeed, the finite moment assumption determines the type of spatial diffusion we get in the limit, and as we shall see later, the symmetry assumption yields that all the moments of Ψ of odd order are 0. A typical example of admissible connectivity kernel in our framework is a Gaussian function.

The main purpose of this chapter is to derive a macroscopic model of the neural network from the transport equation (4.1.1), which accounts for the evolution of the average membrane potential of neurons at each position $\mathbf{x}$. Yet, the macroscopic values computed from f^ε a solution to (4.1.1) do not satisfy a closed system of equations. Indeed, let us consider ρ^ε the average density of neurons, V^ε the average membrane potential and W^ε the average adaptation variable, defined through

$$\begin{cases} \rho^\varepsilon(t, \mathbf{x}) := \displaystyle\int_{\mathbb{R}^2} f^\varepsilon(t, \mathbf{x}, v, w) \, \mathrm{d}v \, \mathrm{d}w, \\[2mm] \rho^\varepsilon(t, \mathbf{x}) \, V^\varepsilon(t, \mathbf{x}) := \displaystyle\int_{\mathbb{R}^2} v \, f^\varepsilon(t, \mathbf{x}, v, w) \, \mathrm{d}v \, \mathrm{d}w, \\[2mm] \rho^\varepsilon(t, \mathbf{x}) \, W^\varepsilon(t, \mathbf{x}) := \displaystyle\int_{\mathbb{R}^2} w \, f^\varepsilon(t, \mathbf{x}, v, w) \, \mathrm{d}v \, \mathrm{d}w. \end{cases} \tag{4.1.6}$$

We directly get from (4.1.1) the conservation of mass, that is for all $t > 0$, $\rho^\varepsilon(t, \cdot) = \rho^\varepsilon(0, \cdot) = \rho_0^\varepsilon$. Then, these macroscopic quantities formally satisfy the following system for all $t > 0$ and $\mathbf{x} \in \mathbb{R}^d$:

$$\begin{cases} \partial_t(\rho_0^\varepsilon \, V^\varepsilon)(t, \mathbf{x}) - \dfrac{1}{\varepsilon^2} \displaystyle\int_{\mathbb{R}^d} \Psi_\varepsilon(\|\mathbf{x} - \mathbf{x}'\|) \left(V^\varepsilon(t, \mathbf{x}') - V^\varepsilon(t, \mathbf{x}) \right) \rho_0^\varepsilon(\mathbf{x}) \, \rho_0^\varepsilon(\mathbf{x}') \, \mathrm{d}\mathbf{x}' \\[3mm] \qquad\qquad = \displaystyle\int_{\mathbb{R}^2} N(v) \, f^\varepsilon(t, \mathbf{x}, v, w) \, \mathrm{d}v \, \mathrm{d}w - \rho_0^\varepsilon \, W^\varepsilon(t, \mathbf{x}), \\[3mm] \partial_t(\rho_0^\varepsilon \, W^\varepsilon)(t, \mathbf{x}) = \rho_0^\varepsilon(\mathbf{x}) \, A\left(V^\varepsilon(t, \mathbf{x}), W^\varepsilon(t, \mathbf{x}) \right). \end{cases} \tag{4.1.7}$$

The problem comes from the fact that the function N is not linear. The whole interest of the scaling of the nonlocal term in (4.1.1) is to consider the regime of strong local interactions, in order to circumvent this issue. Indeed, in the asymptotic limit $\varepsilon \to 0$, the interaction kernel Ψ_ε converges towards a Dirac distribution. From a biological viewpoint, this seems definitely justified, since at the macroscopic scale, if we consider a whole portion of the cortex, any neuron seems to interact only with its very closest neighbours, so the nonlocal effect is insignificant.

As in Chapter 3, we expect the solution f^ε of the transport equation (4.1.1) as ε goes to 0 to converge towards a monokinetic solution, that is:

$$f^\varepsilon(t, \mathbf{x}, v, w) \underset{\varepsilon \to 0}{\rightharpoonup} F(t, \mathbf{x}, w) \otimes \delta_0(v - V(t, \mathbf{x})), \tag{4.1.8}$$

where the pair (F, V) has to be determined. If we define

$$\rho(t, \mathbf{x}) := \int_{\mathbb{R}} F(t, \mathbf{x}, w) \mathrm{d}w, \quad \rho(t, \mathbf{x}) \, W(t, \mathbf{x}) := \int_{\mathbb{R}} F(t, \mathbf{x}, w) \, w \, \mathrm{d}w,$$

then, following the steps from the general introduction, we get that the pair (V, F) formally satisfies for $t > 0$, $\mathbf{x} \in \mathbb{R}^d$ and $w \in \mathbb{R}$ the system:

$$\begin{cases} \partial_t F + \partial_w \left(A(V, w) F \right) = 0, \\ \\ \partial_t \left(\rho_0 V \right) - \sigma \left[\rho_0 \Delta_{\mathbf{x}} \left(\rho_0 V \right) - \left(\Delta_{\mathbf{x}} \rho_0 \right) \rho_0 V \right] = \rho_0 N(V) - \rho_0 W, \end{cases} \tag{4.1.9}$$

Therefore, the limit triple $\mathcal{Z} := \left(\rho_0, \rho_0 V, \rho_0 W \right)$ is expected to satisfy the reaction-diffusion system

$$\partial_t \mathcal{Z} = \rho_0 \begin{pmatrix} 0 \\ N(V) - W + \sigma \left[\Delta_{\mathbf{x}}(\rho_0 V) - \Delta_{\mathbf{x}} \rho_0 V \right] \\ A(V, W) \end{pmatrix}. \tag{4.1.10}$$

Let us discuss the structure of the system (4.1.10). It is worth noticing that it is not well-defined for $\mathbf{x} \in \mathbb{R}^d$ if $\rho_0(\mathbf{x}) = 0$. In the case $\rho_0 > 0$, it reduces to the FHN reaction-diffusion system for $t > 0$ and $\mathbf{x} \in \mathbb{R}^d$:

$$\begin{cases} \partial_t V(t, \mathbf{x}) - \sigma \left[\Delta_{\mathbf{x}} \left(\rho_0 V \right) (t, \mathbf{x}) - \Delta_{\mathbf{x}} \rho_0(\mathbf{x}) V(t, \mathbf{x}) \right] = N(V(t, \mathbf{x})) - W(t, \mathbf{x}), \\ \\ \partial_t W(t, \mathbf{x}) = A(V(t, \mathbf{x}), W(t, \mathbf{x})). \end{cases} \tag{4.1.11}$$

We stress that the rescaling ε^{-2} in the nonlocal term in (4.1.1) is crucial. From a biological viewpoint, we only need it to go to infinity as ε goes to 0 to provide strong interactions, but from a mathematical viewpoint, this power -2 is the only one which enables us to get local interactions in the limit $\varepsilon \to 0$. We refer to [6, 7], in which the authors use the same rescaling to prove the convergence of the traveling wave solutions of a nonlocal bistable equation towards solutions of a standard local one.

The system (4.1.11) has been extensively studied, namely regarding the formation and propagation of traveling fronts and pulses for example (see e.g. [36, 38, 92]). We also mention some recent works on the FHN system in the discrete case [88, 89]. The contribution of this chapter is thus to prove that the system (4.1.9), which can be reduced under some assumptions to the FHN reaction-diffusion system (4.1.11), is a macroscopic description of the neural network.

Our approach to prove the asymptotic limit follows ideas from [49, 63, 94, 95], where the authors derive macroscopic equations using a relative entropy argument, as developed in the works by Dafermos [51] and Di Perna [56] for conservation laws. Yet, the entropy used in the [49] for instance is the standard energy functional, so the associated relative entropy actually corresponds to the notion of modulated energy as introduced in [20] to prove the convergence of the Vlasov-Poisson system in the quasi-neutral regime towards the incompressible Euler equations. This modulated energy argument consists in estimating the modulation of the energy functional with the solution of the limit equation. It was developed precisely to derive asymptotic limits of kinetic equations without velocity transport, as in our framework, or in [21] for instance. In the rest of this chapter, the two notions of modulated energy and relative entropy being equivalent in this framework, we stick with the relative entropy method.

The specificity of our problem is the absence of noise in the considered neural network, which implies the absence of a Laplace operator in v in the mean-field equation (4.1.1). Hence, without the regularizing effect of noise, the solution f^ε of (4.1.1) converges towards a Dirac distribution in v, which prevents us from using the decay of a usual entropy of type $f \log(f)$ as in [95]. As in [49, 63, 94], we rather focus on the evolution of moments of second order in v and w of f^ε. Then, we encounter two main difficulties. The first one comes from the term $\partial_v(f^\varepsilon N(v))$ in (4.1.1), which introduces moments of f^ε in v of higher order. Similarly as in [49], it will be sufficient to control moments of f^ε of fourth order to circumvent this problem. Then, unlike [49], we have to precisely determine the regularity in space we need for the solutions of the limit system (4.1.9) to estimate the modulated energy.

Outline of the paper. The rest of this paper is organised as follows. In Section 4.2, we present our hypotheses, and our results on the existence of solutions to the transport equation (4.1.1) and to the limit equation (4.1.9), and our main result about the asymptotic limit from (4.1.1) to (4.1.9). Then, in Section 4.3, we prove some *a priori* estimates which will be key arguments for the proof of our main result. Then, Section 4.4 is devoted to the relative entropy estimate and the proof of our main result. Finally, in Section 4.5, we study the well-posedness of the limit equation (4.1.9), constructing a solution from a pair (V, W) satisfying the reaction-diffusion system (4.1.11) in a weak sense.

4.2 Main result

In this section, we state our main result on the asymptotic limit of a weak solution $(f^\varepsilon)_{\varepsilon > 0}$ of the transport equation (4.1.1) towards a solution (V, F) of the reaction-diffusion equation (4.1.9). Before that, we have to precisely define our notion of solutions of the transport model (4.1.1) and of the system (4.1.9).

4.2.1 Existence of a weak solution of the transport equation

In this subsection, we focus on the well-posedness of the mesoscopic model. First, let us specify our notion of weak solution of the transport equation (4.1.1).

Definition 4.2.1. *We say that f^ε is a weak solution of (4.1.1) with initial condition $f_0^\varepsilon \geq 0$ if for any $T > 0$,*

$$f^\varepsilon \in \mathscr{C}^0\left([0, T], L^1(\mathbb{R}^{d+2})\right) \cap L^\infty\left((0, T) \times \mathbb{R}^{d+2}\right),$$

and for any $\varphi \in \mathscr{C}_c^\infty([0, T) \times \mathbb{R}^{d+2})$, the following weak formulation of (4.1.1) holds,

$$\int_0^T \int f^\varepsilon \left[\partial_t \varphi + (N(v) - w - \mathcal{K}_\varepsilon[f^\varepsilon]) \, \partial_v \varphi + A(v, w) \, \partial_w \varphi\right] \mathrm{d}\mathbf{z} \, \mathrm{d}t \ + \ \int f_0^\varepsilon(\mathbf{z}) \, \varphi(0, \mathbf{z}) \, \mathrm{d}\mathbf{z} \ = \ 0,$$
(4.2.1)

where $\mathbf{z} = (\mathbf{x}, v, w) \in \mathbb{R}^{d+2}$.

In the rest of this paper, if f^ε is a weak solution of (4.1.1), we note $\mathcal{Z}^\varepsilon := (\rho_0^\varepsilon, \rho_0^\varepsilon V^\varepsilon, \rho_0^\varepsilon W^\varepsilon)$ the triple of macroscopic quantities computed from f^ε as in (1.3.1). Then, let us quote our result of existence and uniqueness of a weak solution to the transport equation (4.1.1), whose proof can be found in Proposition 2.2 from [49].

Proposition 4.2.2. *Let $\varepsilon > 0$. We consider a connectivity kernel Ψ satisfying (4.1.5), and an initial data f_0^ε such that*

$$f_0^\varepsilon \geq 0, \quad \|f_0^\varepsilon\|_{L^1(\mathbb{R}^{d+2})} = 1, \quad f_0^\varepsilon, \nabla_{\mathbf{u}} f_0^\varepsilon \in L^\infty(\mathbb{R}^{d+2}),$$
(4.2.2)

where $\mathbf{u} = (v, w)$, and there exists a positive constant $R_0^\varepsilon > 0$ such that for all $\mathbf{x} \in \mathbb{R}^d$,

$$\mathrm{Supp}(f_0^\varepsilon(\mathbf{x}, \cdot)) \subseteq B(0, R_0^\varepsilon) \subset \mathbb{R}^2.$$
(4.2.3)

Then, for any $T > 0$, there exists a unique non-negative weak solution f^ε of (4.1.1) in the sense of Definition 4.2.1, which is compactly supported in $\mathbf{u} = (v, w) \in \mathbb{R}^2$.

Remark 4.2.3.

1. *In the following, since the conservation of the L^1 norm of a weak solution f^ε of (4.1.1) holds, we get that for all $t \in [0, T]$, $\|f^\varepsilon(t, \cdot)\|_{L^1(\mathbb{R}^{d+2})} = \|f_0^\varepsilon\|_{L^1(\mathbb{R}^{d+2})} = 1$.*

2. *It is worth noticing that we do not need the weak solution f^ε of (4.1.1) to be differentiable in space.*

4.2.2 Existence of a solution of the limit system

Our purpose is to prove the existence of a solution to the system (4.1.9). We proceed in two steps: first, we prove the existence and uniqueness of a solution to the FHN reaction-diffusion system (4.1.11), and then we construct a solution to the system (4.1.9) from the solution to (4.1.11). Thus, we start by studying the following Cauchy problem for a given initial data (V_0, W_0):

$$
\begin{cases}
\partial_t V(t, \mathbf{x}) - \sigma \left[\rho_0(\mathbf{x}) \, \Delta_\mathbf{x} V(t, \mathbf{x}) + 2 \nabla_\mathbf{x} \rho_0(\mathbf{x}) \cdot \nabla_\mathbf{x} V(t, \mathbf{x}) \right] = N(V(t, \mathbf{x})) - W(t, \mathbf{x}), \\[2mm]
\partial_t W(t, \mathbf{x}) = A(V(t, \mathbf{x}), W(t, \mathbf{x})), \\[2mm]
V|_{t=0} = V_0, \quad W|_{t=0} = W_0.
\end{cases}
\tag{4.2.4}
$$

Before stating our existence result, we have to precisely define the notion of weak solution to the reaction-diffusion system (4.2.4). Since all the mathematical difficulties come from the first equation in (4.2.4), we consider the second component W as a reaction term.

Definition 4.2.4. *For any $T > 0$ and any given initial data $V_0, W_0 \in H^2(\mathbb{R}^d)$, the pair (V, W) is a weak solution of (4.2.4) on $[0, T]$ with initial data (V_0, W_0) if $V \in L^\infty([0, T], H^2(\mathbb{R}^d)) \cap W^{1,\infty}([0, T], L^2(\mathbb{R}^d))$, and (V, W) verifies for all $\varphi \in H^1(\mathbb{R}^d)$, for all $t \in [0, T]$ and almost every $\mathbf{x} \in \mathbb{R}^d$:*

$$
\begin{cases}
\displaystyle \int \partial_t V \, \varphi \, \mathrm{d}\mathbf{x} = -\sigma \int \rho_0 \, \nabla_\mathbf{x} V \cdot \nabla_\mathbf{x} \varphi \, \mathrm{d}\mathbf{x} + \sigma \int \nabla_\mathbf{x} \rho_0 \cdot \nabla_\mathbf{x} V \, \varphi \, \mathrm{d}\mathbf{x} + \int (N(V) - W) \, \varphi \, \mathrm{d}\mathbf{x}, \\[4mm]
\displaystyle W(t, \mathbf{x}) = e^{-\tau \, b \, t} W_0(\mathbf{x}) + \tau \int_0^t e^{-\tau \, b \, (t-s)} V(s, \mathbf{x}) \, \mathrm{d}s, \\[4mm]
V|_{t=0} = V_0.
\end{cases}
\tag{4.2.5}
$$

Now, we can give the details of our result of existence and uniqueness for the reaction-diffusion system (4.2.4).

Proposition 4.2.5. *Let Ψ be a connectivity kernel satisfying (4.1.5). Consider an initial data ρ_0 such that*

$$
\rho_0 \geq 0, \quad \rho_0 \in \mathscr{C}_b^3(\mathbb{R}^d), \quad \|\rho_0\|_{L^1} = 1,
\tag{4.2.6}
$$

and also consider an initial data (V_0, W_0) such that

$$
V_0, W_0 \in H^2(\mathbb{R}^d).
\tag{4.2.7}
$$

Then, for all $T > 0$, there exists a unique function (V, W) weak solution of the reaction-diffusion equation (4.2.4) on $[0, T]$ in the sense of Definition 4.2.4 such that

$$
V, W \in L^\infty \left([0, T], H^2(\mathbb{R}^d) \right) \cap \mathscr{C}^0 \left([0, T], H^1(\mathbb{R}^d) \right).
$$

We postpone the proof of Proposition 4.2.5 to Section 4.5. Our strategy consists in approximating the reaction-diffusion system (4.2.4) with an uniformly parabolic system, and then to pass to the limit.

It remains to deduce from this proposition the existence of a solution to the limit system (4.1.9). In order to work with a well-defined system on $\mathbb{R}^d$, we make the convention that for all

$\mathbf{x} \in \mathbb{R}^d$ such that $\rho_0(\mathbf{x}) = 0$, $V(\cdot, \mathbf{x}) = 0$ and $F(\cdot, \mathbf{x}, \cdot) = 0$. From a modeling viewpoint, it means that there is no electrical activity wherever there is no neuron. Hence, we are led to study the following Cauchy problem for any given initial data (V_0, F_0), for all $t > 0$, $\mathbf{x} \in \mathbb{R}^d$ and $w \in \mathbb{R}$:

$$
\begin{cases}
\partial_t F \, + \, \partial_w \left(A(V, w) \, F \right) \, = \, 0, \\[2mm]
\partial_t \left(\rho_0 \, V \right) \, - \, \sigma \left[\rho_0 \, \Delta_\mathbf{x} \left(\rho_0 \, V \right) \, - \, \left(\Delta_\mathbf{x} \rho_0 \right) \rho_0 \, V \right] \, = \, \rho_0 \, N(V) \, - \, \rho_0 \, W, \\[2mm]
V(t, \mathbf{x}) \, = \, 0, \quad t > 0 \text{ and } \mathbf{x} \in \mathbb{R}^d \backslash \mathrm{Supp}_{\mathrm{ess}}(\rho_0), \\[2mm]
W(t, \mathbf{x}) \, = \, \begin{cases} \dfrac{1}{\rho_0(\mathbf{x})} \displaystyle\int_\mathbb{R} w \, F(t, \mathbf{x}, \mathrm{d}w) & \text{if } \rho_0(\mathbf{x}) > 0, \\[4mm] 0 & \text{else,} \end{cases} \\[6mm]
V|_{t=0} \, = \, V_0, \quad F|_{t=0} \, = \, F_0, \quad \rho_0(\mathbf{x}) \, = \, \displaystyle\int_\mathbb{R} F_0(\mathbf{x}, w) \, \mathrm{d}w.
\end{cases}
\tag{4.2.8}
$$

To conclude this subsection, we state our notion of solution to the limit system (4.2.8), and then our result of existence and uniqueness of a solution. In the rest of this chapter, we denote by $\mathcal{M}(\mathbb{R}^{d+1})$ the set of non-negative Radon measures on $\mathbb{R}^{d+1}$.

Definition 4.2.6. *For any $T > 0$, and any initial data $V_0 \in H^2(\mathbb{R}^d)$ and $F_0 \in \mathcal{M}(\mathbb{R}^{d+1})$ satisfying*

$$
\int_{\mathbb{R}^{d+1}} |w|^2 \, F_0(\mathrm{d}\mathbf{x}, \mathrm{d}w) \, < \, +\infty, \quad \rho_0 := \int_\mathbb{R} F_0(\cdot, \mathrm{d}w) \in L^1(\mathbb{R}^d),
$$

we say that (V, F) is a solution of (4.2.8) if F is a measure solution of the first equation in (4.1.9), that is for all $\varphi \in \mathscr{C}_c^\infty(\mathbb{R}^{d+1})$, for all $t \in [0, T]$,

$$
\frac{\mathrm{d}}{\mathrm{d}t} \int_{\mathbb{R}^{d+1}} \varphi(\mathbf{x}, w) \, F(t, \mathrm{d}\mathbf{x}, \mathrm{d}w) \, - \, \int_{\mathbb{R}^{d+1}} A(V(t, \mathbf{x}), w) \, \partial_w \varphi \, F(t, \mathrm{d}\mathbf{x}, \mathrm{d}w) \, = \, 0,
\tag{4.2.9}
$$

and $V \in L^\infty([0, T], H^2(\mathbb{R}^d)) \cap W^{1,\infty}([0, T], L^2(\mathbb{R}^d))$ satisfies for all $\varphi \in H^1(\mathbb{R}^d)$ and all $t \in [0, T]$,

$$
\begin{cases}
\displaystyle\int \partial_t(\rho_0 \, V) \, \varphi \, \mathrm{d}\mathbf{x} \, = \, \sigma \int \left[(\rho_0 \, V) \nabla_\mathbf{x} \rho_0 - \rho_0 \, \nabla_\mathbf{x}(\rho_0 \, V) \right] \cdot \nabla_\mathbf{x} \varphi \, \mathrm{d}\mathbf{x} \, + \, \int \rho_0 \, (N(V) - W) \, \varphi \, \mathrm{d}\mathbf{x}, \\[4mm]
W(t, \mathbf{x}) \, = \, \begin{cases} 0 & \text{if } \rho_0(\mathbf{x}) = 0, \\[3mm] \dfrac{1}{\rho_0(\mathbf{x})} \displaystyle\int w \, F(t, \mathbf{x}, \mathrm{d}w) & \text{else,} \end{cases}
\end{cases}
\tag{4.2.10}
$$

Corollary 4.2.7. *Let Ψ be a connectivity kernel satisfying (4.1.5). Consider an initial data (V_0, F_0) such that $F_0 \in \mathcal{M}(\mathbb{R}^{d+1})$ satisfies*

$$
\int |w|^2 \, F_0(\mathrm{d}\mathbf{x}, \mathrm{d}w) \, < \, +\infty,
\tag{4.2.11}
$$

and define for all $\mathbf{x} \in \mathbb{R}^d$,

$$
\rho_0 := \int F_0(\cdot, \mathrm{d}w), \quad W_0(\mathbf{x}) := \begin{cases} \dfrac{1}{\rho_0(\mathbf{x})} \displaystyle\int w \, F_0(\mathbf{x}, \mathrm{d}w), & \text{if } \rho_0(\mathbf{x}) > 0, \\[4mm] 0, & \text{else.} \end{cases}
\tag{4.2.12}
$$

Let us assume that ρ_0 satisfies (4.2.6), (V_0, W_0) *satisfies* (4.2.7), *and that*

$$V_0(\mathbf{x}) = 0 \qquad \text{if } \mathbf{x} \in \mathbb{R}^d \backslash Supp_{ess}(\rho_0). \tag{4.2.13}$$

Then, for all $T > 0$, there exists a unique pair (V, F) solution of the reaction-diffusion equation (4.2.8) *on $[0, T]$ in the sense of Definition 4.2.6 such that*

$$\begin{cases} \rho_0 V \in L^\infty \left([0, T], H^2(\mathbb{R}^d)\right) \cap \mathscr{C}^0 \left([0, T], H^1(\mathbb{R}^d)\right), \\[2mm] F \in L^\infty \left([0, T], \mathcal{M}(\mathbb{R}^{d+1})\right), \end{cases}$$

and such that there exists a constant $C_T > 0$ such that for all $t \in [0, T]$,

$$\int |w|^2 F(t, \mathrm{d}\mathbf{x}, \mathrm{d}w) \leq C_T.$$

We postpone the proof of Corollary 4.2.7 to Section 4.5.

4.2.3   Main result

Now, we can state our main theorem about the asymptotic limit.

Theorem 4.2.8. *Let $T > 0$, and let Ψ be a connectivity kernel satisfying* (4.1.5). *Consider a set of initial data $(f_0^\varepsilon)_{\varepsilon > 0}$ satisfying the assumptions* (4.2.2)-(4.2.3), *and there exists a positive constant $M > 0$ such that*

$$\int \left(1 + \|\mathbf{x}\|^4 + |v|^4 + |w|^4\right) f_0^\varepsilon(\mathbf{x}, v, w) \, \mathrm{d}\mathbf{x} \, \mathrm{d}v \, \mathrm{d}w \leq M, \tag{4.2.14}$$

$$\|\rho_0^\varepsilon\|_{L^\infty(\mathbb{R}^d)} \leq M. \tag{4.2.15}$$

Also consider the initial data (ρ_0, V_0, W_0) satisfying the assumptions (4.2.6)-(4.2.7) *such that $\rho_0 \in H^2(\mathbb{R}^d)$, and verifying:*

$$\frac{1}{\varepsilon^2} \|\rho_0^\varepsilon - \rho_0\|_{L^2(\mathbb{R}^d)} \longrightarrow 0, \tag{4.2.16}$$

$$\int \rho_0^\varepsilon(\mathbf{x}) \left[|V_0^\varepsilon(\mathbf{x}) - V_0(\mathbf{x})|^2 + |W_0^\varepsilon(\mathbf{x}) - W_0(\mathbf{x})|^2\right] \mathrm{d}\mathbf{x} \longrightarrow 0 \tag{4.2.17}$$

as $\varepsilon \to 0$. Consider (V, W) the weak solution of the reaction-diffusion equation (4.2.4) *on $[0, T]$ provided by Proposition 4.2.5. For any $\varepsilon > 0$, let f^ε be the weak solution of the transport equation* (4.1.1) *on $[0, T]$ provided by Proposition 4.2.2. Then, for all $\varepsilon > 0$, the macroscopic functions $(\rho_0^\varepsilon, V^\varepsilon, W^\varepsilon)$ computed from f^ε satisfy*

$$\lim_{\varepsilon \to 0} \sup_{t \in [0, T]} \int \rho_0^\varepsilon(\mathbf{x}) \left[|V^\varepsilon(t, \mathbf{x}) - V(t, \mathbf{x})|^2 + |W^\varepsilon(t, \mathbf{x}) - W(t, \mathbf{x})|^2\right] \mathrm{d}\mathbf{x} = 0. \tag{4.2.18}$$

Moreover, assume that there exists a measure $F_0 \in \mathcal{M}(\mathbb{R}^{d+1})$ satisfying (4.2.11)-(4.2.13). *Further consider $(F_0^\varepsilon)_{\varepsilon > 0}$ the functions defined for all $\varepsilon > 0$, $(\mathbf{x}, w) \in \mathbb{R}^{d+1}$, with*

$$F_0^\varepsilon(\mathbf{x}, w) := \int_{\mathbb{R}} f_0^\varepsilon(\mathbf{x}, v, w) \, \mathrm{d}v.$$

Therefore, if $F_0^\varepsilon \rightharpoonup F_0$ weakly-$\star$ in $\mathcal{M}(\mathbb{R}^{d+1})$, then we have for all $\varphi \in \mathscr{C}_b^0(\mathbb{R}^{d+2})$,

$$\iint \varphi(\mathbf{x}, v, w) \, f^\varepsilon(t, \mathbf{x}, v, w) \, \mathrm{d}\mathbf{x} \, \mathrm{d}v \, \mathrm{d}w \longrightarrow \int \varphi(\mathbf{x}, V(t, \mathbf{x}), w) \, F(t, \mathbf{x}, w) \, \mathrm{d}\mathbf{x}, \tag{4.2.19}$$

strongly in $L_{loc}^1(0, T)$ as $\varepsilon \to 0$, where (V, F) is the solution of (4.1.9) *provided by Corollary 4.2.7.*

The proof is postponed to Section 4.4. Our approach is similar to the work done in [49]. To show that the relative entropy vanishes as ε goes to 0, we encounter some difficulties, coming from the reaction term $\partial_v(f^\varepsilon N(v))$, which makes appear some moments of f^ε of order higher than 2 that we need to control, and from the fact that V^ε and W^ε are not *a priori* differentiable in space, and not uniformly bounded. We circumvent these issues with an *a priori* dissipation estimate, detailed in Section 4.3.

Remark 4.2.9. *We can further precise that the convergence of the estimate* (4.2.18) *is of order* $\varepsilon^{2/(d+6)}$ *with further assumptions on the initial conditions. More precisely, we need to replace the assumption* (4.2.16) *with*

$$\|\rho_0^\varepsilon - \rho_0\|_{L^2(\mathbb{R}^d)} \leq C\, \varepsilon^{2+1/(d+6)},$$

to assume that the convergence of the initial conditions in (4.2.17) *is of rate* $\varepsilon^{2/(d+6)}$, *and to suppose some additional regularity of* (ρ_0, V_0, W_0) *so that* $\rho_0\, V, \rho_0\, W \in L^\infty([0,T], H^4(\mathbb{R}^d))$.

4.3 *A priori* estimates for the transport equation

In this section, we prove an *a priori* estimate of the moments of a solution of (4.1.1), in order to estimate a dissipation. First of all, we define for all $i \in \mathbb{N}$ and $u \in \{v, w\}$ the moment of order i in u of f^ε, denoted by $\mathbf{u}_i^u$, and the moment of order i in $\mathbf{x}$ of f^ε, denoted by $\mathbf{u}_i^\mathbf{x}$, with

$$\mathbf{u}_i^u(t) := \int_{\mathbb{R}^{d+1}} |u|^i\, f^\varepsilon(t, \mathbf{x}, v, w)\, \mathrm{d}\mathbf{x}\, \mathrm{d}v\, \mathrm{d}w\,, \quad \mathbf{u}_i^\mathbf{x}(t) := \int_{\mathbb{R}^{d+1}} \|\mathbf{x}\|^i\, f^\varepsilon(t, \mathbf{x}, v, w)\, \mathrm{d}\mathbf{x}\, \mathrm{d}v\, \mathrm{d}w.$$

We also define for all $\varepsilon > 0$ and for all $p \geq 1$ the dissipation

$$\mathcal{D}_p : t \mapsto \frac{1}{2}\, \frac{1}{\varepsilon^d} \iint \Psi\left(\frac{\|\mathbf{x} - \mathbf{x}'\|}{\varepsilon}\right) (v^{2p-1} - v'^{2p-1})\,(v - v')\, f^\varepsilon(t, \mathbf{z}')\, f^\varepsilon(t, \mathbf{z})\, \mathrm{d}\mathbf{z}'\, \mathrm{d}\mathbf{z} \geq 0, \quad (4.3.1)$$

using the notation $\mathbf{z} = (\mathbf{x}, v, w) \in \mathbb{R}^{d+2}$. In the following, let $T > 0$, and $\varepsilon > 0$ and suppose that there exists f^ε a well-defined solution of (4.1.1) on $[0, T]$.

Proposition 4.3.1. *Consider* f^ε *a weak solution of the transport equation* (4.1.1) *on* $[0, T]$ *provided by Proposition 4.2.2. Assume that there exists* $p^* \in \mathbb{N}$ *such that*

$$\mathbf{u}_{2p^*}^v(0) + \mathbf{u}_{2p^*}^w(0) < +\infty. \quad (4.3.2)$$

Then, for all $1 \leq p \leq p^*$, *there exists a constant* C_p *which depends on* p *such that for all* $t \in [0, T]$, *we have:*

$$\frac{1}{2p}\, \frac{\mathrm{d}}{\mathrm{d}t}\left(\mathbf{u}_{2p}^v(t) + \mathbf{u}_{2p}^w(t)\right) + \kappa_1'\, \mathbf{u}_{2(p+1)}^v(t) + \frac{1}{\varepsilon^2}\, \mathcal{D}_p(t) \leq C_p\left(\mathbf{u}_{2p}^v(t) + \mathbf{u}_{2p}^w(t)\right), \quad (4.3.3)$$

where $\kappa_1' > 0$ *is the positive constant defined in* (4.1.3).

Proof. Let $t \in [0, T]$. In the rest of this proof, we use the notation $\mathbf{u} = (v, w) \in \mathbb{R}^2$ and $\mathbf{z} = (\mathbf{x}, \mathbf{u}) \in \mathbb{R}^{d+2}$. Since f^ε is a solution of the transport equation (4.1.1), we have:

$$\frac{1}{2p}\, \frac{\mathrm{d}}{\mathrm{d}t}\left(\mathbf{u}_{2p}^v(t) + \mathbf{u}_{2p}^w(t)\right) = I_1 + I_2,$$

where

$$
\begin{cases}
I_1 := \displaystyle\int_{\mathbb{R}^{d+2}} v^{2p-1}\,(N(v)-w)\,f^\varepsilon(t,\mathbf{z})\,\mathrm{d}\mathbf{z} \;+\; \int_{\mathbb{R}^{d+2}} w^{2p-1}\,A(v,w)\,f^\varepsilon(t,\mathbf{z})\,\mathrm{d}\mathbf{z},\\[3mm]
I_2 := \dfrac{1}{\varepsilon^{d+2}} \displaystyle\iint \Psi\left(\dfrac{\|\mathbf{x}-\mathbf{x}'\|}{\varepsilon}\right) v^{2p-1}\,(v'-v)\,f^\varepsilon(t,\mathbf{z}')\,f^\varepsilon(t,\mathbf{z})\,\mathrm{d}\mathbf{z}'\,\mathrm{d}\mathbf{z}.
\end{cases}
$$

First of all, using Young's inequality and the properties of N given in (4.1.3), we treat the first term I_1 as follows:

$$
\begin{aligned}
I_1 &\leq \int \left(\kappa_1\, v^{2p} - \kappa_1'\, v^{2p+2} + \frac{2p-1}{2p} v^{2p} + \frac{1}{2p} w^{2p} \right) f^\varepsilon(t,\mathbf{z})\,\mathrm{d}\mathbf{z}\\
&\quad + \tau \int \left(\frac{2p-1}{p} w^{2p} + \frac{1}{2p} v^{2p} - b\,w^{2p} \right) f^\varepsilon(t,\mathbf{z})\,\mathrm{d}\mathbf{z}\\
&= \frac{2p(1+\kappa_1)+\tau-1}{2p}\, \mathbf{u}_{2p}^v(t) + \frac{4\tau p - 2\tau + 1}{2p}\, \mathbf{u}_{2p}^w(t) - \kappa_1'\, \mathbf{u}_{2p+2}^v(t).
\end{aligned}
$$

Then, to deal with the second term I_2, we reformulate it using the symmetry of Ψ. Indeed, we have:

$$
\begin{aligned}
I_2 &= -\frac{1}{2}\frac{1}{\varepsilon^{d+2}} \iint \Psi\left(\frac{\|\mathbf{x}-\mathbf{x}'\|}{\varepsilon}\right) \left(v^{2p-1}-v'^{2p-1}\right)(v-v')\,f^\varepsilon(t,\mathbf{z}')\,f^\varepsilon(t,\mathbf{z})\,\mathrm{d}\mathbf{z}'\,\mathrm{d}\mathbf{z}\\
&= -\frac{1}{\varepsilon^2}\,\mathcal{D}_p(t).
\end{aligned}
$$

This enables us to conclude that there exists a constant $C_p > 0$ such that for all $t \in [0,T]$,

$$
\frac{1}{2p}\frac{\mathrm{d}}{\mathrm{d}t}\left(\mathbf{u}_{2p}^v(t) + \mathbf{u}_{2p}^w(t)\right) \leq C_p\left(\mathbf{u}_{2p}^v(t) + \mathbf{u}_{2p}^w(t)\right) - \kappa_1'\mathbf{u}_{2(p+1)}^v(t) - \frac{1}{\varepsilon^2}\mathcal{D}_p(t).
$$

$\square$

Corollary 4.3.2. *Under the same assumptions than in Proposition 4.3.1 with $p^* = 2$, if we assume that for all $\varepsilon > 0$, (4.2.14) is satisfied, then there exists a constant $C_T > 0$ such that for all $k \in [0,4]$, for all $\varepsilon > 0$ and for all $t \in [0,T]$,*

$$
\begin{cases}
\mathbf{u}_k^v(t) + \mathbf{u}_k^w(t) + \mathbf{u}_k^{\mathbf{x}}(t) \leq C_T,\\[3mm]
\displaystyle\int_0^T \mathbf{u}_{k+2}^v(t)\,\mathrm{d}t \leq C_T.
\end{cases}
\tag{4.3.4}
$$

Proof. This result is a direct consequence of Proposition 4.3.1, integrating the inequality (4.3.3) between 0 and t. $\square$

Now, let us estimate the dissipation $\mathcal{D}_1$ as defined in (4.3.1). Let $\varepsilon > 0$. Under the same assumptions as in Proposition 4.3.1 with $p^* = 1$, there exists a constant C_T such that:

Corollary 4.3.3. *Let $\varepsilon > 0$. Under the same assumptions as in Proposition 4.3.1 with $p^* = 1$, there exists a constant C_T such that:*

$$
\int_0^T \mathcal{D}_1(t)\,\mathrm{d}t = \frac{1}{2}\frac{1}{\varepsilon^d}\int_0^T \iint \Psi\left(\frac{\|\mathbf{x}-\mathbf{x}'\|}{\varepsilon}\right)|v-v'|^2\,f^\varepsilon(t,\mathbf{z})\,f^\varepsilon(t,\mathbf{z}')\,\mathrm{d}\mathbf{z}\,\mathrm{d}\mathbf{z}'\,\mathrm{d}t \leq C_T\,\varepsilon^2. \tag{4.3.5}
$$

Proof. This dissipation estimate comes from the inequality (4.3.3) with $p = 1$. Indeed, integrating between 0 and T, we get that

$$\frac{1}{\varepsilon^2} \int_0^T \mathcal{D}_1(t) \, \mathrm{d}t \ \leq \ C \int_0^T \left(\mathbf{u}_2^v(t) \, + \, \mathbf{u}_2^w(t) \right) \, \mathrm{d}t \, + \, \mathbf{u}_2^v(0) \, + \, \mathbf{u}_2^w(0).$$

We conclude using the moment estimate from Corollary 4.3.2. $\qquad\square$

It turns ou that this result is not enough to conclude the proof of Theorem 4.2.8. Actually, we need to remove the weight $\Psi_\varepsilon(\| \cdot \|) \star_{\mathbf{x}} \rho_0^\varepsilon$ in the integrand of the previous estimate. In the following, we use the shorthand notation $\Psi_\varepsilon \star_{\mathbf{x}} \rho_0^\varepsilon$.

Proposition 4.3.4. *Let $\varepsilon > 0$. We make the same assumptions than in Proposition 4.3.1 with $p^\star = 2$, and we further assume that there exists a function $\rho_0 \in H^2(\mathbb{R}^d)$ such that for all $\varepsilon > 0$ small enough,*

$$\| \rho_0^\varepsilon - \rho_0 \|_{L^2(\mathbb{R}^d)} \ \leq \ C \, \varepsilon^2, \tag{4.3.6}$$

for some positive constant $C > 0$. Then, there exists a constant C_T such that for all $t \in [0, T]$, we have:

$$\int_0^T \int_{\mathbb{R}^{d+2}} f^\varepsilon(t, \mathbf{x}, v, w) \, |v - V^\varepsilon(t, \mathbf{x})|^2 \, \mathrm{d}\mathbf{x} \, \mathrm{d}v \, \mathrm{d}w \ \leq \ C_T \, \varepsilon^{4/(d+6)}. \tag{4.3.7}$$

Proof. Let $\varepsilon > 0$ and $T > 0$. We define the integral

$$I_\varepsilon \ := \ \int_0^T \int_{\mathbb{R}^{d+2}} f^\varepsilon(t, \mathbf{x}, v, w) \, |v - V^\varepsilon(t, \mathbf{x})|^2 \, \mathrm{d}\mathbf{x} \, \mathrm{d}v \, \mathrm{d}w \, \mathrm{d}t.$$

Using the definition of V^ε, let us notice that for all $t \in [0, T]$ and all $\mathbf{x} \in \mathbb{R}^d$,

$$\int_{\mathbb{R}^2} f^\varepsilon(t, \mathbf{x}, v, w) \, |v - V^\varepsilon(t, \mathbf{x})|^2 \, \mathrm{d}v \, \mathrm{d}w \ = \ \int_{\mathbb{R}^2} f^\varepsilon(t, \mathbf{x}, v, w) \, |v|^2 \, \mathrm{d}v \, \mathrm{d}w \, - \, \rho_0^\varepsilon(\mathbf{x}) \, |V^\varepsilon(t, \mathbf{x})|^2 \, .$$

In the rest of this proof, we use the notation $\mathbf{z} = (\mathbf{x}, v, w) \in \mathbb{R}^{d+2}$. First of all, we restrict our analysis to the nontrivial case $\rho_0^\varepsilon \not\equiv 0$. Since $\Psi > 0$ almost everywhere and $\rho_0^\varepsilon \geq 0$, we get that for all $\mathbf{x} \in \mathbb{R}^d$, $\Psi_\varepsilon \star_{\mathbf{x}} \rho_0^\varepsilon(\mathbf{x}) > 0$. Our strategy to estimate I_ε consists in dividing the set of integration into subsets on which the integrand is easier to control. Let $\eta > 0$ be a constant depending on ε to be determined later. We define:

$$\begin{cases} \mathcal{A}_\varepsilon^\eta \ := \ \left\{ \mathbf{x} \in \mathbb{R}^d, \, \Psi_\varepsilon \star_{\mathbf{x}} \rho_0^\varepsilon(\mathbf{x}) \, \geq \, \eta \right\}, \\[2mm] \mathcal{B}_\varepsilon^\eta \ := \ \left\{ \mathbf{x} \in \mathbb{R}^d, \, 0 < \Psi_\varepsilon \star_{\mathbf{x}} \rho_0^\varepsilon(\mathbf{x}) \, < \, \eta \right\}, \end{cases}$$

and hence $\mathbb{R}^d = \mathcal{A}_\varepsilon^\eta \cup \mathcal{B}_\varepsilon^\eta$. Then, we have that

$$
\int_0^T \iint_{\mathcal{A}_\varepsilon^\eta \times \mathbb{R}^2} f^\varepsilon \, |v - V^\varepsilon|^2 \, \mathrm{d}\mathbf{z} \, \mathrm{d}t \le \frac{1}{\eta} \int_0^T \iint_{\mathcal{A}_\varepsilon^\eta \times \mathbb{R}^2} f^\varepsilon \, |v - V^\varepsilon|^2 \, \Psi_\varepsilon \star_\mathbf{x} \rho_0^\varepsilon(\mathbf{x}) \, \mathrm{d}\mathbf{z} \, \mathrm{d}t
$$

$$
= \frac{1}{\eta} \int_0^T \iint_{\mathcal{A}_\varepsilon^\eta \times \mathbb{R}^2} f^\varepsilon \, |v|^2 \, \Psi_\varepsilon \star_\mathbf{x} \rho_0^\varepsilon(\mathbf{x}) \, \mathrm{d}\mathbf{z} \, \mathrm{d}t \; - \; \frac{1}{\eta} \int_0^T \int_{\mathcal{A}_\varepsilon^\eta} \rho_0^\varepsilon \, |V^\varepsilon|^2 \, \Psi_\varepsilon \star_\mathbf{x} \rho_0^\varepsilon(\mathbf{x}) \, \mathrm{d}\mathbf{x} \, \mathrm{d}t
$$

$$
= \frac{1}{\eta} \int_0^T \iint_{\mathcal{A}_\varepsilon^\eta \times \mathbb{R}^2} f^\varepsilon \, |v|^2 \, \Psi_\varepsilon \star_\mathbf{x} \rho_0^\varepsilon(\mathbf{x}) \, \mathrm{d}\mathbf{z} \, \mathrm{d}t \; - \; \frac{1}{\eta} \int_0^T \int_{\mathcal{A}_\varepsilon^\eta} \rho_0^\varepsilon \, V^\varepsilon \, \Psi_\varepsilon \star_\mathbf{x} [\rho_0^\varepsilon \, V^\varepsilon](\mathbf{x}) \, \mathrm{d}\mathbf{x} \, \mathrm{d}t
$$

$$
+ \frac{1}{\eta} \int_0^T \iint_{\mathcal{A}_\varepsilon^\eta \times \mathbb{R}^2} \rho_0^\varepsilon \, V^\varepsilon \, \Psi_\varepsilon \star_\mathbf{x} [\rho_0^\varepsilon \, V^\varepsilon](\mathbf{x}) \, \mathrm{d}\mathbf{z} \, \mathrm{d}t \; - \; \frac{1}{\eta} \int_0^T \int_{\mathcal{A}_\varepsilon^\eta} \rho_0^\varepsilon \, |V^\varepsilon|^2 \, \Psi_\varepsilon \star_\mathbf{x} \rho_0^\varepsilon(\mathbf{x}) \, \mathrm{d}\mathbf{x} \, \mathrm{d}t
$$

$$
= \frac{1}{\eta} \frac{1}{\varepsilon^d} \frac{1}{2} \int_0^T \iint \Psi\left(\frac{\|\mathbf{x} - \mathbf{x}'\|}{\varepsilon} \right) |v - v'|^2 \, f^\varepsilon(t, \mathbf{z}) \, f^\varepsilon(t, \mathbf{z}') \, \mathrm{d}\mathbf{z}' \, \mathrm{d}\mathbf{z} \, \mathrm{d}t
$$

$$
- \frac{1}{\eta} \frac{1}{\varepsilon^d} \frac{1}{2} \int_0^T \iint \Psi\left(\frac{\|\mathbf{x} - \mathbf{x}'\|}{\varepsilon} \right) |V^\varepsilon(t, \mathbf{x}) - V^\varepsilon(t, \mathbf{x}')|^2 \, \rho_0^\varepsilon(\mathbf{x}) \, \rho_0^\varepsilon(\mathbf{x}') \, \mathrm{d}\mathbf{x}' \, \mathrm{d}\mathbf{x} \, \mathrm{d}t
$$

$$
\le \frac{1}{\eta} \int_0^T \mathcal{D}_1(t) \, \mathrm{d}t,
$$

where $\mathcal{D}_1$ is defined in (4.3.1). Consequently, using Corollary 4.3.3, we conclude that there exists a positive constant $C_T > 0$ such that

$$
\int_0^T \iint_{\mathcal{A}_\varepsilon^\eta \times \mathbb{R}^2} f^\varepsilon \, |v - V^\varepsilon|^2 \, \mathrm{d}\mathbf{z} \, \mathrm{d}t \; \le \; C_T \, \frac{\varepsilon^2}{\eta}. \tag{4.3.8}
$$

Then, it remains to estimate

$$
\int_0^T \iint_{\mathcal{B}_\varepsilon^\eta \times \mathbb{R}^2} f^\varepsilon \, |v - V^\varepsilon|^2 \, \mathrm{d}\mathbf{z} \, \mathrm{d}t \; \le \; \int_0^T \iint_{\mathcal{B}_\varepsilon^\eta \times \mathbb{R}^2} f^\varepsilon \, |v|^2 \, \mathrm{d}\mathbf{z} \, \mathrm{d}t \; = \; I_1 + I_2 + I_3,
$$

where

$$
\begin{cases}
I_1 := \displaystyle \int_0^T \int_{\mathcal{B}_\varepsilon^\eta} \int_{\{|v|>R\}} f^\varepsilon \, |v|^2 \, \mathrm{d}\mathbf{z} \, \mathrm{d}t, \\[2ex]
I_2 := \displaystyle \int_0^T \int_{\mathcal{B}_\varepsilon^\eta \cap B^c(0,R)} \int_{\{|v| \le R\}} f^\varepsilon \, |v|^2 \, \mathrm{d}\mathbf{z} \, \mathrm{d}t, \\[2ex]
I_3 := \displaystyle \int_0^T \int_{\mathcal{B}_\varepsilon^\eta \cap B(0,R)} \int_{\{|v| \le R\}} f^\varepsilon \, |v|^2 \, \mathrm{d}\mathbf{z} \, \mathrm{d}t,
\end{cases}
$$

where $R > 0$ is a constant depending on η and ε to be determined later. For $k > 2$, we get that

$$
I_1 \; \le \; \frac{1}{R^{k-2}} \int_0^T \int_{\mathcal{B}_\varepsilon^\eta} \int_{\{|v|>R\}} f^\varepsilon \, |v|^k \, \mathrm{d}\mathbf{z} \, \mathrm{d}t \; \le \; \frac{1}{R^{k-2}} \int_0^T \mathbf{u}_k^v(t) \, \mathrm{d}t.
$$

Then, for $q > 2$, we also have that

$$
I_2 \; \le \; \int_0^T \int f^\varepsilon \, R^2 \, \frac{|\mathbf{x}|^q}{R^q} \, \mathrm{d}\mathbf{z} \, \mathrm{d}t \; \le \; \frac{1}{R^{q-2}} \int_0^T \mathbf{u}_q^\mathbf{x}(t) \, \mathrm{d}t.
$$

As for the last term, we compute:

$$I_3 \leq R^2 \int_0^T \int_{\mathcal{B}_\varepsilon^\eta \cap B(0,R)} \rho_0^\varepsilon(\mathbf{x}) \, \mathrm{d}\mathbf{x} \, \mathrm{d}t$$

$$\leq R^2 \int_0^T \int_{\mathcal{B}_\varepsilon^\eta \cap B(0,R)} \Psi_\varepsilon \star \rho_0^\varepsilon(\mathbf{x}) \, \mathrm{d}\mathbf{x} \, \mathrm{d}t \; + \; R^2 \int_0^T \int_{\mathcal{B}_\varepsilon^\eta \cap B(0,R)} |\rho_0^\varepsilon(\mathbf{x}) - \Psi_\varepsilon \star \rho_0^\varepsilon(\mathbf{x})| \, \mathrm{d}\mathbf{x} \, \mathrm{d}t$$

$$\leq C \, T \, R^{d+2} \, \eta \; + \; R^2 \, T \left(\int_{\mathcal{B}_\varepsilon^\eta \cap B(0,R)} 1 \, \mathrm{d}\mathbf{x} \right)^{1/2} \|\rho_0^\varepsilon - \Psi_\varepsilon \star \rho_0^\varepsilon\|_{L^2(\mathbb{R}^d)}$$

$$\leq C \, T \, R^{d+2} \, \eta \; + \; C^{1/2} \, T \, R^{2+d/2} \|\rho_0^\varepsilon - \Psi_\varepsilon \star \rho_0^\varepsilon\|_{L^2(\mathbb{R}^d)}.$$

Then, using Young's inequality, we notice that

$$\|\rho_0^\varepsilon - \Psi_\varepsilon \star \rho_0^\varepsilon\|_{L^2(\mathbb{R}^d)} \leq \|\rho_0^\varepsilon - \rho_0\|_{L^2(\mathbb{R}^d)} \; + \; \|\rho_0 - \Psi_\varepsilon \star \rho_0\|_{L^2(\mathbb{R}^d)} \; + \; \|\Psi_\varepsilon \star (\rho_0^\varepsilon - \rho_0)\|_{L^2(\mathbb{R}^d)}$$

$$\leq (1 + \|\Psi_\varepsilon\|_{L^1(\mathbb{R}^d)}) \, \|\rho_0^\varepsilon - \rho_0\|_{L^2(\mathbb{R}^d)} \; + \; \|\rho_0 - \Psi_\varepsilon \star \rho_0\|_{L^2(\mathbb{R}^d)}$$

$$\leq 2 \, \|\rho_0^\varepsilon - \rho_0\|_{L^2(\mathbb{R}^d)} \; + \; \|\rho_0 - \Psi_\varepsilon \star \rho_0\|_{L^2(\mathbb{R}^d)}.$$

On the one hand, we have assumed that the initial data satisfies the estimate (4.3.6). On the other hand, we can estimate $\|\rho_0 - \Psi_\varepsilon \star \rho_0\|_{L^2(\mathbb{R}^d)}$ with similar arguments as in [7]. Indeed, using the change of variable $\mathbf{y} = (\mathbf{x} - \mathbf{x}')/\varepsilon$ and a Taylor expansion, we get that

$$\|\rho_0 - \Psi_\varepsilon \star \rho_0\|_{L^2(\mathbb{R}^d)}^2 \leq \int \left| \frac{1}{\varepsilon^d} \int \Psi\left(\frac{\mathbf{x} - \mathbf{x}'}{\varepsilon} \right) (\rho_0(\mathbf{x}') - \rho_0(\mathbf{x})) \, \mathrm{d}\mathbf{x}' \right|^2 \mathrm{d}\mathbf{x}$$

$$\leq \int \left| \int \Psi(\mathbf{y}) \, (\rho_0(\mathbf{x} - \varepsilon\mathbf{y}) - \rho_0(\mathbf{x})) \, \mathrm{d}\mathbf{y} \right|^2 \mathrm{d}\mathbf{x}$$

$$\leq \varepsilon^4 \int \left| \int \Psi(\mathbf{y}) \int_0^1 (1 - s) \, \mathbf{y}^T \cdot \nabla_{\mathbf{x}}^2 \rho_0(\mathbf{x} - \varepsilon s \mathbf{y}) \cdot \mathbf{y} \, \mathrm{d}s \, \mathrm{d}\mathbf{y} \right|^2 \mathrm{d}\mathbf{x}.$$

Furthermore, using Cauchy-Schwarz inequality for the integral in s and then for the integral in $\mathbf{y}$, we get

$$\|\rho_0 - \Psi_\varepsilon \star \rho_0\|_{L^2(\mathbb{R}^d)}^2$$

$$\leq \varepsilon^4 \int \left| \int \Psi(\mathbf{y}) \left(\int_0^1 |1 - s| \|\mathbf{y}\|^2 \, \mathrm{d}s \right)^{1/2} \left(\int_0^1 |1 - s| \|\mathbf{y}\|^2 \, \|\nabla_{\mathbf{x}}^2 \rho_0(\mathbf{x} - \varepsilon s \mathbf{y})\|^2 \mathrm{d}s \right)^{1/2} \mathrm{d}\mathbf{y} \right|^2 \mathrm{d}\mathbf{x}$$

$$\leq \varepsilon^4 \int \left(\int \Psi(\|\mathbf{y}\|) \frac{\|\mathbf{y}\|^2}{2} \, \mathrm{d}\mathbf{y} \right) \left(\int \Psi(\|\mathbf{y}\|) \int_0^1 |1 - s| \|\mathbf{y}\|^2 \, \|\nabla_{\mathbf{x}}^2 \rho_0(\mathbf{x} - \varepsilon s \mathbf{y})\|^2 \mathrm{d}s \, \mathrm{d}\mathbf{y} \right) \mathrm{d}\mathbf{x}$$

Consequently,

$$\|\rho_0 - \Psi_\varepsilon \star \rho_0\|_{L^2(\mathbb{R}^d)}^2 \leq \sigma \, \varepsilon^4 \int \Psi(\|\mathbf{y}\|) \int_0^1 |1 - s| \|\mathbf{y}\|^2 \int \|\nabla_{\mathbf{x}}^2 \rho_0(\mathbf{x} - \varepsilon s \mathbf{y})\|^2 \, \mathrm{d}\mathbf{x} \, \mathrm{d}s \, \mathrm{d}\mathbf{y}$$

$$\leq \sigma^2 \, \|\rho_0\|_{H^2(\mathbb{R}^d)}^2 \, \varepsilon^4.$$

Finally, we get that there exists a positive constant $C > 0$ such that

$$I_3 \leq C \, T \left(R^{d+2} \eta \; + \; R^{(d+4)/2} \varepsilon^2 \right). \tag{4.3.9}$$

Finally, using the moment estimates, and the estimate (4.3.8), we get that there exists a positive constant C_T such that

$$I_\varepsilon \leq C_T \left(\frac{\varepsilon^2}{\eta} \; + \; R^{d+2} \eta \; + \; R^{(d+4)/2} \varepsilon^2 \; + \; \frac{1}{R^{k-2}} \; + \; \frac{1}{R^{q-2}} \right). \tag{4.3.10}$$

It remains to optimize the values of η and R. For the sake of simplicity, we choose $k = q = 4$. We consider $R = \eta^{-1/(d+4)}$, so that

$$R^{d+2}\eta = \frac{1}{R^2}.$$

Then, we take $\eta = \varepsilon^{2(d+4)/(d+6)}$, so that

$$R^{d+2}\eta = \frac{\varepsilon^2}{\eta} = \varepsilon^{4/(d+6)}.$$

This leads to

$$I_\varepsilon \leq C_T \left(\varepsilon^{4/(d+6)} + \varepsilon^{(d+8)/(d+6)} \right) \leq \widetilde{C}_T \, \varepsilon^{4/(d+6)}, \qquad (4.3.11)$$

for a positive constant $\widetilde{C}_T > 0$ and $\varepsilon > 0$ small enough. $\qquad \square$

4.4 Proof of Theorem 4.2.8

Our proof of Theorem 4.2.8 relies on a relative entropy argument, as developed in [20]. This leads to estimate the distance between the macroscopic functions derived from the solution of the transport equation (4.1.1), and the solution of the limit system (4.1.9). First, we introduce the notion of relative entropy we use in this chapter. Then, we prove that it converges to 0 as ε goes to 0. Finally, we explain how this argument enables us to prove Theorem 4.2.8.

In the rest of this chapter, for any given $\varepsilon > 0$ and for $\rho : \mathbb{R}^d \to \mathbb{R}$ and $V : (0, \infty) \times \mathbb{R}^d \to \mathbb{R}$ regular enough, we define the following local and nonlocal differential operators:

$$\begin{cases} \mathcal{L}_\rho(V) := \sigma\left[\Delta_{\mathbf{x}}(\rho V) - \Delta_{\mathbf{x}}\rho \, V\right] = \sigma\left[\rho \, \Delta_{\mathbf{x}} V + 2 \, \nabla_{\mathbf{x}}\rho \cdot \nabla_{\mathbf{x}} V\right], \\[2mm] \mathscr{L}_\rho(V) := \Psi_\varepsilon \star_{\mathbf{x}} [\rho V] - [\Psi_\varepsilon \star_{\mathbf{x}} \rho] \, V \\[1mm] \qquad\quad = \frac{1}{\varepsilon^{d+2}} \iint \Psi\left(\frac{\|\mathbf{x} - \mathbf{x}'\|}{\varepsilon}\right) \left(V(t, \mathbf{x}') - V(t, \mathbf{x})\right) \rho(\mathbf{x}') \, \mathrm{d}\mathbf{x}', \end{cases} \qquad (4.4.1)$$

respectively defined on $H^2(\mathbb{R}^d)$ and $L^\infty(\mathbb{R}^d)$.

4.4.1 Definition of relative entropy

Consider $\mathcal{Z}^\varepsilon = (\rho_0^\varepsilon, \rho_0^\varepsilon V^\varepsilon, \rho_0^\varepsilon W^\varepsilon)$ the triple of macroscopic quantities computes from f^ε the solution to the transport equation (4.1.1), and $\mathcal{Z} = (\rho_0, \rho_0 V, \rho_0 W)$ the solution of the reaction-diffusion equation (4.1.10). Then, similarly as in Chapter 3, we define the relative entropy between $\mathcal{Z}^\varepsilon$ and $\mathcal{Z}$ through:

$$\eta\left(\mathcal{Z}^\varepsilon \,|\, \mathcal{Z}\right) := \rho_0^\varepsilon \, \frac{|V - V^\varepsilon|^2 + |W - W^\varepsilon|^2}{2}. \qquad (4.4.2)$$

4.4.2 relative entropy estimate

This subsection is devoted to the proof of the relative entropy estimate (4.2.18) under the same assumptions as in Theorem 4.2.8. For all $\varepsilon > 0$, let f^ε be the solution of the transport equation (4.1.1). According to Corollary 4.3.2, we know that for all $t \in [0, T]$, the moment of order 4 of $f^\varepsilon(t)$ is uniformly bounded with respect to $\varepsilon > 0$. Therefore, using Hölder's inequality, we obtain that for all $\mathbf{x} \in \mathbb{R}^d$ such that $\rho_0^\varepsilon(\mathbf{x}) > 0$ and for all $t \in [0, T]$,

$$\begin{aligned} \rho_0^\varepsilon(\mathbf{x}) \, |V^\varepsilon(t, \mathbf{x})|^4 &= \frac{1}{|\rho_0^\varepsilon(\mathbf{x})|^3} \left(\int v \, f^\varepsilon(t, \mathbf{x}, v, w) \, \mathrm{d}v \, \mathrm{d}w \right)^4 \\ &\leq \int |v|^4 \, f^\varepsilon(t, \mathbf{x}, v, w) \, \mathrm{d}v \mathrm{d}w. \end{aligned} \qquad (4.4.3)$$

This last inequality (4.4.3) remains true where $\rho_0^\varepsilon(\mathbf{x}) = 0$ and with W^ε instead of V^ε. Consequently, since $\|\rho_0^\varepsilon\|_{L^1(\mathbb{R}^d)} = 1$, we get that for any $0 \le p \le 4$ and for all $t \in [0, T]$,

$$\rho_0^\varepsilon \left(|V^\varepsilon(t)|^p + |W^\varepsilon(t)|^p \right) \in L^1(\mathbb{R}^d).$$

Let (V, W) be the weak solution of the reaction-diffusion system (4.2.4) provided by Proposition 4.2.5. In the following, we consider the triples $\mathcal{Z}^\varepsilon$ and $\mathcal{Z}$ as defined in Subsection 4.4.1. Since V and W are in $W^{1,\infty}([0, T], L^2(\mathbb{R}^d))$ by definition, for all $t \in [0, T]$, we can compute :

$$
\begin{aligned}
\int_{\mathbb{R}^d} \eta\left(\mathcal{Z}^\varepsilon \mid \mathcal{Z}\right)(t, \mathbf{x})\, \mathrm{d}\mathbf{x} ={}& \int_{\mathbb{R}^d} \eta\left(\mathcal{Z}^\varepsilon \mid \mathcal{Z}\right)(0, \mathbf{x})\, \mathrm{d}\mathbf{x} \\
&+ \int_0^t \int (V^\varepsilon - V)\left(\partial_t(\rho_0^\varepsilon V^\varepsilon) - \rho_0^\varepsilon \partial_t V\right) \mathrm{d}\mathbf{x}\, \mathrm{d}s \\
&+ \int_0^t \int (W^\varepsilon - W)\left(\partial_t(\rho_0^\varepsilon W^\varepsilon) - \rho_0^\varepsilon \partial_t W\right) \mathrm{d}\mathbf{x}\, \mathrm{d}s \\
={}& \int_{\mathbb{R}^d} \eta\left(\mathcal{Z}^\varepsilon \mid \mathcal{Z}\right)(0, \mathbf{x})\, \mathrm{d}\mathbf{x} + \int_0^t \left[\mathcal{T}_1(s) + \mathcal{T}_2(s) + \mathcal{T}_3(s)\right] \mathrm{d}s,
\end{aligned}
$$

where for all $s \in [0, T]$, we define

$$
\begin{cases}
\mathcal{T}_1(s) := \displaystyle\int \rho_0^\varepsilon\, (W^\varepsilon - W)\,(A(V^\varepsilon, W^\varepsilon) - A(V, W))\, \mathrm{d}\mathbf{x} - \int \rho_0^\varepsilon\, (V^\varepsilon - V)\,(W^\varepsilon - W)\, \mathrm{d}\mathbf{x}, \\[2ex]
\mathcal{T}_2(s) := \displaystyle\int_{\mathbb{R}^d} (V^\varepsilon - V) \int_{\mathbb{R}^2} (N(v) - N(V))\, f^\varepsilon(s, \mathbf{x}, \mathbf{u})\, \mathrm{d}\mathbf{u}\, \mathrm{d}\mathbf{x}, \\[2ex]
\mathcal{T}_3(s) := \displaystyle\int \rho_0^\varepsilon\, (V^\varepsilon - V)\, \left(\mathscr{L}_{\rho_0^\varepsilon}(V^\varepsilon) - \mathcal{L}_{\rho_0}(V)\right)\, \mathrm{d}\mathbf{x},
\end{cases}
$$

which respectively stand for the difference between the linear reaction terms, the nonlinear reaction terms, and the diffusion terms.

Estimate of the linear reaction terms.   First of all, we can directly treat the first term $\mathcal{T}_1$ with Young's inequality, which yields that,

$$\int_0^T \mathcal{T}_1(t)\, \mathrm{d}t \le (1 + \tau) \int_0^T \int_{\mathbb{R}^d} \eta\left(\mathcal{Z}^\varepsilon \mid \mathcal{Z}\right)(t, \mathbf{x})\, \mathrm{d}\mathbf{x}\, \mathrm{d}t. \tag{4.4.4}$$

Estimate of the nonlinear reaction terms.   Then, we deal with the second term $\mathcal{T}_2$ using the assumptions (4.1.3) satisfied by N, as in [49]. For all $t \in [0, T]$, we have:

$$
\begin{aligned}
\mathcal{T}_2(t) ={}& \int_{\mathbb{R}^d} (V^\varepsilon - V) \int_{\mathbb{R}^2} (N(v) - N(V^\varepsilon))\, f^\varepsilon(t, \mathbf{x}, \mathbf{u})\, \mathrm{d}\mathbf{u}\, \mathrm{d}\mathbf{x} \\
&+ \int_{\mathbb{R}^d} (V^\varepsilon - V)\,(N(V^\varepsilon) - N(V))\, \rho_0^\varepsilon(\mathbf{x})\, \mathrm{d}\mathbf{x} \\
\le{}& \kappa_3 \int_{\mathbb{R}^{d+2}} |V^\varepsilon - V|\,|V^\varepsilon - v|\, \left[1 + v^2 + (V^\varepsilon)^2\right] f^\varepsilon(t, \mathbf{x}, \mathbf{u})\, \mathrm{d}\mathbf{x}\, \mathrm{d}\mathbf{u} \\
&+ 2\,\kappa_2 \int_{\mathbb{R}^d} \eta\left(\mathcal{Z}^\varepsilon \mid \mathcal{Z}\right)(t, \mathbf{x})\, \mathrm{d}\mathbf{x},
\end{aligned}
$$

where the constants κ_2 and κ_3 are given in (4.1.3). Then, in order to estimate $\mathcal{T}_2$ using the dissipation estimate from Proposition 4.3.4, Cauchy-Schwarz inequality yields that

$$\mathcal{T}_2(t) \leq \alpha(t) \left(\int |V^\varepsilon(t) - v|^2 \, f^\varepsilon(t, \mathbf{x}, \mathbf{u}) \, \mathrm{d}\mathbf{x} \, \mathrm{d}\mathbf{u} \right)^{1/2} + 2\,\kappa_2 \int_{\mathbb{R}^d} \eta \left(\mathcal{Z}^\varepsilon \,|\, \mathcal{Z} \right)(t, \mathbf{x}) \, \mathrm{d}\mathbf{x},$$

where

$$\alpha(t) := \kappa_3 \left(\int \left[1 + (V^\varepsilon(t))^2 + v^2 \right]^2 \left[V^\varepsilon(t) - V(t) \right]^2 \, f^\varepsilon(t, \mathbf{x}, \mathbf{u}) \, \mathrm{d}\mathbf{x} \, \mathrm{d}\mathbf{u} \right)^{1/2}.$$

We recall that $V \in L^\infty([0, T], H^2(\mathbb{R}^d))$, and $H^2(\mathbb{R}^d) \subset L^\infty(\mathbb{R}^d)$ since $d \leq 3$. Hence, using the moment estimate from Corollary 4.3.2, and the fact that for all $t \in [0, T]$ and $\mathbf{x} \in \mathbb{R}^d$,

$$\rho_0^\varepsilon(\mathbf{x}) \, |V^\varepsilon(t, \mathbf{x})|^6 \leq \int |v|^6 \, f^\varepsilon(t, \mathbf{x}, \mathbf{u}) \, \mathrm{d}\mathbf{x} \, \mathrm{d}\mathbf{u},$$

we can conclude that there exists a positive constant $C_T > 0$ such that

$$\int_0^T \alpha(t)^2 \, \mathrm{d}t \leq C_T.$$

Consequently, according to the estimate from Proposition 4.3.4,

$$\int_0^T \mathcal{T}_2(t) \, \mathrm{d}t \leq C_T \, \varepsilon^{2/(d+6)} + 2\,\kappa_2 \int_0^T \int_{\mathbb{R}^d} \eta \left(\mathcal{Z}^\varepsilon \,|\, \mathcal{Z} \right)(t, \mathbf{x}) \, \mathrm{d}\mathbf{x} \, \mathrm{d}t. \tag{4.4.5}$$

Estimate of the diffusion terms.   Finally, it remains to estimate the third term $\mathcal{T}_3$, involving the difference between the nonlocal diffusion term $\mathscr{L}_{\rho_0^\varepsilon}(V^\varepsilon)$ and the local diffusion term $\mathcal{L}_\rho(V)$. On the one hand, since V^ε is not regular enough in space, we cannot apply the operator $\mathcal{L}_{\rho_0}$ to it. On the other hand, we can apply the nonlocal operator $\mathscr{L}_{\rho_0^\varepsilon}$ to both V^ε and V. This leads to rewrite $\mathcal{T}_3$ as follows:

$$\mathcal{T}_3 = \mathcal{T}_{3,1} + \mathcal{T}_{3,2},$$

where for all $t \in [0, T]$

$$\begin{cases} \mathcal{T}_{3,1}(t) := \int \rho_0^\varepsilon \left(V^\varepsilon - V \right) \left(\mathscr{L}_{\rho_0^\varepsilon}(V^\varepsilon) - \mathscr{L}_{\rho_0}(V) \right) \mathrm{d}\mathbf{x}, \\[2mm] \mathcal{T}_{3,2}(t) := \int \rho_0^\varepsilon \left(V^\varepsilon - V \right) \left(\mathscr{L}_{\rho_0}(V) - \mathcal{L}_{\rho_0}(V) \right) \mathrm{d}\mathbf{x}. \end{cases} \tag{4.4.6}$$

To estimate the first term $\mathcal{T}_{3,1}$, using the shorthand notations $V := V(t, \mathbf{x})$, $V' := V(t, \mathbf{x}')$, and the same for V^ε and $V^{\varepsilon\,\prime}$, we compute:

$$\mathcal{T}_{3,1}(t)$$
$$= \frac{1}{\varepsilon^{d+2}} \iint \Psi \left(\frac{\|\mathbf{x} - \mathbf{x}'\|}{\varepsilon} \right) \rho_0^\varepsilon(\mathbf{x}) \left(V^\varepsilon - V \right) \left[\rho_0^\varepsilon(\mathbf{x}') \left(V^{\varepsilon\,\prime} - V^\varepsilon \right) - \rho_0(\mathbf{x}') \left(V' - V \right) \right] \mathrm{d}\mathbf{x} \, \mathrm{d}\mathbf{x}'$$
$$= \frac{1}{\varepsilon^{d+2}} \iint \Psi \left(\frac{\|\mathbf{x} - \mathbf{x}'\|}{\varepsilon} \right) \left(V^\varepsilon - V \right) \rho_0^\varepsilon(\mathbf{x}) \rho_0^\varepsilon(\mathbf{x}') \left[\left(V^{\varepsilon\,\prime} - V' \right) - \left(V^\varepsilon - V \right) \right] \mathrm{d}\mathbf{x} \, \mathrm{d}\mathbf{x}'$$
$$+ \frac{1}{\varepsilon^{d+2}} \iint \Psi \left(\frac{\|\mathbf{x} - \mathbf{x}'\|}{\varepsilon} \right) \left(V^\varepsilon - V \right) \rho_0^\varepsilon(\mathbf{x}) \left(\rho_0^\varepsilon(\mathbf{x}') - \rho_0(\mathbf{x}') \right) \left(V' - V \right) \mathrm{d}\mathbf{x} \, \mathrm{d}\mathbf{x}'$$
$$\leq \frac{1}{\varepsilon^{d+2}} \iint \Psi \left(\frac{\|\mathbf{x} - \mathbf{x}'\|}{\varepsilon} \right) \rho_0^\varepsilon(\mathbf{x}) \, |V^\varepsilon - V| \, |\rho_0^\varepsilon - \rho_0|(\mathbf{x}') \, |V' - V| \, \mathrm{d}\mathbf{x} \, \mathrm{d}\mathbf{x}'$$
$$\leq 2 \, \|V\|_{L^\infty} \frac{1}{\varepsilon^{d+2}} \iint \Psi \left(\frac{\|\mathbf{x} - \mathbf{x}'\|}{\varepsilon} \right) \rho_0^\varepsilon(\mathbf{x}) \, |V^\varepsilon - V| \, |\rho_0^\varepsilon - \rho_0|(\mathbf{x}') \, \mathrm{d}\mathbf{x} \, \mathrm{d}\mathbf{x}',$$

and then, using Young's inequality, we have

$$
\begin{aligned}
\mathcal{T}_{3,1}(t) \leq{}& \|V\|_{L^\infty} \int \rho_0^\varepsilon \, |V - V^\varepsilon|^2 \, \mathrm{d}\mathbf{x} \\
&+ \|V\|_{L^\infty} \int \left[\frac{1}{\varepsilon^{d+2}} \int \Psi\left(\frac{\|\mathbf{x} - \mathbf{x}'\|}{\varepsilon} \right) |\rho_0^\varepsilon - \rho_0| \,(\mathbf{x}') \, \mathrm{d}\mathbf{x}' \right]^2 \rho_0^\varepsilon(\mathbf{x}) \, \mathrm{d}\mathbf{x} \\
\leq{}& 2 \, \|V\|_{L^\infty} \int_{\mathbb{R}^d} \eta\left(\mathcal{Z}^\varepsilon \,|\, \mathcal{Z}\right)(t, \mathbf{x}) \, \mathrm{d}\mathbf{x} + \frac{1}{\varepsilon^4} \|V\|_{L^\infty} \|\rho_0^\varepsilon\|_{L^\infty} \|\Psi_\varepsilon\|_{L^1} \|\rho_0 - \rho_0^\varepsilon\|_{L^2}^2 .
\end{aligned}
$$

This leads to the estimate

$$
\mathcal{T}_{3,1}(t) \leq C_T \left(\frac{1}{\varepsilon^4} \|\rho_0^\varepsilon - \rho_0\|_{L^2(\mathbb{R}^d)}^2 + \int_{\mathbb{R}^d} \eta\left(\mathcal{Z}^\varepsilon \,|\, \mathcal{Z}\right)(t, \mathbf{x}) \, \mathrm{d}\mathbf{x} \right), \tag{4.4.7}
$$

where $C_T > 0$ is a positive constant independent of ε. It remains to control the final term $\mathcal{T}_{3,2}$. We start by separating the diffusions on $\rho_0 V$ and on ρ_0 alone, as follows:

$$
\mathcal{T}_{3,2} = \mathcal{T}_{3,2,1} + \mathcal{T}_{3,2,2},
$$

where for all $t \in [0, T]$

$$
\left\{
\begin{aligned}
\mathcal{T}_{3,2,1}(t) &:= \int \rho_0^\varepsilon \left(V^\varepsilon - V\right) \left[\frac{1}{\varepsilon^2} \left(\Psi_\varepsilon \star_{\mathbf{x}} [\rho_0 \, V](t, \mathbf{x}) - \rho_0 \, V(t, \mathbf{x})\right) - \sigma \, \Delta_{\mathbf{x}}(\rho_0 \, V)(t, \mathbf{x}) \right] \mathrm{d}\mathbf{x}, \\
\mathcal{T}_{3,2,2}(t) &:= -\int \rho_0^\varepsilon \left(V^\varepsilon - V\right) V(t, \mathbf{x}) \left[\frac{1}{\varepsilon^2} \left(\Psi_\varepsilon \star_{\mathbf{x}} \rho_0(\mathbf{x}) - \rho_0(\mathbf{x})\right) - \sigma \, \Delta_{\mathbf{x}}\rho_0(\mathbf{x}) \right] \mathrm{d}\mathbf{x}.
\end{aligned}
\right.
$$

Our strategy to estimate both $\mathcal{T}_{3,2,1}$ and $\mathcal{T}_{3,2,2}$ follows the idea from [7] with a Taylor expansion. Using Young's inequality, we get that

$$
\left\{
\begin{aligned}
\mathcal{T}_{3,2,1}(t) \leq{}& \int_{\mathbb{R}^d} \eta\left(\mathcal{Z}^\varepsilon \,|\, \mathcal{Z}\right)(t, \mathbf{x}) \, \mathrm{d}\mathbf{x} \\
&+ \frac{1}{2} \|\rho_0^\varepsilon\|_{L^\infty} \int \left| \frac{1}{\varepsilon^2} \left(\Psi_\varepsilon \star_{\mathbf{x}} [\rho_0 \, V](t, \mathbf{x}) - \rho_0 \, V(t, \mathbf{x})\right) - \sigma \, \Delta_{\mathbf{x}}(\rho_0 \, V)(t, \mathbf{x}) \right|^2 \mathrm{d}\mathbf{x}, \\
\mathcal{T}_{3,2,2}(t) \leq{}& \int_{\mathbb{R}^d} \eta\left(\mathcal{Z}^\varepsilon \,|\, \mathcal{Z}\right)(t, \mathbf{x}) \, \mathrm{d}\mathbf{x} \\
&+ \frac{1}{2} \|\rho_0^\varepsilon\|_{L^\infty} \|V\|_{L^\infty}^2 \int \left| \frac{1}{\varepsilon^2} \left(\Psi_\varepsilon \star_{\mathbf{x}} \rho_0(\mathbf{x}) - \rho_0(\mathbf{x})\right) - \sigma \, \Delta_{\mathbf{x}}\rho_0(\mathbf{x}) \right|^2 \mathrm{d}\mathbf{x}.
\end{aligned}
\right.
$$

Then, for all $\mathbf{x} \in \mathbb{R}^d$, we apply in the convolution products the change of variable $\mathbf{y} = (\mathbf{x} - \mathbf{x}')/\varepsilon$, so that using a Taylor expansion, we get:

$$
\begin{aligned}
&\left| \frac{1}{\varepsilon^2} \left(\Psi_\varepsilon \star_{\mathbf{x}} [\rho_0 \, V](t, \mathbf{x}) - \rho_0 \, V(t, \mathbf{x})\right) - \sigma \, \Delta_{\mathbf{x}}(\rho_0 \, V)(t, \mathbf{x}) \right|^2 \\
&= \left| \frac{1}{\varepsilon^2} \int \Psi(\|\mathbf{y}\|) \, (\rho_0 \, V)(t, \mathbf{x} - \varepsilon \mathbf{y}) \, \mathrm{d}\mathbf{y} - \frac{1}{\varepsilon^2} \rho_0 \, V(t, \mathbf{x}) - \sigma \, \Delta_{\mathbf{x}}(\rho_0 \, V)(t, \mathbf{x}) \right|^2 \\
&= \left| \int \Psi(\|\mathbf{y}\|) \int_0^1 (1 - s) \, \mathbf{y}^T \cdot \left(\nabla_{\mathbf{x}}^2(\rho_0 \, V)(t, \mathbf{x} - \varepsilon \, s \, \mathbf{y}) - \nabla_{\mathbf{x}}^2(\rho_0 \, V)(t, \mathbf{x})\right) \cdot \mathbf{y} \, \mathrm{d}s \, \mathrm{d}\mathbf{y} \right|^2 .
\end{aligned}
$$

Besides, we consecutively use the Cauchy-Schwarz inequality in the integrals in s and then in $\mathbf{y}$, which gives:

$$\left| \frac{1}{\varepsilon^2} \left(\Psi_\varepsilon \star_{\mathbf{x}} [\rho_0\, V](t, \mathbf{x}) \,-\, \rho_0\, V(t, \mathbf{x}) \right) \,-\, \sigma\, \Delta_{\mathbf{x}}(\rho_0\, V)(t, \mathbf{x}) \right|^2$$

$$\leq \left| \int \Psi(\|\mathbf{y}\|) \left(\int_0^1 |1 - s|\, \|\mathbf{y}\| \, \mathrm{d}s \right)^{1/2} \right.$$

$$\left. \times \left(\int_0^1 |1 - s|\, \|\mathbf{y}\|^2 \left\| \nabla_{\mathbf{x}}^2(\rho_0\, V)(t, \mathbf{x} - \varepsilon\, s\, \mathbf{y}) - \nabla_{\mathbf{x}}^2(\rho_0\, V)(t, \mathbf{x}) \right\|^2 \mathrm{d}s \right)^{1/2} \mathrm{d}\mathbf{y} \right|^2$$

$$\leq \sigma \int \Psi(\|\mathbf{y}\|) \left(\int_0^1 |1 - s|\, \|\mathbf{y}\|^2 \left\| \nabla_{\mathbf{x}}^2(\rho_0\, V)(t, \mathbf{x} - \varepsilon\, s\, \mathbf{y}) - \nabla_{\mathbf{x}}^2(\rho_0\, V)(t, \mathbf{x}) \right\|^2 \mathrm{d}s \right) \mathrm{d}\mathbf{y}.$$

Consequently, after integrating this last inequality with respect to $\mathbf{x}$, using the fact that $\rho_0\, V$ is in $L^\infty([0, T], H^2(\mathbb{R}^d))$ and the hypotheses (4.1.5) satisfied by Ψ, we get:

$$\int \left| \frac{1}{\varepsilon^2} \left(\Psi_\varepsilon \star_{\mathbf{x}} [\rho_0\, V](t, \mathbf{x}) \,-\, \rho_0\, V(t, \mathbf{x}) \right) \,-\, \sigma\, \Delta_{\mathbf{x}}(\rho_0\, V)(t, \mathbf{x}) \right|^2 \mathrm{d}\mathbf{x}$$

$$\leq \sigma \iint \Psi(\|\mathbf{y}\|) \left(\int_0^1 |1 - s|\, \|\mathbf{y}\|^2 \left\| \nabla_{\mathbf{x}}^2(\rho_0\, V)(t, \mathbf{x} - \varepsilon\, s\, \mathbf{y}) - \nabla_{\mathbf{x}}^2(\rho_0\, V)(t, \mathbf{x}) \right\|^2 \mathrm{d}s \right) \mathrm{d}\mathbf{y}\, \mathrm{d}\mathbf{x}$$

$$\leq 2\, \sigma^2 \, \|\rho_0\, V\|_{L^\infty([0, T], H^2(\mathbb{R}^d))}^2.$$

Then, using these two last inequalities and the Lebesgue's Dominated Convergence Theorem, and the fact that $\|\rho_0^\varepsilon\|_{L^\infty}$ is uniformly bounded, we get that as ε goes to 0, for all $t \in [0, T]$

$$\mathcal{T}_{3,2,1}(t) \,\leq\, \int_{\mathbb{R}^d} \eta\left(\mathcal{Z}^\varepsilon \mid \mathcal{Z}\right)(t, \mathbf{x})\, \mathrm{d}\mathbf{x} \,+\, o_{\varepsilon \to 0}(1), \tag{4.4.8}$$

where $o_{\varepsilon \to 0}(1)$ denotes a function which converges towards 0 as ε goes to 0, uniformly in $t \in [0, T]$. Using similar arguments, and the fact that $\rho_0 \in H^2(\mathbb{R}^d)$ and $V \in L^\infty([0, T], L^\infty(\mathbb{R}^d))$, we also get that

$$\mathcal{T}_{3,2,2}(t) \,\leq\, \int_{\mathbb{R}^d} \eta\left(\mathcal{Z}^\varepsilon \mid \mathcal{Z}\right)(t, \mathbf{x})\, \mathrm{d}\mathbf{x} \,+\, o_{\varepsilon \to 0}(1). \tag{4.4.9}$$

We precise that these two last estimates (4.4.8) and (4.4.9) are not uniform in T in general since they involve norms in $L^\infty([0, T], H^2(\mathbb{R}^d))$ of the macroscopic quantities, which may not be uniform.

Relative entropy estimate. Finally, putting together the estimates (4.4.4)–(4.4.9), we get that there exists a positive constant $C_T > 0$ such that for all $t \in [0, T]$,

$$\int_{\mathbb{R}^d} \eta\left(\mathcal{Z}^\varepsilon \mid \mathcal{Z}\right)(t, \mathbf{x})\, \mathrm{d}\mathbf{x} \,\leq\, \int_{\mathbb{R}^d} \eta\left(\mathcal{Z}^\varepsilon \mid \mathcal{Z}\right)(t, \mathbf{x})\, \mathrm{d}\mathbf{x}$$

$$+\, C_T \left(\frac{1}{\varepsilon^4} \|\rho_0^\varepsilon - \rho_0\|_{L^2(\mathbb{R}^d)}^2 \,+\, \varepsilon^{2/(d+6)} \,+\, o_{\varepsilon \to 0}(1) \,+\, \int_0^t \int_{\mathbb{R}^d} \eta\left(\mathcal{Z}^\varepsilon \mid \mathcal{Z}\right)(s, \mathbf{x})\, \mathrm{d}\mathbf{x}\, \mathrm{d}s \right).$$

According to the assumptions (4.2.16) and (4.2.17) satisfied by the initial conditions, we get

$$\int_{\mathbb{R}^d} \eta\left(\mathcal{Z}^\varepsilon \mid \mathcal{Z}\right)(t, \mathbf{x})\, \mathrm{d}\mathbf{x} \,\leq\, o_{\varepsilon \to 0}(1) \,+\, C_T \int_0^t \int_{\mathbb{R}^d} \eta\left(\mathcal{Z}^\varepsilon \mid \mathcal{Z}\right)(t, \mathbf{x})\, \mathrm{d}\mathbf{x}\, \mathrm{d}s.$$

Therefore, Grönwall's inequality yields that

$$\lim_{\varepsilon \to 0} \sup_{t \in [0, T]} \int_{\mathbb{R}^d} \eta\left(\mathcal{Z}^\varepsilon \mid \mathcal{Z}\right)(t, \mathbf{x})\, \mathrm{d}\mathbf{x} \,=\, 0. \tag{4.4.10}$$

4.4.3 Conclusion

Finally, let us conclude the proof of Theorem 4.2.8 using the relative entropy estimate (4.4.10) established in the previous subsection. Let $T > 0$. We want to prove that the weak solution of the transport equation (4.1.1) converges towards a monokinetic distribution as ε vanishes. First, we set

$$F^\varepsilon(t, \mathbf{x}, w) := \int f^\varepsilon(t, \mathbf{x}, v, w) \, \mathrm{d}v, \quad F^\varepsilon(0, \mathbf{x}, v) = F_0(\mathbf{x}, w) := \int f_0^\varepsilon(\mathbf{x}, v, w) \, \mathrm{d}v.$$

Let us notice that since f^ε is compactly supported in v for any $\varepsilon > 0$, we can choose a test function in (4.2.1) independent of $v \in \mathbb{R}$, so that the ditribution F^ε satisfies the following equation for all $\varphi \in \mathscr{C}_c^\infty([0, T) \times \mathbb{R}^{d+1})$:

$$\int_0^T \int_{\mathbb{R}^{d+1}} \left(F^\varepsilon \, \partial_t \varphi + \tau \left[\int_{\mathbb{R}} v \, f^\varepsilon \, \mathrm{d}v - b \, w \, F^\varepsilon \right] \partial_w \varphi \right) \mathrm{d}\mathbf{x} \, \mathrm{d}w \, \mathrm{d}t + \int_{\mathbb{R}^{d+1}} F_0^\varepsilon \, \varphi(0) \, \mathrm{d}\mathbf{x} \, \mathrm{d}w = 0,$$

which is equivalent to satisfying for all $\varphi \in \mathscr{C}_c^1([0, T) \times \mathbb{R}^{d+1})$ the equation

$$\int_0^T \int_{\mathbb{R}^{d+1}} F^\varepsilon \left[\partial_t \varphi + A\left(V(t, \mathbf{x}), w\right) \partial_w \varphi \right] \mathrm{d}\mathbf{x} \, \mathrm{d}w \, \mathrm{d}t + \int_{\mathbb{R}^{d+1}} F_0^\varepsilon \, \varphi(0) \, \mathrm{d}\mathbf{x} \, \mathrm{d}w$$
$$= \tau \int_0^T \int_{\mathbb{R}^{d+2}} (V(t, \mathbf{x}) - v) \, f^\varepsilon \, \partial_w \varphi \, \mathrm{d}v \, \mathrm{d}w \, \mathrm{d}\mathbf{x} \, \mathrm{d}t, \quad (4.4.11)$$

where V is solution to the second equation in (4.2.8). On the one hand, since $(F^\varepsilon)_{\varepsilon > 0}$ in uniformly bounded by 1 in $L^\infty([0, T], L^1(\mathbb{R}^{d+1}))$, we get that it converges weakly-$\star$ up to extraction in $\mathcal{M}((0, T) \times \mathbb{R}^{d+1})$ towards a limit $F \in \mathcal{M}((0, T) \times \mathbb{R}^{d+1})$. Thus, we can pass to the limit on the left hand side of (4.4.11) by linearity. On the other hand, from the dissipation estimate in Proposition 4.3.4 and the relative entropy estimate (4.4.10), we get that

$$\int_0^T \int f^\varepsilon \, |v - V(t, \mathbf{x})|^2 \, \mathrm{d}\mathbf{x} \, \mathrm{d}v \, \mathrm{d}w \, \mathrm{d}t$$
$$\leq 2 \int_0^T \int f^\varepsilon \left(|v - V^\varepsilon(t, \mathbf{x})|^2 + |V^\varepsilon(t, \mathbf{x}) - V(t, \mathbf{x})|^2 \right) \mathrm{d}\mathbf{x} \, \mathrm{d}v \, \mathrm{d}w \, \mathrm{d}t$$
$$\longrightarrow 0,$$
$$(4.4.12)$$

as $\varepsilon \to 0$. Consequently, since $\|\rho_0^\varepsilon\|_{L^1} = 1$, it yields with Cauchy-Schwarz inequality that:

$$\left| \int_0^T \int_{\mathbb{R}^{d+2}} (V(t, \mathbf{x}) - v) \, f^\varepsilon \, \partial_w \varphi \, \mathrm{d}v \mathrm{d}w \, \mathrm{d}\mathbf{x} \, \mathrm{d}t \right|$$
$$\leq T^{1/2} \, \|\partial_w \varphi\|_\infty \int_0^T \int |V(t, \mathbf{x}) - v|^2 \, f^\varepsilon \, \mathrm{d}v \mathrm{d}w \, \mathrm{d}\mathbf{x} \, \mathrm{d}t \longrightarrow 0,$$

as $\varepsilon \to 0$. Therefore, passing to the limit $\varepsilon \to 0$ in (4.1.1), it proves that (V, F) is a solution of the system (4.1.9). Furthermore, by uniqueness of the solution of (4.1.9), we get the convergence of the sequence $(F^\varepsilon)_{\varepsilon > 0}$.

Now, let us prove that for any $\varphi \in \mathscr{C}_b^0(\mathbb{R}^{d+2})$,

$$\int \varphi(\mathbf{x}, v, w) \, f^\varepsilon(t, \mathbf{x}, v, w) \, \mathrm{d}\mathbf{x} \, \mathrm{d}v \, \mathrm{d}w \longrightarrow \int \varphi(\mathbf{x}, V(t, \mathbf{x}), w) \, F(t, \mathrm{d}\mathbf{x}, \mathrm{d}w),$$

strongly in $L^1_{\text{loc}}(0,T)$ as $\varepsilon \to 0$. We start with proving that for all $0 < t < t' \leq T$, for all $\varphi \in \mathscr{C}^1_c(\mathbb{R}^{d+2})$,

$$\int_t^{t'} \int f^\varepsilon(s, \mathbf{x}, v, w)\, \varphi(\mathbf{x}, v, w)\, \mathrm{d}v\, \mathrm{d}w\, \mathrm{d}\mathbf{x}\, \mathrm{d}s \xrightarrow[\varepsilon \to 0]{} \int_t^{t'} \int \varphi(\mathbf{x}, V(s, \mathbf{x}), w)\, F(s, \mathrm{d}\mathbf{x}, \mathrm{d}w)\, \mathrm{d}s, \quad (4.4.13)$$

where (V, F) is the solution on $[0, T]$ of the reaction-diffusion system (4.1.9) provided by Proposition 4.2.5, and we conclude using a density argument. Let $0 < t < t' \leq T$. We can compute:

$$\mathcal{I} := \left| \int_t^{t'} \left(\int_{\mathbb{R}^{d+2}} f^\varepsilon(s, \mathbf{x}, v, w)\, \varphi(\mathbf{x}, v, w)\, \mathrm{d}v\, \mathrm{d}w\, \mathrm{d}\mathbf{x} - \int_{\mathbb{R}^{d+1}} \varphi(\mathbf{x}, V(s, \mathbf{x}), w)\, F(s, \mathrm{d}\mathbf{x}, \mathrm{d}w) \right) \mathrm{d}s \right|$$

$$\leq \mathcal{I}_1 + \mathcal{I}_2,$$

where

$$\begin{cases} \mathcal{I}_1 := \displaystyle\int_t^{t'} \int f^\varepsilon(s, \mathbf{x}, v, w)\, |\varphi(\mathbf{x}, v, w) - \varphi(\mathbf{x}, V(s, \mathbf{x}), w)|\, \mathrm{d}v\, \mathrm{d}w\, \mathrm{d}\mathbf{x}\, \mathrm{d}s, \\[4mm] \mathcal{I}_2 := \displaystyle\int_t^{t'} \int |\varphi(\mathbf{x}, V(s, \mathbf{x}), w)|\, |F^\varepsilon(s, \mathrm{d}\mathbf{x}, \mathrm{d}w) - F(s, \mathrm{d}\mathbf{x}, \mathrm{d}w)|\, \mathrm{d}s. \end{cases}$$

On the one hand, using Cauchy-Schwarz inequality, we have

$$\mathcal{I}_1 \leq \|\partial_v \varphi\|_\infty \int_t^{t'} \int f^\varepsilon(s, \mathbf{x}, v, w)\, |v - V(s, \mathbf{x})|\, \mathrm{d}v\, \mathrm{d}w\, \mathrm{d}\mathbf{x}\, \mathrm{d}s$$

$$\leq \|\partial_v \varphi\|_\infty \left(\int_0^T \int f^\varepsilon(s, \mathbf{x}, v, w)\, \mathrm{d}v\, \mathrm{d}w\, \mathrm{d}\mathbf{x}\, \mathrm{d}s \right)^{1/2}$$

$$\times \left(\int_0^T \int f^\varepsilon(s, \mathbf{x}, v, w)\, |v - V(s, \mathbf{x})|^2\, \mathrm{d}v\, \mathrm{d}w\, \mathrm{d}\mathbf{x}\, \mathrm{d}s \right)^{1/2}$$

$$= \|\partial_v \varphi\|_\infty T^{1/2} \left(\int_0^T \int f^\varepsilon(s, \mathbf{x}, v, w)\, |v - V(s, \mathbf{x})|^2\, \mathrm{d}v\, \mathrm{d}w\, \mathrm{d}\mathbf{x}\, \mathrm{d}s \right)^{1/2}.$$

Consequently, using the convergence from (4.4.12), we get

$$\lim_{\varepsilon \to 0} \mathcal{I}_1 = 0. \quad (4.4.14)$$

On the other hand, the second term $\mathcal{I}_2$ converges to zero as ε goes to zero since $(F^\varepsilon)_{\varepsilon>0}$ converges weakly-$\star$ towards F in $\mathcal{M}((0,T) \times \mathbb{R}^{d+1})$. Consequently, we can conclude that

$$\lim_{\varepsilon \to 0} \mathcal{I} = 0. \quad (4.4.15)$$

Using a density argument, this shows the convergence of f^ε in $L^1_{\text{loc}}((0,T), \mathcal{M}(\mathbb{R}^{d+2}))$ towards a monokinetic distribution, which concludes the proof of Theorem 4.2.8.

4.5 Proof of Proposition 4.2.5

This subsection is devoted to the proofs of Proposition 4.2.5 and its Corollary 4.2.7, that is to the construction of a solution to the system (4.2.8). The main difficulty lies in the fact that the function ρ_0 can reach 0, so the second equation in (4.2.8) is not well-defined on $\mathbb{R}^d$. A solution to overcome this problem is to construct a solution to (4.2.8) from a weak solution of the reaction-diffusion FHN system (4.2.4) in the sense of Definition 4.2.4.

Furthermore, we have to be especially careful to prove the existence and uniqueness of a weak solution to the reaction-diffusion system (4.2.4) since it is not a parabolic system. A way to circumvent this issue is to consider for all $\delta \geq 0$ the linear operator:

$$\mathcal{L}_{\rho_0+\delta} : V \mapsto \sigma\big[(\rho_0 + \delta)\,\Delta_{\mathbf{x}}V \,+\, 2\,\nabla_{\mathbf{x}}\rho_0 \,\cdot\, \nabla_{\mathbf{x}}V\big]. \tag{4.5.1}$$

First of all, for any given initial data $V_0 \in L^2(\mathbb{R}^d)$ and for all $\delta > 0$, we prove the existence and uniqueness of V_δ a weak solution of the approximated parabolic system

$$\partial_t V_\delta \,+\, \mathcal{L}_{\rho_0+\delta}(V_\delta) \,=\, N(V_\delta) \,-\, W[V_\delta], \tag{4.5.2}$$

where for all $V : \mathbb{R}^+ \times \mathbb{R}^d \to \mathbb{R}$, we define

$$W[V] : (t,\mathbf{x}) \mapsto e^{-\tau\,b\,t}W_0(\mathbf{x}) \,+\, \tau \int_0^t e^{-\tau\,b\,(t-s)}V(s,\mathbf{x})\,\mathrm{d}s, \tag{4.5.3}$$

where $W_0 : \mathbb{R}^d \to \mathbb{R}$ is a given initial data in $H^2(\mathbb{R}^d)$. We will be able to pass to the limit $\delta \to 0$ thanks to *a priori* estimates of the H^2 norm of the solution of (4.5.2) which are uniform in δ.

In the rest of this chapter, for all $k \in \{0,1,2\}$, we note $\langle \cdot, \cdot \rangle_{H^k(\mathbb{R}^d)}$ the scalar product of $H^k(\mathbb{R}^d)$ defined as follows:

$$\langle U, V \rangle_{H^k(\mathbb{R}^d)} \,:=\, \sum_{\alpha \in \mathbb{N}^d, |\alpha| \leq k} \int \partial^\alpha U \, \partial^\alpha V \,\mathrm{d}\mathbf{x},$$

for all $U, V \in H^k(\mathbb{R}^d)$, where for all $\alpha = (\alpha_1, ..., \alpha_d) \in \mathbb{N}^d$, $\partial^\alpha = \partial_{\mathbf{x}_1}^{\alpha_1} ... \partial_{\mathbf{x}_d}^{\alpha_d}$.

4.5.1 *A priori* estimates

The purpose of this subsection is to derive an *a priori* estimate of the H^2 norm of a weak solution to the FHN reaction-diffusion system (4.5.2) uniform in δ.

Lemma 4.5.1. *Let $T > 0$. Consider an initial data ρ_0 satisfying (4.2.6) and $V_0 \in H^2(\mathbb{R}^d)$ satisfying (4.2.7). Let $\delta \geq 0$. Assume that there exists*

$$V_\delta \in L^\infty([0,T], H^2(\mathbb{R}^d)) \cap \mathscr{C}^0([0,T], L^2(\mathbb{R}^d))$$

a weak solution of the reaction-diffusion equation for $t > 0$ and $\mathbf{x} \in \mathbb{R}^d$:

$$\partial_t V_\delta \,-\, \mathcal{L}_{\rho_0+\delta}V_\delta \,=\, S, \tag{4.5.4}$$

where $S \in L^\infty([0,T], H^2(\mathbb{R}^d))$ are two general source terms. Then, there exists a positive constant $C > 0$ independent of δ such that for all $t \in [0,T]$

$$\|V_\delta(t)\|^2_{H^2(\mathbb{R}^d)} \,+\, \delta \int_0^t \|V_\delta(s)\|^2_{H^3(\mathbb{R}^d)}$$

$$\leq \|V_0\|^2_{H^2(\mathbb{R}^d)} \,+\, C \int_0^t \Big(\|V_\delta(s)\|^2_{H^2(\mathbb{R}^d)} \,+\, \langle S(s)\,, V_\delta(s)\rangle_{H^2(\mathbb{R}^d)}\Big)\,\mathrm{d}s. \tag{4.5.5}$$

Proof. We postpone the proof to Appendix 4.7. $\qquad\qquad\square$

Corollary 4.5.2. *Let $\delta \geq 0$. Consider an initial data ρ_0 satisfying (4.2.6) and (V_0, W_0) satisfying (4.2.7). Let $T > 0$ such that there exists*

$$V_\delta \in L^\infty([0,T], H^2(\mathbb{R}^d)) \cap \mathscr{C}^0([0,T], L^2(\mathbb{R}^d))$$

a weak solution of the reaction-diffusion system (4.5.2). Then, there exists a finite constant $C_T > 0$ independant of δ such that for all $t \in [0,T]$,

$$\|V_\delta(t)\|_{H^2(\mathbb{R}^d)} \,\leq\, C_T. \tag{4.5.6}$$

Proof. We postpone the proof to Appendix 4.8. $\qquad\qquad\square$

4.5.2 Case of a positive δ

Let $\delta > 0$. This subsection focuses on the existence and uniqueness of the reaction-diffusion equation (4.5.2).

Lemma 4.5.3. *Consider an initial data ρ_0 satisfying* (4.2.6) *and $V_0 \in H^2(\mathbb{R}^d)$. Then, for all $T > 0$ and for all $\delta > 0$, there exists a unique weak solution V_δ of the diffusion equation*

$$\partial_t V_\delta \, - \, \mathcal{L}_{\rho_0 + \delta} V_\delta \, = \, N(V_\delta) \, - \, W[V_\delta], \tag{4.5.7}$$

such that

$$V_\delta \in L^\infty([0,T], H^2(\mathbb{R}^d)) \cap L^2([0,T], H^3(\mathbb{R}^d)) \cap \mathscr{C}^0([0,T], L^2(\mathbb{R}^d)),$$

and V_δ satisfies the energy estimate (4.5.5) *with $S = N(V_\delta) - W[V_\delta]$.*

Proof. The proof relies on classical methods explained in Section 7.1 in [59]. According to Lemma 4.5.1, V_δ satisfies the energy estimate (4.5.5) with $S = N(V_\delta) - W[V_\delta]$. $\square$

4.5.3 Proof of Proposition 4.2.5

Step 1: Existence. Now, let us pass to the limit $\delta \to 0$ in the approximated equation (4.5.2), to prove Proposition 4.2.5. Let V_0 and $W_0 \in H^2(\mathbb{R}^d)$. For all $\delta > 0$, Lemma 4.5.3 yields the existence of a weak solution V_δ to the reaction-diffusion equation (4.5.2). According to Corollary 4.5.2, there exists a positive constant $K_1 > 0$ independent of δ such that for all $\delta > 0$,

$$\|V_\delta\|_{L^\infty([0,T], H^2(\mathbb{R}^d))} \leq K_1.$$

Let $(\delta_n)_{n \in \mathbb{N}}$ be a sequence of positive reals such that $\delta_n \to 0$ as $n \to \infty$. Therefore, there exists a function $V \in L^\infty([0,T], H^2(\mathbb{R}^d))$ such that up to extraction,

$$V_{\delta_n} \rightharpoonup V,$$

weakly-$\star$ in $L^\infty([0,T], H^2(\mathbb{R}^d))$ as $\delta \to 0$. Let us prove that the sequence $(V_{\delta_n})_{n \in \mathbb{N}}$ also converges in a strong sense using Arzelà-Ascoli Theorem. On the one hand, since for all $n \in \mathbb{N}$ the function V_{δ_n} is a weak solution of (4.5.7), then there exists a constant $K_2 > 0$ independent of n such that for all $n \in \mathbb{N}$,

$$\|\partial_t V_{\delta_n}\|_{L^\infty([0,T], L^2(\mathbb{R}^d))} \leq K_2.$$

On the other hand, for all $t \in [0,T]$, the set $\{V_{\delta_n}(t) \,|\, n \in \mathbb{N}\}$ is not relatively compact in $L^2(\mathbb{R}^d)$. In order to validate this last assumption we have to restrict the domain of integration to open bounded sets. Indeed, for all open bounded subset Ω of $\mathbb{R}^d$, the set $\{V_{\delta_n}(t)|_\Omega \,|\, n \in \mathbb{N}\}$ is relatively compact in $L^2(\Omega)$ since the inclusion $H^2(\Omega) \subset L^2(\Omega)$ is compact. In the following, for all $r > 0$, we note B_r the ball of $\mathbb{R}^d$ of radius r centered in 0.

For all $k \in \mathbb{N}^*$ and all $n \in \mathbb{N}$, let us consider $V_{n,k} := V_{\delta_n}|_{B_k}$. We use a diagonal extraction argument and the Arzelà-Ascoli theorem to obtain that for all $k \in \mathbb{N}^*$, there exists an extraction ϕ_k such that for all $k' \leq k$, the sequence $(V_{\phi_k(n),k'})_{n \in \mathbb{N}}$ converges towards a function $V_{\infty,k'}$ strongly in $\mathscr{C}^0\left(([0,T], L^2(B_{k'})\right)$ as n goes to infinity.

We claim that for all $k \in \mathbb{N}^*$, $V_{\infty,k} = V_{\infty,k+1}|_{B_k}$. Indeed, we have

$$\|V_{\infty,k} - V_{\infty,k+1}\|_{L^\infty([0,T], L^2(B_k))}$$
$$\leq \|V_{\infty,k} - V_{\phi_{k+1}(n),k}\|_{L^\infty([0,T], L^2(B_k))} + \|V_{\infty,k+1} - V_{\phi_{k+1}(n),k+1}\|_{L^\infty([0,T], L^2(B_k))}$$
$$+ \|V_{\phi_{k+1}(n),k} - V_{\phi_{k+1}(n),k+1}\|_{L^\infty([0,T], L^2(B_k))}.$$

Furthermore, we also have that $V_{\phi_{k+1}(n),k} = V_{\phi_{k+1}(n),k+1}|_{B_k}$ according to the definition of the sequence $(V_{n,k})_{n\in\mathbb{N}}$. Thus, passing to the limit $n \to +\infty$ in the last inequality, we can prove our claim.

Consequently, there exists a function $V_\infty \in \mathscr{C}([0,T], L^2_{\mathrm{loc}}(\mathbb{R}^d))$ such that for all $k \in \mathbb{N}^*$, the function $V_{\infty,k}$ is the restriction of V_k to the domain B_k. Thus, the sequence $(V_{\phi_n(n),n})_{n\in\mathbb{N}}$ strongly converges towards V_∞ in $L^\infty([0,T], L^2_{\mathrm{loc}}(\mathbb{R}^d))$. Therefore, $V = V_\infty$, and thus,

$$V \in L^\infty\left([0,T], H^2(\mathbb{R}^d)\right) \cap \mathscr{C}^0\left([0,T], L^2_{\mathrm{loc}}(\mathbb{R}^d)\right).$$

Since the sequence $(V_{\phi_n(n),n})_{n\in\mathbb{N}}$ strongly converges towards V, we can pass to the limit in the weak formulation of the equation (4.5.2) when the space of test functions is $\mathscr{C}_c^\infty(\mathbb{R}^{d+2})$. Consequently, V is a solution in the sense of distributions of (4.2.4) with $\delta = 0$. Furthermore, since $V \in L^\infty([0,T], H^2(\mathbb{R}^d))$, we can deduce that $\partial_t V \in L^\infty([0,T], L^2(\mathbb{R}^d))$, and thus

$$V \in W^{1,\infty}([0,T], L^2(\mathbb{R}^d)).$$

Therefore, using classical arguments detailed in the paragraph 5.9.2 from [59], we get:

$$V \in \mathscr{C}^0([0,T], H^1(\mathbb{R}^d)).$$

Furthermore, since the space of test functions $\mathscr{C}_c^\infty(\mathbb{R}^{d+2})$ is dense in $H^1(\mathbb{R}^{d+2})$, we get that V is a weak solution of (4.2.4) in the sense of Definition 4.2.4.

Step 2: Uniqueness. Finally, let us justify the uniqueness of the solution. Let V and $\widetilde{V}$ be two solutions of the Cauchy problem (4.2.4). If we consider the function $V - \widetilde{V}$, we notice that it satisfies the equation (4.5.4) with $\delta = 0$ and with the source term

$$S = N(V) - N(\widetilde{V}) - \left(W[V] - W[\widetilde{V}]\right).$$

Let us estimate the L^2 norm of $V - \widetilde{V}$. Following the same computations as in Lemma 4.5.1, we find that there exists a positive constant $C > 0$ such that for all $t \in [0,T]$,

$$\|(V - \widetilde{V})(t)\|_{L^2(\mathbb{R}^d)} \leq C \int_0^t \left(\|(V - \widetilde{V})(s)\|_{L^2(\mathbb{R}^d)} + \langle S(s), (V - \widetilde{V})(s)\rangle_{L^2(\mathbb{R}^d)}\right) \mathrm{d}s. \quad (4.5.8)$$

It remains to estimate the scalar product. According to the assumption (4.1.3) satisfied by the nonlinearity N, we get that there exists a positive constant $C_T > 0$ such that for all $s \in [0,t]$,

$$\begin{cases} \displaystyle\int (V - \widetilde{V})(s,\mathbf{x})\,(N(V) - N(\widetilde{V}))(s,\mathbf{x})\,\mathrm{d}\mathbf{x} \leq \kappa_2\,\|(V - \widetilde{V})(s)\|_{L^2(\mathbb{R}^d)}^2, \\[2mm] \displaystyle\int (V - \widetilde{V})(s,\mathbf{x})\,(W[V] - W[\widetilde{V}])(s,\mathbf{x})\,\mathrm{d}\mathbf{x} \leq C_T\,\|V - \widetilde{V}\|_{L^\infty([0,s],L^2(\mathbb{R}^d))}^2. \end{cases}$$

Then, taking the supremum over time in (4.5.8), we get that there exists a positive constant $C_T > 0$ such that for all $t \in [0,T]$:

$$\|V - \widetilde{V}\|_{L^\infty([0,t],L^2(\mathbb{R}^d))} \leq C_T \int_0^t \|V - \widetilde{V}\|_{L^\infty([0,s],L^2(\mathbb{R}^d))}\,\mathrm{d}s.$$

According to Grönwall's inequality, we get that $V = \widetilde{V}$.

4.5.4 Conclusion: proof of Corollary 4.2.7

Let $T > 0$. Let us denote with $(\widetilde{V}, \widetilde{W})$ the weak solution of the equation (4.2.4) provided by Proposition 4.2.5 with initial condition (ρ_0, V_0, W_0). Our proof is organised in two steps. First of all, we claim that for all solution (V, F) of the system (4.1.9), the two functions V and $\widetilde{V}$ coincide almost everywhere on $[0, T] \times \mathbb{R}^d$. Then, we prove the existence of a measure solution F so that $(\widetilde{V}, F)$ is a solution of the system (4.1.9).

Before starting the proof, notice that for all $\mathbf{x} \in \mathbb{R}^d$ such that $\rho_0(\mathbf{x}) = 0$, the system (4.2.4) reduces to the following system of ODEs

$$\begin{cases} \partial_t \widetilde{V} = N(\widetilde{V}) - \widetilde{W}, \\[2mm] \partial_t \widetilde{W} = A(\widetilde{V}, \widetilde{W}). \end{cases} \tag{4.5.9}$$

For almost every $\mathbf{x} \in \mathbb{R}^d$ such that $\rho_0(\mathbf{x}) = 0$, since $V_0(\mathbf{x}) = W_0(\mathbf{x}) = 0$ according to (4.2.12)–(4.2.13), one can directly conclude that for all $t \in [0, T]$,

$$\widetilde{V}(t, \mathbf{x}) = \widetilde{W}(t, \mathbf{x}) = 0.$$

Step 1: Uniqueness. Now, let us prove that for any solution (V, F) on $[0, T]$ of (4.1.9) in the sense of Definition 4.2.6, the function V coincides with $\widetilde{V}$ on $[0, T] \times \mathbb{R}^d$. Suppose that (V, F) is a solution of (4.1.9) such that F has a finite second moment in w. If we define for all $(t, \mathbf{x}) \in [0, T] \times \mathbb{R}^d$

$$\rho_0(\mathbf{x}) \, W(t, \mathbf{x}) := \int w \, F(t, \mathbf{x}, \mathrm{d}w),$$

then the triple $(\rho_0, \rho_0 V, \rho_0 W)$ satisfies the reaction-diffusion equation (4.1.10). On the one hand, by definition, for almost every $\mathbf{x} \in \mathbb{R}^d$ such that $\rho_0(\mathbf{x}) = 0$, for all $t \in [0, T]$,

$$V(t, \mathbf{x}) = \widetilde{V}(t, \mathbf{x}) = 0, \quad W(t, \mathbf{x}) = \widetilde{W}(t, \mathbf{x}) = 0.$$

According to the notion of solution of (4.1.9) from Definition 4.2.6, $V \in L^\infty([0, T], H^2(\mathbb{R}^d))$, so $\Delta_{\mathbf{x}} V(t, \mathbf{x})$ is defined for almost every $\mathbf{x} \in \mathbb{R}^d$. Consequently, the pair (V, W) satisfies (4.2.4) pointwise for all $t \in [0, T]$ and almost every $\mathbf{x} \in \mathbb{R}^d$ such that $\rho_0(\mathbf{x}) = 0$.

On the other hand, for all $\mathbf{x} \in \mathbb{R}^d$ such that $\rho_0(\mathbf{x}) > 0$, the equation (4.1.10) reduces to the reaction-diffusion system (4.2.4). Therefore, (V, W) satisfies the equation (4.2.4) for all $t \in [0, T]$ and almost every $\mathbf{x} \in \mathbb{R}^d$, with initial condition (V_0, W_0). Consequently, the pair (V, W) satisfies the reaction-diffusion system (4.2.4) in the sense of Definition 4.2.4. Thus, by uniqueness of the solution of the equation (4.2.4), we can conclude that

$$(V, W) = (\widetilde{V}, \widetilde{W}).$$

Step 2: Existence. Then, let us prove the existence of a measure solution of the first equation in (4.1.9). With V the first component of the solution of the system (4.2.4), let us consider the transport equation for $t > 0$, $\mathbf{x} \in \mathbb{R}^d$ and $w \in \mathbb{R}$:

$$\begin{cases} \partial_t F(t, \mathbf{x}, w) + \partial_w \left(A(V(t, \mathbf{x}), w) \, F(t, \mathbf{x}, w) \right) = 0, \\[2mm] F|_{t=0} = F_0. \end{cases} \tag{4.5.10}$$

In order to solve (4.5.10), we introduce the associated system of characteristic curves for all $(s, t, \mathbf{x}, w) \in [0, T]^2 \times \mathbb{R}^{d+1}$:

$$\begin{cases} \dfrac{\mathrm{d}}{\mathrm{d}s}\mathcal{W}(s) = A(V(s, \mathbf{x}), \mathcal{W}(s)), \\[2mm] \mathcal{W}(t) = w. \end{cases} \tag{4.5.11}$$

Since the function A grows linearly with respect to w, and the function V is regular enough, we get the global existence and uniqueness of a solution of the characteristic equation (4.5.11). Then, using the theory of characteristics, we get the existence of a unique solution to the transport equation (4.5.10). Then, we directly get from (4.5.10) and the assumptions (4.2.11) and (4.2.12) that there exists a positive constant $C_T > 0$ such that for all $t \in [0, T]$ and all $\mathbf{x} \in \mathbb{R}^d$,

$$\iint_{\mathbb{R}^{d+1}} |w|^2 \, F(t, \mathrm{d}\mathbf{x}, \mathrm{d}w) \leq C_T, \quad \frac{1}{\rho_0(\mathbf{x})} \int_{\mathbb{R}} w \, F(t, \mathbf{x}, \mathrm{d}w) = W(t, \mathbf{x}).$$

Consequently, the unique solution of the system (4.1.9) is (V, F) where (V, W) is the weak solution of (4.2.4) and F is the unique solution of the transport equation (4.5.10).

4.6 Extension to the case of a fat-tailed connectivity kernel

In this section, we extend our main result from Theorem 4.2.8 to another framework of connectivity kernel. More precisely, let us consider a function Ψ satisfying :

$$\int \Psi(\|\mathbf{y}\|) \, \|\mathbf{y}\|^2 \, \mathrm{d}\mathbf{y} = +\infty, \quad \int \Psi(\|\mathbf{y}\|) \, \|\mathbf{y}\|^{2s} \, \mathrm{d}\mathbf{y} < +\infty, \tag{4.6.1}$$

for some fixed constant $s \in (0, 1)$. In order to circumvent the new difficulties caused by this interaction kernel, we have to choose a different rescaling as previously. Following the idea from previous works like [105] for the diffusive limit of collisional kinetic equations, for any rescaling parameter $\varepsilon > 0$, we change the definition of the nonlocal term $\mathcal{K}_\varepsilon[f^\varepsilon]$. More precisely, we now consider the transport equation for $t > 0$ and $(\mathbf{x}, v, w) \in \mathbb{R}^{d+2}$, using the shorthand notation $\mathbf{u} = (v, w)$ and $\mathbf{u}' = (v', w')$:

$$\begin{cases} \partial_t f^\varepsilon(t, \mathbf{x}, \mathbf{u}) + \partial_v \left[f^\varepsilon(t, \mathbf{x}, \mathbf{u}) \left(N(v) - w - \mathcal{K}_\varepsilon[f^\varepsilon](t, \mathbf{x}, v) \right) \right] + \partial_w \left[f^\varepsilon(t, \mathbf{x}, \mathbf{u}) \, A(v, w) \right] = 0, \\[3mm] \mathcal{K}_\varepsilon[f^\varepsilon](t, \mathbf{x}, v) := \dfrac{1}{\varepsilon^{d+2s}} \iint \Psi\left(\dfrac{\|\mathbf{x} - \mathbf{x}'\|}{\varepsilon} \right) (v - v') \, f^\varepsilon(t, \mathbf{x}', \mathbf{u}') \, \mathrm{d}\mathbf{x}' \, \mathrm{d}\mathbf{u}', \\[3mm] f^\varepsilon|_{t=0} = f_0^\varepsilon. \end{cases} \tag{4.6.2}$$

In [105], with a similar rescaling in the collisional terms, the authors recovered in the diffusive limit a fractional diffusion. In the following, we define the fractional Laplace operator of order $s \in (0, 1)$ through

$$(-\Delta_{\mathbf{x}})^s U := \mathcal{F}^{-1} \left(\|\mathbf{k}\|^{2s} \, \mathcal{F}(U)(\mathbf{k}) \right), \tag{4.6.3}$$

where $\mathcal{F}$ stands for the Fourier transform in $\mathbf{x}$. Therefore, passing in the asymptotic limit $\varepsilon \to 0$ in the transport equation (4.6.2), we expect to derive a reaction-diffusion system of FHN type with a fractional spatial diffusion, which reads for any $t > 0$ and $\mathbf{x} \in \mathbb{R}^d$:

$$\begin{cases} \partial_t V(t, \mathbf{x}) + \sigma_s \left[(-\Delta_{\mathbf{x}})^s [\rho_0 V](t, \mathbf{x}) - (-\Delta_{\mathbf{x}})^s [\rho_0](\mathbf{x}) \, V(t, \mathbf{x}) \right] = N(V(t, \mathbf{x})) - W(t, \mathbf{x}), \\[3mm] \partial_t V(t, \mathbf{x}) = A(V(t, \mathbf{x}), W(t, \mathbf{x})). \end{cases} \tag{4.6.4}$$

In the rest of this section, let us assume that the connectivity kernel satisfies the properties (4.6.1) and

$$\Psi > 0 \text{ a.e.,} \quad \int \Psi(\|\mathbf{y}\|) \, \mathrm{d}\mathbf{y} = 1, \quad \lim_{\mathbf{k} \to 0} \left| \widehat{\Psi}(\mathbf{k}) - \left(1 - \sigma_s \|\mathbf{k}\|^{2s} \right) \right| = 0, \qquad (4.6.5)$$

where $\sigma_s > 0$ is a fixed positive constant, and $\widehat{\Psi}$ denotes the Fourier transform of Ψ. A typical example is the connectivity kernel

$$r \mapsto \frac{1}{(1 + r^2)^{s+1/2}}.$$

Then, we state the following Theorem of asymptotic limit from the transport equation (4.6.2) towards the fractional reaction-diffusion system (4.6.4).

Theorem 4.6.1. *Let $T > 0$, and let Ψ be a connectivity kernel satisfying (4.6.1)-(4.6.5). Consider a set of initial data $(f_0^\varepsilon)_{\varepsilon>0}$ satisfying the assumptions (4.2.2)-(4.2.3), and (4.2.14)-(4.2.15). Also consider the initial data (ρ_0, V_0, W_0) satisfying the assumptions (4.2.6)-(4.2.7) such that $\rho_0 \in H^2(\mathbb{R}^d)$, and verifying:*

$$\frac{1}{\varepsilon^{2s}} \|\rho_0^\varepsilon - \rho_0\|_{L^2(\mathbb{R}^d)} \longrightarrow 0, \qquad (4.6.6)$$

$$\int \rho_0^\varepsilon(\mathbf{x}) \left[|V_0^\varepsilon(\mathbf{x}) - V_0(\mathbf{x})|^2 + |W_0^\varepsilon(\mathbf{x}) - W_0(\mathbf{x})|^2 \right] \mathrm{d}\mathbf{x} \longrightarrow 0 \qquad (4.6.7)$$

as $\varepsilon \to 0$. Assume that there exist V and W uniformly bounded on $[0, T] \times \mathbb{R}^d$ and of class $\mathscr{C}^1$ in time, which formally satisfy the fractional reaction-diffusion system (4.6.4) with initial data (V_0, W_0). Then, for all $\varepsilon > 0$, let f^ε be the weak solution of the kinetic equation (4.1.1) on $[0, T]$ provided by Proposition 4.2.2. Then, for all $\varepsilon > 0$, the macroscopic functions $(V^\varepsilon, W^\varepsilon)$ computed from f^ε satisfy

$$\lim_{\varepsilon \to 0} \sup_{t \in [0,T]} \int \rho_0^\varepsilon(\mathbf{x}) \left[|V^\varepsilon(t, \mathbf{x}) - V(t, \mathbf{x})|^2 + |W^\varepsilon(t, \mathbf{x}) - W(t, \mathbf{x})|^2 \right] \mathrm{d}\mathbf{x} = 0. \qquad (4.6.8)$$

Moreover, assume that (ρ_0, V_0, W_0) satisfies (4.2.13), and for all $\mathbf{x} \in \mathbb{R}^d$,

$$\rho_0(\mathbf{x}) = \int F_0(\mathbf{x}, w) \, \mathrm{d}w, \quad W_0(\mathbf{x}) = \begin{cases} \dfrac{1}{\rho_0(\mathbf{x})} \displaystyle\int F_0(\mathbf{x}, w) \, \mathrm{d}w, & \text{if } \rho_0(\mathbf{x}) > 0, \\ \\ 0, & \text{else,} \end{cases}$$

for $F_0 \in \mathcal{M}(\mathbb{R}^{d+1})$. Further consider $(F_0^\varepsilon)_{\varepsilon>0}$ the functions defined for all $\varepsilon > 0$, $(\mathbf{x}, w) \in \mathbb{R}^{d+1}$, with

$$F_0^\varepsilon(\mathbf{x}, w) := \int f_0^\varepsilon(\mathbf{x}, v, w) \, \mathrm{d}v.$$

Therefore, if $F_0^\varepsilon \rightharpoonup F_0$ weakly-$\star$ in $\mathcal{M}(\mathbb{R}^{d+1})$, then we have for all $\varphi \in \mathscr{C}_b^0(\mathbb{R}^{d+2})$,

$$\iint \varphi(\mathbf{x}, v, w) \, f^\varepsilon(t, \mathbf{x}, v, w) \, \mathrm{d}\mathbf{x} \, \mathrm{d}v \, \mathrm{d}w \longrightarrow \int \varphi(\mathbf{x}, V(t, \mathbf{x}), w) \, F(t, \mathbf{x}, w) \, \mathrm{d}\mathbf{x}, \qquad (4.6.9)$$

strongly in $L_{loc}^1(0, T)$ as $\varepsilon \to 0$, where (V, F) is the solution of (4.1.9).

Proof. We follow the same strategy developped in Sections 4.3 and 4.4. We only present the arguments that need to be adapted. Actually, only two results are modified by the new rescaling. First of all, following the steps of the proof of Corollary 4.3.3, we prove that there exists a positive constant $C_T > 0$ such that for all $\varepsilon > 0$:

$$\frac{1}{\varepsilon^d} \int_0^T \iint \Psi\left(\frac{\|\mathbf{x} - \mathbf{x}'\|}{\varepsilon}\right)(v - v')\, f^\varepsilon(t, \mathbf{z})\, f^\varepsilon(t, \mathbf{z}')\, \mathrm{d}\mathbf{z}\, \mathrm{d}\mathbf{z}'\, \mathrm{d}t \ \leq\ C_T\, \varepsilon^{2\,s}. \tag{4.6.10}$$

Consequently, as in Proposition 4.3.4, we also get that there exists another positive constant $\widetilde{C}_T > 0$ such that for all $\varepsilon > 0$,

$$\int_0^T \int |v - V^\varepsilon(t, \mathbf{x})|^2\ f^\varepsilon(t, \mathbf{z})\, \mathrm{d}\mathbf{z}\, \mathrm{d}t\ \leq\ \widetilde{C}_T\, \varepsilon^{2\,s/(d+6)}. \tag{4.6.11}$$

Furthermore, the computation of the relative entropy estimate is follows exactly the same strategy. The only difference is the term $\mathcal{T}_{3,2}$ defined in (4.4.6) in Subsection 4.4.2. As precedently, we separate the diffusions on $\rho_0\, V$ and on ρ_0 as follows:

$$\mathcal{T}_{3,2}\ =\ \mathcal{T}_{3,2,1}\ +\ \mathcal{T}_{3,2,2},$$

where

$$\begin{cases} \mathcal{T}_{3,2,1} := \int \rho_0^\varepsilon\, (V^\varepsilon - V)\, \left[\frac{1}{\varepsilon^{2s}}\left(\Psi_\varepsilon \star_{\mathbf{x}} [\rho_0\, V](t, \mathbf{x}) - \rho_0\, V(t, \mathbf{x})\right) + \sigma_s\, (-\Delta_{\mathbf{x}})^s (\rho_0\, V)(t, \mathbf{x})\right] \mathrm{d}\mathbf{x}, \\[2mm] \mathcal{T}_{3,2,2} := -\int \rho_0^\varepsilon\, (V^\varepsilon - V)\, V(t, \mathbf{x})\, \left[\frac{1}{\varepsilon^{2s}}\left(\Psi_\varepsilon \star_{\mathbf{x}} \rho_0(\mathbf{x}) - \rho_0(\mathbf{x})\right) + \sigma_s\, (-\Delta_{\mathbf{x}})^s \rho_0(\mathbf{x})\right] \mathrm{d}\mathbf{x}. \end{cases}$$

Then, using Young's inequality and the fact that $V \in L^\infty([0, T], L^\infty(\mathbb{R}^d))$, we get:

$$\begin{cases} \mathcal{T}_{3,2,1} \leq \eta(\mathcal{Z}^\varepsilon\,|\,\mathcal{Z}) \\[1mm] \qquad + \frac{1}{2}\,\|\rho_0^\varepsilon\|_{L^\infty} \int \left|\frac{1}{\varepsilon^{2s}}\left(\Psi_\varepsilon \star_{\mathbf{x}} [\rho_0\, V](t, \mathbf{x}) - \rho_0\, V(t, \mathbf{x})\right) + \sigma_s\, (-\Delta_{\mathbf{x}})^s (\rho_0\, V)(t, \mathbf{x})\right|^2 \mathrm{d}\mathbf{x}, \\[3mm] \mathcal{T}_{3,2,2} \leq \eta(\mathcal{Z}^\varepsilon\,|\,\mathcal{Z}) \\[1mm] \qquad + \frac{1}{2}\|\rho_0^\varepsilon\|_{L^\infty}\,\|V\|_{L^\infty}^2 \int \left|\frac{1}{\varepsilon^{2s}}\left(\Psi_\varepsilon \star_{\mathbf{x}} \rho_0(\mathbf{x}) - \rho_0(\mathbf{x})\right) + \sigma_s\, (-\Delta_{\mathbf{x}})^s \rho_0(\mathbf{x})\right|^2 \mathrm{d}\mathbf{x}. \end{cases}$$

The arguments are similar for both terms $\mathcal{T}_{3,2,1}$ and $\mathcal{T}_{3,2,2}$, so we only give the details for the first one. We want to use the fact that the Fourier transform is an isometry in $L^2(\mathbb{R}^d)$. Consequently, if we note $\widetilde{\rho_0\, V}$ the Fourier transform of $\rho_0\, V$, we get for all $t \in [0, T]$:

$$\int \left|\frac{1}{\varepsilon^{2s}}\left(\Psi_\varepsilon \star_{\mathbf{x}} [\rho_0\, V](t, \mathbf{x}) - \rho_0\, V(t, \mathbf{x})\right) + \sigma_s\, (-\Delta_{\mathbf{x}})^s (\rho_0\, V)(t, \mathbf{x})\right|^2 \mathrm{d}\mathbf{x}$$

$$\leq \int \left|\frac{1}{\varepsilon^{2s}}\left(\widehat{\Psi_\varepsilon}(\mathbf{k})\, \widehat{\rho_0\, V}(t, \mathbf{k}) - \widehat{\rho_0\, V}(t, \mathbf{k})\right) + \sigma_s\, \|\mathbf{k}\|^{2s}\, \widehat{\rho_0\, V}(t, \mathbf{k})\right|^2 \mathrm{d}\mathbf{k}$$

$$\leq \int \left|\left[\frac{1}{\varepsilon^{2s}}\left(\widehat{\Psi_\varepsilon}(\mathbf{k}) - 1\right) + \sigma_s\, \|\mathbf{k}\|^{2s}\right] \widehat{\rho_0\, V}(t, \mathbf{k})\right|^2 \mathrm{d}\mathbf{k}.$$

Furthermore, for all $\mathbf{k} \in \mathbb{R}^d$,

$$\widehat{\Psi_\varepsilon}(\mathbf{k})\ =\ \widehat{\Psi}(\varepsilon\,\mathbf{k}).$$

Consequently, using the assumptions (4.6.5) satisfied by Ψ, we get:

$$\int \left| \frac{1}{\varepsilon^{2s}} \left(\Psi_\varepsilon \star_\mathbf{x} [\rho_0 \, V](t, \mathbf{x}) - \rho_0 \, V(t, \mathbf{x}) \right) + \sigma_s \, (-\Delta_\mathbf{x})^s (\rho_0 \, V)(t, \mathbf{x}) \right|^2 \mathrm{d}\mathbf{x}$$

$$\leq \int \left| \frac{1}{\varepsilon^{2s}} \left(\widehat{\Psi}(\varepsilon \, \mathbf{k}) - 1 + \sigma_s \, \|\varepsilon \, \mathbf{k}\|^{2s} \right) \widehat{\rho_0 \, V}(t, \mathbf{k}) \right|^2 \mathrm{d}\mathbf{k}.$$

Hence, using Lebesgue's dominated convergence theorem, we obtain that

$$\begin{cases} \mathcal{T}_{3,2,1} \leq \eta(\mathcal{Z}^\varepsilon \,|\, \mathcal{Z}) + o_{\varepsilon \to 0}(1), \\[2mm] \mathcal{T}_{3,2,2} \leq \eta(\mathcal{Z}^\varepsilon \,|\, \mathcal{Z}) + o_{\varepsilon \to 0}(1). \end{cases} \tag{4.6.12}$$

Thus, we can conclude with the same strategy as in Section 4.4. $\qquad \square$

4.7 Appendix: proof of Lemma 4.5.1

Our approach consists in studying the variations of $\|V_\delta\|_{L^2(\mathbb{R}^d)}$ and $\|\Delta_\mathbf{x} V_\delta\|_{L^2(\mathbb{R}^d)}$, in order to conclude with interpolations. Let $t \in [0, T]$. For the sake of simplicity, in the rest of this proof, we note V instead of V_δ. First of all, we get:

$$\frac{1}{2} \frac{\mathrm{d}}{\mathrm{d}t} \|V\|^2_{L^2(\mathbb{R}^d)} = -\sigma \left(\int (\rho_0 + \delta) \, |\nabla_\mathbf{x} V|^2 \, \mathrm{d}\mathbf{x} - \int (\nabla_\mathbf{x} \rho_0 \cdot \nabla_\mathbf{x} V) \, V \, \mathrm{d}\mathbf{x} \right) + \int S \, V \, \mathrm{d}\mathbf{x}$$

$$= -\sigma \left(\int (\rho_0 + \delta) \, |\nabla_\mathbf{x} V|^2 \, \mathrm{d}\mathbf{x} + \frac{1}{2} \int \Delta_\mathbf{x} \rho_0 \, |V|^2 \, \mathrm{d}\mathbf{x} \right) + \int S \, V \, \mathrm{d}\mathbf{x}.$$

Thus, since $\rho_0 \in \mathscr{C}^3_b(\mathbb{R}^d)$, we can conclude that there exists a constant $C > 0$ such that

$$\frac{1}{2} \frac{\mathrm{d}}{\mathrm{d}t} \|V\|^2_{L^2(\mathbb{R}^d)} + \sigma \int (\rho_0 + \delta) \, |\nabla_\mathbf{x} V|^2 \, \mathrm{d}\mathbf{x} \leq C \, \|V\|^2_{L^2(\mathbb{R}^d)} + \int S \, V \, \mathrm{d}\mathbf{x}. \tag{4.7.1}$$

Then, we also get that

$$\frac{1}{2} \frac{\mathrm{d}}{\mathrm{d}t} \|\Delta_\mathbf{x} V\|^2_{L^2(\mathbb{R}^d)}$$

$$= -\int \Delta_\mathbf{x}((\rho_0 + \delta) \, \nabla_\mathbf{x} V) \cdot \nabla_\mathbf{x} \Delta_\mathbf{x} V \, \mathrm{d}\mathbf{x} + \int \Delta_\mathbf{x}(\nabla_\mathbf{x} \rho_0 \cdot \nabla_\mathbf{x} V) \, \Delta_\mathbf{x} V \, \mathrm{d}\mathbf{x} + \int \Delta_\mathbf{x} S \, \Delta_\mathbf{x} V \, \mathrm{d}\mathbf{x}$$

$$= -\int [\Delta_\mathbf{x} \rho_0 \, \nabla_\mathbf{x} V + 2 \, \Delta_\mathbf{x} V \, \nabla_\mathbf{x} \rho_0 + (\rho_0 + \delta) \, \nabla_\mathbf{x} \Delta_\mathbf{x} V] \cdot \nabla_\mathbf{x} \Delta_\mathbf{x} V \, \mathrm{d}\mathbf{x}$$

$$+ \int [\nabla_\mathbf{x} \Delta_\mathbf{x} \rho_0 \cdot \nabla_\mathbf{x} V + 2 \, \Delta_\mathbf{x} \rho_0 \, \Delta_\mathbf{x} V + \nabla_\mathbf{x} \rho_0 \cdot \nabla_\mathbf{x} \Delta_\mathbf{x} V] \, \Delta_\mathbf{x} V \, \mathrm{d}\mathbf{x} + \int \Delta_\mathbf{x} S \, \Delta_\mathbf{x} V \, \mathrm{d}\mathbf{x}.$$

Using Green's formula on the term $\int \Delta_{\mathbf{x}} \rho_0 \, \nabla_{\mathbf{x}} V \cdot \nabla_{\mathbf{x}} \Delta_{\mathbf{x}} V \, \mathrm{d}\mathbf{x}$, we compute that

$$
\begin{aligned}
\frac{1}{2} &\frac{\mathrm{d}}{\mathrm{d}t} \| \Delta_{\mathbf{x}} V \|_{L^2(\mathbb{R}^d)}^2 \\
&= - \int (\rho_0 + \delta) \, |\nabla_{\mathbf{x}} \Delta_{\mathbf{x}} V|^2 \, \mathrm{d}\mathbf{x} \, + \, 3 \int \Delta_{\mathbf{x}} \rho_0 \, |\Delta_{\mathbf{x}} V|^2 \, \mathrm{d}\mathbf{x} \, + \, \int \nabla_{\mathbf{x}} \Delta_{\mathbf{x}} \rho_0 \cdot \nabla_{\mathbf{x}} V \, \Delta_{\mathbf{x}} V \, \mathrm{d}\mathbf{x} \\
&\quad + \int \Delta_{\mathbf{x}} S \, \Delta_{\mathbf{x}} V \, \mathrm{d}\mathbf{x} \\
&\leq - \int (\rho_0 + \delta) \, |\nabla_{\mathbf{x}} \Delta_{\mathbf{x}} V|^2 \, \mathrm{d}\mathbf{x} \, + \, 3 \, \| \rho_0 \|_{\mathscr{C}^2(\mathbb{R}^d)} \| \Delta_{\mathbf{x}} V \|_{L^2(\mathbb{R}^d)}^2 \\
&\quad + \, \| \rho_0 \|_{\mathscr{C}^3(\mathbb{R}^d)} \| \nabla_{\mathbf{x}} V \|_{L^2(\mathbb{R}^d)} \| \Delta_{\mathbf{x}} V \|_{L^2(\mathbb{R}^d)} \, + \, \int \Delta_{\mathbf{x}} S \, \Delta_{\mathbf{x}} V \, \mathrm{d}\mathbf{x} \\
&\leq - \int (\rho_0 + \delta) \, |\nabla_{\mathbf{x}} \Delta_{\mathbf{x}} V|^2 \, \mathrm{d}\mathbf{x} \, + \, C \left(\| V \|_{L^2(\mathbb{R}^d)}^2 \, + \, \| \Delta_{\mathbf{x}} V \|_{L^2(\mathbb{R}^d)}^2 \right) \, + \, \int \Delta_{\mathbf{x}} S \, \Delta_{\mathbf{x}} V \, \mathrm{d}\mathbf{x},
\end{aligned}
$$

where $C > 0$ is a positive constant. Consequently, we get that for all $t \in [0, T]$,

$$
\begin{aligned}
\frac{1}{2} \frac{\mathrm{d}}{\mathrm{d}t} \, \| \Delta_{\mathbf{x}} V(t) \|_{L^2(\mathbb{R}^d)}^2 \, &+ \, \int (\rho_0 + \delta) \, |\nabla_{\mathbf{x}} \Delta_{\mathbf{x}} V|^2 \, \mathrm{d}\mathbf{x} \\
&\leq C \left(\| \Delta_{\mathbf{x}} V(t) \|_{L^2(\mathbb{R}^d)}^2 \, + \, \| V(t) \|_{L^2(\mathbb{R}^d)}^2 \right) \, + \, \int \Delta_{\mathbf{x}} S(t) \, \Delta_{\mathbf{x}} V(t) \, \mathrm{d}\mathbf{x}. \quad (4.7.2)
\end{aligned}
$$

Finally, integrating the estimates (4.7.1) and (4.7.2) between 0 and t for $t \in [0, T]$, we get the estimate (4.5.5) since the H^2 norm is equivalent to the norm $\| \cdot \|_{L^2(\mathbb{R}^d)} + \| \Delta_{\mathbf{x}} \cdot \|_{L^2(\mathbb{R}^d)}$.

4.8   Appendix: proof of Corollary 4.5.2

For the sake of simplicity, in the rest of this section, we note V instead of V_δ. According to Lemma 4.5.1, the estimate (4.5.5) holds with $S = N(V) - W[V]$. To obtain Corollary 4.5.2 from the energy estimate (4.5.5), we need to estimate the scalar product $\langle V, N(V) \rangle_{H^2(\mathbb{R}^d)}$. First of all, for all $t \in [0, T]$, since N satisfies the property (4.1.3), we have:

$$
\int V \, N(V) \, \mathrm{d}\mathbf{x} \, \leq \, \kappa_1 \, \| V \|_{L^2(\mathbb{R}^d)}^2 \, - \, \kappa_1' \| V \|_{L^4(\mathbb{R}^d)}^4 \, \leq \, \kappa_1 \, \| V \|_{L^2(\mathbb{R}^d)}^2.
$$

Then, we only give details of computation of the integral of the product of $\Delta_{\mathbf{x}} V$ and $\Delta_{\mathbf{x}} N(V)$. Using Young's inequality for some small parameter $\lambda > 0$, we also obtain:

$$
\begin{aligned}
\int &\Delta_{\mathbf{x}} V \, \Delta_{\mathbf{x}} N(V) \, \mathrm{d}\mathbf{x} \\
&= \int |\Delta_{\mathbf{x}} V|^2 \left[-3|V|^2 + 2(1 + \theta) V - \theta \right] \mathrm{d}\mathbf{x} \, + \, \int \Delta_{\mathbf{x}} V \, |\nabla_{\mathbf{x}} V|^2 \left[-6V + 2(1 + \theta) \right] \mathrm{d}\mathbf{x} \\
&\leq -3 \int |\Delta_{\mathbf{x}} V|^2 \, |V|^2 \, \mathrm{d}\mathbf{x} \, - \, \theta \int |\Delta_{\mathbf{x}} V|^2 \, \mathrm{d}\mathbf{x} \\
&\quad + \frac{(1 + \theta)}{\lambda} \int |\Delta_{\mathbf{x}} V|^2 \, \mathrm{d}\mathbf{x} \, + \, (1 + \theta) \, \lambda \int |\Delta_{\mathbf{x}} V|^2 \, |V|^2 \, \mathrm{d}\mathbf{x} \\
&\quad + \frac{3}{\lambda} \int |\nabla_{\mathbf{x}} V|^4 \, \mathrm{d}\mathbf{x} \, + \, 3 \, \lambda \int |V|^2 \, |\Delta_{\mathbf{x}} V|^2 \, \mathrm{d}\mathbf{x} \\
&\quad + (1 + \theta) \int |\Delta_{\mathbf{x}} V|^2 \, \mathrm{d}\mathbf{x} \, + \, (1 + \theta) \int |\nabla_{\mathbf{x}} V|^4 \, \mathrm{d}\mathbf{x}.
\end{aligned}
$$

Consequently, if we consider λ small enough so that $(1 + \theta)\lambda + 3\lambda \leq 3$, we obtain:

$$\int \Delta_{\mathbf{x}} V \, \Delta_{\mathbf{x}} N(V) \, \mathrm{d}\mathbf{x} \leq \left(1 + \frac{1}{\lambda}\right)(1 + \theta) \int |\Delta_{\mathbf{x}} V|^2 \, \mathrm{d}\mathbf{x} + \left(1 + \theta + \frac{3}{\lambda}\right) \int |\nabla_{\mathbf{x}} V|^4 \, \mathrm{d}\mathbf{x}. \quad (4.8.1)$$

Therefore, to conclude, we only need to find a uniform bound of the L^4 norm of $\nabla_{\mathbf{x}} V(t)$. We apply the Gagliardo-Nirenberg inequality on $\|\nabla_{\mathbf{x}} V_0\|_{L^4(\mathbb{R}^d)}$, which yields that there exists a positive constant $C > 0$ such that:

$$\|\nabla_{\mathbf{x}} V_0\|_{L^4(\mathbb{R}^d)} \leq C \|V_0\|_{H^2(\mathbb{R}^d)}^{\frac{d}{4}} \|\nabla_{\mathbf{x}} V_0\|_{L^2(\mathbb{R}^d)}^{1 - \frac{d}{4}} < +\infty,$$

Hence, since $V_0 \in H^2(\mathbb{R}^d)$, we have $\nabla_{\mathbf{x}} V_0 \in L^4(\mathbb{R}^d)$, and it still holds if we replace V_0 with W_0. Furthermore, $\nabla_{\mathbf{x}} V$ satisfies in the weak sense the following equation on $(0, T] \times \mathbb{R}^d$

$$\partial_t (\nabla_{\mathbf{x}} V) = \sigma \left[\nabla_{\mathbf{x}} (\rho_0 \Delta_{\mathbf{x}} V) + 2 \nabla_{\mathbf{x}} (\nabla_{\mathbf{x}} \rho_0 \cdot \nabla_{\mathbf{x}} V) \right] + \nabla_{\mathbf{x}} V \, N'(V) - \nabla_{\mathbf{x}} W[V].$$

We can use this last equation and similar computations as before to estimate the L^4 norm of $\nabla_{\mathbf{x}} V$. Thus, we get that there exists a positive constant $K_T > 0$ such that

$$\sup_{t \in [0,T]} \|\nabla_{\mathbf{x}} V(t)\|_{L^4(\mathbb{R}^d)}^4 \leq K_T. \quad (4.8.2)$$

Therefore, we conclude from (4.8.1)-(4.8.2) that there exists a positive constant C such that for all $t \in [0, T]$:

$$\int \Delta_{\mathbf{x}} V \, \Delta_{\mathbf{x}} N(V) \, \mathrm{d}\mathbf{x} \leq C \|V\|_{H^2(\mathbb{R}^d)}^2 + K_T.$$

Chapter 5

Asymptotic preserving schemes for the FitzHugh-Nagumo transport equation with strong local interactions

Article soumis en 2020, en collaboration avec mon directeur de thèse Francis Filbet.

Contents

Abstract

This paper is devoted to the numerical approximation of the spatially-extended FitzHugh-Nagumo transport equation with strong local interactions based on a particle method. In this regime, the time step can be subject to stability constraints related to the interaction kernel. To avoid this limitation, our approach is based on higher-order implicit-explicit numerical schemes. Thus, when the magnitude of the interactions becomes large, this method provides a consistent discretization of the macroscopic reaction-diffusion FitzHugh-Nagumo system. We carry out some theoretical proofs and perform several numerical experiments that establish a solid validation of the method and its underlying concepts.

5.1 Introduction

As in the last chapter, let us consider a set of neurons which can be described at any time $t > 0$ and any position $\mathbf{x} \in \mathbb{R}^d$, $d \in \{1, 2, 3\}$ with a distribution function $f^\varepsilon(t, \mathbf{x}, \cdot)$ solution to the following nonlocal mean-field equation:

$$\begin{cases} \partial_t f^\varepsilon + \partial_v \left[f^\varepsilon \left(N(v) - w + \mathcal{K}_\varepsilon[f^\varepsilon] \right) \right] + \partial_w \left[f^\varepsilon A(v, w) \right] = 0, \\ f^\varepsilon(t = 0, \mathbf{x}, .) = f_0^\varepsilon(\mathbf{x}, .), \end{cases} \tag{5.1.1}$$

with $\mathcal{K}_\varepsilon[f^\varepsilon]$ and A given for all pair voltage-adaptation $(v, w) \in \mathbb{R}^2$ by

$$\begin{cases} \mathcal{K}_\varepsilon[f^\varepsilon](t, \mathbf{x}, v) = \dfrac{1}{\varepsilon^2} \displaystyle\int_{\mathbb{R}^d} \int_{\mathbb{R}^2} \Psi_\varepsilon \left(\|\mathbf{x} - \mathbf{x}'\| \right) (v' - v) f^\varepsilon(t, \mathbf{x}', dv', dw') d\mathbf{x}', \\ A(v, w) = \tau (v + a - b w), \end{cases} \tag{5.1.2}$$

where $\tau \geq 0$, $a \in \mathbb{R}$ and $b \geq 0$ are three given constants. Up to consider the translated variable $v + a$ instead of v, we assume in the following that $a = 0$. Furthermore, we set $N(v) = v (1 - v) (v - \theta)$, with $\theta \in (0, 1)$ a fixed parameter, the nonlinearity which models the cell excitability. Then, we consider a small scaling parameter $\varepsilon > 0$ which is involved in spatial coupling through

$$\Psi_\varepsilon(\|\mathbf{y}\|) := \frac{1}{\varepsilon^d} \Psi \left(\frac{\|\mathbf{y}\|}{\varepsilon} \right), \quad \mathbf{y} \in \mathbb{R}^d,$$

where $\Psi : \mathbb{R}^+ \to \mathbb{R}^+$. This scaling with respect to ε means that when ε goes to zero, space interactions are highly dominated by local ones compared to long range correlations. In the rest of this chapter, we assume that the connectivity kernel Ψ is nonnegative and rapidly vanishing at infinity, hence we introduce the following quantities,

$$\begin{cases} \overline{\Psi} := \displaystyle\int_{\mathbb{R}^d} \Psi(\|\mathbf{y}\|) \, d\mathbf{y} > 0, \\ \overline{\sigma} := \dfrac{1}{2} \displaystyle\int_{\mathbb{R}^d} \Psi(\|\mathbf{y}\|) \|\mathbf{y}\|^2 d\mathbf{y} > 0, \end{cases} \tag{5.1.3}$$

which will play an important role later. A typical example for Ψ is a Gaussian function, or the indicator function in a compact set.

Here, we want to construct numerical solutions to (5.1.1)–(5.1.2) using particle methods, which consist in approximating the distribution function by a finite number of macro-particles. The trajectories of these particles are determined from the characteristic curves corresponding to the (5.1.1). Indeed, for any initial data f_0^ε with finite second moments in $\mathbf{x} \in \mathbb{R}^d$ and

$(v, w) \in \mathbb{R}^2$, the solution to (5.1.1)–(5.1.2) is uniquely defined as the push-forward of f_0^ε by the flow of the characteristic system of equations associated to (5.1.1)–(5.1.2), which can be written for $(t, \mathbf{x}) \in \mathbb{R}^+ \times \mathbb{R}^d$ and $(v, w) \in \mathbb{R}^2$ as

$$
\begin{cases}
\dfrac{\mathrm{d}\mathcal{V}^\varepsilon}{\mathrm{d}t} = N(\mathcal{V}^\varepsilon) - \mathcal{W}^\varepsilon + \mathcal{K}_\varepsilon[f^\varepsilon](t, \mathbf{x}, \mathcal{V}^\varepsilon), \\[2mm]
\dfrac{\mathrm{d}\mathcal{W}^\varepsilon}{\mathrm{d}t} = A(\mathcal{V}^\varepsilon, \mathcal{W}^\varepsilon), \\[2mm]
\mathcal{V}^\varepsilon(0) = v, \quad \mathcal{W}^\varepsilon(0) = w.
\end{cases}
\tag{5.1.4}
$$

Then we denote by $\Phi_{t,\mathbf{x}}$ the flow $(v, w) \in \mathbb{R}^2 \mapsto \Phi_{t,\mathbf{x}}(v, w) = (\mathcal{V}^\varepsilon, \mathcal{W}^\varepsilon)(t, \mathbf{x}, v, w) \in \mathbb{R}^2$, hence the solution to (5.1.1)–(5.1.2) is given by

$$
f^\varepsilon(t, \mathbf{x}, .) = \Phi_{t,\mathbf{x}} \# f_0^\varepsilon(\mathbf{x}, .),
\tag{5.1.5}
$$

that is, for any test-function φ and $B \subset \mathbb{R}^2$,

$$
\int_B \varphi(v, w) \, f^\varepsilon(t, \mathbf{x}, \mathrm{d}v, \mathrm{d}w) = \int_{\Phi_{t,\mathbf{x}}^{-1}(B)} \varphi \circ \Phi_{t,\mathbf{x}} \, f_0^\varepsilon(\mathbf{x}, \mathrm{d}v, \mathrm{d}w).
$$

We also define for all $(t, \mathbf{x}) \in \mathbb{R}^+ \times \mathbb{R}^d$ and $\varepsilon > 0$ the following macroscopic quantities,

$$
\rho^\varepsilon \begin{pmatrix} 1 \\ V^\varepsilon \\ W^\varepsilon \end{pmatrix}(t, \mathbf{x}) := \int_{\mathbb{R}^2} \begin{pmatrix} 1 \\ v \\ w \end{pmatrix} f^\varepsilon(t, \mathbf{x}, \mathrm{d}v, \mathrm{d}w),
\tag{5.1.6}
$$

so that $\rho^\varepsilon(t, \mathbf{x})$ is the average neuron density in the network at time t and location $\mathbf{x}$, and $(V^\varepsilon, W^\varepsilon)$ is the average pair membrane potential - adaptation variable. Therefore, we observe that $\mathcal{K}_\varepsilon[f^\varepsilon]$ may be written with respect to the macroscopic quantities ρ^ε and $\rho^\varepsilon V^\varepsilon$ as

$$
\mathcal{K}_\varepsilon[f^\varepsilon](., v) = \frac{1}{\varepsilon^2} \left[\Psi_\varepsilon \star (\rho^\varepsilon V^\varepsilon) - \Psi_\varepsilon \star \rho^\varepsilon v \right],
\tag{5.1.7}
$$

where $\star$ denotes the standard convolution product in $\mathbf{x}$.

Before describing and analyzing a class of numerical methods for (5.1.1)–(5.1.2) in the presence of strong local space interactions ($\varepsilon \ll 1$), we first briefly expound what may be expected from the continuous model in the limit $\varepsilon \to 0$.

On the one hand, by integrating (5.1.1) with respect to $(v, w) \in \mathbb{R}^2$, we observe that for all $t \geq 0$

$$
\rho^\varepsilon(t, \mathbf{x}) = \rho_0^\varepsilon(\mathbf{x}), \quad \mathbf{x} \in \mathbb{R}^d
$$

and moreover we suppose that it does not depend neither on ε, so that $\rho^\varepsilon(t, .) = \rho_0$ with

$$
\rho_0 \geq 0, \quad \rho_0 \in L^\infty(\mathbb{R}^d).
\tag{5.1.8}
$$

On the other hand, using (5.1.7), we observe that

$$
\int_{\mathbb{R}^2} \mathcal{K}_\varepsilon[f^\varepsilon](t, \mathbf{x}, v) \, f^\varepsilon(t, \mathbf{x}, \mathrm{d}v \, \mathrm{d}w) = \frac{\rho_0}{\varepsilon^2} \left[\Psi_\varepsilon \star (\rho_0 \, V^\varepsilon) - (\Psi_\varepsilon \star \rho_0) \, V^\varepsilon \right].
\tag{5.1.9}
$$

Hence, multiplying (5.1.1) by v (resp. w) and integrating with respect to $(v, w) \in \mathbb{R}^2$ and using (5.1.9), we get a time evolution equation for the macroscopic quantities $(\rho_0 V^\varepsilon, \rho_0 W^\varepsilon)$ as

$$
\begin{cases}
\partial_t(\rho_0 \, V^\varepsilon) - \dfrac{\rho_0}{\varepsilon^2} \left[\Psi_\varepsilon \star (\rho_0 \, V^\varepsilon) - (\Psi_\varepsilon \star \rho_0) \, V^\varepsilon \right] = \displaystyle\int_{\mathbb{R}^2} N(v) \, f^\varepsilon(., \mathrm{d}v, \mathrm{d}w) - \rho_0 W^\varepsilon, \\[3mm]
\partial_t(\rho_0 \, W^\varepsilon) = \rho_0 \, A(V^\varepsilon, W^\varepsilon).
\end{cases}
\tag{5.1.10}
$$

Of course, this system is not closed since the right hand side of the equation on $\rho_0 V^\varepsilon$ again depends on the distribution function f^ε. However, in the regime of strong local interactions [47], that is, in the limit $\varepsilon \to 0$, the singular term in ε^{-2} indicates that the distribution function f^ε converges towards a Dirac distribution in v centered in V^ε. Then applying a Taylor expansion of the solution V^ε, the right hand side of (5.1.10) gives rise to a diffusive operator for the spatial interactions at zeroth order with respect to ε. It yields that $(\rho_0 V^\varepsilon, \rho_0 W^\varepsilon)$ converges towards a limit pair $(\rho_0 V, \rho_0 W)$ satisfying the FHN reaction-diffusion system,

$$
\begin{cases}
\rho_0 \left(\partial_t V - \overline{\sigma} \left[\Delta \left(\rho_0 V \right) - V \Delta \rho_0 \right] - N(V) + W \right) = 0, \\[2mm]
\rho_0 \left(\partial_t W - A(V, W) \right) = 0,
\end{cases}
\tag{5.1.11}
$$

where $\overline{\sigma}$ is defined in (5.1.3). We refer to [47] for more details on this asymptotic analysis.

We now come to our main concern in the present chapter and seek after a numerical method that is able to capture these expected asymptotic properties, even when numerical discretization parameters are kept independent of ε hence are not adapted to the stiffness degree of the space interactions. Our objective enters in the general framework of so-called Asymptotic Preserving (AP) schemes, first introduced and widely studied for dissipative systems as in [90, 98]. Yet, in opposition with collisional kinetic equations in hydrodynamic or diffusion limits, transport equations like (5.1.1) involve of course some stiffness in time but it is also crucial to take care of the space discretization in order to capture the correction terms of the non-local operator $\mathcal{K}_\varepsilon[f^\varepsilon]$. By many respects this makes the identification of suitable schemes much more challenging.

In [48], the author proposed a numerical approximation to (5.1.1)–(5.1.2) using a standard particle method. However, as the parameter ε goes to 0, that is when the range of interactions between neurons shrinks and their amplitude grows, the time step and spatial grid size have to tend to zero too, hence the scheme cannot be consistent with the limit system (5.1.11) in the limit $\varepsilon \to 0$. In a different context [68], F. Filbet & L. M. Rodrigues developed a particle method for the Vlasov-Poisson system with a strong external magnetic field, which is able to capture accurately the non stiff part of the evolution while allowing for coarse discretization parameters.

Here, we show how this approach may be extended to transport equations like (5.1.1) to deal with the time discretization. However, it is not sufficient since an appropriate space discretization technique is mandatory to capture the diffusive operator in (5.1.11) in the limit $\varepsilon \to 0$. In [29], the authors apply a spectral collocation method to provide numerical approximations of reaction-diffusion equations, with fractional spatial diffusion. Their method obviously can also be applied for local diffusions as in the FitzHugh-Nagumo reaction-diffusion system (5.1.11). On the other hand, the spectral collocation method also provides numerical approximations of differential equations with integral terms. For example, in [64, 66, 67, 69, 114] the authors use fast spectral methods for the non-local Boltzmann operator, which lead to compute the time evolution of Fourier coefficients of the solution instead of the solution itself. Therefore, this approach considerably simplifies the computation of the integral collision term and may be applied in our context. Moreover, we will show that a suitable formulation allows to perform a Taylor expansion of the solution in the Fourier space and to recover a consistent discretization of the macroscopic system (5.1.11) in the limit $\varepsilon \to 0$, which guarantee the asymptotic preserving property. Finally, another difficulty in our framework is to prove the convergence when ε vanishes of the nonlinear term in (5.1.4) involving the cubic function N. The idea to circumvent this issue is to use, as in the continuous framework [47], the stiff term in (5.1.4), which stands for the interactions between neurons throughout the network to prove that the solution f^ε converges towards a Dirac mass in v, that is all the membrane potential of the neurons at position $\mathbf{x}$ are synchronized. Thus, it is possible to identify the asymptotic of the nonlinear term in (5.1.4). We will show that the particle approximation of the distribution in $(v, w) \in \mathbb{R}^2$ is particularly well suited to achieve this.

The rest of the paper is organized as follows. In Section 5.2, we present the particle method for the transport equation (5.1.1)–(5.1.2) and propose an apropriate time discretization technique in order to preserve the correct asymptotic when $\varepsilon \ll 1$. Then, we provide first and second order schemes and verify the consistency when ε tends to zero. Finally, in Section 5.3, we present some numerical simulations to illustrate our results, and to study the dynamics of (5.1.1)–(5.1.2) with different different sets of parameters and different heterogeneous neuron densities.

5.2 A numerical scheme for the FitzHugh-Nagumo transport equation

This section is devoted to the construction of the numerical schemes for (5.1.1)- (5.1.2). We first focus on the discretization of the nonlocal operator $\mathcal{K}_\varepsilon[f^\varepsilon]$ in (5.1.2), for which we propose a spectral collocation method based on the discrete fast Fourier method. Then, we treat the transport equation (5.1.1) using a particle method for the microscopic variable $(v, w) \in \mathbb{R}^2$ and provide first and second order semi-implicit schemes for the time discretization. This algorithm is constructed in order to get a consistent approximation in the limit $\varepsilon \to 0$.

For sake of clarity, we drop the dependence with respect to ε on the distribution function f^ε and on the non-local operator $\mathcal{K}_\varepsilon[f^\varepsilon]$.

5.2.1 Computation of the Non-local operator

We first look for an approximation of the operator $\mathcal{K}[f]$ given in (5.1.2). In view of applying a Fourier spectral method in space, we write $\mathcal{K}[f]$ as

$$\mathcal{K}[f](t, \mathbf{x}, v) = \frac{1}{\varepsilon^2} \int_{\mathbb{R}^d} \Psi_\varepsilon(\|\mathbf{y}\|) \, \rho_0(\mathbf{x} - \mathbf{y}) \, (V(t, \mathbf{x} - \mathbf{y}) - v) \, \mathrm{d}\mathbf{y} \, .$$

Then we define a truncated operator $\mathcal{K}^S[f]$ in the following way.

Lemma 5.2.1. *Suppose that* $\mathrm{Supp}\,(\rho_0) \subset \mathcal{B}(0, S)$*, where* $\mathcal{B}(0, S)$ *is the ball of radius* $S > 0$ *centered at the origin and choose* $\varepsilon \in (0, 1)$*. Then, for any* $(t, \mathbf{x}, v, w) \in \mathbb{R}^+ \times \mathcal{B}(0, S) \times \mathbb{R}^2$*,* f *is solution to*

$$\partial_t f + \partial_v \left[f \left(N(v) - w + \mathcal{K}^S[f] \right) \right] + \partial_w \left[f A(v, w) \right] = 0,$$

where for any $(\mathbf{x}, v) \in \mathcal{B}(0, S) \times \mathbb{R}$*,*

$$\mathcal{K}^S[f](t, \mathbf{x}, v) = \frac{\chi_{\mathcal{B}(0,S)}}{\varepsilon^2}(\mathbf{x}) \int_{\mathcal{B}(0,2S)} \Psi_\varepsilon(\|\mathbf{y}\|) \, \rho_0(\mathbf{x} - \mathbf{y}) \, (V(t, \mathbf{x} - \mathbf{y}) - v) \, \mathrm{d}\mathbf{x}', \qquad (5.2.1)$$

where $\chi_{\mathcal{B}(0,S)}$ *denotes the characteristic function in the ball* $\mathcal{B}(0, S)$*.*

Proof. On the one hand, since $\mathrm{Supp}\,(\rho_0) \subset \mathcal{B}(0, S)$ and for all $t \geq 0$, the density $\rho(t) = \rho_0$, we get that for any $\mathbf{x} \in \mathbb{R}^d$, the transport equation (5.1.1) can be written as

$$\partial_t f + \partial_v \left[f \left(N(v) - w + \chi_{\mathcal{B}(0,S)} \mathcal{K}[f] \right) \right] + \partial_w \left[f A(v, w) \right] = 0 \, .$$

Then it is enough to consider only $\mathbf{x} \in \mathcal{B}(0, S)$. On the other hand, the domain of integration of the operator $\mathcal{K}[f]$ is such that

$$\|\mathbf{y}\| \leq \|\mathbf{x}\| + \|\mathbf{y} - \mathbf{x}\| \leq 2 \, S,$$

hence for any $(t, \mathbf{x}, v) \in \mathbb{R}^+ \times \mathcal{B}(0, S) \times \mathbb{R}$,

$$\mathcal{K}[f](t, \mathbf{x}, v) = \frac{1}{\varepsilon^2} \int_{\mathcal{B}(0,2S)} \Psi_\varepsilon(\|\mathbf{y}\|) \, \rho_0(\mathbf{x} - \mathbf{y}) \, (V(t, \mathbf{x} - \mathbf{y}) - v) \, \mathrm{d}\mathbf{y}.$$

Thus, we define the truncated operator (5.2.1) as $\varepsilon^2 \, \mathcal{K}^S[f] = \chi_{B(0,S)} \, \mathcal{K}[f]$. $\qquad \square$

Actually the operator $\mathcal{K}^S[f]$ can be seen as convolution products between $(\rho_0, \rho_0 V)$ and the connectivity kernel Ψ_ε, that is,

$$\mathcal{K}^S[f](t, \mathbf{x}, v) = \frac{1}{\varepsilon^2} \left(\mathcal{L}^S[\rho_0 V](t, \mathbf{x}) - v\, \mathcal{L}^S[\rho_0](\mathbf{x}) \right),$$

where $\mathcal{L}^S$ is given by

$$\mathcal{L}^S[u] = \Psi_\varepsilon \star u, \quad u \in \{\rho_0, \rho_0 V\}. \tag{5.2.2}$$

In the sequel, we choose for simplicity $S = \pi/2$ such that $\mathcal{B}(0, S) \subset \mathbb{T} := [-\pi, \pi]^d$, and consider a set of equidistant points $(\mathbf{x}_j)_{j \in \mathbf{J}_{n_x}} \subset \mathbb{T}$ with $\mathbf{J}_{n_x} := [\![-n_x/2, n_x/2 - 1]\!]^d$ where n_x is an even integer. An efficient strategy to approximate this nonlocal term is the spectral or spectral collocation methods [82, 114]. We suppose that the density ρ_0 and the macroscopic membrane potential V are both known at the mesh points $(\mathbf{x}_j)_{j \in \mathbf{J}_{n_x}}$, then we compute an approximation of the Fourier coefficients for $u \in \{\rho_0, \rho_0 V\}$ as,

$$\widetilde{u}(t, \mathbf{k}) := \frac{1}{n_x^d} \sum_{j \in \mathbf{J}_{n_x}} u(t, \mathbf{x}_j)\, e^{-i\, \mathbf{k} \cdot \mathbf{x}_j}, \quad \mathbf{k} \in \mathbf{J}_{n_x}.$$

and get a trigonometric polynomial

$$u_{n_x}(t, \mathbf{x}) := \sum_{\mathbf{k} \in \mathbf{J}_{n_x}} \widetilde{u}(t, \mathbf{k})\, e^{i\, \mathbf{k} \cdot \mathbf{x}}, \quad u \in \{\rho_0, \rho_0 V\}.$$

Therefore, we substitute this polynomials in (5.2.2), which yields a discrete operator $\mathcal{L}^S_{n_x}$ given by

$$\mathcal{L}^S_{n_x}[u] := \sum_{\mathbf{k} \in \mathbf{J}_{n_x}} \widetilde{\mathcal{L}}^S[u](t, \mathbf{k})\, e^{i\, \mathbf{k} \cdot \mathbf{x}}, \tag{5.2.3}$$

where $\widetilde{\mathcal{L}}^S[u]$ is given by

$$\widetilde{\mathcal{L}}^S[u](t, \mathbf{k}) = (2\pi)^d\, \widehat{\Psi}_\varepsilon(\mathbf{k})\, \widetilde{u}(t, \mathbf{k}) \tag{5.2.4}$$

and $\widehat{\Psi}_\varepsilon$ is the expansion coefficient depending on the connectivity kernel

$$\widehat{\Psi}_\varepsilon(\mathbf{k}) = \frac{1}{(2\pi)^d} \int_{\mathbb{T}} \Psi_\varepsilon(\|\mathbf{x}\|)\, e^{-i\, \mathbf{k} \cdot \mathbf{x}}\, \mathrm{d}\mathbf{x}. \tag{5.2.5}$$

Finally the approximation $\mathcal{K}^S_{n_x}[f]$ of the operator $\mathcal{K}^S[f]$ is provided by

$$\mathcal{K}^S_{n_x}[f](t, \mathbf{x}, v) = \frac{1}{\varepsilon^2} \left(\mathcal{L}^S_{n_x}[\rho_0 V](t, \mathbf{x}) - v\, \mathcal{L}^S_{n_x}[\rho_0](\mathbf{x}) \right). \tag{5.2.6}$$

Let us focus on the computation of the kernel modes $(\widehat{\Psi}_\varepsilon(\mathbf{k}))_{\mathbf{k} \in \mathbf{J}_{n_x}}$ for any fixed parameter $\varepsilon > 0$. In the spirit of [114] for the Boltzmann equation, our purpose is to prove that these coefficients can be computed as one-dimensional integrals, so that we can store them in an array, but also to compute the asymptotic limit when $\varepsilon \to 0$ in order to ensure that the scheme is consistent and stable when $\varepsilon \ll 1$.

Using the change of variable $\mathbf{x} = r\, \omega$, for $r \geq 0$ and $\omega \in \mathbb{S}^{d-1}$, we get:

$$\widehat{\Psi}_\varepsilon(\mathbf{k}) = \frac{1}{(2\pi)^d} \int_0^\pi \Psi_\varepsilon(r)\, r^{d-1}\, I(\mathbf{k}, r)\, \mathrm{d}r,$$

where

$$I(\mathbf{k}, r) := \int_{\mathbb{S}^{d-1}} \exp(-i\, r\, \mathbf{k} \cdot \omega)\, \mathrm{d}\omega.$$

128

Then, changing the variable r into $s = r/\varepsilon$, we get

$$\widehat{\Psi}_\varepsilon(\mathbf{k}) = \frac{1}{(2\pi)^d} \int_0^{\pi/\varepsilon} \Psi(s)\, s^{d-1} I(\mathbf{k}, \varepsilon\, s)\, \mathrm{d}s.$$

To complete the computation of the function I, we have to study separately each possible value for the spatial dimension $d \in \{1, 2, 3\}$.

One-dimensional case: $d = 1$.   Since $\mathbb{S}^0 = \{-1, 1\}$, it is straightforward to check that for any $\mathbf{k} \in \mathbf{J}_{n_x}$,

$$I(\mathbf{k}, r) = 2 \cos(r\, |\mathbf{k}|),$$

hence we get:

$$\widehat{\Psi}_\varepsilon(\mathbf{k}) = \frac{1}{\pi} \int_0^{\pi/\varepsilon} \Psi(s)\, \cos(\varepsilon\, s\, |\mathbf{k}|)\, \mathrm{d}s.$$

Two-dimensional case: $d = 2$.   Let $r \geq 0$ and $\mathbf{k} \in \mathbf{J}_{n_x}$. In this case, if we note $\mathbf{q} = -r\, \mathbf{k}$, then using spherical coordinates, we have

$$I(\mathbf{k}, r) = \int_{\mathbb{S}^1} \exp\left(i\, \mathbf{q} \cdot \omega\right) \mathrm{d}\omega = \int_0^{2\pi} \exp\left(i\, r\, \|\mathbf{k}\|\, \cos\theta\right) \mathrm{d}\theta = 2 \int_0^\pi \cos\left(r\, \|\mathbf{k}\|\, \sin\theta\right) \mathrm{d}\theta$$
$$= 2\pi\, \mathcal{J}_0(r\, \|\mathbf{k}\|),$$

where $\mathcal{J}_0$ is the Bessel function of order 0, defined with

$$\mathcal{J}_0 : x \in \mathbb{R} \mapsto \frac{1}{\pi} \int_0^\pi \cos\left(x\, \sin\theta\right) \mathrm{d}\theta = \sum_{l=0}^\infty \frac{(-1)^l}{(l!)^2} \left(\frac{x}{2}\right)^{2l}.$$

Consequently, we get

$$\widehat{\Psi}_\varepsilon(\mathbf{k}) = \frac{1}{2\pi} \int_0^{\pi/\varepsilon} \Psi(s)\, s\, \mathcal{J}_0\left(\varepsilon\, s\, \|\mathbf{k}\|\right) \mathrm{d}s.$$

Three-dimensional case: $d = 3$.   Let $r \geq 0$ and $\mathbf{k} \in \mathbf{J}_{n_x}$. Hence, if we note $\mathbf{q} = -r\, \mathbf{k}$, and then using spherical coordinates, we get

$$I(\mathbf{k}, r) = \int_{\mathbb{S}^2} \exp\left(i\, \mathbf{q} \cdot \omega\right) \mathrm{d}\omega = 2\pi \int_0^\pi \exp\left(i\, \|\mathbf{q}\|\, \cos(\theta)\right) \sin\theta\, \mathrm{d}\theta = 2\pi \int_{-1}^1 \exp\left(i\, \|\mathbf{q}\|\, \mu\right) \mathrm{d}\mu$$
$$= 4\pi\, \mathrm{Sinc}\left(r\, \|\mathbf{k}\|\right),$$

where $\mathrm{Sinc}(x) := \sin(x)/x$. Thus, the kernel mode $\widehat{\Psi}_\varepsilon(\mathbf{k})$ is given by

$$\widehat{\Psi}_\varepsilon(\mathbf{k}) = \frac{1}{2\pi^2} \int_0^{\pi/\varepsilon} \Psi(s)\, |s|^2\, \mathrm{Sinc}\left(\varepsilon\, s\, \|\mathbf{k}\|\right) \mathrm{d}s.$$

Now let us investigate the asymptotic behavior of the discrete operator $\mathcal{L}_{n_x}^S[u]$ when $\varepsilon \ll 1$. To this aim we set $\mathcal{S}_{n_x}$ the space of trigonometric polynomial of degree $n_x/2$ in each direction, defined as [35]

$$\mathcal{S}_{n_x} = \mathrm{span}\left\{ e^{i\mathbf{k} \cdot \mathbf{x}}, \quad -n_x/2 \leq \mathbf{k}_s \leq n_x/2 - 1,\ s = 1, \ldots, d \right\},$$

equipped with the classical L^2 norm $\|.\|_{L^2}$, which satisfies [35] for any $u \in \mathcal{S}_{n_x}$

$$\|u\|_{L^2}^2 = \left(\frac{2\pi}{n_x}\right)^d \sum_{j \in \mathbf{J}_{n_x}} |u(\mathbf{x}_j)|^2$$

and for any u and $v \in \mathcal{S}_{n_x}$, we also have

$$\int_{\mathbb{T}} u(\mathbf{x})\, \overline{v}(\mathbf{x})\, \mathrm{d}\mathbf{x} = \left(\frac{2\pi}{n_x}\right)^d \sum_{j \in \mathbf{J}_{n_x}} u(\mathbf{x}_j)\, \overline{v}(\mathbf{x}_j).$$

Finally we define by $\mathcal{I}_{n_x}$ the projection operator from $\mathcal{C}(\mathbb{T})$ to $\mathcal{S}_{n_x}$ such that $\mathcal{I}_{n_x} u(\mathbf{x}_j) = u(\mathbf{x}_j)$, for all $j \in \mathbf{J}_{n_x}$.

Proposition 5.2.2. *Let $d \in \{1, 2, 3\}$ and consider a connectivity kernel Ψ satisfying* (5.1.3) *with*

$$\int_{\mathbb{R}^d} \Psi(\|\mathbf{y}\|)\, \|\mathbf{y}\|^4\, \mathrm{d}\mathbf{y} < \infty. \tag{5.2.7}$$

Then, for all $\mathbf{k} \in \mathbf{J}_{n_x}$, there exists a positive constant $C > 0$, depending on Ψ, such that for all $\varepsilon > 0$,

$$\left| (2\pi)^d\, \widehat{\Psi}_\varepsilon(\mathbf{k}) - \overline{\Psi} + \overline{\sigma}\, \varepsilon^2\, \|\mathbf{k}\|^2 \right| \leq C \left(\|\mathbf{k}\|^4 + 1 \right) \varepsilon^4. \tag{5.2.8}$$

Moreover for any trigonometric polynomial $u \in \mathcal{S}_{n_x}$, we have

$$\left\| \mathcal{L}_{n_x}^S[u] - \overline{\Psi}\, u - \overline{\sigma}\, \varepsilon^2\, \Delta u \right\|_{L^2} \leq C\, \varepsilon^4 \left(\|\Delta^2 u\|_{L^2} + \|u\|_{L^2} \right). \tag{5.2.9}$$

Proof. On the one hand, for any $\mathbf{k} \in \mathbf{J}_{n_x}$, we perform a Taylor expansion of $I(\mathbf{k}, .)$ at $r = 0$ and using the assumptions (5.2.7) on Ψ, it yields

$$\left| (2\pi)^d\, \widehat{\Psi}_\varepsilon(\mathbf{k}) - \int_0^{\pi/\varepsilon} \Psi(s) s^{d-1} \mathrm{d}s - \varepsilon^2\, \|\mathbf{k}\|^2 \int_0^{\pi/\varepsilon} \Psi(s) s^{d+1} \mathrm{d}s \right| \leq \|\mathbf{k}\|^4\, \varepsilon^4 \int_{\mathbb{R}^d} \|\mathbf{y}\|^4\, \Psi(\|\mathbf{y}\|) \mathrm{d}\mathbf{y}.$$

On the other hand, we have

$$\int_{\pi/\varepsilon}^\infty \Psi(s) s^{d-1} \mathrm{d}s + \varepsilon^2 \int_{\pi/\varepsilon}^\infty \Psi(s) s^{d+1} \mathrm{d}s \leq \varepsilon^4 \left(\frac{1}{\pi^4} + \frac{1}{\pi^2} \right) \int_{\mathbb{R}^d} \|\mathbf{y}\|^4\, \Psi(\|\mathbf{y}\|) \mathrm{d}\mathbf{y}.$$

Gathering these results and using (5.1.3), there exists a constant $C > 0$, depending on Ψ, such that

$$\left| (2\pi)^d\, \widehat{\Psi}_\varepsilon(\mathbf{k}) - \overline{\Psi} + \overline{\sigma}\, \varepsilon^2\, \|\mathbf{k}\|^2 \right| \leq C \left(\|\mathbf{k}\|^4 + 1 \right) \varepsilon^4.$$

Then, we consider $u \in \mathcal{S}_{n_x}$ and for $\mathbf{k} \in \mathbf{J}_{n_x}$, we substitute the latter result in the expression (5.2.4) of $\widetilde{\mathcal{L}}^S[u](\mathbf{k})$, it yields for each

$$\left| \widetilde{\mathcal{L}}^S[u](\mathbf{k}) - \left(\overline{\Psi} + \overline{\sigma}\, \varepsilon^2\, \|\mathbf{k}\|^2 \right) \widetilde{u}(\mathbf{k}) \right| \leq C\, \varepsilon^2 \left(\|\mathbf{k}\|^4 + 1 \right) |\widetilde{u}(\mathbf{k})|.$$

Thus, from the definition of (5.2.3), we know that $\mathcal{L}_{n_x}^S[u] \in \mathcal{S}_{n_x}$ and get

$$
\begin{aligned}
\left\| \mathcal{L}_{n_x}^S[u] - \overline{\Psi}\, u - \overline{\sigma}\, \varepsilon^2 \Delta u \right\|_{L^2} &= \left(\sum_{\mathbf{k} \in \mathbf{J}_{n_x}} \left| \widetilde{\mathcal{L}}^S[u](\mathbf{k}) - \left(\overline{\Psi} + \overline{\sigma}\, \varepsilon^2\, \|\mathbf{k}\|^2 \right) \widetilde{u}(\mathbf{k}) \right|^2 \right)^{1/2}, \\
&\leq C\, \varepsilon^4 \left(\|\Delta^2 u\|_{L^2} + \|u\|_{L^2} \right).
\end{aligned}
$$

$\square$

5.2.2 Particle/Spectral methods for (5.1.1)

We now consider the transport equation (5.1.1) and apply a standard particle method. This kind of numerical scheme was first introduced by Harlow [79] for the numerical computation of specific problems in fluid dynamics, and precisely mathematically studied later [120]. Thus a large diversity of particle methods were developed for the simulation in fluid mechanics and plasma physics (see for instance [68] and references therein). The method consists in approximating the solution f to (5.1.1) with a sum of Dirac masses centered in a finite number of solutions of the characteristic system (5.1.4). These solutions stand for some particles characterized by a pair membrane potential-adaptation variable $(v, w) \in \mathbb{R}^2$.

We approximate the solution f to the transport equation (5.1.1) at each point $\mathbf{x} \in \mathbb{T}$,

$$f_M(t, \mathbf{x}, \mathrm{d}v, \mathrm{d}w) := \frac{\rho_0(\mathbf{x})}{M} \sum_{p=1}^{M} \delta_{\mathcal{V}_p(t, \mathbf{x})}(\mathrm{d}v) \otimes \delta_{\mathcal{W}_p(t, \mathbf{x})}(\mathrm{d}w),$$

where $M \in \mathbb{N}^*$, δ stands for the Dirac measure, and for any $t \geq 0$, $(\mathcal{V}_p, \mathcal{W}_p)(t) \in \mathcal{S}_{n_x}$ is the solution of the spatially discretized characteristic system which can be written as follows, $\mathbf{x} \in \mathbb{T}$ and $1 \leq p \leq M$

$$\begin{cases} \dfrac{\mathrm{d}\mathcal{V}_p}{\mathrm{d}t} = \mathcal{I}_{n_x} \left(N(\mathcal{V}_p) + \mathcal{K}_{n_x}^S[f_M](\mathcal{V}_p) \right) - \mathcal{W}_p, \\[2mm] \dfrac{\mathrm{d}\mathcal{W}_p}{\mathrm{d}t} = A(\mathcal{V}_p, \mathcal{W}_p), \end{cases} \tag{5.2.10}$$

with a given initial data $(\mathcal{V}_p^0, \mathcal{W}_p^0) \in \mathcal{S}_{n_x}$ for $1 \leq p \leq M$ and $\mathcal{I}_{n_x}$ is the projection operator on $\mathcal{S}_{n_x}$. Moreover, we define the macroscopic potential V_M at each point $(t, \mathbf{x}) \in \mathbb{R}^+ \times \mathbb{T}$, as

$$\begin{cases} \rho_0 = \displaystyle\int_{\mathbb{R}^2} f_M(t, \mathbf{x}, \mathrm{d}v, \mathrm{d}w), \\[4mm] \rho_0 V_M(t, \mathbf{x}) := \displaystyle\int_{\mathbb{R}^2} v\, f_M(t, \mathbf{x}, \mathrm{d}v, \mathrm{d}w) = \dfrac{1}{M} \sum_{p=1}^{M} \rho_0(\mathbf{x})\, \mathcal{V}_p(t, \mathbf{x}), \\[4mm] \rho_0 W_M(t, \mathbf{x}) := \displaystyle\int_{\mathbb{R}^2} w\, f_M(t, \mathbf{x}, \mathrm{d}v, \mathrm{d}w) = \dfrac{1}{M} \sum_{p=1}^{M} \rho_0(\mathbf{x})\, \mathcal{W}_p(t, \mathbf{x}). \end{cases} \tag{5.2.11}$$

From these macroscopic quantities, it is then possible to compute the discrete operator $\mathcal{K}_{n_x}^S[f_M]$ given in (5.2.6), where (5.2.10)–(5.2.11) are solved at each mesh point $(\mathbf{x}_j)_{j \in \mathbf{J}_{n_x}}$.

5.2.3 Time discretization

The time discretization of the system (5.2.10) is the key point to get an Asymptotic-Preserving of the transport equation (5.1.1). We have to be especially careful about the stiff nonlocal terms in (5.1.4): on the one hand, we cannot use a fully explicit scheme, which does not provide an AP-scheme, and on the other hand, a fully implicit time discretization would be too costly because of the spectral collocation method for the nonlocal terms.

Therefore, our strategy consists in applying implicit-explicit numerical scheme, and to treat $\mathcal{V}_M$ as an additional unknown of the system. In the following, we consider $\Delta t > 0$ and for all $n \in \mathbb{N}$, we set $t^n = n\,\Delta t$.

A first order semi-implicit scheme

We propose a first order semi-implicit scheme, that is for any time step $n \in \mathbb{N}$ and any particle index $1 \le p \le M$, we approximate $(\mathcal{V}_p(t^n), \mathcal{W}_p(t^n))$ solution to (5.2.10) by $(\mathcal{V}_p^n, \mathcal{W}_p^n) \in \mathcal{S}_{n_x} \times \mathcal{S}_{n_x}$ given by the following system

$$
\begin{cases}
\dfrac{\mathcal{V}_p^{n+1} - \mathcal{V}_p^n}{\Delta t} = \mathcal{I}_{n_x}\left(N(\mathcal{V}_p^n) + \dfrac{1}{\varepsilon^2}\left[\mathcal{L}_{n_x}^S[\rho_0 V_M^n] - \mathcal{V}_p^{n+1}\mathcal{L}_{n_x}^S[\rho_0]\right]\right) - \mathcal{W}_p^n, \\[4mm]
\dfrac{\mathcal{W}_p^{n+1} - \mathcal{W}_p^n}{\Delta t} = A\left(\mathcal{V}_p^{n+1}, \mathcal{W}_p^n\right),
\end{cases}
\tag{5.2.12}
$$

where V_M^n denotes an approximation of the macroscopic membrane potential. Using the linearity of A and the fact that $(\mathcal{V}_p^n, \mathcal{W}_p^n) \in \mathcal{S}_{n_x} \times \mathcal{S}_{n_x}$, the system (5.2.12) yields that $(\mathcal{V}_p^{n+1}, \mathcal{W}_p^{n+1}) \in \mathcal{S}_{n_x} \times \mathcal{S}_{n_x}$. Moreover, since the projection $\mathcal{I}_{n_x}$ is linear, and $\mathcal{L}_{n_x}^S[\rho_0 V_M^n] \in \mathcal{S}_{n_x}$ according to its definition (5.2.3), we get that the right term in the first equation in (5.2.12) reads

$$
\mathcal{I}_{n_x}\left(N(\mathcal{V}_p^n) + \dfrac{1}{\varepsilon^2}\left[\mathcal{L}_{n_x}^S[\rho_0 V_M^n] - \mathcal{V}_p^{n+1}\mathcal{L}_{n_x}^S[\rho_0]\right]\right) - \mathcal{W}_p^n
$$
$$
= \mathcal{I}_{n_x}\left(N(\mathcal{V}_p^n)\right) + \dfrac{1}{\varepsilon^2}\left[\mathcal{L}_{n_x}^S[\rho_0 V_M^n] - \mathcal{I}_{n_x}\left(\mathcal{V}_p^{n+1}\mathcal{L}_{n_x}^S[\rho_0]\right)\right] - \mathcal{W}_p^n.
$$

On the one hand, let us emphasize that the stiff term, for $\varepsilon \ll 1$, is treated implicitly but can be solved exactly whereas other terms, nonlinear with respect to $\mathcal{V}_p$, are considered explicitly. Formally speaking, when ε tends to zero, at each point $\mathbf{x}_j \in \mathbb{T}$, $j \in \mathbf{J}_{n_x}$, the microscopic potential $\mathcal{V}_p^{n+1}$ converges to $\mathcal{L}_{n_x}^S[\rho_0 V_M^n]/\mathcal{L}_{n_x}^S[\rho_0]$.

On the other hand, the macroscopic membrane potential V_M^n might be given by (5.2.11) from the values $(\mathcal{V}_p^n)_{1 \le p \le M}$. Unfortunately, this approach would not give the correct asymptotic behavior of the macroscopic membrane potential when $\varepsilon \to 0$. Therefore, we consider $V_M^n \in \mathcal{S}_{n_x}$ as an additional variable solution to the following scheme

$$
\dfrac{V_M^{n+1} - V_M^n}{\Delta t} = \dfrac{1}{M}\sum_{p=1}^M \mathcal{I}_{n_x}\left(N(\mathcal{V}_p^{n+1})\right) + \dfrac{1}{\varepsilon^2}\left[\mathcal{L}_{n_x}^S[\rho_0 V_M^n] - \mathcal{I}_{n_x}\left(V_M^n \mathcal{L}_{n_x}^S[\rho_0]\right)\right] - W_M^n. \tag{5.2.13}
$$

Observe here that the nonlinear term is computed implicitly from $(\mathcal{V}_p^{n+1})_{1 \le p \le M}$ whereas the stiff term is now explicit.

Now, we define a numerical parameter $\mathbf{h} \in \mathbb{R}^3$ as $\mathbf{h} = (\Delta t, \Delta x, 1/M)$, where $\Delta x = 2\pi/n_x$ and let us show the consistency of the numerical scheme (5.2.12)–(5.2.13) in the limit $\varepsilon \to 0$ for a fixed numerical parameter $\mathbf{h}$.

Proposition 5.2.3 (Consistency in the limit $\varepsilon \to 0$ for fixed numerical parameters $\mathbf{h}$). *Let $\mathbf{h}$ be a fixed parameter and consider a connectivity kernel $\Psi : \mathbb{R}^+ \to \mathbb{R}^+$ satisfying (5.1.3), (5.2.7) and a neuron density $\rho_0 \in \mathcal{S}_{n_x}$ satisfying (5.1.8) at each grid point $\mathbf{x}_j$, $j \in \mathbf{J}_{n_x}$. For all $\varepsilon > 0$, $p \in \{1, \dots, M\}$ and $n \in \mathbb{N}$, let us assume that the triplet $(\mathcal{V}_p^{\varepsilon,n}, \mathcal{W}_p^{\varepsilon,n}, V_M^{\varepsilon,n})$ given by (5.2.12)–(5.2.13) is uniformly bounded with respect to $\varepsilon > 0$. Then we define*

$$
W_M^{\varepsilon,n} = \dfrac{1}{M}\sum_{p=1}^M \mathcal{W}_p^{\varepsilon,n}
$$

132

and for all $j \in \mathbf{J}_{n_x}$, $(V_M^{\varepsilon,n}, W_M^{\varepsilon,n})(\mathbf{x}_j)$ converges to $(\overline{V}_M^n, \overline{W}_M^n)(\mathbf{x}_j)$, as ε goes to 0, solution to

$$
\begin{cases}
\dfrac{\overline{V}_M^{n+1} - \overline{V}_M^n}{\Delta t} = \mathcal{I}_{n_x}\left(N\left(\overline{V}_M^n\right)\right) - \overline{W}_M^n + \overline{\sigma}\left(\Delta\mathcal{I}_{n_x}\left(\rho_0 \overline{V}_M^n\right) - \mathcal{I}_{n_x}\left(\overline{V}_M^n\Delta\rho_0\right)\right), \\[4mm]
\dfrac{\overline{W}_M^{n+1} - \overline{W}_M^n}{\Delta t} = A\left(\overline{V}_M^n, \overline{W}_M^n\right).
\end{cases}
\tag{5.2.14}
$$

Proof. For any $p \in \{1,\ldots,M\}$ and $n \geq 0$, we denote by $\left(\mathcal{V}_p^{\varepsilon,n}, \mathcal{W}_p^{\varepsilon,n}, V_M^{\varepsilon,n}\right)_{\varepsilon>0}$ the solution to (5.2.12)–(5.2.13) computed at the grid points $(\mathbf{x}_j)_{j\in\mathbf{J}_{n_x}}$. Since this sequence, abusively labeled by ε, is uniformly bounded, there exists a sub-sequence, still labeled in the same manner, which converges to $\left(\overline{\mathcal{V}}_p^n, \overline{\mathcal{W}}_p^n, \overline{V}_M^n\right)$ when $\varepsilon \to 0$.

On the one hand using the scheme (5.2.12) on $\mathcal{V}_p^{n+1}$, we may write

$$
\varepsilon^2 \frac{\mathcal{V}_p^{\varepsilon,n+1} - \mathcal{V}_p^{\varepsilon,n}}{\Delta t} = \varepsilon^2 \mathcal{I}_{n_x}\left(N(\mathcal{V}_p^{\varepsilon,n})\right) - \varepsilon^2 \mathcal{W}_p^{\varepsilon,n} + \left[\mathcal{L}_{\varepsilon,n_x}^S[\rho_0 V_M^{\varepsilon,n}] - \mathcal{I}_{n_x}\left(\mathcal{V}_p^{\varepsilon,n+1}\mathcal{L}_{\varepsilon,n_x}^S[\rho_0]\right)\right],
$$

and pass to the limit with respect to ε, it yields that for any $j \in \mathbf{J}_{n_x}$,

$$
\mathcal{L}_{\varepsilon,n_x}^S[\rho_0 V_M^{\varepsilon,n}](\mathbf{x}_j) - \mathcal{I}_{n_x}\left(\mathcal{V}_p^{\varepsilon,n+1}\mathcal{L}_{\varepsilon,n_x}^S[\rho_0]\right)(\mathbf{x}_j) = \mathcal{L}_{\varepsilon,n_x}^S[\rho_0 V_M^{\varepsilon,n}](\mathbf{x}_j) - \mathcal{V}_p^{\varepsilon,n+1}(\mathbf{x}_i)\mathcal{L}_{\varepsilon,n_x}^S[\rho_0](\mathbf{x}_j)
$$
$$
\xrightarrow[\varepsilon\to 0]{} 0.
$$

Then, applying Proposition 5.2.2 to $\rho_0 \in \mathcal{S}_{n_x}$, we have $\|\mathcal{L}_{\varepsilon,n_x}^S[\rho_0] - \overline{\Psi}\rho_0\|_{L^2} \to 0$, when ε goes to 0, that is, for any $j \in \mathbf{J}_{n_x}$

$$
\left|\mathcal{L}_{\varepsilon,n_x}^S[\rho_0](\mathbf{x}_j) - \overline{\Psi}\rho_0(\mathbf{x}_j)\right| \xrightarrow[\varepsilon\to 0]{} 0.
$$

Furthermore, applying again Proposition 5.2.2 to $\mathcal{I}_{n_x}(\rho_0 V_M^{\varepsilon,n}) \in \mathcal{S}_{n_x}$, we also get

$$
\left|\mathcal{L}_{\varepsilon,n_x}^S[\rho_0 V_M^{\varepsilon,n}](\mathbf{x}_j) - \overline{\Psi}\rho_0\overline{V}_M^n(\mathbf{x}_j)\right| \xrightarrow[\varepsilon\to 0]{} 0,
$$

hence for any $j \in \mathbf{J}_{n_x}$ and $p \in \{1,\ldots,M\}$, the limit $\overline{\mathcal{V}}_p^{n+1}(\mathbf{x}_j)$ does no depend on p and is given by

$$
\overline{\mathcal{V}}_p^{n+1}(\mathbf{x}_j) = \begin{cases} \overline{V}_M^n(\mathbf{x}_j), & \text{if } \rho_0(\mathbf{x}_j) > 0, \\[2mm] 0, & \text{else.} \end{cases}
$$

Now we consider $W_M^{\varepsilon,n}$ given by

$$
W_M^{\varepsilon,n} = \frac{1}{M}\sum_{p=1}^M \mathcal{W}_p^{\varepsilon,n}
$$

and apply the second relation in (5.2.12), it gives by linearity of A,

$$
\frac{W_M^{\varepsilon,n+1} - W_M^{\varepsilon,n}}{\Delta t} = A\left(\frac{1}{M}\sum_{p=1}^M \mathcal{V}_p^{\varepsilon,n+1}, W_M^{\varepsilon,n}\right),
$$

Passing to the limit $\varepsilon \to 0$, we get an equation on the limit $\overline{W}_M^n$ given by

$$
\frac{\overline{W}_M^{n+1} - \overline{W}_M^n}{\Delta t} = A\left(\overline{V}_M^n, \overline{W}_M^n\right).
$$

On the other hand, we start from (5.2.13) and again apply Proposition 5.2.2, it yields that

$$
\frac{V_M^{\varepsilon,n}\left(\mathcal{L}_{\varepsilon,n_x}^S[\rho_0] - \overline{\overline{\Psi}}\rho_0\right)}{\varepsilon^2} \xrightarrow[\varepsilon \to 0]{} \overline{\sigma}\,\overline{V}_M^n\,\Delta\rho_0\,,
$$

whereas

$$
\frac{\mathcal{L}_{\varepsilon,n_x}^S[\rho_0 V_M^{\varepsilon,n}] - \overline{\overline{\Psi}}\,\mathcal{I}_{n_x}\left(\rho_0 V_M^{\varepsilon,n}\right)}{\varepsilon^2} \xrightarrow[\varepsilon \to 0]{} \overline{\sigma}\,\Delta\mathcal{I}_{n_x}\left(\rho_0\overline{V}_M^n\right)\,.
$$

Gathering these latter results, we get that when ε goes to zero,

$$
\frac{\mathcal{L}_{\varepsilon,n_x}^S[\rho_0 V_M^{\varepsilon,n}] - \mathcal{I}_{n_x}\left(V_M^{\varepsilon,n}\,\mathcal{L}_{\varepsilon,n_x}^S[\rho_0]\right)}{\varepsilon^2} \xrightarrow[\varepsilon \to 0]{} \overline{\sigma}\left[\Delta\mathcal{I}_{n_x}\left(\rho_0\overline{V}_M^n\right) - \mathcal{I}_{n_x}\left(\overline{V}_M^n\Delta\rho_0\right)\right].
$$

Therefore the limit $\overline{V}_M^{n+1}$ is solution to

$$
\frac{\overline{V}_M^{n+1} - \overline{V}_M^n}{\Delta t} = \mathcal{I}_{n_x}\left(N\left(\overline{V}_M^n\right)\right) - \overline{W}_M^n + \overline{\sigma}\left(\Delta\mathcal{I}_{n_x}(\rho\,\overline{V}_M^n) - \mathcal{I}_{n_x}\left(\Delta\rho_0\,\overline{V}_M^n\right)\right).
$$

Finally, since the limit point $(\overline{V}_M^n, \overline{W}_M^n)$ is uniquely determined, actually all the sequence $(V_M^{\varepsilon,n}, W_M^{\varepsilon,n})_{\varepsilon>0}$ converges. □

A second order implicit-explicit Runge-Kutta scheme

Now let us adapt the previous strategy to a second order implicit-explicit Runge-Kutta scheme for the system (5.2.10). We propose a combination of Heun's method for the explicit part, and an A-stable second order singly diagonally implicit Runge-Kutta (SDIRK) method for the implicit part. According to the classification from [14], we call it H-SDIRK2 (2,2,2).

For all $n \in \mathbb{N}$ and $p \in \{1\ldots M\}$, we apply a first stage,

$$
\begin{cases}
\mathcal{V}_p^{(1)} = \mathcal{V}_p^n + \dfrac{\Delta t}{2}\left[\mathcal{I}_{n_x}\left(N(\mathcal{V}_p^n)\right) + \dfrac{1}{\varepsilon^2}\left[\mathcal{L}_{n_x}^S[\rho_0 V_M^n] - \mathcal{I}_{n_x}\left(\mathcal{V}_p^{(1)}\,\mathcal{L}_{n_x}^S[\rho_0]\right)\right] - \mathcal{W}_p^n\right], \\[2ex]
\mathcal{W}_p^{(1)} = \mathcal{W}_p^n + \dfrac{\Delta t}{2}\,A\left(\mathcal{V}_p^{(1)}, \mathcal{W}_p^n\right),
\end{cases}
\tag{5.2.15}
$$

Hence we compute the additional variable $V_M^{(1)} \in \mathcal{S}_{n_x}$ solution to the following scheme

$$
V_M^{(1)} = V_M^n + \frac{\Delta t}{2}\left[\frac{1}{M}\sum_{p=1}^{M}\mathcal{I}_{n_x}\left(N(\mathcal{V}_p^{(1)})\right) + \frac{1}{\varepsilon^2}\left[\mathcal{L}_{n_x}^S[\rho_0 V_M^n] - \mathcal{I}_{n_x}\left(V_M^n\,\mathcal{L}_{n_x}^S[\rho_0]\right)\right] - W_M^n\right],
\tag{5.2.16}
$$

with

$$
W_M^n := \frac{1}{M}\sum_{p=1}^{M}\mathcal{W}_p^n.
$$

Then, we set

$$
\begin{cases}
\hat{\mathcal{V}}_p^{(1)} = 2\,\mathcal{V}_p^{(1)} - \mathcal{V}_p^n, \\[1.5ex]
\hat{\mathcal{W}}_p^{(1)} = 2\,\mathcal{W}_p^{(1)} - \mathcal{W}_p^n, \\[1.5ex]
\hat{V}_M^{(1)} = 2\,V_M^{(1)} - V_M^n
\end{cases}
$$

and compute the second stage with a semi-implicit step on $(\mathcal{V}_p^{(2)}, \mathcal{W}_p^{(2)})$,

$$\begin{cases} \mathcal{V}_p^{(2)} = \mathcal{V}_p^n + \dfrac{\Delta t}{2} \left[\mathcal{I}_{n_x} \left(N(\hat{\mathcal{V}}_p^{(1)}) \right) + \dfrac{1}{\varepsilon^2} \left[\mathcal{L}_{n_x}^S [\rho_0 \hat{V}_M^{(1)}] - \mathcal{I}_{n_x} \left(\mathcal{V}_p^{(2)} \mathcal{L}_{n_x}^S [\rho_0] \right) \right] - \hat{\mathcal{W}}_p^{(1)} \right], \\[3mm] \mathcal{W}_p^{(2)} = \mathcal{W}_p^n + \dfrac{\Delta t}{2} A \left(\mathcal{V}_p^{(2)}, \hat{\mathcal{W}}_p^{(1)} \right), \end{cases}$$

(5.2.17)

Moreover, $V_M^{(2)} \in \mathcal{S}_{n_x}$ is given by

$$V_M^{(2)} = V_M^n + \dfrac{\Delta t}{2} \left[\dfrac{1}{M} \sum_{p=1}^M \mathcal{I}_{n_x} \left(N(\mathcal{V}_p^{(2)}) \right) + \dfrac{1}{\varepsilon^2} \left[\mathcal{L}_{n_x}^S [\rho_0 \hat{V}_M^{(1)}] - \mathcal{I}_{n_x} \left(\hat{V}_M^{(1)} \mathcal{L}_{n_x}^S [\rho_0] \right) \right] - \hat{W}_M^{(1)} \right],$$

(5.2.18)

where $\hat{W}_M^{(1)} = 2 W_M^{(1)} - W_M^n$ and

$$W_M^{(1)} := \dfrac{1}{M} \sum_{p=1}^M \mathcal{W}_p^{(1)}.$$

Finally, we get the numerical solution at time t^{n+1} through

$$\begin{cases} \mathcal{V}_p^{n+1} = \mathcal{V}_p^{(1)} + \mathcal{V}_p^{(2)} - \mathcal{V}_p^n, \\[2mm] \mathcal{W}_p^{n+1} = \mathcal{W}_p^{(1)} + \mathcal{W}_p^{(2)} - \mathcal{W}_p^n, \\[2mm] V_M^{n+1} = V_M^{(1)} + V_M^{(2)} - V_M^n. \end{cases}$$

(5.2.19)

Now, we prove an analogous result to Proposition 5.2.3 for the numerical scheme (5.2.15)–(5.2.19) as the parameter ε goes to 0 with a fixed numerical parameter $\mathbf{h} \in \mathbb{R}^3$ given by $\mathbf{h} = (\Delta t, \Delta x, 1/M)$, where $\Delta x = 2\pi/n_x$, $\Delta t > 0$ and $M \in \mathbb{N}^*$.

Proposition 5.2.4 (Consistency in the limit $\varepsilon \to 0$ for a fixed numerical parameter $\mathbf{h}$). *Let $\mathbf{h}$ to be fixed and consider a connectivity kernel $\Psi : \mathbb{R}^+ \to \mathbb{R}^+$ satisfying (5.1.3), (5.2.7) and a neuron density $\rho_0 \in \mathcal{S}_{n_x}$ satisfying (5.1.8) at each grid point $\mathbf{x}_j$, $j \in \mathbf{J}_{n_x}$. For all $\varepsilon > 0$, $p \in \{1, \dots, M\}$ and $n \in \mathbb{N}$, let us assume that the triplet $(\mathcal{V}_p^{\varepsilon,n}, \mathcal{W}_p^{\varepsilon,n}, V_M^{\varepsilon,n})$ given by (5.2.15)–(5.2.19) is uniformly bounded with respect to $\varepsilon > 0$. Then we define*

$$W_M^{\varepsilon,n} = \dfrac{1}{M} \sum_{p=1}^M \mathcal{W}_p^{\varepsilon,n}$$

and for all $j \in \mathbf{J}_{n_x}$, $(V_M^{\varepsilon,n}, W_M^{\varepsilon,n})(\mathbf{x}_j)$ converges to $(\overline{V}_M^n, \overline{W}_M^n)(\mathbf{x}_j)$, as ε goes to 0, solution to

$$\begin{cases} \overline{V}_M^{(1)} = \overline{V}_M^n + \dfrac{\Delta t}{2} \left[\mathcal{I}_{n_x} \left(N \left(\overline{V}_M^n \right) \right) - \overline{W}_M^n + \overline{\sigma} \left(\Delta \mathcal{I}_{n_x} \left(\rho_0 \overline{V}_M^n \right) - \mathcal{I}_{n_x} \left(\overline{V}_M^n \Delta \rho_0 \right) \right) \right], \\[3mm] \overline{W}_M^{(1)} = \overline{W}_M^n + \dfrac{\Delta t}{2} A \left(\overline{V}_M^n, \overline{W}_M^n \right), \end{cases}$$

(5.2.20)

where the second stage is given by

$$\begin{cases} \overline{V}_M^{(2)} = \overline{V}_M^n + \dfrac{\Delta t}{2} \left[N \left(\hat{V}_M^{(1)} \right) - \hat{W}_M^{(1)} + \overline{\sigma} \left(\Delta \mathcal{I}_{n_x} \left(\rho_0 \hat{V}_M^{(1)} \right) - \mathcal{I}_{n_x} \left(\hat{V}_M^{(1)} \Delta \rho_0 \right) \right) \right] \\[3mm] W_M^{(2)} = W_M^n + \dfrac{\Delta t}{2} A \left(\hat{V}_M^{(1)}, \hat{W}_M^{(1)} \right), \end{cases}$$

(5.2.21)

where $\hat{V}_M^{(1)} = 2\overline{V}_M^{(1)} - \overline{V}_M^n$, $\hat{W}_M^{(1)} = 2\overline{W}_M^{(1)} - \overline{W}_M^n$. The next time step is given by

$$\begin{cases} V_M^{n+1} = V_M^{(1)} + V_M^{(2)} - V_M^n, \\ \\ W_M^{n+1} = W_M^{(1)} + W_M^{(2)} - W_M^n. \end{cases} \tag{5.2.22}$$

Remark 5.2.5. *The numerical scheme* (5.2.15)–(5.2.19) *is an explicit second order A-stable approximation of the reaction-diffusion system* (5.1.11).

Proof. We fix a time step $\Delta t > 0$, a set of equidistant points $(\mathbf{x}_j)_{j \in \mathbf{J}_{n_x}} \subset \mathbb{T}$ and $p \in \{1, \dots, M\}$. Then we denote by $\left(\mathcal{V}_p^{\varepsilon,n}, \mathcal{W}_p^{\varepsilon,n}, V_M^{\varepsilon,n}\right)_{\varepsilon>0}$ the solution to (5.2.15)–(5.2.19). Up to a sub-sequence, $\left(\mathcal{V}_p^{\varepsilon,n}, \mathcal{W}_p^{\varepsilon,n}, V_M^{\varepsilon,n}\right)_{\varepsilon>0}$ converges to $\left(\overline{\mathcal{V}}_p^n, \overline{\mathcal{W}}_p^n, \overline{V}_M^n\right)$ when $\varepsilon \to 0$, hence we proceed exactly as in Proposition 5.2.3 and set

$$W_M^{\varepsilon,(1)} = \frac{1}{M} \sum_{p=1}^M \mathcal{W}_p^{\varepsilon,(1)} \xrightarrow[\varepsilon \to 0]{} \overline{W}_M^{(1)}.$$

Thus, we prove that $\left(\overline{V}_M^{(1)}, \overline{W}_M^{(1)}\right)$ corresponds to the solution of the first stage (5.2.20) and we have

$$\begin{cases} \overline{V}_M^{(1)} = 2\overline{V}_M^{(1)} - \overline{V}_M^n, \\ \\ \overline{W}_M^{(1)} = 2\overline{W}_M^{(1)} - \overline{W}_M^n. \end{cases}$$

Furthermore, we treat the second stage in the same manner for any $j \in \mathbf{J}_{n_x}$ and $p \in \{1, \dots, M\}$, the limit $\overline{\mathcal{V}}_p^{(2)}(\mathbf{x}_j)$ does not depend on p and is given by

$$\overline{\mathcal{V}}_p^{(2)}(\mathbf{x}_j) = \begin{cases} \hat{V}_M^{(1)}(\mathbf{x}_j), & \text{if } \rho_0(\mathbf{x}_j) > 0, \\ \\ 0, & \text{else.} \end{cases}$$

Passing to the limit $\varepsilon \to 0$ in (5.2.18) and in the second equation in (5.2.17), it yields that $\left(\overline{V}_M^{(2)}, \overline{W}_M^{(2)}\right)$ satisfies (5.2.21) and finally (5.2.22). $\qquad \square$

Let us notice that the present strategy can be applied to a large class of second order schemes and can also be extended to a third order semi-implicit scheme. We refer to [14] for the detailed description of the schemes.

5.3 Numerical simulations

In this section, we provide examples of numerical computations to validate and compare the different time discretization schemes (5.2.12)–(5.2.13) and (5.2.15)–(5.2.19) introduced in the previous section.

First of all, we focus on the order of accuracy when ε is fixed and the numerical parameter **h** goes to zero. Then we study the behaviour of the numerical solutions for a fixed **h** and in the limit $\varepsilon \to 0$, to show the convergence towards the solutions of the approximations (5.2.14) and (5.2.20)–(5.2.22) of the reaction-diffusion system (5.1.11).

Then, we display some simulations of the behaviour of a solution to (5.1.1)–(5.1.2) with a heterogeneous neuron density, and finally, we show some two-dimensional dynamics.

Throughout this section, except for the first subsection, we fix the parameter of the non-linearity N to $\theta = 0.1$ and the other constants to $\tau = 0.005$ and $b = 5$, expect in the first subsection. This framework corresponds to the "excitable" regime of the well-known FHN

$\|\mathbf{h}\|$	L^2 error for (5.2.12)–(5.2.13)	Order	$\|\mathbf{h}\|$	L^2 error for (5.2.15)–(5.2.19)	Order
1.e-01	5.48e-04	XXX	1.e-01	1.23e-07	XXX
5.e-02	2.73e-04	1.63	5.e-02	3.56e-08	2.69
2.e-02	1.09e-04	1.00	2.e-02	8.35e-09	2.02
1.e-02	5.47e-05	1.00	1.e-02	2.07e-08	2.01
5.e-03	2.73e-05	1.00	5.e-03	5.01e-09	2.01
2.e-03	1.09e-05	1.00	2.e-03	1.23e-09	2.01
1.e-03	5.47e-06	1.00	1.e-03	2.95e-10	2.01
5.e-04	2.73e-06	1.00	5.e-04	2.95e-10	2.00

Table 5.1: **Order of accuracy in $\|\mathbf{h}\| \to 0$:** evaluation of the numerical error at fixed time $T = 10$ of the numerical schemes (5.2.12)–(5.2.13) (left table) and (5.2.15)–(5.2.19) (right table).

reaction-diffusion system (5.3.5). Therefore, the system only admits one steady state which is the stable fixed point 0, and according to [36], τ is small enough so that the solution to (5.3.5) exhibits slow/fast dynamics like traveling pulses.

Moreover, as for the connectivity kernel, we use the following truncated gaussian function

$$\Psi(\|\mathbf{z}\|) = \frac{1}{(2\pi\sigma_0)^{d/2}} \exp\left(-\frac{\|\mathbf{z}\|^2}{2\sigma_0}\right), \qquad (5.3.1)$$

with $\sigma_0 = 0.005$ such that we have in (5.1.3),

$$\overline{\Psi} = 1 \quad \text{and} \quad \overline{\sigma} = \frac{\sigma_0}{2}.$$

5.3.1 Order of accuracy in the numerical parameters

In this subsection, we aim to verify the order of accuracy of our numerical methods proposed in Section 5.2 with respect to the numerical parameters $\mathbf{h} = (\Delta t, \Delta x, 1/M)$, when it goes to zero. We consider a simplified version of the nonlocal transport equation (5.1.1) with $N(v) = -\alpha v$ and $\tau = 0$, that is, for $t > 0$ and $\mathbf{x} \in \mathbb{R}$

$$\begin{cases} \partial_t f^\varepsilon + \partial_v \left(f^\varepsilon \left[-\alpha v - w + \mathcal{K}_\varepsilon[f^\varepsilon] \right] \right) = 0, \\ f^\varepsilon|_{t=0}(\mathbf{x}, v, w) = \delta_{V_0(\mathbf{x})}(v) \otimes \delta_0(w), \end{cases} \qquad (5.3.2)$$

with V_0 given by

$$V_0(\mathbf{x}) = \exp\left(-100\,|\mathbf{x}|^2\right), \quad \mathbf{x} \in \mathbb{R}.$$

Consequently, in this configuration, we have $\rho_0 \equiv 1$, and the solution to (5.1.1)–(5.1.2) is given by $f^\varepsilon = \delta_{V^\varepsilon}(v) \otimes \delta_0(w)$ where V^ε is the unique solution to the following reaction-diffusion equation for $t > 0$ and $\mathbf{x} \in \mathbb{R}$,

$$\begin{cases} \partial_t V^\varepsilon - \frac{1}{\varepsilon^2} \left(\Psi_\varepsilon \star V^\varepsilon - \overline{\Psi}\, V^\varepsilon \right) = -\alpha V^\varepsilon, \\ V^\varepsilon(0, \mathbf{x}) = V_0(\mathbf{x}), \quad \mathbf{x} \in \mathbb{R}. \end{cases}$$

Since the term $N(V^\varepsilon)$ is now linear, the macroscopic equation on V^ε is also linear (even if the equation on f^ε is not) and we can exhibit an explicit solution using a Fourier transform in space. It yields that,

$$\widehat{V}^\varepsilon(t, \xi) = \widehat{V_0}(\xi) \exp\left(\left[-\alpha + \frac{1}{\varepsilon^2}\left(\widehat{\Psi}_\varepsilon(\xi) - \overline{\Psi}\right)\right] t\right).$$

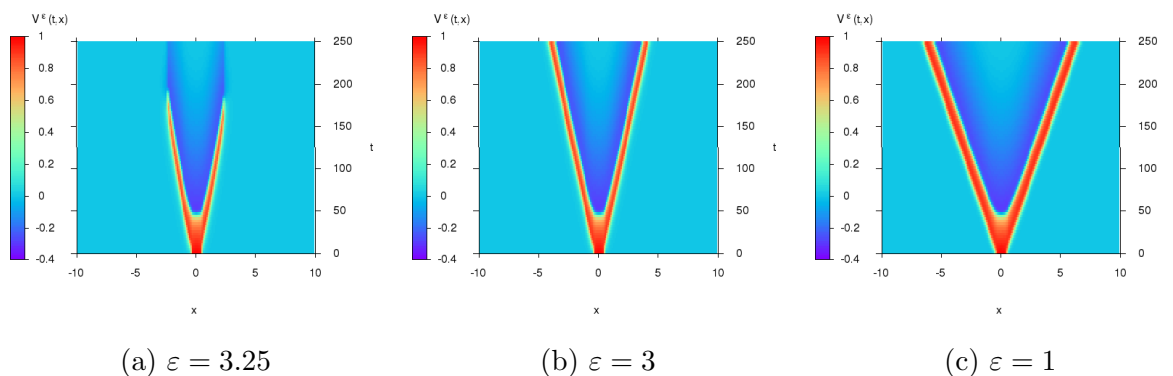(a) $\varepsilon = 3.25$ (b) $\varepsilon = 3$ (c) $\varepsilon = 1$

Figure 5.1: **Order of accuracy in** $\varepsilon \to 0$: spatio-temporal profile of $V^\varepsilon(t, \mathbf{x})$ for (a) $\varepsilon = 3.25$, (b) $\varepsilon = 3$ and (c) $\varepsilon = 1$.

where we choose the parameter $\alpha = 0.001$, and the scaling parameter $\varepsilon = 1$. The domain in space is taken to be $(-1, 1)$. We compute an approximation of the error on the macroscopic quantity V^ε at each time step

$$\mathcal{E}^n \; = \; \|V_M^{\varepsilon,n} - V^\varepsilon(t^n)\|_{L^2}, \quad n = 0, \ldots N_T,$$

with $N_T = [T/\Delta t]$. In Table 5.1, we report the numerical error for different values of $\mathbf{h}$ at fixed time $T = 10$ for the numerical schemes (5.2.12)–(5.2.13) (left panel) and (5.2.15)–(5.2.19) (right panel). A linear regression yields that these numerical methods seems to be respectively first and second order in $\mathbf{h}$. Therefore, with this parametrization, the order of accuracy corresponds to the one given by the time discretization, whereas the error due to the spectral discretization is negligible.

5.3.2 Order of accuracy in ε

We again consider the transport equation (5.1.1)–(5.1.2), with the initial data

$$f_0(\mathbf{x}, v, w) = \delta_{V_0(\mathbf{x})}(v) \otimes \delta_{W_0(\mathbf{x})}(w), \tag{5.3.3}$$

with

$$V_0 \; = \; \chi_{[-1,1]} \quad \text{and} \quad W_0 \equiv 0.$$

In this configuration, we get $\rho_0 \equiv 1$ and the solution of the transport equation (5.1.1) is again a Dirac mass in (v, w) centered in $(V^\varepsilon, W^\varepsilon)$, solution to the nonlocal reaction-diffusion system for $t > 0$ and $\mathbf{x} \in \mathbb{R}^d$,

$$\begin{cases} \partial_t V^\varepsilon - \dfrac{1}{\varepsilon^2} \left(\Psi_\varepsilon \star V^\varepsilon - \overline{\Psi} \, V^\varepsilon \right) \; = \; N(V^\varepsilon) - W^\varepsilon, \\[2mm] \partial_t W^\varepsilon \; = \; A\left(V^\varepsilon, W^\varepsilon\right). \end{cases} \tag{5.3.4}$$

The purpose is now to study the asymptotic when the scaling parameter ε goes to 0. It is expected that the macroscopic quantities $(V^\varepsilon, W^\varepsilon)$ converge towards the solution to the reaction-diffusion FHN system (5.1.11), which reads as follows when $\rho_0 \equiv 1$, for $t > 0$ and $\mathbf{x} \in \mathbb{R}$,

$$\begin{cases} \partial_t V - \overline{\sigma} \, \partial_{\mathbf{x}}^2 V \; = \; N(V) - W, \\[2mm] \partial_t W \; = \; \tau \, (V - b \, W). \end{cases} \tag{5.3.5}$$

138

ε	$\mathcal{D}_\varepsilon(t)$ with (5.2.12)–(5.2.13)	Order
5	1.21	
2	1.73	XX
1	9.16e-01	0.92
5.e-01	2.60e-01	1.37
2.e-01	4.17e-02	1.65
1.e-01	1.04e-02	1.76
5.e-02	2.60e-03	1.82
2.e-02	4.17e-04	1.87
1.e-01	1.04e-04	1.90

ε	$\mathcal{D}_\varepsilon(t)$ with (5.2.15)–(5.2.19)	Order
5	1.21	
2	1.73	XX
1	9.13e-01	0.92
5.e-01	2.59e-01	1.37
2.e-02	4.15e-02	1.65
1.e-01	1.04e-02	1.76
5.e-02	2.59e-03	1.82
2.e-02	4.15e-04	1.87
1.e-02	1.03e-04	1.90

Table 5.2: **Order of accuracy in** $\varepsilon \to 0$**:** approximation of $\mathcal{D}_\varepsilon(t)$ at fixed time $t = 250$ with the first order scheme (5.2.12)–(5.2.13) (left) and the second order scheme (5.2.15)–(5.2.19) (right).

To investigate this asymptotic, we compute an approximation of the relative entropy given at any time $t > 0$ as

$$\mathcal{D}_\varepsilon(t) := \left[\int_{\mathbb{R}} \rho_0(\mathbf{x}) \left[|V^\varepsilon(t, \mathbf{x}) - V(t, \mathbf{x})|^2 + |W^\varepsilon(t, \mathbf{x}) - W(t, \mathbf{x})|^2 \right] \, d\mathbf{x} \right]^{1/2}, \qquad (5.3.6)$$

as ε goes to 0. Here again, we approach $\mathcal{D}_\varepsilon(t)$ with a rectangle rule. Since we compute our simulations on the domain in space $(-10, 10)$, we have for al $n \in \mathbb{N}$:

$$\mathcal{D}_\varepsilon(t^n) \approx \left(\sum_{j=1}^{n_x} \rho_0(\mathbf{x}_j) \left(|V_M^{\varepsilon,n}(\mathbf{x}_j) - \overline{V}_M^n(\mathbf{x}_j)|^2 + |W_M^{\varepsilon,n}(\mathbf{x}_j) - \overline{W}_M^n(\mathbf{x}_j)|^2 \right) \frac{20}{n_x} \right)^{1/2}.$$

In [47], it is proven that for any $t > 0$, $\mathcal{D}_\varepsilon(t)$ tends to 0 as ε goes to 0 with a rate of convergence larger than 2/7. However, when $\rho_0 \equiv 1$ and for compactly supported f^ε, the rate of convergence is formally equal to 2.

Furthermore, since the solution to the transport equation is a Dirac mass in $(v, w) \in \mathbb{R}^2$, we take $M = 1$. Then, we choose $\Delta t = 0.01$ and $n_x = 512$ for the time and space discretization.

In Figure 5.1, we show the spatio-temporal profile of the mean membrane potential V^ε computed from f^ε the solution of the transport equation (5.1.1) for $\varepsilon = 3.25$ (panel (a)), $\varepsilon = 3$ (panel (b)) and $\varepsilon = 1$ (panel (c)). It shows that depending on the value of ε, the solution V^ε presents dramatically different dynamics. If ε is too large compared to the width of the considered interval, as in the case (a), two symmetric waves start to propagate, but quickly disappear, and then V^ε converges to 0 everywhere as time goes on. On the contrary, for smaller values of ε as in the cases (b) and (c), that is $\varepsilon \leq 3$, the function V^ε has the shape of two symmetric counter-propagating traveling pulses. This is typically the kind of slow/fast dynamics expected for the solution of (5.3.5) according to [36] with this set of parameters. Moreover, it seems that the speed of propagation of these waves decreases as ε grows, since in the case (b), the speed of propagation of these traveling pulses is slightly less than in the case (c).

Then, we display in Table 5.2 the numerical approximations of $\mathcal{D}_\varepsilon(t)$ at fixed time $t = 250$ for several values of ε for the first order (left table) and the second order (right table) numerical schemes. Since the function V^ε does not present some traveling pulses only for $\varepsilon = 5$, we display linear regressions only from the line corresponding to $\varepsilon = 2$. These linear regressions yield that $\mathcal{D}_\varepsilon(t)$ seems to be approximately of order two in ε for both numerical schemes, which corresponds to the one obtained by formal computations [47].
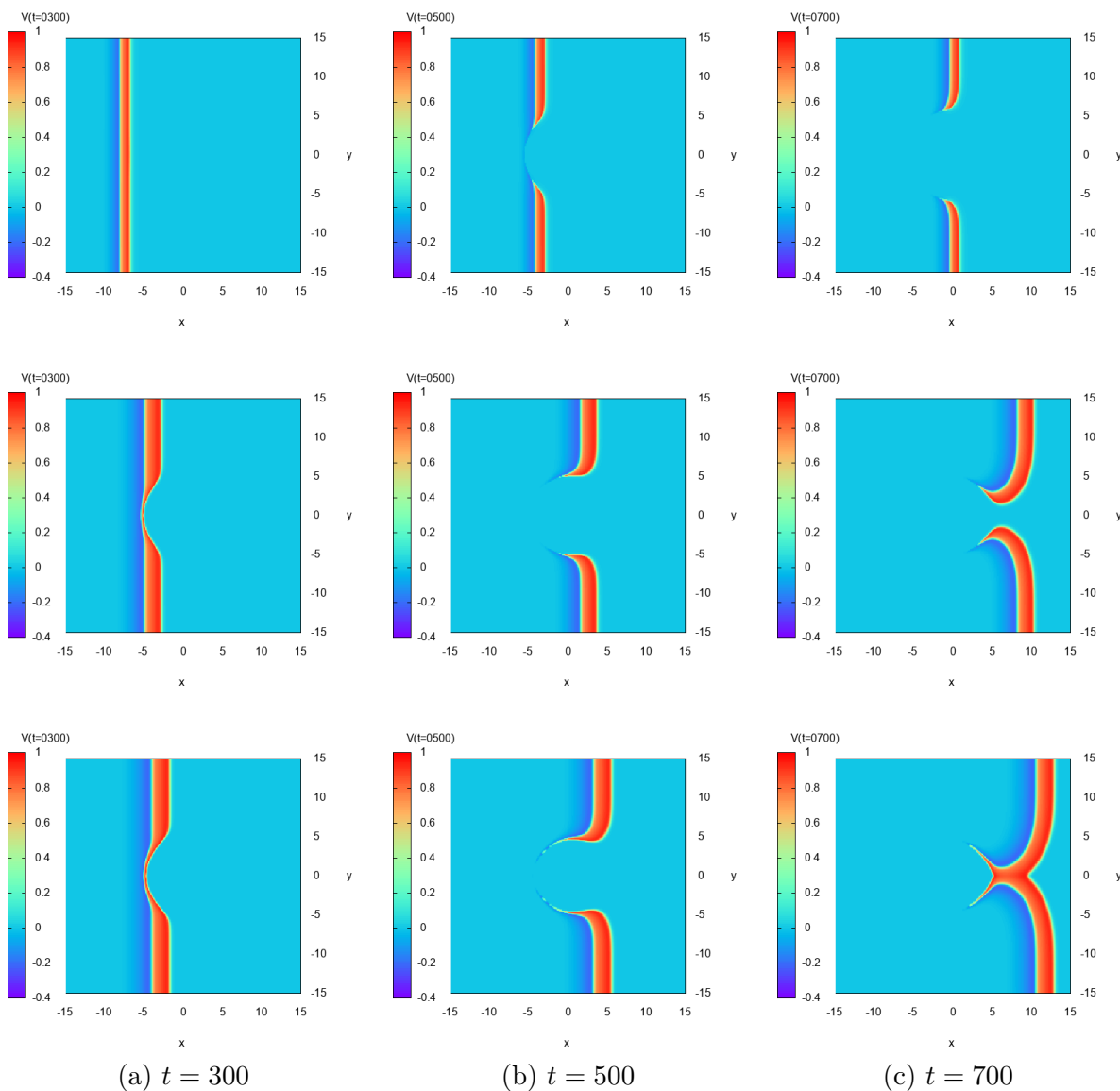
(a) $t = 300$ (b) $t = 500$ (c) $t = 700$

Figure 5.2: **Heterogeneous neuron density** : plot of the solution V^ε at different time $t = 300$, 500 and 700 for $\varepsilon = 5$ (top), $\varepsilon = 2$ (middle) and $\varepsilon = 10^{-2}$ (bottom).

5.3.3   Heterogeneous neuron density

In the spirit of [22, 23], the study of propagating waves in neural networks with spatial heterogeneities seems to be a fruitful topic. This subsection is therefore devoted to the illustration of the behaviour of the solution to the numerical scheme (5.2.12)–(5.2.13) with a non constant neuron density function ρ_0. We choose the initial datum

$$f_0(\mathbf{x}, v, w) = \rho_0(\mathbf{x})\, \chi_A\left(\frac{v - V_0(\mathbf{x})}{10}\right) \chi_A\left(\frac{w - W_0(\mathbf{x})}{100}\right),$$

140

with $A = (-1/2, 1/2)$ where the density ρ_0 is a smooth approximation of $1 - \chi_{\mathcal{B}(0,6)}$ and (V_0, W_0) is chosen as

$$V_0(\mathbf{x}) = \begin{cases} 1 & \text{if } x_1 \in (-14, -13), \\ 0 & \text{else,} \end{cases} \qquad W_0(\mathbf{x}) = \begin{cases} 0.1 & \text{if } x_2 \leq -14, \\ 0 & \text{else.} \end{cases} \qquad (5.3.7)$$

The domain in space is taken to be $(-15, 15)^2$, discretized using $n_x = 512$ points in each spatial coordinate and $M = 50$ particles per cell. It is expected that a wave will propagate initially from the left hand side in the homogeneous density of neurons. Then in the center of the domain, the density becomes inhomogeneous, which will perturb the wave propagation front. In Figure 5.2, we propose different scenario depending on the scaling parameter $\varepsilon > 0$. We display the profile of the solution V^ε at time $t = 300$, 500 and 700 for $\varepsilon = 5$, 2 and 10^{-2}. Clearly, the amplitude of the scaling parameter $\varepsilon > 0$ has an influence on the shape of the pulse but also on the speed of propagation.

First of all, the scrolling wave does not propagate through the ball $\mathcal{B}(0, 6)$, since the neuron density is too weak. Then, we can observe that as ε grows small, the speed of propagation and the width of the scroll wave increase. Thus, the heterogeneity does not have exactly the same effect. For $\varepsilon = 5$ and $\varepsilon = 2$ for example, the width of the gap in the neuron density is too large compared to the width of the traveling pulse. Therefore, the scroll wave breaks at its middle, and then recomposes once the heterogeneity is passed. Then, for smaller values of ε, as $\varepsilon = 0.01$, the traveling pulse starts to wrap the area where it cannot propagate before breaking and recomposing.

5.3.4 Rotating spiral waves

A spiral wave in the broadest sense is a rotating wave traveling outward from a center. Such spiral waves have been observed in many biological systems [107, 134], such as mammalian cerebral cortex [86]. Although circular waves were predicted from early models of cortical activity [11], true spiral wave formation has been already obtained in numerical simulations of reaction-diffusion systems such as the Wilson-Cowan system [29, 132, 133].

In this section, we present numerical evidence for stable spiral waves considering the transport equation (5.1.1)–(5.1.2). We choose the initial datum [29]

$$f_0(\mathbf{x}, v, w) = \rho_0(\mathbf{x}) \, \chi_A\left(\frac{v - V_0(\mathbf{x})}{10}\right) \chi_A\left(\frac{w - W_0(\mathbf{x})}{100}\right),$$

with $A = (-1/2, 1/2)$ where the density ρ_0 is a smooth approximation of the characteristic function on the disk centered in 0 with radius 12, whereas (V_0, W_0) is chosen as

$$V_0(\mathbf{x}) = \begin{cases} 1 & \text{if } x_1 \leq -6 \text{ and } x_2 \in (0, 3), \\ 0 & \text{else,} \end{cases} \qquad W_0(\mathbf{x}) = \begin{cases} 0.1 & \text{if } x_2 \geq 3, \\ 0 & \text{else.} \end{cases} \qquad (5.3.8)$$

Here the trivial state $(V, W) = (0, 0)$ is perturbed by setting the lower-left quarter of the domain to $V = 1$ and the upper half part to $W = 0.1$, which allows the initial condition to curve and rotate clockwise generating the spiral pattern. The domain in space is taken to be $(-15, 15)^2$, discretized using $n_x = 512$ points in each spatial coordinate and $M = 50$ particles per cell.

We first perform several computations changing the value of the scaling parameter and report in Figure 5.3, the profile of the numerical solution V^ε obtained using the second order scheme (5.2.15)–(5.2.17) at the final time of the simulation $t = 800$. On the one hand, when $\varepsilon \geq 6$, we observe that the initial wave first propagates into the domain, then it is damped and the solution converges to the stable steady state $(V, W) = (0, 0)$ when times goes on (see Figure 5.3 (a) at time $t = 800$). On the other hand, when ε becomes smaller $\varepsilon \in (4, 6)$, the solution
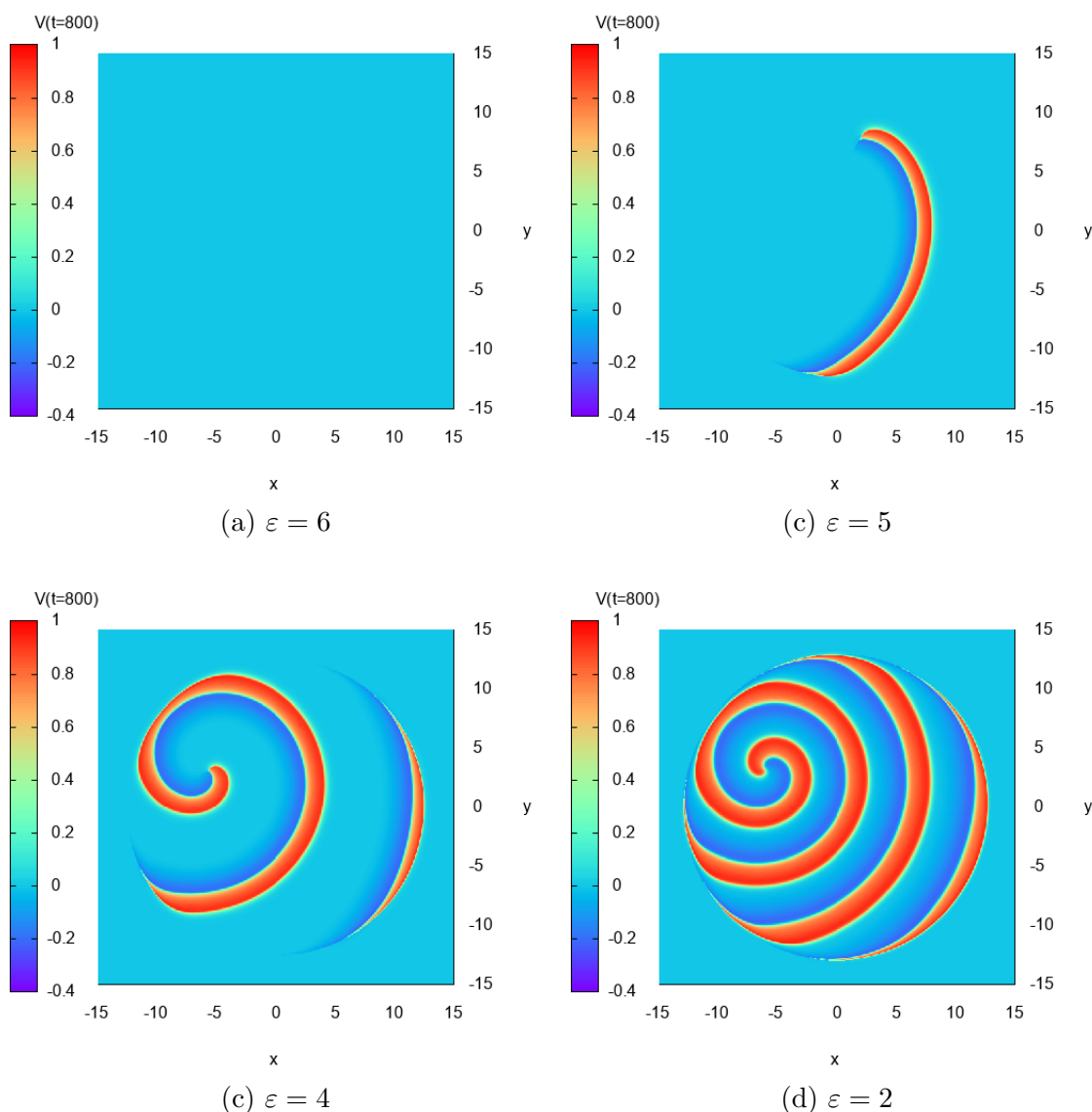
Figure 5.3: **Rotating spiral waves** : plot of the solution V^ε at time $t = 800$ for different values of $\varepsilon > 0$.

evolves in a different manner. Indeed, the initial wave propagates into the physical domain where $\rho_0 > 0$, and a spiral wave appears at time $t \simeq 20$, where a traveling pulse emerges and propagates from the bottom left quarter of the domain, towards the bottom right quarter, which creates a rotating spiral wave at larger time. For these values of ε, the shape of the solution is very sensitive to ε (see for instance (b) and (c) in Figure 5.3). Finally, when $\varepsilon \leq 4$, a spiral wave appears and it seems that the solution is not anymore sensitive to ε.

In Figure 5.4, we report the numerical results for $\varepsilon = 0.5$ at different time $t \in (0, 600)$. It illustrates how the spiral wave is generated from the initial data: a traveling pulse appears and begins to rotate clockwise, while the waves propagate up to the edge of the region where $\rho_0 > 0$. Moreover, it seems that once the spiral wave has appeared, its speed of rotation remains constant (see in (e) and (f) in Figure 5.4). Furthermore, in Figure 5.5, we report a zoom in the

(a) $t = 0$ (b) $t = 100$ (c) $t = 200$

(d) $t = 300$ (e) $t = 400$ (f) $t = 600$
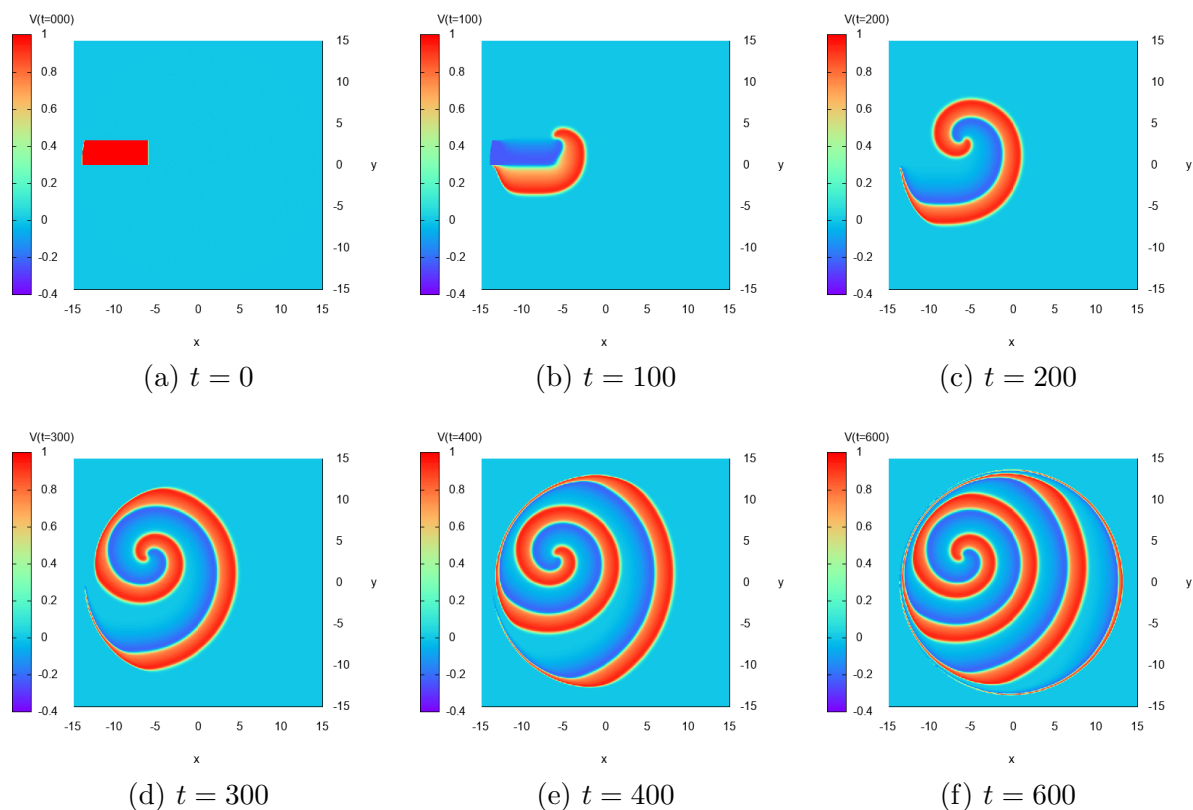
Figure 5.4: **Rotating spiral waves** : plot of the solution V^ε for $\varepsilon = 0.5$ at different time
$t \in [0, 600]$.

region where the traveling pulse appears. We observe that the center of the spiral moves and
oscillates around a point. Finally in Figure 5.6, we propose the time evolution of the solution
V^ε at different points $\mathbf{x} = (-6, 3)$, $\mathbf{x} = (-8, 4)$ and $\mathbf{x} = (-8, 2)$. Close to the point $\mathbf{x} = (-6, 3)$,
around which the spiral oscillates, time oscillations appear with an amplitude between -0.1
and 0.6 whereas in the neighboring points, different oscillations appear with a larger amplitude.
Observe that at $\mathbf{x} = (-8, 4)$ and $\mathbf{x} = (-8, 2)$, the time oscillations look the same but are shifted.

5.4 Conclusion

In the present paper we have proposed a class of semi-implicit time discretization techniques for
particle simulations to (5.1.1)–(5.1.2) coupled with a spectral collocation method for the space
discretization. The main feature of our approach is to guarantee the accuracy and stability on
slow scale variables even when the amplitude of local interactions becomes large, thus allowing
a capture of the correct behavior with a large time step with respect to $\varepsilon > 0$. Even on large
time simulations the obtained numerical schemes also provide an acceptable accuracy on the
membrane potential when $\varepsilon \ll 1$, whereas fast scales are automatically filtered when the time
step is large compared to ε^2.

As a theoretical validation we have proved that under some stability assumptions on numer-
ical approximations, the slow part of the approximation converges when $\varepsilon \to 0$ to the solution
of a limiting scheme for the asymptotic evolution, that preserves the initial order of accuracy.
Yet a full proof of uniform accuracy remains to be carried out in the frame of the continuous
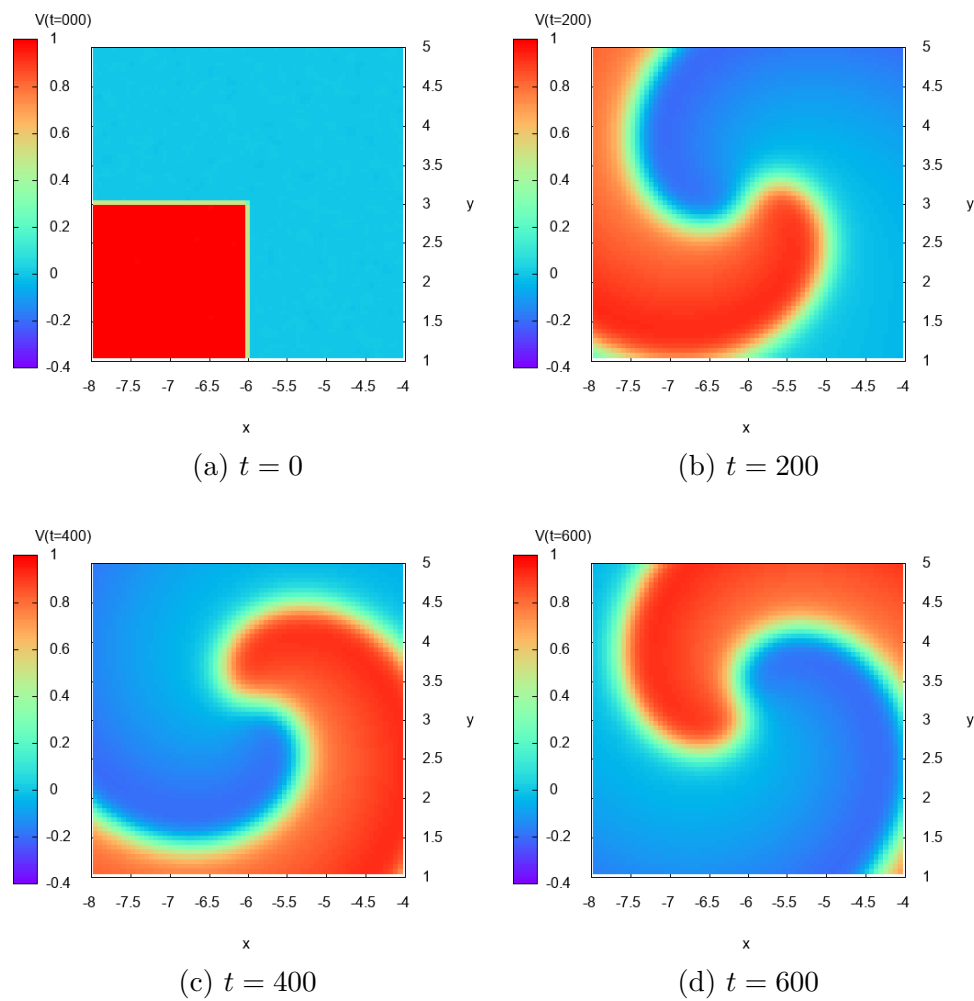
Figure 5.5: **Rotating spiral waves** : zoom on the solution V^ε for $\varepsilon = 0.5$ at different time $t \in [0, 400]$ around the point where the traveling pulse emerges.

case [47].

(a) $\mathbf{x} = (-6, 3)$ (b) $\mathbf{x} = (-8, 4)$ (c) $\mathbf{x} = (-8, 2)$
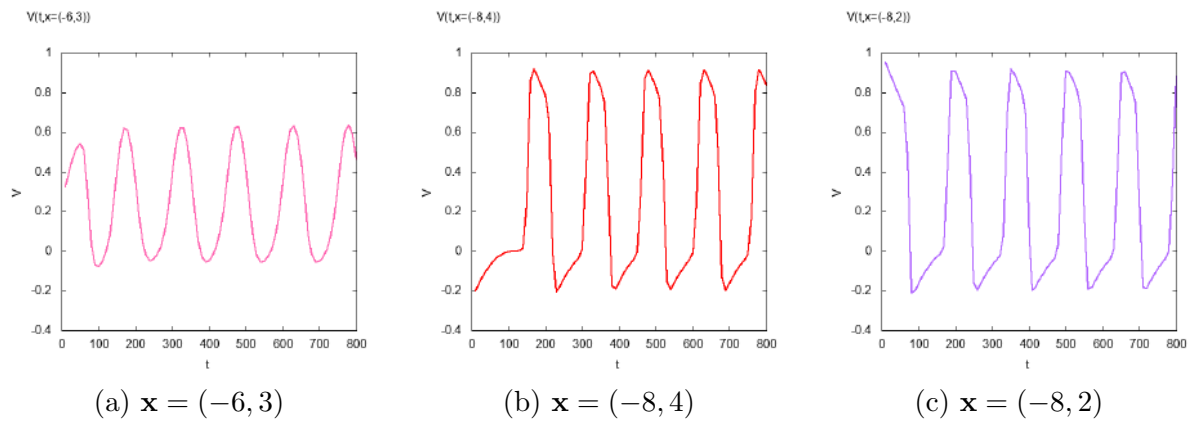
Figure 5.6: **Rotating spiral waves** : time evolution of the solution V^ε for $\varepsilon = 0.5$ at different points around the location where the traveling pulse emerges.

Chapter 6

Conclusion générale et perspectives

Tout le travail effectué dans cette thèse a donc consisté à établir rigoureusement un lien entre le modèle microscopique de FHN spatialement étendu (1.1.8), et des modèles macroscopiques comme (1.3.8) ou (1.3.16). Pour cela, nous avons commencé par établir la limite champ moyen du système (1.1.8) vers l'équation de transport (1.2.2) quand le nombre de neurones dans le réseau tend vers l'infini. Cette équation nous a servi de modèle mésoscopique intermédiaire, à partir duquel nous avons présenté deux redimensionnements possibles afin de considérer le régime d'interactions locales fortes.

Le premier consiste à étudier le cas d'un noyau d'interaction décomposé en deux termes : une fonction intégrable et une masse de Dirac multipliée par un terme qui tend vers l'infini, représentant respectivement les interactions à longue portée et à courte portée. La limite hydrodynamique de l'équation ainsi obtenue est le système de réaction-diffusion nonlocal (1.3.8). Ainsi, d'après ce modèle, le réseau de neurones à l'échelle macroscopique garde des interactions à longue portée. La seconde manière est de redimensionner le noyau d'interaction afin que lorsque le paramètre d'échelonnement tend vers 0, l'amplitude des interactions tend vers l'infini, tandis que leur portée tend vers 0. La limite asymptotique de l'équation nous donne le système de réaction diffusion local (1.3.16). Dans les deux cas, nous avons utilisé une technique d'entropie relative, afin d'estimer l'écart entre les quantités moyennes calculées à partir de la solution de l'équation de transport (1.2.2), et la solution de l'équation de réaction-diffusion limite.

De plus, nous avons présenté une discrétisation du modèle de champ moyen (1.3.11) avec interaction locales fortes qui reste asymptotiquement stable lorsque l'on passe à la limite macroscopique permettant d'obtenir (1.3.16), afin de pouvoir étudier numériquement l'influence du paramètre d'échelonnement, donc de l'intensité et la portée des interactions, sur la dynamique du système.

Ce qui distingue les modèles que nous avons considérés de la littérature, c'est essentiellement le fait d'avoir considéré des liaisons synaptiques uniquement pondérées par l'organisation spatiale du réseau de neurones. De plus, nous n'avons pas ajouté de bruit stochastique, ce qui nous a permis d'utiliser uniquement des techniques déterministes. Une des faiblesses de notre modèle est l'ensemble des hypothèses que nous avons dû faire pour l'obtenir. En particulier, le fait de n'avoir considéré que des synapses électriques, et pas chimiques, n'est pas réaliste. Néanmoins, nous avons réussi à obtenir des modèles macroscopiques connus pour être capables de reproduire certains comportements qualitatifs observés expérimentalement *in vivo* dans le cortex. De manière plus réaliste, ces modèles pourraient donc tout aussi bien s'appliquer pour l'étude des variations de potentiels électriques sur des tissus comme les fibres ventriculaires du cœur, comme le font [2, 74, 99] par exemple.

Présentons à présent avec quelques extensions possibles de nos travaux.

Dynamiques en milieu hétérogène   Comme expliqué plus haut, le modèle nonlocal (1.3.8) permet de décrire l'évolution du voltage moyen des neurones dans un réseau dont la répartition spatiale est hétérogène. Dans le cas homogène, l'existence de solutions de type ondes progressives a déjà été établi dans [62] (voir aussi [8] pour l'existence de front d'invasion dans le cas de l'équation d'Allen-Cahn nonlocale).

Si l'étude de la propagation de signaux dans des réseaux homogènes a un certain intérêt, pour la diffusion le long de colonnes corticales par exemple, à l'échelle macroscopique, le cortex est organisé de manière hétérogène. Dans l'esprit des travaux [22, 23] de P.C. Bressloff, nous souhaitons à présent étudier le cas où la densité de neurones du réseau ρ_0 est une fonction périodique, dans le cas unidimensionnel $d = 1$. Pour simplifier la formulation du problème, retirons la variable d'adaptation. L'équation (1.3.8) devient donc l'équation d'Allen-Cahn non-

locale, qui s'écrit pour tout $t > 0$ et $x \in \mathbb{R}$:

$$\partial_t V(t,x) - \int_{\mathbb{R}} \Psi(|x-y|) \, \rho_0(y) \, (V(t,y) - V(t,x)) \, \mathrm{d}y = N(V(t,x)). \qquad (6.0.1)$$

Soit $\varepsilon > 0$ un paramètre de redimensionnement. Le premier problème qu'il faudrait aborder est de démontrer rigoureusement l'existence, l'unicité, et la stabilité ou non d'ondes progressives, c'est-à-dire de solutions de (6.0.1) de la forme $V(t,x) = V(t, x - \phi(t))$, où ϕ est une fonction de $\mathbb{R}$. Dans le cas homogène $\rho_0 \equiv 1$, la fonction ϕ serait linéaire. Deux cas nous semblent intéressants. D'une part, le cas de perturbation du cas homogène $\rho_0(x) = 1 + \nu(x)$, où ν est une fonction périodique d'amplitude inférieure à 1, afin que ρ_0 reste strictement positive, dans l'esprit de ce qui a été étudié dans [45] pour une équation de champ neuronal. D'autre part, nous pouvons aussi étudier le cas d'une répartition des neurones éparse, c'est-à-dire

$$\rho_0 = \sum_{k \in \mathbb{Z}} \chi_{[2k, 2k+1)}.$$

Ici, le fait que ρ_0 puisse s'annuler peut poser des problèmes analytiques supplémentaires, mais d'un point de vue de modélisation, ce problème reste intéressant pour décrire par exemple les interactions entre deux colonnes corticales. La portée des interactions aura ici un rôle crucial : il faut qu'elle soit suffisamment grande pour franchir l'écart entre deux groupes de neurones. Dans les deux cas, nous pourrons utiliser des techniques développées pour l'étude de fronts de propagation pour les équations de réaction-diffusion locales comme dans [55].

Limites asymptotiques en milieu hétérogène Une fois que l'existence d'ondes progressives solution de (6.0.1) est établie rigoureusement, nous pouvons nous intéresser à l'influence de la fréquence des oscillations de ρ_0, particulièrement lorsque celle-ci est très faible, ou très grande.

- *Hétérogénéités spatiales lentes.* Dans le terme non local dans (6.0.1), on remplace $\rho_0(y)$ par $\rho_0(\varepsilon y)$. Ce problème a été traité formellement dans [22] avec une méthode de Hamilton-Jacobi, pour les fronts de propagation solutions d'une équation de champ neuronal. L'auteur commence par redimensionner le temps et l'espace $t \to t/\varepsilon$ et $x \to x/\varepsilon$, puis fait l'hypothèse que
$$V(t,x) \sim e^{-G(t,x)/\varepsilon},$$
où $G(t,x) > 0$ pour tout $x > x(t)$ avec $x(t)$ la position du front de propagation à l'instant $t > 0$. Cette approximation est nommée WKB (pour Wentzel–Kramers–Brillouin). La méthode d'Hamilton-Jacobi consiste donc à étudier la fonction G plutôt que V, en trouvant une équation différentielle approchant son comportement quand ε tend vers 0. Dans le cas de (6.0.1), notre objectif serait d'obtenir des résultats rigoureux similaires à ceux de [22].

- *Hétérogénéités spatiales rapides.* Ensuite, nous pouvons plutôt remplacer $\rho_0(y)$ par remplacer $\rho_0(y/\varepsilon)$. Là encore, nous nous référons à l'article [23], dans lequel P.C. Bressloff utilise des techniques de théorie d'homogénéisation pour observer le comportement d'une équation de champ neuronal dans le cas d'oscillations locales rapides de la densité de neurones. En utilisant une méthode formelle de perturbation du cas homogène, l'auteur parvient à obtenir des approximations sur le comportement des solutions de type ondes progressives lorsque la fréquence des oscillations des hétérogénéités tend vers l'infini. Notre objectif serait là aussi d'obtenir des résultats similaires pour (6.0.1) de manière rigoureuse.

Appendix A

CEMRACS research project: influence of the mode of reproduction on dispersal evolution during species invasion

Ce proceeding est à paraître dans *ESAIM: Proceedings and Surveys*. Il est issu d'un projet de recherche encadré par Vincent Calvez et Gaël Raoul, réalisé en collaboration avec Léonard Dekens, Florian Lavigne et Frédéric Kuczma.

Contents

Abstract

We consider a reaction-diffusion-reproduction equation, modeling a spatially and phenotypically organised population. The dispersion of each individuals is influenced by its phenotype. In the literature, the asymptotic propagation speed of an asexual population has already been rigorously determined. In this paper we focus on the difference between the asexual reproduction case, and the sexual reproduction case, involving a non-local term modeling the reproduction. This comparison leads to a different invasion speed according to the reproduction.

After a formal analysis of both cases, leading to a heuristic of the asymptotic behaviour of the invasion fronts, we give some numerical evidence that the acceleration rate of the spatial spreading of a sexual population is slower than the acceleration rate of an asexual one. The main difficulty to get sharper results on a transient comes from the non-local sexual reproduction term.

Introduction

Biological populations are often evolving in a heterogeneous environment, to which individuals can be more or less fitted, according to their phenotypes. Phenotypic distributions are shaped through processes like survival, reproduction and migration. Biological invasions are archetypal of a process where spatial heterogeneities are constitutive. Successful species manage to thrive due to some selective advantage in a new environment, and to expand in a new area. Different causes can promote the success of an invasion: wind or birds can disperse seeds (*e.g.* widespreading of lodgepole pine in western North America [50]) or climate change modifies the local environment and may influence species range (*e.g.* invasion of butterfly and bush cricket species in Britain [122]). Also, many species invasions result from an introduction, either voluntary or involuntary, by human beings (*e.g.* invasion of cane toads in Australia [1, 118, 121]), etc.

Recently, much attention was paid to evolutionary dynamics at the vanguard of species range expansion, see for instance [12, 121, 127, 128]. Among other, dispersal evolution, that is the evolution of the dispersal abilities of individuals, was the subject of biological and mathematical studies in the past decade. In particular, the phenomenon of *spatial sorting*, *i.e.* the assembly of more dispersive individuals ahead of the range expansion by pure spatial effect (all other phenotypes being identical within the population), was the subject of several modelling and analytical studies [9, 17, 18, 39, 129]. In particular, it has been established that front acceleration results from sustained spatial sorting in the case of possibly unbounded dispersal rates (or equivalently in the transient regime before the physiological limits are reached) [10, 16, 33]. So far, analytical results were obtained based on the modeling assumption that reproduction is clonal (as for asexual reproduction) with possible mutations affecting the dispersal ability of offsprings. In particular, recent techniques borrowed from the approximation of geometric optics for front propagation were used successfully to compute quantitative features such as the asymptotic speed of propagation, or the rate of acceleration in the transient regime [33, 129].

Besides, similar techniques were developed recently in a different context: the asymptotic description of equilibria in quantitative genetics models involving a sexual mode of reproduction in the regime of small variance. This methodology was recently completed for Fisher's infinitesimal model [70]. It is a simple model for the inheritance of quantitative traits in a population with a sexual mode of reproduction. It assigns to an offspring the average parental phenotypic trait up to a random normal deviation with constant variance [16].

Preliminary heuristics seem to show that this mode of reproduction significantly slows down the wave expansion as compared to an asexual reproduction. It is expected that, in the transient

accelerating regime, the population spreads as $t^{5/4}$ under the infinitesimal model of inheritance, whereas it was previously shown that the spreading occurs at a rate of order $t^{3/2}$ with the asexual mode of reproduction [10, 19].

In this paper, we present formal calculations in order to compare the rates of expansion for the two modes of reproduction under study. To validate these heuristics, we present also numerical results, which help us to catch a transient regime and its main features.

A.1 Our model

In this paper, we study the time evolution and the spatial and phenotypical propagation of population encowed with either an asexual or a sexual reproduction mode. More precisely, the population is distributed according to its location $x \in \mathbb{R}$ and its phenotypic trait $\theta \in (\theta_{\min}, +\infty)$, with $\theta_{\min} > 0$, and is modeled with the following reaction-diffusion equation for all $t > 0$:

$$\partial_t f(t,x,\theta) = r_1 f(t,x,\theta)\left[1 - K^{-1}\varrho(t,x)\right] + \theta\Delta_x f(t,x,\theta) + B[f](t,x,\theta), \qquad \text{(A.1.1)}$$

where $r_1 > 0$ and $K > 0$ are fixed constants, $f(t,x,\theta)$ is the density of individuals presenting the trait θ at location $x \in \mathbb{R}$ at time $t \geq 0$, and $\rho(t,x) := \int_{\theta_{\min}}^{\infty} f(t,x,\theta)\,\mathrm{d}\theta$ is the population size at $x \in \mathbb{R}$ and time $t > 0$. The reaction term $B[f]$ will be detailed later. We also assume that initially, the density support is compact. Let us discuss the modeling interest of each term.

Firstly, the term $r_1 f \left[1 - K^{-1}\varrho\right]$ stands for an adaptation force called *selection*. At point $x \in \mathbb{R}$ and at time $t \geq 0$, any individual is in competition with the others for resources: when the density $\varrho(t,x)$ at x is less than a threshold K, named the *carrying capacity*, there is enough resources for everyone so the population can grow; whereas, if $\varrho(t,x) > K$, then competition is involved, and the population is decreasing. The constants $r_1 > 0$ is therefore called *competition rate*.

Then, the term $\theta\,\Delta_x f$ models the *migration* phenomenon. Individuals are assumed to diffuse through space at each time t, at a rate given by the phenotypic trait θ. For example, those with long legs or bigger wings can be faster to go into a new environment, and so help the invasion. In fact, the equation (A.1.1) without the last reaction term $B[f]$ is the generalized non-local Fisher-KPP equation, where the diffusion depends on the phenotypic traits, which can be seen as a given constant. In the case that ϱ is a convolution term with f, the previous equation has been studied in some different ways [60, 73, 76, 78].

Finally, the last reaction term $B[f]$ models the *reproduction* event. Let us turn to explain this new term.

Asexual case. For asexual populations, reproduction is clonal: the offspring receives at birth the same trait as its sole parent, but mutations change the value of the trait. Assuming the variance of the mutation effects is very small, we can model the phenomenon by the following evolutionary equation, as in [9]:

$$\partial_t f(t,x,\theta) = r_1 f(t,x,\theta)\left[1 - K^{-1}\varrho(t,x)\right] + \theta\Delta_x f(t,x,\theta) + \mu\,\Delta_\theta f(t,x,\theta), \qquad \text{(A.1.2)}$$

where $\mu > 0$ is a constant depending on the mutation rate and on the variance of the mutation effects. Replacing f by $\theta_{\min}K^{-1}f(\theta_{\min}^2 t/\mu, \sqrt{\theta_{\min}^3/\mu}\,x, \theta_{\min}\theta)$ yields us to simplify the initial problem and to study:

$$\partial_t f(t,x,\theta) = r f(t,x,\theta)\left[1 - \varrho(t,x)\right] + \theta\Delta_x f(t,x,\theta) + \Delta_\theta f(t,x,\theta), \qquad \text{(A.1.3)}$$

with $\theta \in (1, +\infty)$, $r > 0$ and $\varrho(t,x) = \int_1^{\infty} f(t,x,\theta)\mathrm{d}\theta$. In this case, the reproduction term is just $Bf(t,x,\theta) = \Delta_\theta f(t,x,\theta)$.

Remark. The variation deduced by the mutation event is an approximation of an infinitesimal model [70, 97], taking the limit of the equation when the variance of the mutation effect $\lambda^2 > 0$ tends to 0. In this infinitesimal model, this variation follows a centred normally distributed random variable. Without selection and migration, the mutations [97] can be modeled by the evolutionary equation:

$$\partial_t f(t,x,\theta) = r_2 \left[J * f(t,x,\theta) - f(t,x,\theta) \right],$$

where $r_2 > 0$ is the *mutation rate*, J is the gaussian distribution of $\mathcal{N}(0, \lambda^2)$ and the "convolution term" $J * f(t,x,\theta) = \int_{\theta_{\min}}^{\infty} J(\theta - \theta') f(t,x,\theta') d\theta'$. Linearising the previous equation, when λ is very small, we retrieve the same term as in (A.1.3), with $\mu = r_2 \lambda$.

Boundary condition for the asexual case. By definition of phenotypic trait, no individual can have a phenotype in $(-\infty, 1)$ or generate a descendent with such phenotype: there is no phenotypical exchange at $\theta = 1$, which means that:

$$\forall t \geq 0, \ \forall x \in \mathbb{R}, \ \partial_\theta f(t,x,1) = 0.$$

Sexual case. During sexual reproduction, at the opposite of the asexual one, recombinations of the DNA happen, which changes the mathematical model and so the reproduction term in (A.1.2). We assume that individuals can breed only with those which are at the same location $x \in \mathbb{R}$.

Let us turn to the sexual reproduction model, introduced by Bülmer in 1980's. At time t, an individual of trait θ_1 can find and copulate with a partner of trait θ_2 with probability density $f(t,x,\theta_2)/\varrho(t,x)$. The offspring has originally the trait $(\theta_1 + \theta_2)/2$, which suffers directly from recombinations of variance $\lambda^2 > 0$:

$$\partial_t f(t,x,\theta) = r_1 f(t,x,\theta) \left[1 - K^{-1} \varrho(t,x) \right] + \theta \Delta_x f(t,x,\theta)$$
$$+ r_3 \left[\int_{\theta_{\min}}^{\infty} \int_{\theta_{\min}}^{\infty} \mathcal{G}_\theta \left(\theta - \frac{\theta_1 + \theta_2}{2} \right) f(t,x,\theta_1) \frac{f(t,x,\theta_2)}{\varrho(t,x)} d\theta_1 d\theta_2 - f(t,x,\theta) \right],$$

with $r_3 > 0$ the *rate of reproduction/recombination*. The term $\mathcal{G}_\theta \left(\theta - \dfrac{\theta_1 + \theta_2}{2} \right)$, symbolizing the stochasticity of the recombinations, is a normalized truncated centred gaussian, with variance $\lambda^2 > 0$, such that $\theta - \dfrac{\theta_1 + \theta_2}{2} > \theta_{\min}$. As a prospect, a further article could study the influence of the variance λ^2 of the recombination event; for the sake of simplicity, we take here $\lambda^2 = 1/2$. Replacing here f by $\theta_{\min} K^{-1} f(t/r_3, \sqrt{\theta_{\min}/r_3}\, x, \theta_{\min}\theta)$, and noting $r := r_1 K/\theta_{\min}$, we can simplify the previous PDE into:

$$\partial_t f(t,x,\theta) = r f(t,x,\theta) \left[1 - \varrho(t,x) \right] + \theta \Delta_x f(t,x,\theta)$$
$$+ \int_1^{\infty} \int_1^{\infty} \mathcal{G}_\theta \left(\theta - \frac{\theta_1 + \theta_2}{2} \right) f(t,x,\theta_1) \frac{f(t,x,\theta_2)}{\varrho(t,x)} d\theta_1 d\theta_2 - f(t,x,\theta), \quad \text{(A.1.4)}$$

with $\mathcal{G}_\theta$ is a normalized truncated centred gaussian, such that $\theta - \dfrac{\theta_1 + \theta_2}{2} > 1$. By this simplification, the reproduction is:

$$Bf(t,x,\theta) = \int_1^{\infty} \int_1^{\infty} \mathcal{G}_\theta \left(\theta - \frac{\theta_1 + \theta_2}{2} \right) f(t,x,\theta_1) \frac{f(t,x,\theta_2)}{\varrho(t,x)} d\theta_1 d\theta_2 - f(t,x,\theta).$$

A.2   Formal analysis

If we consider the asexual reproduction case without the competition, then the PDE that we obtained becomes linear and therefore calls for exponential solutions. Aligning thereby with others studies about diffusion of individuals and speed of the invasion (see for instance [19, 33]), where the common method is to define the function u such that:

$$f(t,x,\theta) = \exp\left[-t\, u\left(s(t), t^{-\alpha}x, t^{-\beta}\theta\right)\right], \tag{A.2.1}$$

where s is a time parametrization, and α and β are introduced to re-scale the spatial and phenotypic variables.

Finding (α, β) crystallizes the main issue tackled by the formal analysis, as it is the crucial key to get asymptotically a non trivial PDE satisfied by u (that is taking into account all the biological forces, namely selection, migration and reproduction), as it is shown in figure A.1.

Asexual case.   Thanks to (A.1.3), we can check that:

$$
\begin{aligned}
-u(s(t),y,\eta) &- ts'(t)\,\partial_s u(s(t),y,\eta) + \alpha y \partial_y u(s(t),y,\eta) + \beta\eta\partial_\eta u(s(t),y,\eta) \\
&= -\eta t^{1-2\alpha+\beta}\Delta_y u(s(t),y,\eta) + \eta t^{2-2\alpha+\beta}[\partial_y u(s(t),y,\eta)]^2 \\
&\qquad - t^{1-2\beta}\Delta_\eta u(s(t),y,\eta) + t^{2-2\beta}[\partial_\eta u(s(t),y,\eta)]^2 + r(1-\varrho),
\end{aligned}
$$

with $\varrho = t^\beta \int_{t^{-\beta}}^\infty \exp(-tu(s(t),y,\eta))\mathrm{d}\eta$. We choose the parametrization $s = \log(t)$ so that $ts'(t) = 1$. In this case, we obtain an viscous Hamilton-Jacobi PDE :

$$
\begin{aligned}
-u - \partial_s u + \alpha y \partial_y u + \beta\eta\partial_\eta u &= -\eta e^{(1-2\alpha+\beta)s}\Delta_y u + \eta e^{(2-2\alpha+\beta)s}(\partial_y u)^2 \\
&\qquad - e^{(1-2\beta)s}\Delta_\eta u + e^{(2-2\beta)s}(\partial_\eta u)^2 + r(1-\varrho) \\
&= e^{(2-2\alpha+\beta)s}\big(\eta(\partial_y u)^2 - \eta e^{-s}\Delta_y u\big) \\
&\qquad + e^{(2-2\beta)s}\big((\partial_\eta u)^2 - e^{-s}\Delta_\eta u\big) + r(1-\varrho). \tag{A.2.2}
\end{aligned}
$$

Remark A.2.1. *In large time t, which is equivalent to taking the limit as s tends to $+\infty$, the factor $\exp(-\,Cste\,s)$ in front of the laplacians terms will make the second order terms vanish. Nevertheless, the transformation (A.2.1) enables to capture the long time asymptotics. In fact, it transforms the nature of the problem, from a second order parabolic equation to a nonlinear viscous Hamilton-Jacobi, for which characteristic lines can be analytically computed. However, reviewing the rigorous derivation of the viscous Hamilton-Jacobi equation relies on the theory of viscosity solutions, which is beyond our scope, and we refer to [33] for details.*

Formally, our purpose is to determine the asymptotic behaviour of (A.2.2) in the limit $s \to +\infty$, that is to derive a PDE in which all biological phenomena intervene, especially:

$\diamond$ the reproduction term: as the factor $e^{(2-2\beta)s}(\partial_\eta u)^2$ tends to $+\infty$ or 0 depending on the sign of $(2-2\beta)$, the reproduction term will either annihilate the contribution of the others or vanish. Thus the only relevant choice derives from $2 - 2\beta = 0$.

$\diamond$ the diffusion term: the same considerations lead us to $2 - 2\alpha + \beta = 0$.

We thereby get the following system for (α, β):

$$
\begin{cases}
2 - 2\beta = 0, \\
2 - 2\alpha + \beta = 0.
\end{cases}
$$

which leads to:

$$(\alpha, \beta) = \left(\frac{3}{2}, 1\right).$$

Sexual case. Although the PDE obtained without taking the competition in account is in this case non linear, it keeps the same homogeneity as the asexual one, for only the reproduction term differs between the two models. We thus proceed by analogy with the asexual case by looking for exponential solutions using the transformation (A.2.1). Taking again $s(t) = \log(t)$, equation (A.1.4) yields:

$$-u - \partial_s u + \alpha y \partial_y u + \beta \eta \partial_\eta u = \eta e^{(2-2\alpha+\beta)s}\big((\partial_y u)^2 - e^{-s}\Delta_y u\big) + \left(\frac{B[f]}{f} - 1\right) + r(1-\varrho), \quad \text{(A.2.3)}$$

with $\varrho = e^{\beta s}\int_{e^{-\beta s}}^{\infty}\exp(-e^s\,u(s,y,\eta))\mathrm{d}\eta$ and:

$$\frac{B[f]}{f} = \frac{1}{\sqrt{2\pi}e^{-\beta s}\varrho}\int_{e^{-\beta s}}^{\infty}\int_{e^{-\beta s}}^{\infty}\exp\left[e^{2\beta s}\left(-\frac{\left(\eta - \frac{\eta_1+\eta_2}{2}\right)^2}{2}\right.\right.$$
$$\left.\left. + e^{s(1-2\beta)}\big[u(s,y,\eta) - u(s,y,\eta_1) - u(s,y,\eta_2)\big]\right)\right]\mathrm{d}\eta_1\,\mathrm{d}\eta_2. \quad \text{(A.2.4)}$$

As the sole difference between the asexual and sexual cases is the reproduction term, only the condition on the reproduction term will differ (and not the condition on the diffusion term that is coupling α and β). Since it dictated entirely the choice β in the previous case, we have to look precisely at the term $\frac{B[f]}{f}$ in order to deduce formally a reasonable β. By the same heuristics as in the previous case, as we want reproduction term neither to vanish nor to undermine the contributions of the other terms as s goes to $+\infty$, we need all the terms in the double integral to be treated equally with respect to s, which yields $1 - 2\beta = 0$. Thereby, we get the following system:

$$\begin{cases} 1 - 2\beta = 0, \\ 2 - 2\alpha + \beta = 0. \end{cases}$$

which leads to:

$$(\alpha, \beta) = \left(\frac{5}{4}, \frac{1}{2}\right).$$

A.3 Schemes and numerical results

Here, we present some numerical schemes to approximate the solutions of the equations (A.1.3) and (A.1.4). During this CEMRACS project, we have simulated the solutions of the different PDEs with *Fortran* and *Python*. We have used the packages *numpy*, *matplotlib* and *pythran*.

A.3.1 Asexual case

In this section, we present two different numerical schemes to approximate the diffusion with asexual reproduction.

We consider $x_{\max} \geq 0$ and $\theta_{\max} \geq 1$ so that we work with couples (x, θ) in the bounded domain $[0, x_{\max}] \times [1, \theta_{\max}]$, discretized with the meshes $(x_i)_{1 \leq i \leq N_x}$ and $(\theta_j)_{1 \leq j \leq N_\theta}$, respectively of step $\Delta x > 0$ and $\Delta \theta > 0$. As for the time discretization, let $\Delta t > 0$ be a time step, and let us define for all $n \in \mathbb{N}$, $t_n := n\,\Delta t$.

In the following, we denote by A_x^D and A_x^N the matrix of the discrete Laplace operator in x

of size N_x respectively with Dirichlet and Neumann boundary conditions:

$$A_x^D = \frac{1}{\Delta x^2} \begin{pmatrix} -2 & 1 & & & (0) \\ 1 & -2 & 1 & & \\ & \ddots & \ddots & \ddots & \\ & & 1 & -2 & 1 \\ (0) & & & 1 & -2 \end{pmatrix} \text{ and } A_x^N = \frac{1}{\Delta x^2} \begin{pmatrix} -1 & 1 & & & (0) \\ 1 & -2 & 1 & & \\ & \ddots & \ddots & \ddots & \\ & & 1 & -2 & 1 \\ (0) & & & 1 & -1 \end{pmatrix}.$$

We consider A_θ^D and A_θ^N the matrix of the discrete Laplace operator in θ of size N_θ respectively with Dirichlet and Neumann boundary conditions with similar definitions. In the following, we choose to work with the fixed parameter $r = 1$.

A.3.1.1   Euler explicit scheme

For all $n \in \mathbb{N}$, we approximate $(f(t_n, x_i, \theta_j))_{1 \leq i \leq N_x, 1 \leq j \leq N_\theta}$ with a matrix

$$F^n = \left(F_{ij}^n\right)_{1 \leq i \leq N_x, 1 \leq j \leq N_\theta}.$$

Then, for all $n \in \mathbb{N}$, we approach $(\varrho(t_n, x_i))_{1 \leq i \leq N_x}$ by a vector $(\widetilde{\varrho}_i^n)_{1 \leq i \leq N_x}$ computed with an approximation of the integral in θ using the trapezoidal rule. We have chosen an initial truncated Gaussian distribution:

$$f(0, x, \theta) = \frac{2}{\sqrt{\pi}} \exp\left[-\frac{x^2 + (1-\theta)^2}{2}\right] \mathbb{1}_{\theta \geq 1}. \tag{A.3.1}$$

First of all, we approximate the reaction-diffusion equation (A.1.3). We start by discretizing the diffusion terms in x and θ with the matrix of discrete Laplace operator with Dirichlet boundary conditions A_x^D and A_θ^D. Then, we approximate in time using an explicit Euler scheme that is for all $n \in \mathbb{N}$, we compute the new value of F^{n+1} by:

$$F^{n+1} = F^n + \Delta t \left[A_x^D \times F^n \times D_\theta + r\left(F^n - D_\varrho^n \times F^n\right) + F^n \times A_\theta^D \right], \tag{A.3.2}$$

where $D_\varrho^n := \mathrm{diag}\left((\widetilde{\varrho}_i^n)_{1 \leq i \leq N_x}\right)$, and $D_\theta := \mathrm{diag}\left((\theta_j)_{1 \leq j \leq N_\theta}\right)$. In the following, the steps Δt, Δx and $\Delta \theta$ have been chosen to satisfied the stability condition:

$$2\,\Delta t \left[\frac{\theta_{\max}}{\Delta x^2} + \frac{1}{\Delta \theta^2}\right] \leq 1.$$

In Figure A.1 (a), we plot the density of population $\varrho(t, \cdot)$ at different fixed times at regular intervals from the instant $t = 10$ to $t = 150$. As expected, the function ϱ seems to quickly converge towards an invasion front propagating towards right connecting 0 to 1. Moreover, we observe that the front of propagation in space seems to accelerate. Theoretically, according to [10, 19], we should observe a propagation of the front of order $t^{3/2}$ in space and of order t in phenotype.

On Figure A.1 (b), we verify the order of the spatial acceleration plotting the same curves with respect to the auto-similar variable $y = xt^{-3/2}$. We observe that the spatial densities ϱ converge towards an Heaviside distribution in y, centered at a constant y_c which is approximately 1.25. Theoretically, according to [19], this constant is approximately $y_c \approx 1.315$.

Then, we focus on the shape of the transition front. We plot in Figure A.1 (c) the spatial distribution ϱ with respect to a re-centered scale in $X_{1/2}(t)$, where $\varrho(t, X_{1/2}(t)) = 1/2$ for all $t \geq 0$. We can observe that the shape of the front flattens as time goes to infinity. In order to study this evolution, we display in Figure A.1 (d) the same curves with respect to the re-scaled
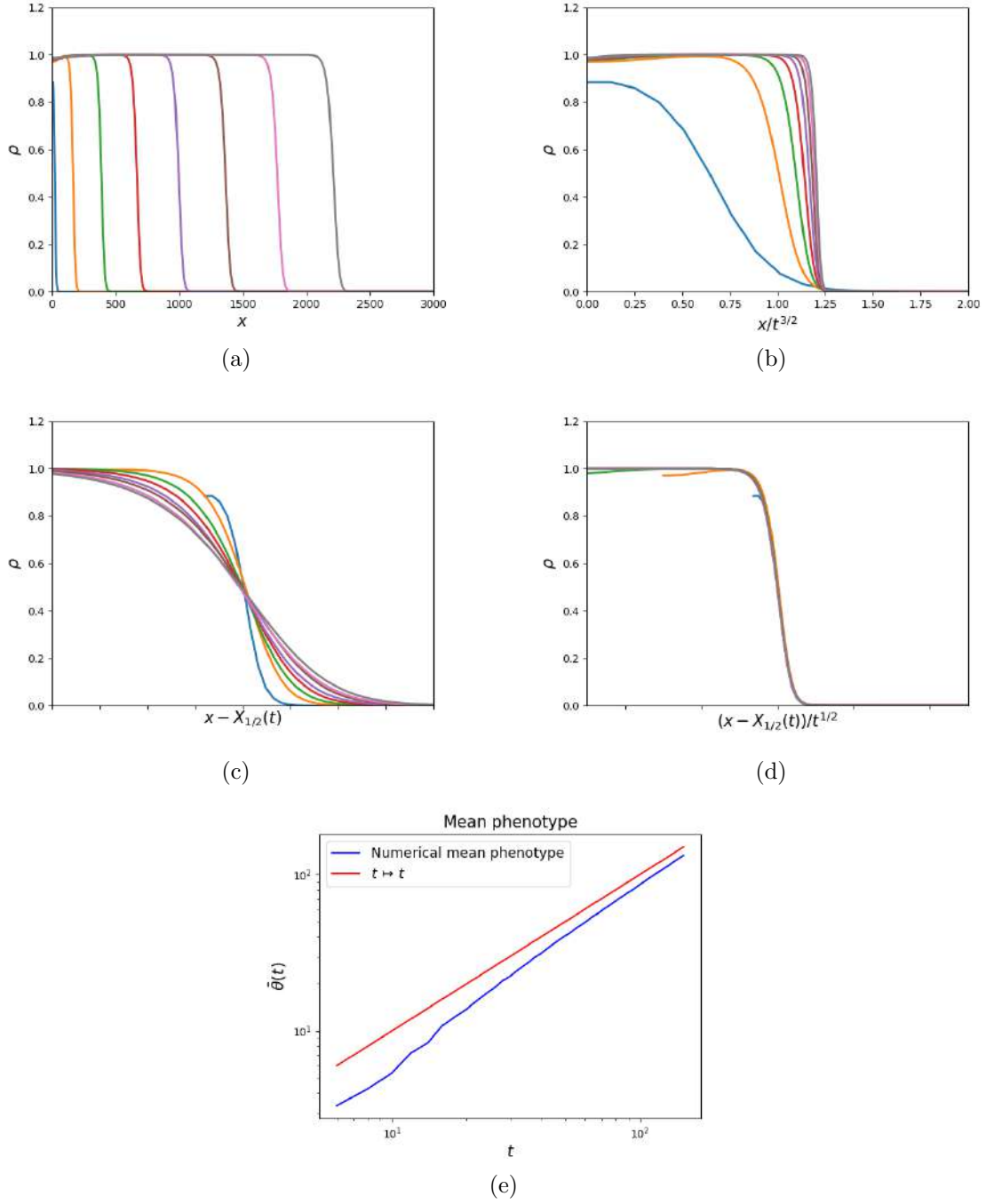
Figure A.1: Simulations associated to the equation (A.1.3) with parameters $r = 1$, $\Delta t = 0.02$, $\Delta x = 4$, $\Delta \theta = 2/3$, $x_{\max} = 3,000$ and $\theta_{\max} = 201$. Plots of the density of population $\varrho(t, \cdot)$ for successive fixed times at regular intervals from $t = 0$ to $t = 150$, with respect to (a) the position x, (b) to the auto-similar variable $x t^{-3/2}$, (c) to the re-centered variable $x - X_{1/2}(t)$, and (d) to the re-scaled variable $(x - X_{1/2}(t)) t^{-1/2}$, where for all $t \geq 0$, $\varrho(t, X_{1/2}(t)) = 1/2$. (e) Plot of the main phenotype $\bar{\theta}(t)$ (see (A.3.4)) at the front position with respect to time (blue curve) and of the function $t \to t$ (red curve), in $\log - \log$ scale.

variable $\left(x - X_{1/2}(t)\right) t^{-1/2}$. We can see that all curves are superposed. Therefore, the shape of the front seems to flatten at order $t^{1/2}$.

Finally, in order to numerically study the accelerations in phenotype of the solution of the

equation (A.1.3), we define for all $t \geq 0$ the position of the front at time t with:

$$X(t) := \underset{x \in [0, x_{\max}]}{\operatorname{argmin}} |\varrho(t, x) - 0.01|, \qquad (A.3.3)$$

and the main phenotype at the head of the front $\bar{\theta}(t)$ with:

$$\bar{\theta}(t) := \frac{\int_{\mathbb{R}} \theta f(t, X(t), \theta) \, d\theta}{\varrho(t, X(t))}. \qquad (A.3.4)$$

In Figure A.1 (e), we show in log-log scale the evolution of the numerical and formal results of $\bar{\theta}$ with respect to time, and the identity function $t \mapsto t$, in order to compare their slopes. We can observe that for high times, these two curves seem to be parallel. Using a linear regression without taking into account the values where t is too small in order not to consider an eventual transitory state, we find that our numerical approximation of the main phenotype $\bar{\theta}(t)$ is of order $t^{1.01}$. Therefore, this explicit Euler scheme seems to be efficient to reproduce the expected acceleration phenomenon in the asexual case.

A.3.1.2 Auto-similar variables

In this section, we focus on the approximation of the variable $u(s, y, \eta)$ defined in (A.2.1), with reparametrized time $s := \log(t)$, and auto-similar variables $y := x \, t^{-\alpha}$ and $\eta := \theta \, t^{-\beta}$ with α and $\beta > 0$. Thus, the equation (A.2.2) satisfied by u can be written as follows:

$$\partial_s u - \eta \, e^{(1-2\alpha+\beta)s} \, \Delta_y u - e^{(1-2\alpha+\beta)s} \, \Delta_\eta u + \mathcal{H}_1(s, \partial_y u) + \mathcal{H}_2(s, \partial_\eta u) = -u - r \, (1 - \varrho), \quad (A.3.5)$$

where for all $s > 0$, and $p \in \mathbb{R}$, the Hamiltonians in y and η are defined with:

$$\begin{cases} \mathcal{H}_1(s, p)(y, \eta) & := & e^{(2-2\alpha+\beta)s} \, \eta \, p^2 - \alpha \, y \, p, \\[2mm] \mathcal{H}_2(s, p)(y, \eta) & := & e^{(2-2\beta)s} \, p^2 - \beta \, \eta \, p. \end{cases}$$

To be consistent with the last paragraph, we also choose a polynomial initial condition:

$$u(0, y, \eta) = \frac{y^2 + \eta^2}{2}.$$

We consider $y_{\max} \geq 0$ and $\eta_{\max} \geq 1$ so that we work with couples (y, η) in the bounded domain $[0, y_{\max}] \times [1, \eta_{\max}]$, discretized with the meshes $(y_i)_{1 \leq i \leq N_y}$ and $(\eta_j)_{1 \leq j \leq N_\eta}$, respectively of step $\Delta y > 0$ and $\Delta \eta > 0$. In the following, we define A_y^N and A_η^N the matrix of the discrete Laplace operator with Neumann boundary conditions respectively in y of size N_y and in η of size N_η. We also define a time step $\Delta s > 0$ and for all $n \in \mathbb{N}$, $s_n = n \, \Delta s$. We want to approximate for all $1 \leq i \leq N_y$, $1 \leq j \leq N_\eta$, and $n \in \mathbb{N}$ the function $u(s_n, y_i, \eta_j)$ with a matrix $\left(U_{ij}^n \right) \in \mathbb{R}^{N_y \times N_\eta}$, defined for all $n \in \mathbb{N}$ with:

$$\begin{aligned} U^{n+1} := &(1 - \Delta s) \, U^n - \Delta s \, H_1(s_n, U^n) - \Delta s \, H_2(s_n, U^n) + r \, \Delta s \, e^{(1-2\beta)s} \, U^n \times A_\eta^N \\ &+ \Delta s \, e^{(\beta-2\alpha+1)s} \, A_y^N \times U^n \times D_\eta - r \, \Delta s \, (\mathbb{1} - M_\varrho^n), \end{aligned}$$

where $D_\eta := \operatorname{diag}\left((\eta_j)_{1 \leq j \leq N_\eta} \right)$, and for all $1 \leq i \leq N_y$, $1 \leq j \leq N_\eta$,

$$(\mathbb{1} - M_\varrho^n)_{ij} := 1 - \widetilde{\varrho}_i^n,$$

where $\widetilde{\varrho}_i^n$ is the approximation of $\varrho\left(\exp(s_n), y_i \times s_n^{5/4}\right)$ computed from U^n. Furthermore, the matrix $H_1(s_n, U^n)$ and $H_2(s_n, U^n) \in \mathbb{R}^{N_y \times N_\eta}$ are the respective approximations of the Hamiltonians in y and η. To choose good approximations H_1 and H_2, we used the idea of the scheme of [46]. This method consists in rewriting the Hamiltonian $\mathcal{H}_1(s, \cdot)$ (resp. $\mathcal{H}_2(s, \cdot)$) into the sum of an increasing function $\mathcal{H}_1^+(s, \cdot)$ and a decreasing function $\mathcal{H}_1^-(s, \cdot)$, which gives for all $s > 0$, $y \in \mathbb{R}$, $\eta > 0$ and $p \in \mathbb{R}$:

$$
\begin{cases}
\mathcal{H}_1^+(s,p)(y,\eta) = \left[e^{(\beta-2\alpha+2)s}\eta\, p^2 - \alpha\, y\, p\right]\mathbb{1}_{p \geq c_1} - \dfrac{\alpha}{2} y\, c_1 \mathbb{1}_{p < c_1}, \\[2ex]
\mathcal{H}_1^-(s,p)(y,\eta) = \left[e^{(\beta-2\alpha+2)s}\eta\, p^2 - \alpha\, y\, p\right]\mathbb{1}_{p \leq c_1} - \dfrac{\alpha}{2} y\, c_1 \mathbb{1}_{p > c_1}, \\[2ex]
\mathcal{H}_2^+(s,p)(y,\eta) = \left[e^{(2-2\beta)s}p^2 - \beta\,\eta\, p\right]\mathbb{1}_{p \geq c_2} - \dfrac{\beta}{2}\eta\, c_2\, \mathbb{1}_{p < c_2}, \\[2ex]
\mathcal{H}_2^-(s,p)(y,\eta) = \left[e^{(2-2\beta)s}p^2 - \beta\,\eta\, p\right]\mathbb{1}_{p \leq c_2} - \dfrac{\beta}{2}\eta\, c_2\, \mathbb{1}_{p > c_2},
\end{cases}
$$

and:

$$
\begin{cases}
c_1 = \dfrac{\alpha}{2}e^{-(\beta-2\alpha+2)s}\dfrac{y}{\eta}, \\[2ex]
c_2 = \dfrac{\beta}{2}e^{-(2-2\beta)s}\,\eta.
\end{cases}
$$

Then, we approximate $\mathcal{H}_1(s, \partial_y u)$ (resp. $\mathcal{H}_2$) with:

$$
\mathcal{H}_1(s_n, \partial_y u) \approx \max[\mathcal{H}_1^+(s, \partial_y^- u), \mathcal{H}_1^-(s, \partial_y^+ u)]
$$
$$
(\text{resp. } \mathcal{H}_2(s_n, \partial_\eta u) \approx \max[\mathcal{H}_2^+(s, \partial_\eta^- u), \mathcal{H}_2^-(s, \partial_\eta^+ u)]),
$$

where $\partial_y^- u$ and $\partial_y^+ u$ (resp. $\partial_\eta^- u$ and $\partial_\eta^+ u$) are the derivatives of u with respect to y (resp. η) respectively on the left and on the right. Thus, if we define the matrices D_y^l and D_y^r of size $N_y \times N_y$ and D_η^l and D_η^r of size $N_\eta \times N_\eta$ with:

$$
D_y^l = \frac{1}{\Delta y}
\begin{pmatrix}
1 & 0 & & & (0) \\
-1 & 1 & 0 & & \\
& \ddots & \ddots & \ddots & \\
& & -1 & 1 & 0 \\
(0) & & & -1 & 1
\end{pmatrix}
, \quad
D_y^r = \frac{1}{\Delta y}
\begin{pmatrix}
1 & -1 & & & (0) \\
0 & 1 & -1 & & \\
& \ddots & \ddots & \ddots & \\
& & 0 & 1 & -1 \\
(0) & & & 0 & 1
\end{pmatrix},
$$

and:

$$
D_\eta^r = \frac{1}{\Delta \eta}
\begin{pmatrix}
1 & 0 & & & (0) \\
-1 & 1 & 0 & & \\
& \ddots & \ddots & \ddots & \\
& & -1 & 1 & 0 \\
(0) & & & -1 & 1
\end{pmatrix}
, \quad
D_\eta^l = \frac{1}{\Delta \eta}
\begin{pmatrix}
1 & -1 & & & (0) \\
0 & 1 & -1 & & \\
& \ddots & \ddots & \ddots & \\
& & 0 & 1 & -1 \\
(0) & & & 0 & 1
\end{pmatrix},
$$

we approximate $\mathcal{H}_1(s_n, \partial_y u)(y_i, \eta_j)$ and $\mathcal{H}_2(s_n, \partial_\eta u)(y_i, \eta_j)$ with:

$$
\begin{cases}
H_1(s_n, U^n)_{ij} := \max\left\{\mathcal{H}_1^+(s_n, D_y^l U^n)(y_i, \eta_j), \mathcal{H}_1^-(s_n, D_y^r U^n)(y_i, \eta_j)\right\}, \\[2ex]
H_2(s_n, U^n)_{ij} := \max\left\{\mathcal{H}_2^+(s_n, U^n D_\eta^l)(y_i, \eta_j), \mathcal{H}_2^-(s_n, U^n D_\eta^r)(y_i, \eta_j)\right\}.
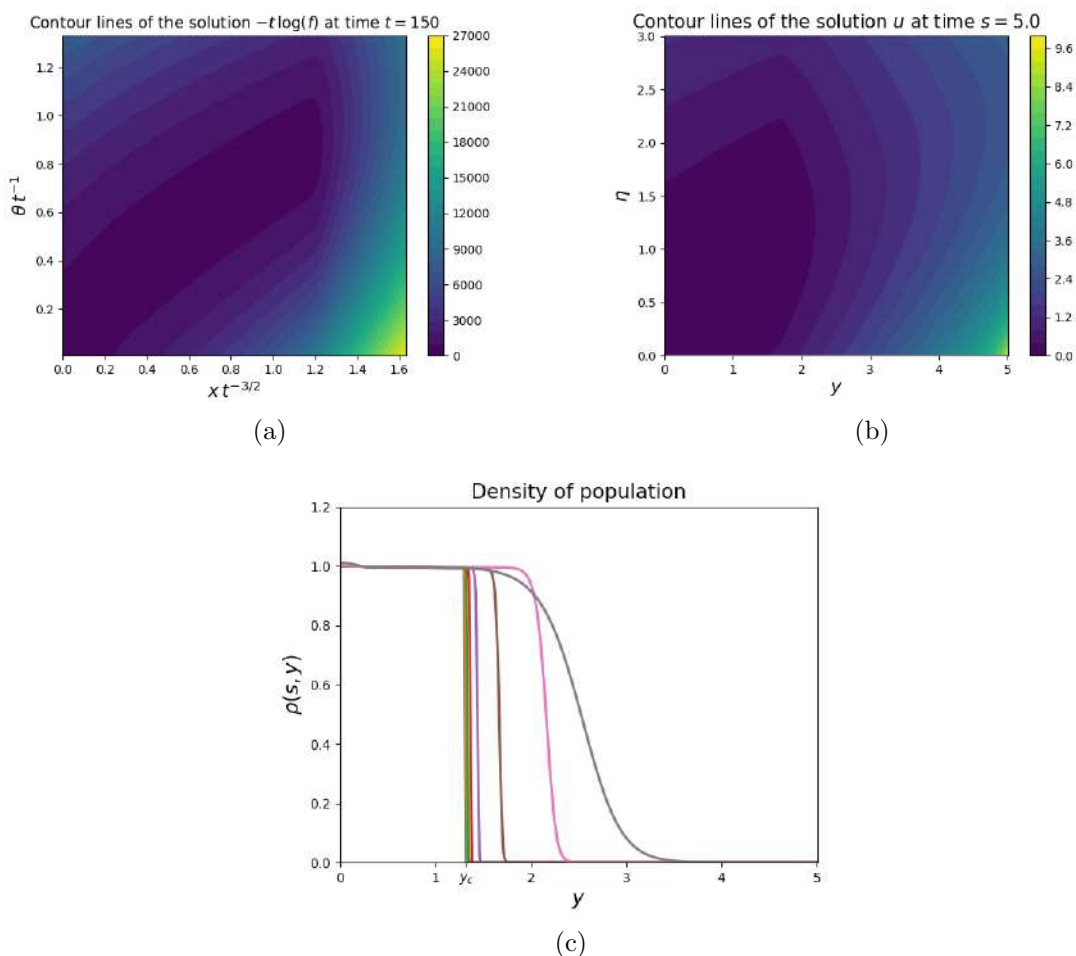\end{cases}
$$

(a)

(b)

(c)

Figure A.2: (a) Plot of $-t \log(f)$ where f is the approximation (see Section 4.1.1) of the solution of the equation (A.1.3) at time $t = 150$, with parameters $r = 1$, $\Delta t = 0.02$, $\Delta x = 4$, $\Delta \theta = 2/3$, $x_{\max} = 3,000$ and $\theta_{\max} = 201$. (b) Plot of the solution u of the viscous Hamilton-Jacobi equation (A.2.2) at time $s = 5$, approximated with the scheme presented in Section 4.1.2). (c) Plot of the population density $\varrho(s, y)$, computed with the approximation of the solution u of (A.2.2) (given by the scheme in Section 4.1.2), with respect to the auto-similar y, at different fixed times at regular intervals from $s = 0$ to $s = 7$, with the same parameters. The parameters used for Figures (b) and (c) are $r = 1$, $ds = 10^{-5}$, $dy = 10^{-2}$, $d\eta = 10^{-2}$, $\eta_{\max} = 3$ and $y_{\max} = 5$.

At the end of an iteration, we compute F by the relation:

$$F_{ij}^n = \exp\left(-e^{s+\Delta s} U_{ij}^n\right).$$

In Figure A.2 (a), we display the function $-t \log(f)$ at fixed time $t = 150$ with respect to the re-scaled variable $y = x \, t^{-3/2}$ and $\eta = \theta \, t^{-1}$, where f is the solution of the reaction-diffusion (A.1.3) in the asexual case. We can compare this plot with the Figure A.2 (b), where we display the function u at fixed re-parametrized time $s = 5$, with respect to y and η. First of all, the shape of these two functions seems to be roughly similar. Nevertheless, since $f(t, x, \theta)$ is close to 0 for large enough x and small enough θ, the function $-t \log(f)$ drawn in Figure A.2 (a) reaches high values for $y = 1.6$ and $\eta = 0$. On the contrary, the function u plotted in Figure A.2 (b) does not explode for large y and small η. Therefore, the numerical scheme with auto-similar variables provides more information than the explicit Euler scheme explained in Section A.3.1.1

on the behaviour of the solution at the head of the front.

Furthermore, in Figure A.2 (c), we show the density population $\varrho(s, y)$ computed from the solution u of the equation (A.2.2), with respect to the re-scaled variable y, at different fixed times from $s = 0$ to $s = 7$ at regular interval. We observe that the function ϱ seems to converge as expected towards an Heaviside function $H(y_c - y)$. This is coherent with the theoretical results explained previously in Section A.2. Moreover, the numerical estimate for $y_c \approx 1.32$ is close to the theoretical value from [33] (approximately 1.315), and is consistent with theorem 1.2 from [19] which establishes $y_c \leq 4/3$ and an acceleration of order $t^{3/2}$. Consequently, this numerical scheme enables us to approximate more accurately the order of acceleration of the front than the previous one explained in Section A.3.1.1.

Besides, the position of the front y_c depends on the value of the birth rate r. For small values of this parameter, we expect y_c to be increasing with respect to r. Indeed, allowing individuals to mutate according to a stronger rate would lead to a larger range in the dispersal rates and build a faster front wave for the invasion. This phenomenon can be illustrated through a comparison with [10], in which the authors have analytically studied the same model with a different set of parameters. Up to a time scale, their model is equivalent to ours with $r = 2$ and we see that:

$$y_c(r = 2) = \frac{2}{3} 2^{\frac{1}{4}} 2^{\frac{3}{2}} = \frac{4}{3} 2^{\frac{3}{4}} \approx 2.24 > \frac{4}{3}.$$

A.3.2 Sexual case

The most challenging problem for the simulation of the sexual case is the approximation of the reproduction term $B[f]$. In this article, a straightforward approach is sufficient to display what we seek. Thus, for all $n \in \mathbb{N}$, $1 \leq i \leq N_x$ and $1 \leq j \leq N_\theta$, we approximate $B[f](t_n, x_i, \theta_j)$ with:

$$S_{ij}^n := \frac{\Delta \theta^2}{\widehat{\varrho}_i^n} \sum_{k=1}^{N_\theta} \sum_{l=1}^{N_\theta} K\left[\theta_j - \frac{1}{2}(\theta_k + \theta_l)\right] F_{ik}^n F_{il}^n,$$

with the function $K : \theta \mapsto \exp\left(-\theta^2\right) / \sqrt{\pi}$.

Similarly as in the asexual case, we discretize the time using an explicit Euler scheme, that is for all $n \in \mathbb{N}$, we compute the matrix F^{n+1} using:

$$F^{n+1} := F^n + \Delta t \left[A_x^N \times F^n \times D_\theta + r\left(F^n - D_\varrho^n \times F^n\right) + (S^n - F^n)\right], \tag{A.3.6}$$

with $D_\varrho^n := \mathrm{diag}\left((\widehat{\varrho}_i^n)_{1 \leq i \leq N_x}\right)$, and $D_\theta := \mathrm{diag}\left((\theta_j)_{1 \leq j \leq N_\theta}\right)$.

In Figure A.3, we show some simulations of the solution of the equation (A.1.4). First of all, in Figure A.3 (a) and (b), we display the contour lines of the function f respectively at fixed time $t = 800$ and $t = 1,600$. We can observe the propagation both in space and phenotype of the function f as time passes. Moreover, the shape of the function f before the head of the front seems to be invariant with respect to time. Therefore, once the population is settled at a position x, it does not evolve any more.

Then, let us more precisely focus on the propagation in space. In Figure A.3 (c), we plot the density function ϱ for different fixed times between $t = 40$ and $t = 1600$. As expected, if we do not take into account the values of x too close to the boundary, ϱ seems to quickly converge towards an invasion front. Moreover, this invasion front seems to accelerate. One can notice that for small x, the density function $\varrho(t, x)$ seems to remain below 1 for all time. Indeed, unlike in the asexual case, this is possible since in the sexual case (A.1.4), the maximum principle is false.

To validate our formal analysis, we display in Figure A.3 (d) the same functions with respect to the auto-similar variable $y = xt^{-5/4}$. As expected, as t increases, the function ϱ tends towards
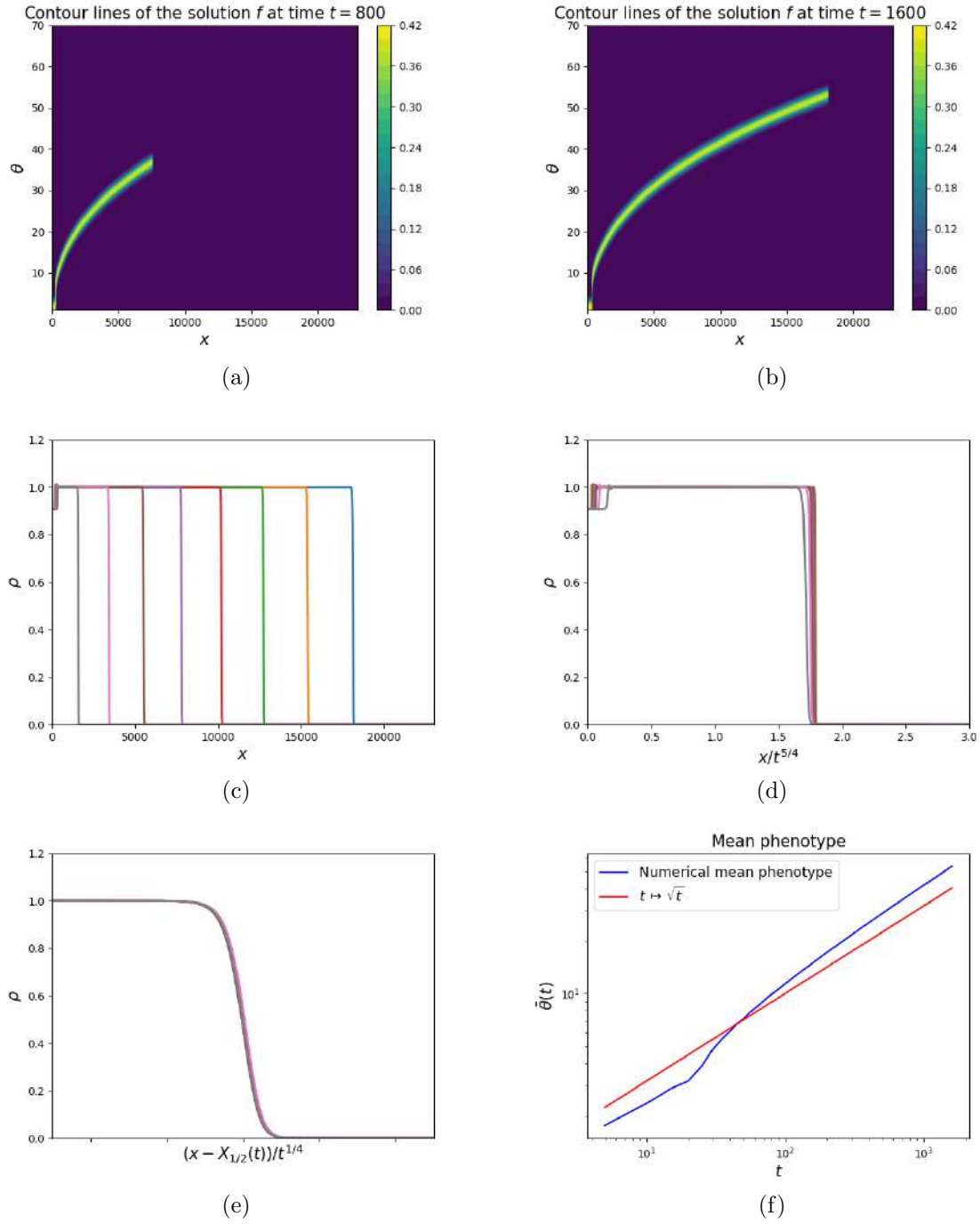
(a)

(b)

(c)

(d)

(e)

(f)

Figure A.3: Simulations associated to the equation (A.1.4) with parameters $r = 1$, $\Delta t = 0.05$, $\Delta x = 4$, $\Delta \theta = 0.69$, $x_{\max} = 2.3 \cdot 10^4$ and $\theta_{\max} = 70$. Plot of the function $f(t, \cdot, \cdot)$ at time (a) $t = 800$ and (b) $t = 1,600$. Plots of the density of population $\varrho(t, \cdot)$ for succesive fixed times at regular intervals from $t = 40$ to $t = 1,600$, with respect to (c) the position x, (d) to the auto-similar variable $xt^{-5/4}$, and (e) to the re-scaled and re-centered variable $(x - X_{1/2}(t))t^{-1/4}$, where for all $t \geq 0$, $\varrho(t, X_{1/2}(t)) = 1/2$. (f) Plot of the main phenotype $\bar{\theta}(t)$ (see (A.3.4)) at the front position with respect to time in $\log - \log$ scale.

a stiff and stationary state. This shows that the acceleration of the invasion front showed in Figure A.3 (c) seems to accelerate at the order $y_c t^{5/4}$. Nevertheless, similarly as in the asexual case, the approximation of the constant y_c is not sharp.

Finally, as done in Section A.3.1.1, let us study the deformation of the invasion front. In

163

Figure A.3 (e), we display the same functions as previously with respect to the re-scale and re-centered variable $(x - X_{1/2}(t)) \, t^{-1/4}$. Since the graphs in Figure A.3 seem to be merged, we can conjecture that the the typical width of the front in the sexual reproduction case is of order $t^{1/4}$.

Finally, in order to study more precisely the acceleration of the invasion front in phenotype, we proceed as previously for the asexual case, computing for all time $t \geq 0$ the front position $X(t)$ and the mean phenotype $\bar{\theta}(t)$ at position $X(t)$, respectively defined with (A.3.3) and (A.3.4). In Figure A.3 (f), we display in log-log scale the numerical approximation of the mean phenotype $\bar{\theta}$ with respect to time, and the function $t \mapsto \sqrt{t}$, in order to compare the slope of the two curves for large times. A formal derivation and approximation of the multiplicative constant in the expression of the mean phenotype will be the objects of an upcoming work. We can observe that for t large enough, the two graphs seem to remain parallel. Proceeding with a linear regression, we find that $\bar{\theta}$ is approximately of order $t^{0.52}$. In the same way that the explicit Euler scheme provides a good approximation of the asexual case (A.1.3), here the numerical results seem to fit with our formal analysis in Section A.2.

A.4   Conclusion

Dispersal evolution at the vanguard of species range expansion can bring intricated dynamics such as spatial sorting [121] and front wave acceleration [10, 19]. As mentioned in the Introduction, some heuristics predict that the sexual reproduction slows down the wave expansion in comparison to the asexual reproduction. In this paper, we have developed numerical schemes to bring elements of confirmation to this phenomenon.

As seen in section 4, the numerical simulations supports the formal analysis in confirming the predicted asymptotic order of the propagation speed in space and in the phenotypic range, for both the asexual and sexual type of reproduction (respectively $(t^{3/2}, t)$ and $(t^{5/4}, t^{1/2})$). Therefore, it does appear that the mode of reproduction does bear a strong influence on the speed of the invasion, as well as on the genetic mixing: a species using a sexual reproduction will be slower to expand on both levels than a species using an asexual reproduction.

However satisfactory bringing a numerical confirmation to this question is, the formal analysis performed for the sexual case in Section 3 could not be considered as complete, as it does arise some new remarks. The knowledge of the values of the rescaling constants $(\alpha, \beta) = (5/4, 1/2)$ allows us to take a new look at the equation involving the re-scaled variables, obtained by the transformation (A.2.3):

$$-u - \partial_s u + \frac{5}{4} \, y \, \partial_y u + \frac{1}{2} \, \eta \, \partial_\eta u = \eta \, \left[(\partial_y u)^2 - e^{-s} \, \Delta_y u \right] + \left(\frac{B[f]}{f} - 1 \right) + r(1 - \varrho), \quad \text{(A.4.1)}$$

with $\varrho = e^{s/2} \int_{e^{-s/2}}^{\infty} \exp(-e^s u(s, y, \eta)) \mathrm{d}\eta$ and:

$$\frac{B[f]}{f}$$
$$= \frac{e^{s/2}}{\sqrt{2\pi} \varrho} \int_{e^{-s/2}}^{\infty} \int_{e^{-s/2}}^{\infty} \exp\left[e^s \left(-\frac{\left(\eta - \frac{\eta_1 + \eta_2}{2} \right)^2}{2} + \left[u(s, y, \eta) - u(s, y, \eta_1) - u(s, y, \eta_2) \right] \right) \right] \mathrm{d}\eta_1 \, \mathrm{d}\eta_2.$$
$$\text{(A.4.2)}$$

The presence of factors like e^s, only in terms where η is variable at a given point of space y, implies that there is a hierarchy between the different equilibria in the variables η and y on how fast they are reached. More precisely, it suggests that we can consider that the equilibrium towards the variable η is always reached at each spatial point y. Moreover, its mathematical

description should clearly state its dependence towards the space variable y, which surely calls for a more thorough analysis.

Numerically, we have observed in the asexual case that a stable code computing u in terms of the re-scaled variables (s, y, η) was far more efficient to capture the complexity of the asymptotic state. Thus, the isolation of such subtle phenomena of hierarchy between phenotypic and space equilibria requires a similar code in the sexual case. Both of these are prospects of an upcoming work.

Bibliography

[1] R. Alford et al. Comparisons through time and space suggest rapid evolution of dispersal behaviour in an invasive species. *Wildlife Research*, 36(1):23–28, 2009.

[2] R. R. Amari and A. V. Panfilov. A simple two-variable modelof cardiac excitation. *Chaos, Solitons and Fractals*, 7(3):293–301, 1996.

[3] S.-I. Amari. Dynamics of pattern formation in lateral-inhibition type neural fields. *Biological Cybernetics*, 27(2):77–87, 1977.

[4] J. Baladron, D. Fasoli, and O. Faugeras. Three applications of gpu computing in neuroscience. *Computing in Science and Engineering*, 14(3), 2012.

[5] J. Baladron, D. Fasoli, O. Faugeras, and J. Touboul. Mean-field description and propagation of chaos in networks of hodgkin-huxley and fitzhugh-nagumo neurons. *The Journal of Mathematical Neuroscience*, 2(10), 2012.

[6] P. W. Bates, X. Chen, and A. J. J. Chmaj. Traveling waves of bistable dynamics on a lattice. *SIAM Journal on Mathematical Analysis*, 35(2):520–546, 2003.

[7] P. W. Bates, X. Chen, and A. J. J. Chmaj. Heteroclinic solutions of a van der waals model with indefinite nonlocal interactions. *Calc. Var. Partial Differential Equations*, 24(3):261–281, 2005.

[8] P.W. Bates, P.C. Fife, X. Ren, and X. Wang. Traveling waves in a convolution model for phase transitions. *Arch. Rational Mech. Anal*, 138:105–136, 1997.

[9] O. Benichou, V. Calvez, N. Meunier, and R. Voituriez. Front acceleration by dynamic selection in fisherpopulation waves. *Physical review E*, 86(4-1):041908, 2012.

[10] N. Berestycki, C. Mouhot, and G. Raoul. Existence of self-accelerating fronts for a nonlocal reaction-diffsuion equations. *arXiv preprint arXiv:1512.00903*, 2015.

[11] R.L. Beurle. Properties of a mass of cells capable of regenerating pulses. *Philos. Trans. R. Soc. London B, Biol. Sci.*, 240(669):55–94, 1956.

[12] G. Birzu, O. Hallatschek, and K. S. Korolev. Neither pulled nor pushed: Genetic drift and front wandering uncover a new class of reaction-diffusion waves. *arXiv preprint arXiv:1709.01601*, 2017.

[13] F. Bolley, J.A. Cañizo, and J.A. Carrillo. Stochastic mean-field limit: Non-lipschitz forces and swarming. *Mathematical Models and Methods in Applied Sciences*, 21(11):2179–2210, 2011.

[14] S. Boscarino, F. Filbet, and G. Russo. High order semi-implicit schemes for time dependent partial differential equations. *J. Sci. Comput.*, 68(3):975–1001, 2016.

[15] M. Bossy, O. Faugeras, and D. Talay. Clarification and complement to "mean-field description and propagation of chaos in networks of hodgkin-huxley and fitzhugh-nagumo neurons". *The Journal of Mathematical Neuroscience*, 5(1), 2015.

[16] E. Bouin, T. Bourgeron, V. Calvez, O. Corro, J. Garnier, T. Lepoutre, and O. Ronce. Equilibria of quantitative genetics models beyond the gaussian approximation i :maladaptation to a changing environment. *in preparation*, 2018.

[17] E. Bouin and V. Calvez. A kinetic eikonal equation. *Comptes Rendus Mathematique*, 350(5-6):243–248, 2012.

[18] E. Bouin and V. Calvez. Travelling waves for the cane toads equation with bounded traits. *Nonlinearity*, 27(9):2233, 2014.

[19] E. Bouin, C. Henderson, and L. Ryzhik. Super-linear spreading in local and non-local cane toads equations. *Journal de Mathématiques Pures et Appliquées*, 108(5):724–750, 2017.

[20] Y. Brenier. Convergence of the vlasov-poisson system to the incompressible euler equations. *Communications in Partial Differential Equations*, 25(3-4):737–754, 2000.

[21] Y. Brenier, R. Natalini, and M. Puel. On a relaxation approximation of the incompressible navier-stokes equations. *Proceedings of the American Mathematical Society*, 132(4):1021–1028, 2004.

[22] P.C. Bressloff. From invasion to extinction in heterogeneous neural fields. *The Journal of Mathematical Neuroscience*, 2, 2001.

[23] P.C. Bressloff. Traveling fronts and wave propagation failure in an inhomogeneous neural network. *Physica D*, 155:83–100, 2001.

[24] P.C. Bressloff. Spatially periodic modulation of cortical patterns by long-range horizontal connections. *Physica D: Nonlinear Phenomena*, 27185(3):131–157, 2003.

[25] P.C. Bressloff. Spatiotemporal dynamics of continuum neural fields. *J. Phys. A: Math. Theor.*, 45(3), 2012.

[26] P.C. Bressloff. *Waves in Neural Media: From single Neurons to Neural Fields*. Springer, 2014.

[27] P.C. Bressloff, Cowan J.D., M. Golubitsky, P.J. Thomas, and M. Wiener. Geometric visual hallucinations, euclidean symmetry and the functional architecture of striate cortex. *Philosophical Transactions of the Royal Society London B*, 40:299–300, 2001.

[28] N. Brunel and Hakim V. Fast global oscillations in networks of integrate-and-fire neurons with low firing rates. *Neural computation*, 11(7):1621–1671, 1999.

[29] A. Bueno-Orovio, D. Kay, and K. Burrage. Fourier spectral methods for fractional-in-space reaction-diffusion equations. *BIT*, 54(4):937–954, 2014.

[30] J.A. Cañizo, J.A. Carrillo, and J. Rosado. A well-posedness theory in measures for some kinetic models of collective motion. *Math. Mod. Meth. Appl. Sci.*, 21:515–539, 2011.

[31] T. Cabana and J.D. Touboul. Large deviations for randomly connected neural networks: I. spatially extended systems. *Advances in Applied Probability*, 50(3):944–982, 2018.

[32] M.J. Caceres, J.A. Carrillo, and B. Perthame. Analysis of nonlinear noisy integrate and fire neuron models: blow-up and steady states. *Journal of Mathematical Neuroscience*, 1:7, 2011.

[33] V. Calvez, C. Henderson, S. Mirrahimi, O. Turanova, and T. Dumont. Non-local competition slows down front acceleration during dispersal evolution. *arXiv preprint arXiv:1810.07634*, 2018.

[34] M. Campos Pinto, E. Sonnendrücker, A. Friedman, D.P. Grote, and S.M. Lund. Noiseless vlasov-poisson simulations with linearly transformed particles. *Journal of Computational Physics*, 275:236–256, 2014.

[35] C. Canuto, M.Y. Hussaini, A. Quarteroni, and T.A. Zang. *Spectral Methods in Fluid Dynamics.* Berlin, Springer-Verlag, 1987.

[36] G. Carpenter. A geometric approach to singular perturbation problems with applications to nerve impulse equations. *J. Differential Equations*, 23:335–367, 1977.

[37] J.A. Carrillo, B. Perthame, D. Salort, and D. Smets. Qualitative properties of solutions for the noisy integrate and fire model in computational neuroscience. *Nonlinearity*, 28:3365–3388, 2015.

[38] P. Carter and A. Scheel. Wave train selection by invasion fronts in the fitzhugh-nagumo equation. *Nonlinearity*, 31(12):5536–5572, 2018.

[39] N. Champagnat and S. Méléard. Invasion and adaptive evolution for individual-based spatially structured populations. *J. Math. Biol.*, 55(147), 2007.

[40] J. Chevallier. Mean-field limit of generalized hawkes processes. *Stochastic Processes and their Applications*, 127(12):3870–3912, 2017.

[41] J. Chevallier, M.J. Caceres, M. Doumic, and P. Reynaud-Bouret. Microscopic approach of a time elapsed neural model. *Mathematical Models and Methods in Applied Sciences*, 25(14):2669–2719, 2015.

[42] J. Chevallier, A. Duarte, E. Löcherbach, and G. Ost. Mean-field limits for nonlinear spatially extended hawkes processes with exponential memory kernels. *Stochastic Processes and their Applications*, 129(1):1–27, 2019.

[43] H. Chiba and G.S. Medvedev. The mean field analysis for the kuramoto model on graphs i. the mean field equation and transition point formulas. Discrete *&* Continuous Dynamical Systems-A, 39(1):131–155, 2019.

[44] S. Coombes. Waves, bumps, and patterns in neural fields theories. *Biological Cybernetics*, 93(2):91–108, 2005.

[45] S. Coombes and C.R. Laing. Pulsating fronts in periodically modulated neural fields models. *Phys Rev E Stat Nonlin Soft Matter Phys*, 83(1 Pt 1):011912, 2011.

[46] M. Crandall and P. Lions. Two approximations of solutions of hamilton-jacobi equations. *Mathematics of Computation*, 43(167):1–19, 1984.

[47] J. Crevat. Diffusive limit of a spatially-extended kinetic fitzhugh-nagumo model. *submitted*, 2019.

[48] J. Crevat. Mean-field limit of a spatially-extended fitzhugh-nagumo neural network. *Kinetic & Related Models*, 12(6):1329–1358, 2019.

[49] J. Crevat, G. Faye, and F. Filbet. Rigorous derivation of the nonlocal reaction-diffusion fitzhugh-nagumo system. *SIAM J. Math. Anal.*, 51(1):346–373, 2019.

[50] L. Cwynar and G. MacDonald. Geographical variation of lodgepole pine in relation to population history. *The American Naturalist*, 129(3):463–469, 1987.

[51] C.M. Dafermos. The second law of thermodynamics and stability. *Arch. Ration. Anal.*, 70(2):167–179, 1979.

[52] P. Degong. Asymptotic-preserving schemes for fluid models of plasma. *Panoramas et synthèses*, 39-40:1–90, 2013.

[53] F. Delarue, J. Inglis, S. Rubenthaler, and E. Tanré. Global solvability of a networked integrate-and-fire model of mckean–vlasov type. *Ann. Appl. Probab.*, 25(4):2096–2133, 2015.

[54] F. Delarue, J. Inglis, S. Rubenthaler, and E. Tanré. Particle systems with a singular mean-field self-excitation. application to neuronal networks. *Stochastic Processes and their Applications*, 125(6):2451 – 2492, 2015.

[55] W. Ding, F. Hamel, and X. Zhao. Bistable pulsating fronts for reaction-diffusion equations in a periodic habitat. *Indiana Univ. Math. J.*, 66:1189–1265, 2017.

[56] R.J. Diperna. Uniqueness of solutions to hyperbolic conservation laws. *Indiana Univ. Math. J.*, 28(1):137–188, 1979.

[57] R. Dobrushin. Vlasov equations. *Funct. Anal. Appl.*, 13:115–123, 1979.

[58] G. B. Ermentrout and J. D. Cowan. A mathematical theory of visual hallucination patterns. *Biological Cybernetics*, 34:137–150, 1979.

[59] L. C. Evans. *Partial differential equations*. American Mathematical Society, Providence, R.I., 2010.

[60] J. Fang and X. Zhao. Monotone wavefronts of the nonlocal fisher-kpp equation. *Nonlinearity*, 24(11):3043–3054, 2011.

[61] O. Faugeras, J. Touboul, and B. Cessac. A constructive mean-field analysis of multi population neural networks with random synaptic weight and stochastic inputs. *Frontiers in computational neuroscience*, 3:1, 2009.

[62] G. Faye and A. Scheel. Existence of pulses in excitable media with nonlocal coupling. *Advances in Mathematics*, 270:400–456, 2015.

[63] A. Figalli and M.-J. Kang. A rigorous derivation from the kinetic cucker-smale model to the pressureless euler system with nonlocal alignment. *Analysis & PDE*, 12(3):843–866, 2019.

[64] F. Filbet, J. Hu, and S. Jin. A numerical scheme for the quantum boltzmann equation with stiff collision terms. *ESAIM Math. Model. Numer. Anal.*, 46(2):443–463, 2012.

[65] F. Filbet and S. Jin. An asymptotic preserving scheme for the es-bgk model of the boltzmann equation. *J. Sci. Computing*, 46(2):204–224, 2011.

[66] F. Filbet, C. Mouhot, and L. Pareschi. Solving the boltzmann equation in $n \log_2 n$. *SIAM J. Sci. Comput.*, 28(3):1029–1053, 2006.

[67] F. Filbet, L. Pareschi, and Th. Rey. On steady-state preserving spectral methods for homogeneous boltzmann equations. *C. R. Math. Acad. Sci. Paris*, 353(4):309–314, 2015.

[68] F. Filbet and L.M. Rodrigues. Asymptotically stable particle-in-cell methods for the vlasov-poisson system with a strong external magnetic field. *SIAM J. Numer. Analysis*, 54(2):1120–1146, 2016.

[69] F. Filbet and G. Russo. High order numerical methods for the space non-homogeneous boltzmann equation. *J. Comput. Phys.*, 2(2):457–480, 2003.

[70] R. Fisher. *The Genetical Theory of Natural Selection*. 1930.

[71] R. FitzHugh. Impulses and physiological sates in theoretical models of nerve membrane. *Biophysical journal*, 1(6):445–466, 1961.

[72] M.A. Geise. *Neural Field Theory for Motion Perception*. Kluwer Academic Publishers, 1999.

[73] S. Genieys, V. Volpert, and P. Auger. Pattern and waves for a model in population dynamics with nonlocal comsumption of resources. *Mathematical Modelling of Natural Phenomena*, 1(1):63–80, 2006.

[74] L. Glass and M. E. Josephson. Resetting and annihilationof reentrant abnormally rapid heartbeat. *Physical Review Letters*, 75(10):2059–2062, 1995.

[75] F. Golse. *On the Dynamics of Large Particle Systems in the Mean Field Limit*, pages 1–144. Springer International Publishing, Cham, 2016.

[76] S. Gourley. Traveling front solutions of a nonlocal fisher equation. *Journal of Mathematical Biology*, 41(3):272–284, 2000.

[77] S.-Y. Ha and J.-G. Liu. A simple proof of the cucker-smale flocking dynamics and mean-field limit. *Commun. Math. Sci.*, 7(2):297–325, 2009.

[78] F. Hamel and L. Ryzhik. On the nonlocal fisher-kpp equation: steady states, spreading speed and global bounds. *Nonlinearity*, 27(11), 2013.

[79] F.H. Harlow. The particle-in-cell method for numerical solution of problems in fluid dynamics. *Method in Computational Physics*, 3:319–343, 1964.

[80] S. Hastings. On traveling wave solutions of the hodgkin-huxley equations. *Arch. Ration. Mech. Anal.*, 60:229–257, 1976.

[81] M. Hauray and P.-E. Jabin. n-particles approximation of the vlasov equations with singular potential. *Archive for Rational Mechanics and Analysis*, 183(3):489–524, 2007.

[82] J.S. Hesthaven, S. Gottlieb, and D. Gottlieb. *Spectral methods for time-dependent problems*. Cambridge University Press, 2007.

[83] D.W. Hewett. Fragmentation, merging, and internal dynamics for pic simulation with finite size particles. *Journal of Computational Physics*, 189(2):390–426, 2003.

[84] A.L. Hodgkin and A.F. Huxley. Action potentials recorded from inside a nerve fibre. *Nature*, 144:710–711, 1939.

[85] A.L. Hodgkin and A.F. Huxley. A quantitative description of membrane current and its application to conduction and excitation in nerve. *The Journal of Physiology*, 117(4):500–544, 1952.

[86] X. Huang, X. Wu, J. Liang, K. Takagaki, X. Gao, and J.Y. Wu. Spiral wave dynamics in neocortex. *Neuron*, 68(5):978–990, 2010.

[87] K. Huffman, M.W. Vernoy, and J. Vernoy. *Psychology in action*. John Wiley & Sons, Inc., 2000.

[88] H.J. Hupkes and B. Sandstede. Traveling pulse solutions for the discrete fitzhugh-nagumo system. *SIAM J. Applied Dynamical Systems*, 9(3):827–882, 2010.

[89] H.J. Hupkes and B. Sandstede. Stability of pulse solutions for the discrete fitzhugh-nagumo system. *Transactions of the American Mathematical Society*, 365:251–301, 2013.

[90] S. Jin. Efficient asymptotic-preserving (ap) schemes for some multiscale kinetic equations. *SIAM J. Sci. Comput.*, 21(2):441–454, 1999.

[91] S. Jin. Asymptotic preserving (ap) schemesfor multiscale kinetic and hyperbolic equations: a review. *Riv. Mat. Univ. Parma*, 3:177–216, 2012.

[92] C.K. Jones. Stability of the travelling wave solution of the fitzhugh-nagumo system. *Transactions of the American Mathematical Society*, 286(2):431–469, 1984.

[93] M.-J. Kang, B. Perthame, and D. Salort. Dynamics of time elapsed inhomogeneous neuron network model. *C. R. Acad. Sci. Paris*, 353(12):1111–1115, 2015.

[94] M.-J. Kang and A. Vasseur. Asymptotic analysis of vlasov-type equations under strong local alignment regime. *Math. Mod. Meth. Appl. Sci.*, 25(11):2153–2173, 2015.

[95] T. Karper, A. Mellet, and K. Trivisa. Hydrodynamic limit of the kinetic cucker-smale flocking model. *Mathematical Models and Methods in Applied Sciences*, 2012.

[96] T. Karper, A. Mellet, and K. Trivisa. Existence of weak solutions to kinetic flocking models. *SIAM J. Math. Anal.*, 45(1):215–243, 2013.

[97] M. Kimura. A stochastic model concerning the maintenance of genetic variability in quantitative characters. *Proceedings of the National Academy of Sciences USA*, 54(3):731–736, 1965.

[98] A. Klar. An asymptotic-induced scheme for nonstationary transport equations in the diffusive limit. *SIAM J. Numer. Anal.*, 35(3):1073–1094, 1998.

[99] T. Krogh-Madsen and D.J. Christini. Resetting and terminationof reentry in a loop-and-tail cardiac model. *Phys. Rev. E*, 77:011916, 2008.

[100] C.R. Laing and W.C. Troy. Two bump solutions of amari-type models of working memory. *Physica D*, 178:190–218, 2003.

[101] C.R. Laing, W.C. Troy, Gutkin B., and Ermentrout G.B. Multiple bumps in a neuronal model of working memory. *SIAM Journal on Applied Mathematics*, 63:62–97, 2002.

[102] E. Luçon. Quenched asymptotics for interacting diffusions on inhomogeneous random graphs. *preprint*, 2018.

[103] E. Luçon and W. Stannat. Mean-field limit for disordered diffusions with singular interactions. *The annals of applied probability*, 24(5):1946–1993, 2014.

[104] J. S. Lund, A. Angelucci, and P. C. Bressloff. Anatomical substrates for functional columns in macaque monkey primary visual cortex. *Cerebral Cortex*, 13(1):15–24, 2003.

[105] A. Mellet, S. Mischler, and C. Mouhot. Fractional diffusion limit for collisional kinetic equations. *Archive for Rational Mechanics and Analysis*, 199(2):493–525, 2011.

[106] S. Mischler, C. Quiñinao, and J. Touboul. On a kinetic fitzhugh-nagumo model of neuronal network. *Comm. Math. Phys.*, 342(3):1001–1042, 2015.

[107] J.D. Murray. *Mathematical biology II: spatial models and biomedical applications*. New York, Springer, 2003.

[108] J. Nagumo, S. Arimoto, and S. Yoshizawa. An active pulse transmission line simulating nerve axon. *Proceedings of the IRE*, 50:2061–2070, 1962.

[109] P. I. Nunez. *Neocortical Dynamics and Human EEG Rhythms*. Oxford University Press, 1995.

[110] I. Omelchenko, B. Riemenschneider, P. Hövel, Y. Maistrenko, and E. Schöll. Transition from spatial coherence to incoherence in coupled chaotic systems. *Physical review. E, Statistical, nonlinear, and soft matter physics*, 85:026212, 2012.

[111] K. Pakdaman, B. Perthame, and D. Salort. Dynamics of a structured neuron population. *Nonlinearity*, 23(1):55–75, 2010.

[112] K. Pakdaman, B. Perthame, and D. Salort. Relaxation and self-sustained oscillations in the time elapsed neuron network model. *SIAM Journal on Applied Mathematics*, 73, 2011.

[113] K. Pakdaman, B. Perthame, and D. Salort. Adaptation and fatigue model for neuron networks and large time asymptotics in a nonlinear fragmentation equation. *Journal of mathematical neuroscience*, 4(14):14, 2014.

[114] L. Pareschi and G. Russo. Numerical solution of the boltzmann equation i: Spectrally accurate approximation of the collision operator. *SIAM J. Numer. Analysis*, 37(4):1217–1245, 2000.

[115] L. Pareschi and G. Russo. *Efficient asymptotic preserving deterministic methods for the Boltzmann equation*. Models and Computational Methods for Rarefied Flows, Lecture Series held at the von Karman Institute, Rhode St. Genèse, Belgium, 24 -28 January, 2011.

[116] B. Perthame and D. Salort. Derivation of an integrate fire equation for neural networks from a voltage-conductance kinetic model. *Communications in Mathematical Sciences*, 17(5):1193–1211, 2019.

[117] B. Perthame, D. Salort, and G. Wainrib. Distributed synaptic weights in a lif neural network and learning rules. *Physica D: Nonlinear Phenomena*, 353, 2017.

[118] B. Phillips, G. Brown, J. Webb, and R. Shine. Invasion and the evolution of speed in toads. *Nature*, 439(7078):803, 2006.

[119] C. Quiñinao and J. Touboul. Clamping and synchronization in the strongly coupled fitzhugh-nagumo model. *preprint*, 2018.

[120] P. A. Raviart. An analysis of particle methods. In Franco Brezzi, editor, *Numerical Methods in Fluid Dynamics*, pages 243–324, Berlin, Heidelberg, 1985. Springer Berlin Heidelberg.

[121] R. Shine, G. Brown, and P. Phillips. An evolutionary process that assembles phenotypes through space rather than through time. *PNAS*, 108(14):5708–5711, 2011.

[122] C. Thomas, E. Bodworth, R. Wikson, et al. Ecological and evolutionary processes at expanding range margins. *Nature*, 411:577–581, 2001.

[123] J. Touboul. Mean-field equations for stochastic firing rate neural fields with delays: Derivation and noise-induced transitions. *Physica D*, 24(1):1223–1244, 2012.

[124] J. Touboul. Propagation of chaos in neural fields. *The Annals of Applied Probability*, 24(3):298–1328, 2014.

[125] J. Touboul. Erratum: "propagation of chaos in neural fields". *The Annals of Applied Probability*, 28(5):3287–3289, 2018.

[126] J. Touboul, G. Hermann, and O. Faugeras. Noise-induced behaviors in neural mean field dynamics. *SIAM Journal on Applied Dynamical Systems*, 11(1):49–81, 2012.

[127] J. M.-J. Travis and C. Dytham. Dispersal evolution during invasions. *Evolutionary Ecology Research*, 4(8):1119–1129, 2002.

[128] J. M.-J. Travis, K. Mustin, and C. Benton, T. G .and Dytham. Accelerating invasion rates result from the evolution of density-dependent dispersal. *Journal of theoretical biology*, 259(1):151–158, 2009.

[129] O. Turanova. On a model of a population with variable motility. *Mathematical models and methods in applied sciences*, 25(10):1961–2014, 2015.

[130] C. Villani. *Topics in Optimal Transportation*. American Mathematical Society, 2003.

[131] G. Wainrib and J. Touboul. Topological and dynamical complexity of random neural networks. *Physical Review Letters*, 110:118101, 2013.

[132] H.R. Wilson and J.D. Cowan. Excitatory and inhibitory interactions in localized populations of model neurons. *Biophys. J.*, 12:1–24, 1972.

[133] H.R. Wilson and J.D. Cowan. A mathematical theory of the functional dynamics of cortical and thalamic nervous tissue. *Biological Cybernetics*, 13(2):50–80, 1973.

[134] A.T. Winfree. *The geometry of biological time*. New York: Springer, 2001.